SLAC-375
CONF-8907190
UC-414
(A)

PROCEEDINGS OF THE 1st INTERNATIONAL WORKSHOP ON ACCELERATOR ALIGNMENT

Stanford Linear Accelerator Center
Stanford University
Stanford, California 94309
July 31 – August 2, 1989

October 1990

Prepared for the Department of Energy
under contract number DE-AC03-76SF00515

Printed in the United States of America. Available from the National Technical Information Service, U.S. Department of Commerce, 5285 Port Royal Road, Springfield, Virginia 22161. Price: Printed Copy A14, Microfiche A01.

PROCEEDINGS OF THE 1ST INTERNATIONAL WORKSHOP ON ACCELERATOR ALIGNMENT

TABLE OF CONTENTS

Session 2B: Toolboxes, Instrumentation, Software, and Methods

Session 3: Fiducialization of Conventional Magnets

Session 4: Fiducialization of Superconducting Magnets

Session 5: Next Generation Linear Colliders

Opening Remarks

Welcome to our workshop!

I must say that I am happy and, to be honest, relieved to see that you all came, in spite of the very short notice of our announcement. I am especially grateful because this workshop depends on your participation to achieve its goals. I see many familiar faces of friends and colleagues whom I have had the pleasure of meeting earlier. For the ones I missed, my name is Robert Ruland, I am involved in the alignment effort here at SLAC.

Before we go any further into the purpose and technicalities of our meeting, let me introduce to you the director of SLAC whom we are fortunate enough to have with us this morning in order to open the meeting.

---- * * * ----

The idea for this workshop goes back quite a few years when we started aligning the SLC. At that time, we knocked at CERN's and DESY's doors to ask for help. The original one way information street eventually evolved into a relationship where we exchanged mutual experiences and developments. One day, we noticed that we had been reinventing the wheel a number of times. Then came a time when others started knocking on our door for support and exchange of ideas. We had the same feeling again: a great deal of work had been done over again, not because of competition, but because we were always unaware what our neighbors were doing. This is the reason for initiating this workshop. We want to establish lines of communication; we want everyone to share not only their accomplishments, but also their problems. By the way, this is what the upcoming first session is all about.

But let me go somewhat beyond this.

Up to now we have been tackling the millimeter world; achieving accuracies in the order of a tenth or some tenths of millimeters. The next generation of linear colliders, however, is confronting us with the micrometer world. Microns, one thousands of a millimeter, and we thought it was already difficult enough to achieve 0.1 mm or in microns: 100 μm accuracies. The traditional tools of our trade cannot measure to this new standard. I am tempted to compare our situation with the one Jean Gervaise at CERN and Kurt Marzahn at DESY faced roughly 30 years ago when they were asked to align the first synchrotrons at these facilities to what at that time was an unbelievably tight 0.1 mm. When we are talking about the micron world we are not talking about some distant future. The micron world has already arrived! Groups at CERN, KEK, Novosibirsk and SLAC are brainstorming linear colliders and related micron alignment techniques today. Here at SLAC, the proposed Final Focus Test Beam Project is scheduled for construction in Fiscal Year 91/92, i.e. roughly 14 months from now and will require positioning tolerances in the order of 5 μm. It is my belief that living in the micron world will require all of us pulling together, and for that matter, on the same end on the rope.

Before turning to the next session, let me say a few words about the fact that we dedicated two sessions to the fiducialization of magnets. Fiducialization is a fancy name for relating the effective magnetic axis of a component to some kind of surveying reference marks, fiducials, which can be tooling balls, CERN sockets or just some reachable mechanical feature on the component's body. The alignment process is one in which we move a component's reference mark to its called for coordinate. But this is only one part of the story. The beam does not know anything about fiducials, the beam is influenced only by the electromagnetic field of a component. We have, therefore, to relate the magnetic axis to the fiducial marks with the same care as we do the final positioning. I hope, these sessions will give an overview of some of the new approaches of making the fiducialization process more reliable and improving what is now a weak link.

But now I don't want to take any more time away from our "Get-to-meet-each-other" session. Let me trade seats now with Gerry Fischer whom I have pressed to take the chair. As a physicist, he has been involved in the construction of many machines, the latest being the SLC and is actively involved in the alignment R&D for the FFTB and NLC. He was recently on sabbatical for 6 months each at DESY and CERN working with their alignment groups where I hope he learnt something.

Gerry, do something.

BUILDING 919 FLOOR STABILITY*

A. PENDZICK, F. KARL, J. MILLS, J. SULLIVAN

Alternating Gradient Synchrotron Department
Brookhaven National Laboratory
Associated Universities, Inc.
Upton, New York

The g-2 ring is to be installed in the old 80" Bubble Chamber high bay. The ring is approximately 50′ diameter, consists of 30° segments weighing 50 tons apiece and supported near their ends. Since the value of the muon magnetic moment depends heavily on knowing the effective field integral of the ring, a study was implemented to determine how the ring survey data varied with time and what factors may contribute to changes in the survey data.

919 Floor

The concrete floor of the old 80" bubble chamber consists of three different sections. The center section consists of 5′ thick concrete slab approximately 20′W x 60′L. The two outer sections consist of a 1′ thick slab approximately 20′W x 75′L. The sections have an expansion joint at their interface.

Method

The floor was loaded, simulating the ring, in 12-4′ x 5′ areas of 50 tons apiece. 12 elevation points were placed along the ring I.D. and 6 elevation points were placed

* Work performed under the auspices of the U.S. Department of Energy.

along the ring O.D. Two diametrical distances were measured, one along the center slab and one across the three slabs (and 2 expansion joints). Additionally, thermocouples were placed in the floor in five places. Each position included a thermocouple close to the concrete surface and one approximately 12"-deep. All measurements were taken once a week from August 3, 1988 to February 22, 1989. Thus, we believe we went through a freeze-thaw cycle. We off-loaded the floor on March 15, 1989 and continued survey to look for rebound and load dampening effects.

Point #1 was used as the reference point and all elevations were measured relative to this point. A Wild N-3 level was set up on the ring center and 3-4 elevations were taken on each point, the average being recorded in the data. This method of data-taking has been statistically analyzed during AGS ring surveys and has been found to be accurate within ± .002". Diametrical distances are typically good to ± .0005" using a laser interferometer.

General Observations

1. The maximum positive excursion occurred in almost all points the week of December 6-13, with a drop in floor temperature. The maximum positive excursion was .020" in Point #13.

2. The maximum weekly change occurred at the same time.

3. The horizontal distance along the center slab tracked very well with temperature, with a maximum change of approximately .064".

4. The horizontal distance across the slabs varied by approximately .030", with the diameter *increasing* with an overall decrease in temperature.

5. The maximum weekly change in roll of .013" occurred between Points 7 and 17 on the thin slab. The thick slab did not fare much better with a maximum of .009" roll in two weeks.

6. Continued survey of the unloaded floor has shown that the excursions seen before the floor was loaded have come back. The load on the floor seems to damp out the vertical excursions.

g-2 Issues

We have looked at the data to better understand how the g-2 ring will behave for pitch, roll and diametrical changes during an experimental run. For pitch we looked at the different inner elevations with time and produced a typical ring profile. For roll we looked at the difference in radial elevations with time. For diametrical changes we looked at the horizontal measurements vs time and temperature. To summarize these results:

Pitch: Maximum excursions will be .012" in one magnet.

Roll: Maximum roll will be .21 mrad; most magnets will roll in the same direction.

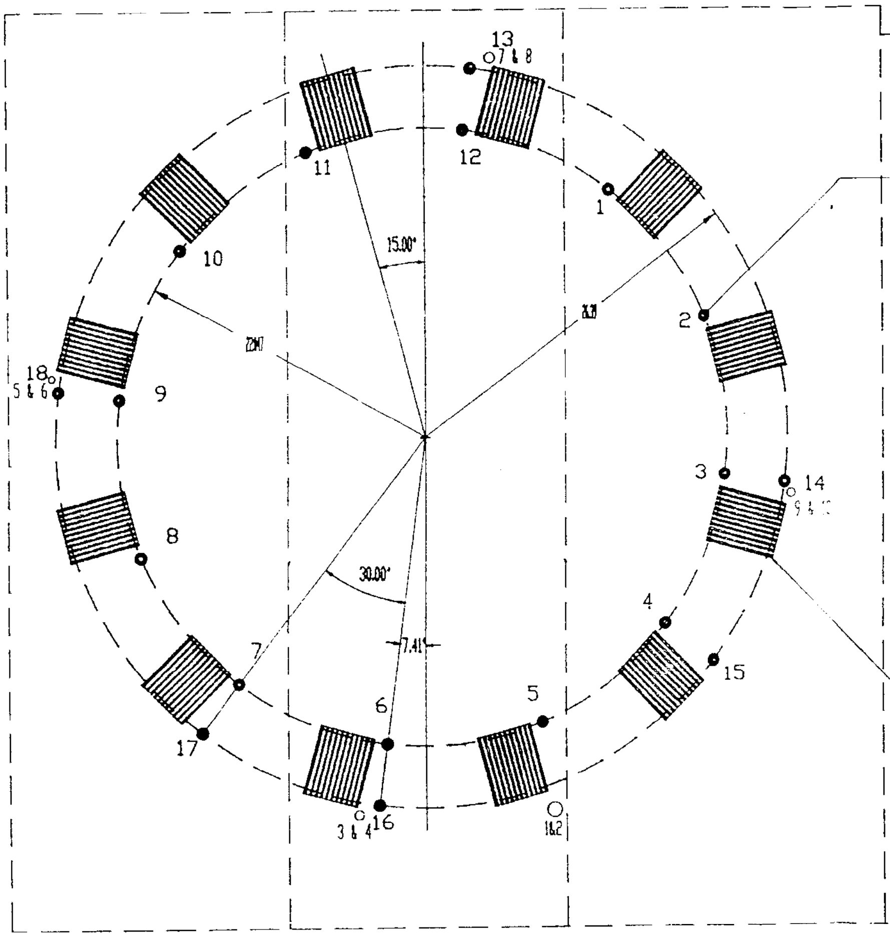

NOTES
THERMOCOUPLES LOCATED AT 13,14,16,18
DISTANCES MEASURED FROM 13 TO 16, 14 TO 18

D18-M-XXXX-4

DEC ± .005 ANG ± 1/2°	1/32 1/64	BROOKHAVEN NATIONAL LABORATORY UPTON, N.Y. 11973
±1/64 ±1/32 ±1/16	125 √	
7-21-88	V .254	EXPERIMENT 881
JM		A

1 #AUTOCAD

Diametrical distance: Expect a .030" contraction along the slabs while incurring a .020" expansion across the slabs.

Each of these issues is addressed separately in the following.

Roll

To estimate the amount of roll that may occur during a running period for the ring, we looked at the difference between two radial floor elevations approximately 60" apart. Two graphs are shown, one representing the best case and one the worst case; both occurred on the 12" slabs. The maximum roll of .013" occurred in one week. This could result in a .21 mrad radial tilt in two adjacent magnets. In general, the tilts occurred in the same direction (towards ring center) compounding the error due to roll. A possible reason for this may be due to the fact that the floor is vertically pinned by the building foundation along the perimeter.

ROLL POINTS

DATE	POINT #3	POINT #14	DEVIATION
10-Aug-88	101.215	100.765	0.000
17-Aug-88	101.212	100.766	-0.004
24-Aug-88	101.212	100.766	-0.003
31-Aug-88	101.213	100.763	0.001
07-Sep-88	101.211	100.762	-0.001
14-Sep-88	101.214	100.766	-0.002
21-Sep-88	101.213	100.765	-0.002
28-Sep-88	101.210	100.763	-0.003
05-Oct-88	101.210	100.762	-0.001
12-Oct-88	101.210	100.763	-0.002
19-Oct-88	101.210	100.762	-0.001
26-Oct-88	101.210	100.761	-0.001
02-Nov-88	101.210	100.761	-0.001
09-Nov-88	101.210	100.761	-0.001
16-Nov-88	101.210	100.764	-0.004
23-Nov-88	101.217	100.769	-0.001
30-Nov-88	101.218	100.770	-0.002
07-Dec-88	101.214	100.767	-0.003
14-Dec-88	101.222	100.775	-0.002
21-Dec-88	101.219	100.772	-0.002
28-Dec-88	101.220	100.770	0.000
04-Jan-89	101.214	100.766	-0.001
11-Jan-89	101.217	100.770	-0.003
18-Jan-89	101.215	100.765	0.001
25-Jan-89	101.216	100.767	-0.001
01-Feb-89	101.212	100.762	0.001
08-Feb-89	101.216	100.765	0.001
15-Feb-89	101.217	100.765	0.002
22-Feb-89	101.216	100.767	0.000
01-Mar-89			
08-Mar-89			
15-Mar-89	101.220	100.766	0.004
22-Mar-89			
29-Mar-89			
05-Apr-89			
12-Apr-89	101.216	100.750	0.017

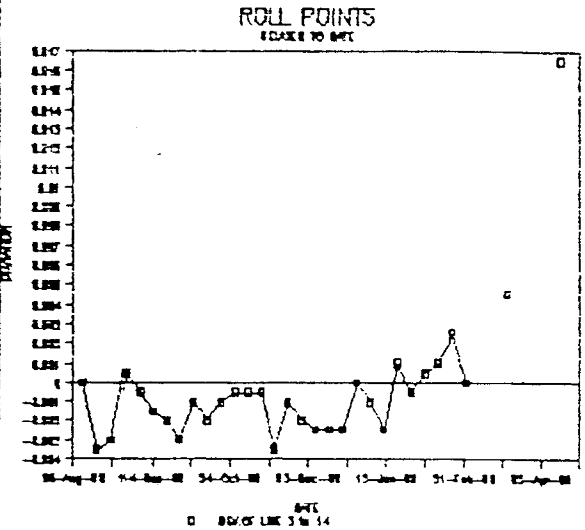

ROLL POINTS

DATE	POINT # 7	POINT #17	DEVIATION
10-Aug-88	100.083	99.774	0.000
17-Aug-88	100.079	99.773	-0.003
24-Aug-88	100.083	99.776	-0.002
31-Aug-88	100.080	99.773	-0.002
07-Sep-88	100.082	99.776	-0.003
14-Sep-88	100.081	99.778	-0.006
21-Sep-88	100.080	99.775	-0.004
28-Sep-88	100.079	99.771	-0.001
05-Oct-88	100.080	99.772	-0.001
12-Oct-88	100.086	99.776	0.001
19-Oct-88	100.080	99.772	-0.002
26-Oct-88	100.079	99.772	-0.001
02-Nov-88	100.080	99.774	-0.003
09-Nov-88	100.080	99.772	-0.001
16-Nov-88	100.080	99.774	-0.003
23-Nov-88	100.085	99.777	-0.001
30-Nov-88	100.087	99.779	-0.001
07-Dec-88	100.085	99.779	-0.002
14-Dec-88	100.096	99.791	-0.003
21-Dec-88	100.093	99.786	-0.002
28-Dec-88	100.091	99.784	-0.002
04-Jan-89	100.088	99.778	0.001
11-Jan-89	100.078	99.781	-0.012
18-Jan-89	100.086	99.779	-0.002
25-Jan-89	100.088	99.781	-0.002
01-Feb-89	100.085	99.770	0.006
08-Feb-89	100.092	99.778	0.005
15-Feb-89	100.088	99.781	-0.002
22-Feb-89	100.090	99.781	-0.001
01-Mar-89			
08-Mar-89			
15-Mar-89	100.091	99.779	0.003
22-Mar-89			
29-Mar-89			
05-Apr-89			
12-Apr-89	100.086	99.765	0.012

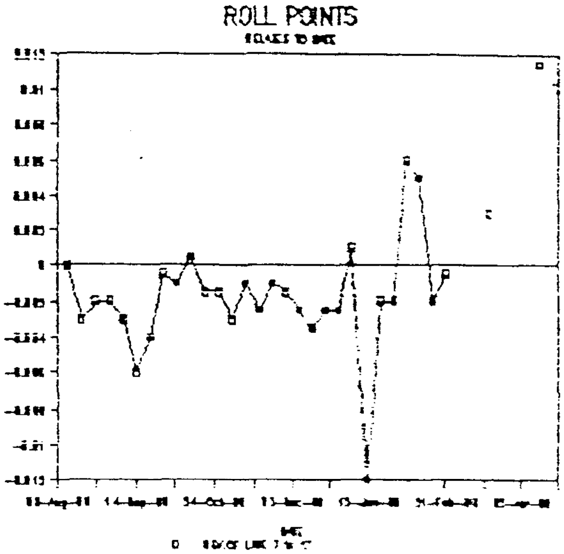

Pitch

To estimate the amount of pitch one would expect during a run, we picked three dates: October 19, December 14, and February 22, and produced a typical ring profile around the inner 12 points and outer 6 points. All elevations were normalized to zero on August 3, 1988. Note that the largest excursions occurred for both inner and out points in December.

Since each inner elevation point is the best representation of pitch in an individual magnet, we use this data for comparisons. The worst case was between points 4 and 5 on February 22, with .012″ pitch. December had two cases of .011″ pitch between points 2 and 3, and 10 and 11.

g-2 PROFILE
INNER DIAMETER

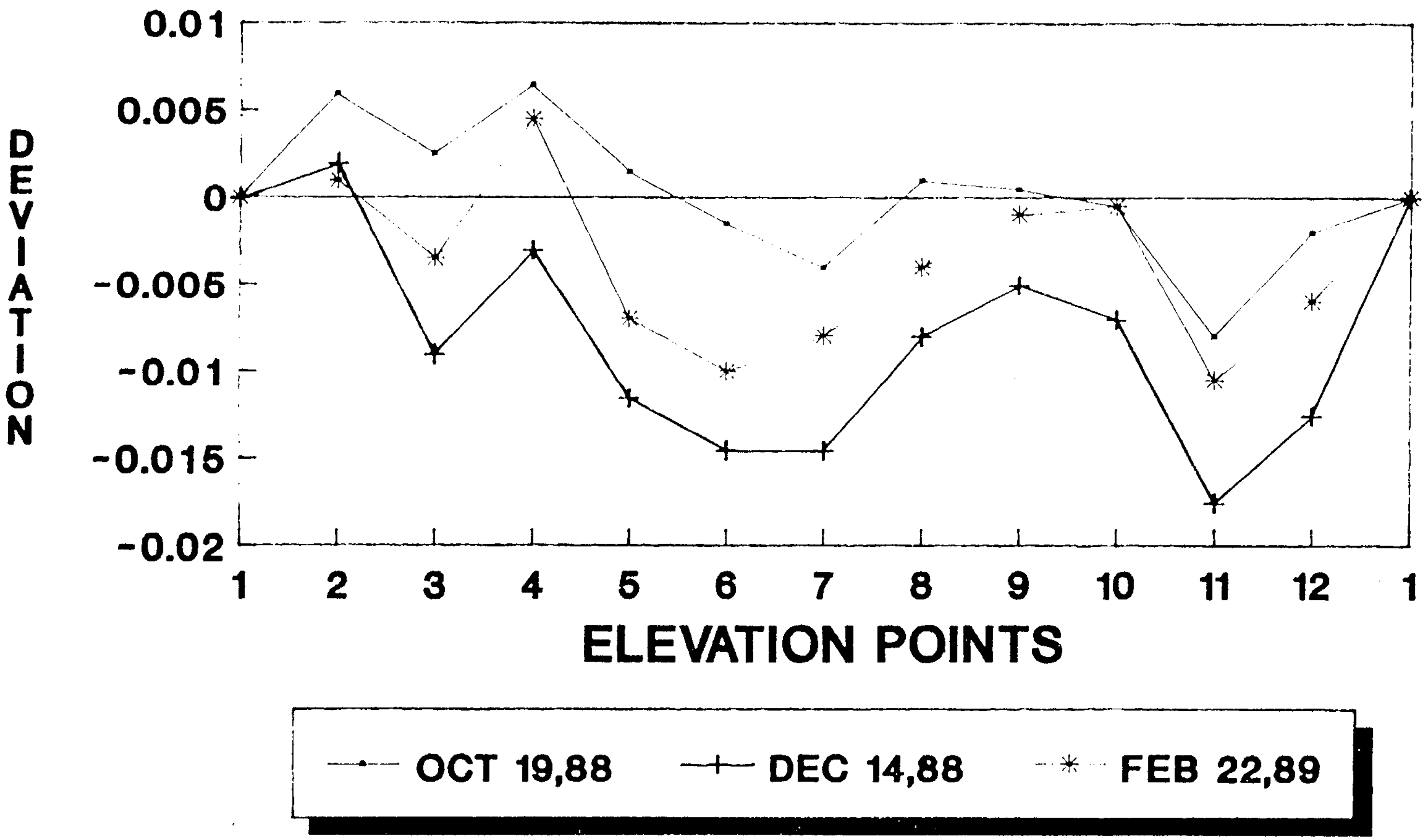

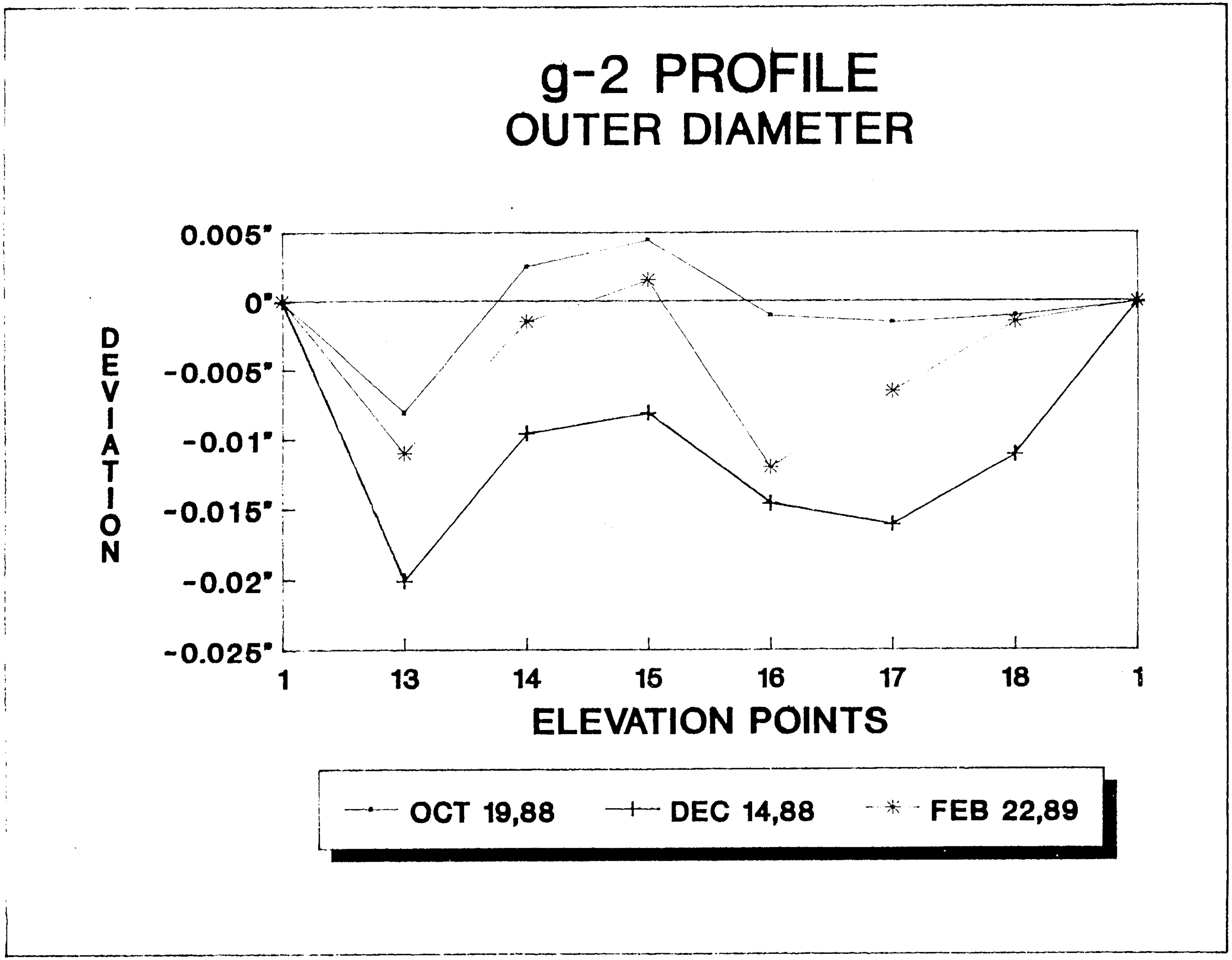
g-2 PROFILE
OUTER DIAMETER
0.005"
0"
-0.005"
-0.01"
-0.015"
-0.02"
-0.025"
DEVIATION
1
13
14
15
16
17
18
1
ELEVATION POINTS
OCT 19,88
DEC 14,88
FEB 22,89

Horizontal Movement

Points 16 to 13 are located along the center slab. On page 12, the horizontal movement is plotted vs two surface temperature probes. There is a clear relationship between temperature and length. Using this data to calculate the coefficient of expansion on concrete

$$\alpha = \frac{\Delta d}{d\Delta t} = \frac{.062''}{(648'')(20K^\circ F)} = 4.78 \times 10^{-6} \frac{in}{in\ ^\circ F}$$

This agrees fairly well with published data of $6 \times 10^{-6} \dfrac{in}{in\ ^\circ F}$.

Points 14 to 18 are located across the slabs and 2 expansion joints. On page 13, the horizontal movement is plotted vs two bottom temperature probes. Temperature and movement are still clearly related, but nonlinear and overall, there is an *increase* in distance for a decrease in temperature. This should not occur if you assume the slabs expand and contract from their centers and the expansion joints are functional. If you assume the outer slabs are pinned to the crane columns, the diameter would increase with a decrease in temperature. There is some evidence that this is happening, but it cannot be confirmed by calculations.

The maximum excursion between the two measured diameters is about .050". This occurred on October 12, 1988 and the late winter of 1989.

g - 2

HZ.MOVEMENT OF FLOOR RELATED TO TEMP.

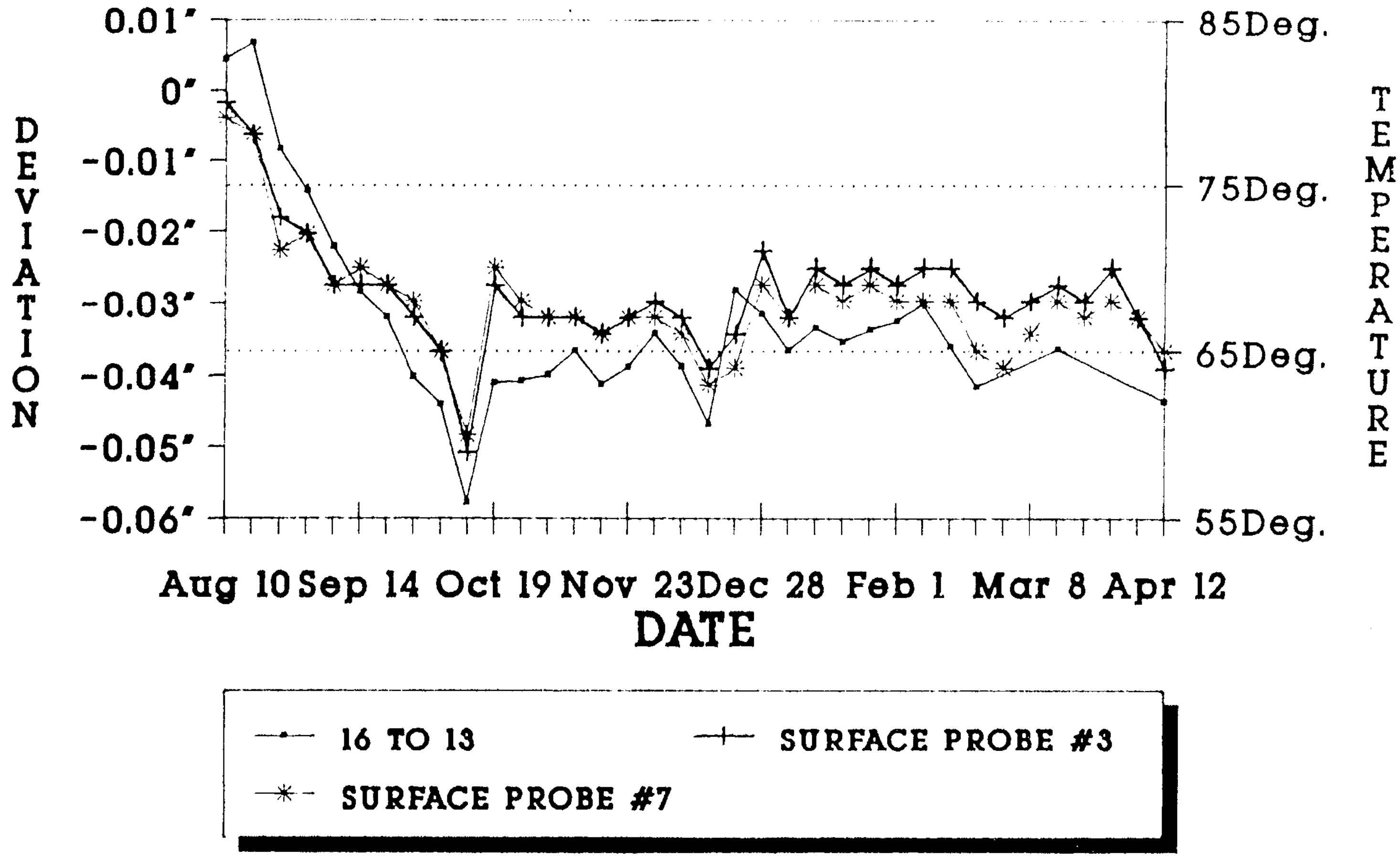

g-2

HZ.MOVEMENT OF FLOOR TO TEMP.

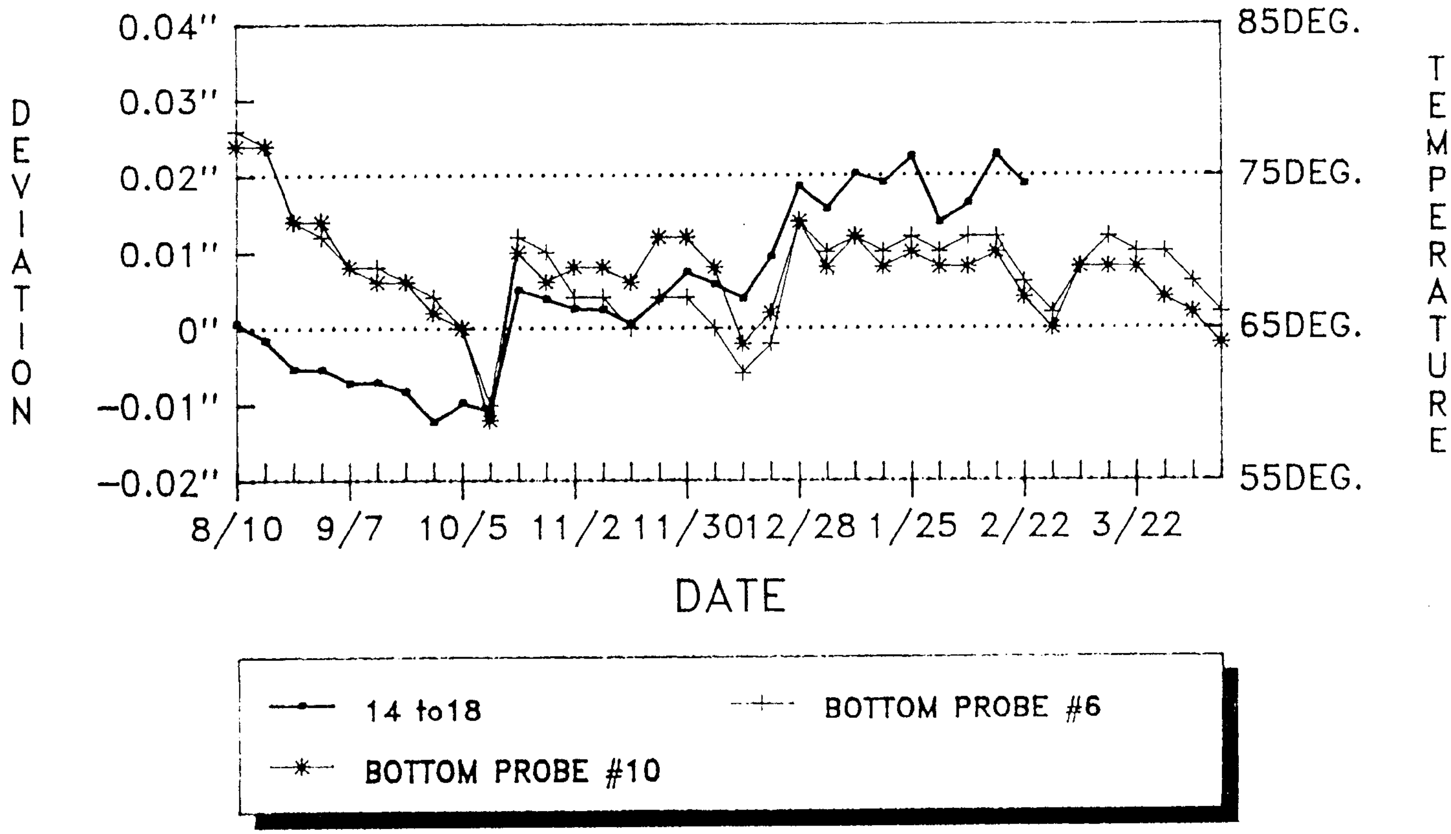

Load Dampening Effects

The following graphs seem to indicate there is an elevation dampening effect due to the simulated load of the g-2 ring on the concrete floor. Graph #1 illustrates the vertical excursion of 4 elevation points before the floor was loaded. Graph #2 represents a typical point with load (note change in scale). Graph #3 represents unloaded data to date using the same points used for the loaded data.

There is a clear indication that the load on the floor dampens the vertical excursions.

The last 3 graphs relate the elevation of a point to temperature. We make no comment on a relationship between the two.

g-2 ELEVATIONS
BEFORE LOADING

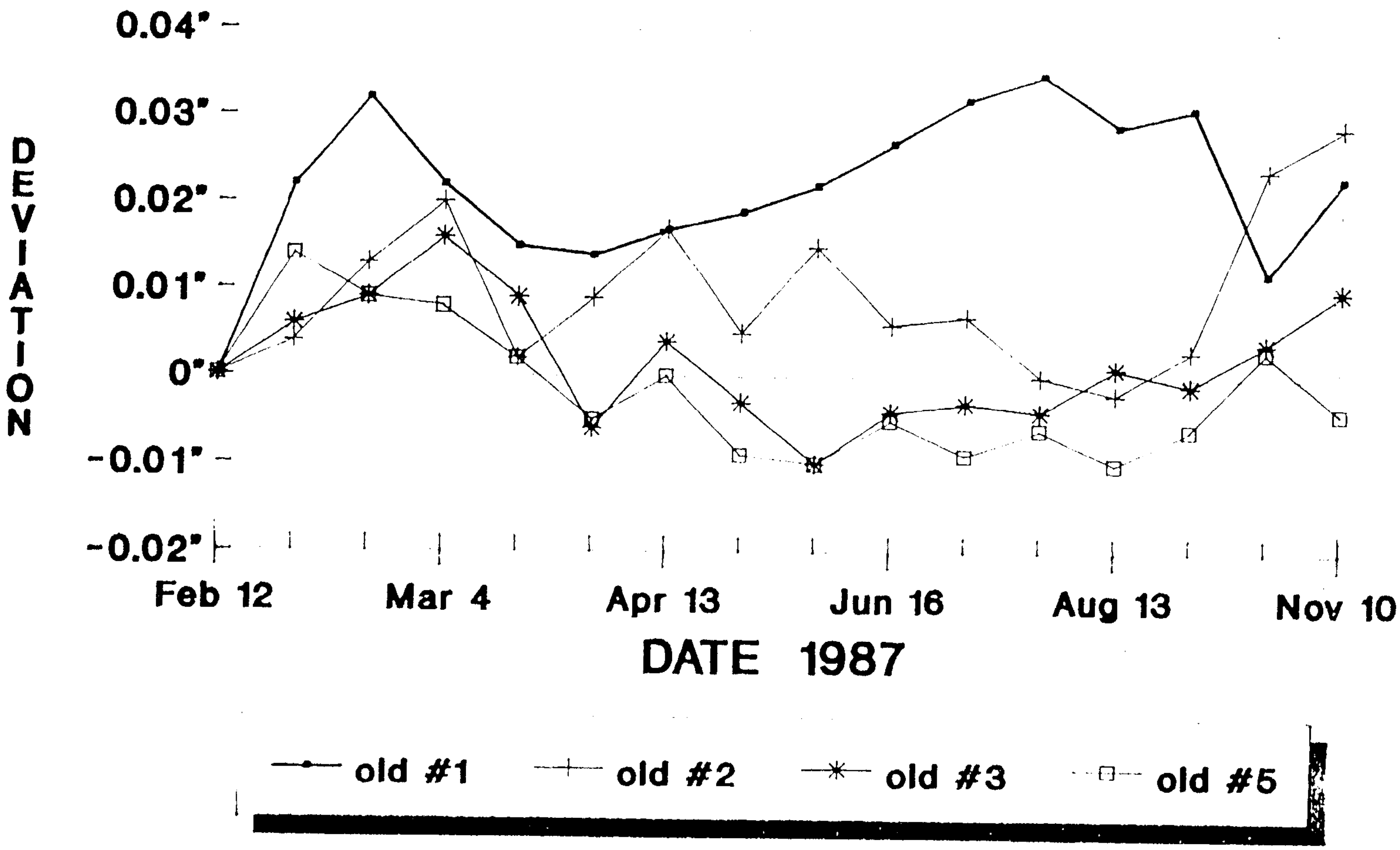

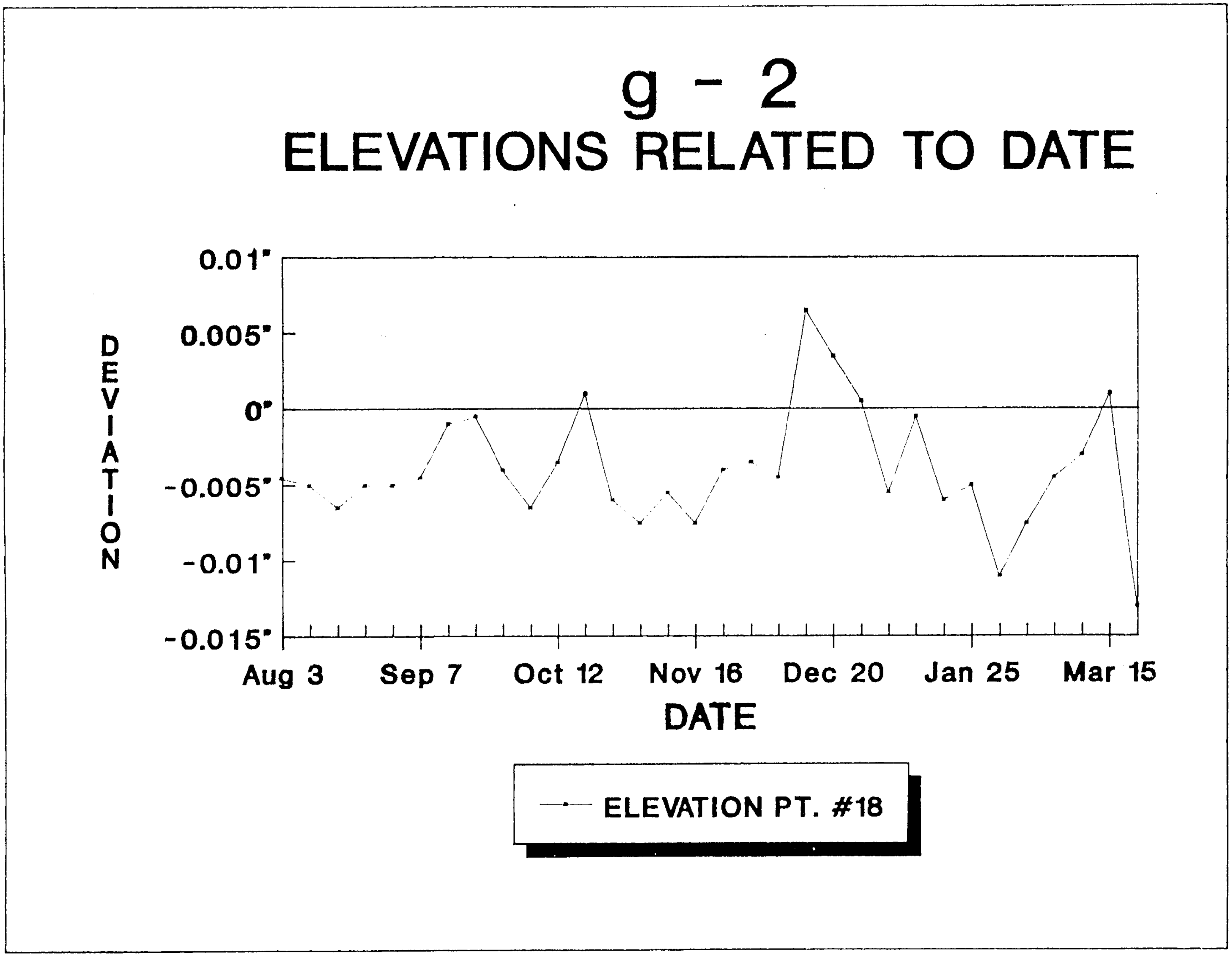
g - 2
ELEVATIONS RELATED TO DATE
DEVIATION
0.01"
0.005"
0"
-0.005"
-0.01"
-0.015"
Aug 3
Sep 7
Oct 12
Nov 16
Dec 20
Jan 25
Mar 15
DATE
ELEVATION PT. #18

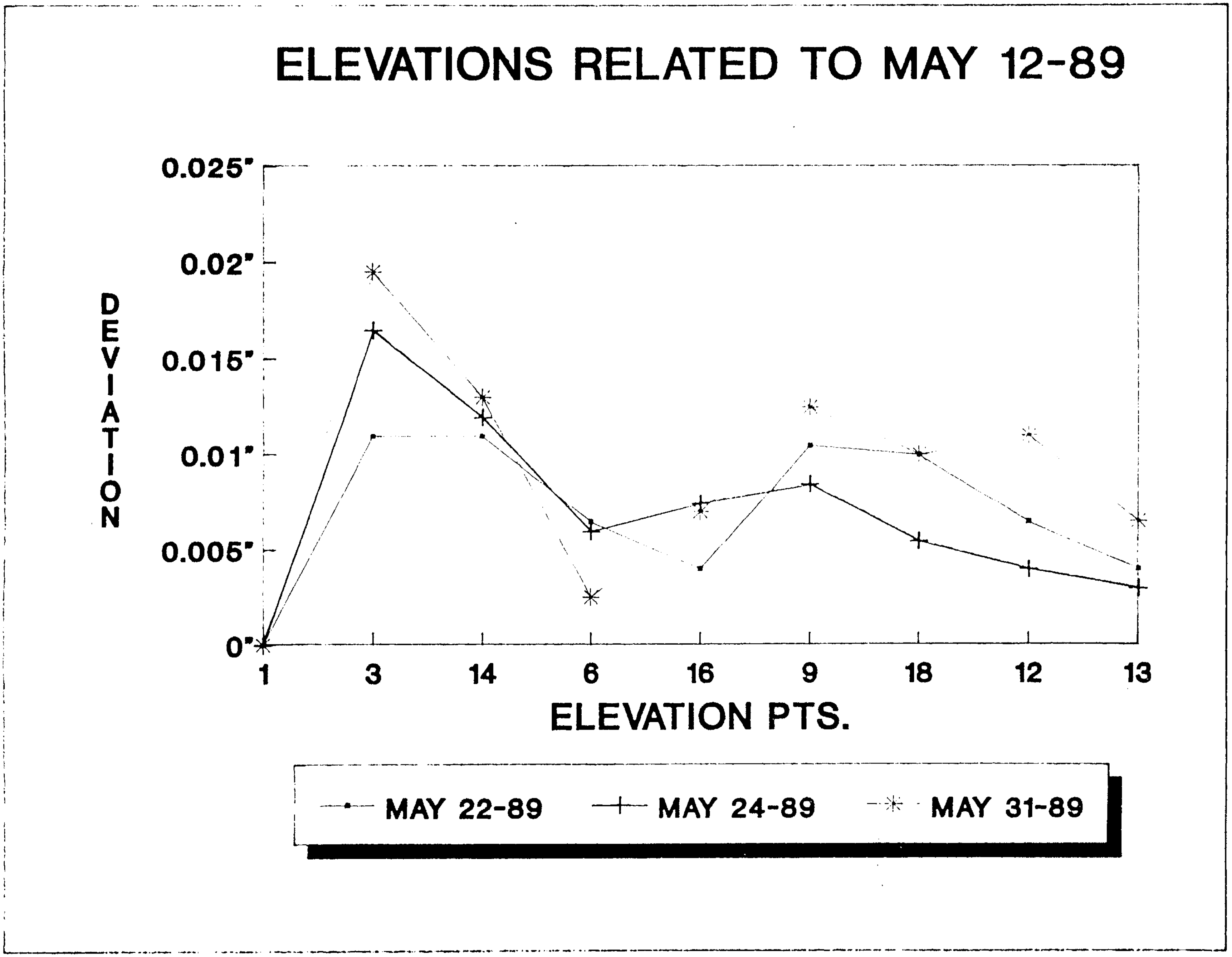

ELEVATIONS RELATED TO MAY 12-89
0.025"
0.02"
0.015"
0.01"
0.005"
0"
DEVIATION
1
3
14
6
16
9
18
12
13
ELEVATION PTS.
MAY 22-89
MAY 24-89
MAY 31-89

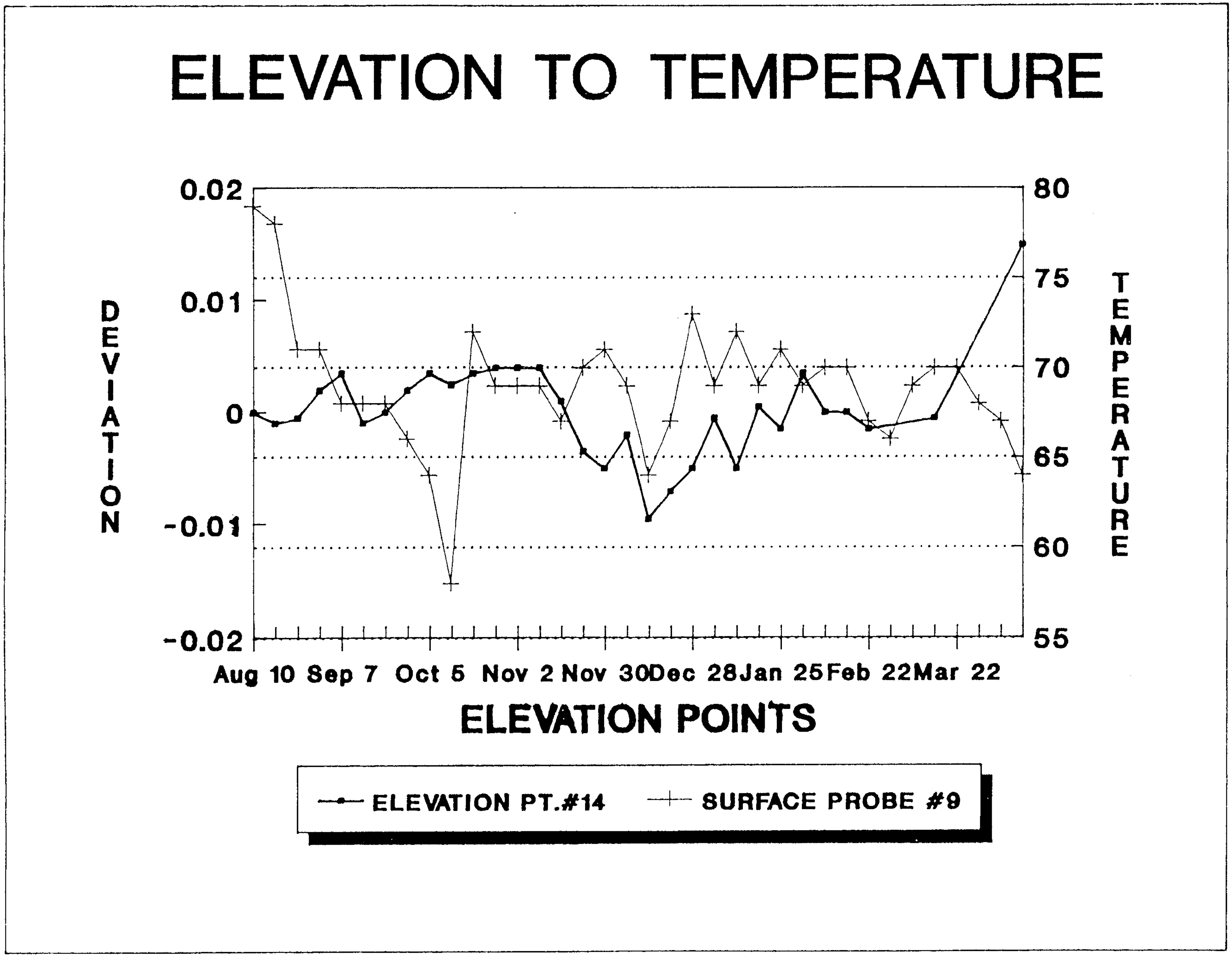

ELEVATION TO TEMPERATURE
DEVIATION
0.02
0.01
0
-0.01
-0.02
TEMPERATURE
80
75
70
65
60
55
Aug 10 Sep 7 Oct 5 Nov 2 Nov 30 Dec 28 Jan 25 Feb 22 Mar 22
ELEVATION POINTS
ELEVATION PT.#14
SURFACE PROBE #9

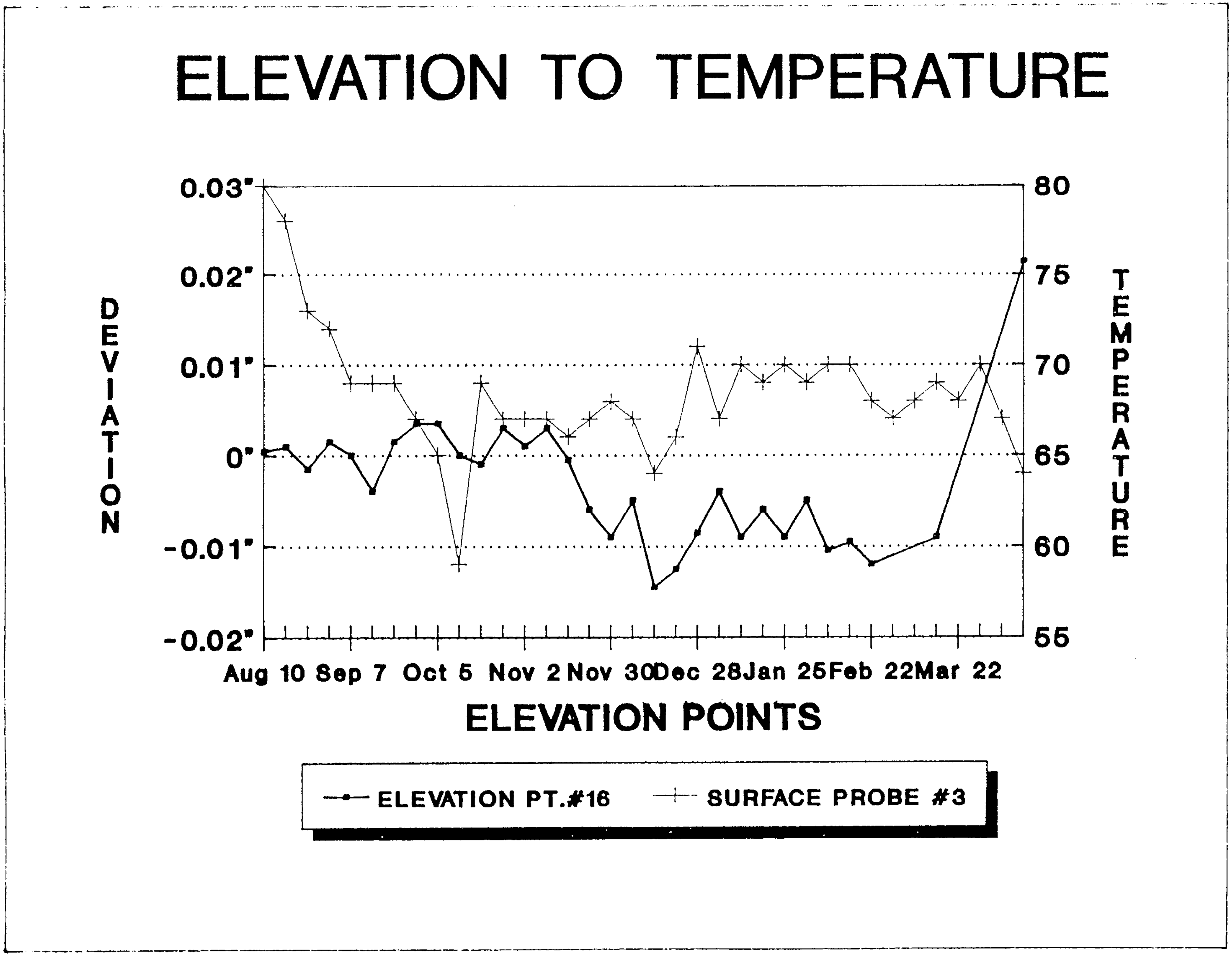
ELEVATION TO TEMPERATURE
DEVIATION
0.03"
0.02"
0.01"
0"
-0.01"
-0.02"
TEMPERATURE
80
75
70
65
60
55
Aug 10 Sep 7 Oct 5 Nov 2 Nov 30 Dec 28 Jan 25 Feb 22 Mar 22
ELEVATION POINTS
ELEVATION PT.#16
SURFACE PROBE #3

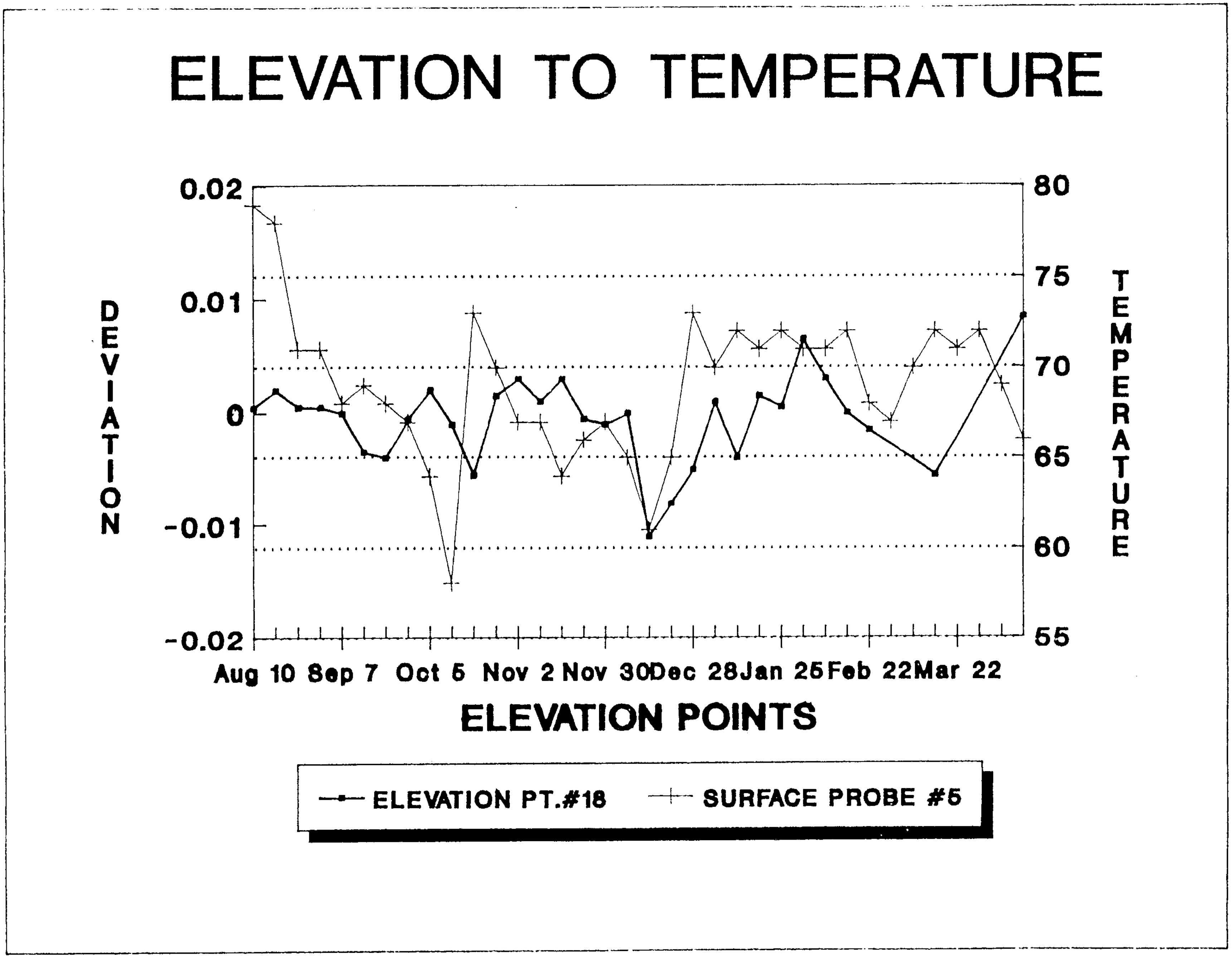
ELEVATION TO TEMPERATURE
0.02
0.01
0
-0.01
-0.02
DEVIATION
80
75
70
65
60
55
TEMPERATURE
Aug 10 Sep 7 Oct 5 Nov 2 Nov 30 Dec 28 Jan 25 Feb 22 Mar 22
ELEVATION POINTS
ELEVATION PT.#18
SURFACE PROBE #5

CURRENT ALIGNMENT TOPICS AT CEBAF

GEORGE BIALLAS
Continuous Electron Beam Accelerator Facility
Newport News, VA.

Overview

The Continuous Electron Beam Accelerator Facility (CEBAF) is a 4 GeV electron accelerator for the Nuclear Physics Community at Newport News, Virginia.* The machine configuration of this accelerator, due to be completed in 1993 and shown in figure 1, is a recirculating linac device that starts with an injector at 50 MeV and continues into a 0.4 GeV linac. The first recirculation is accomplished by arc magnets which bend the beam around 180° in the uppermost of five beam lines, directing the beam into another 0.4 GeV linac. The beam is similarly bent back into the first linac using another recirculating arc. The process continues, the beam gaining energy and cycling to lower arcs until five recirculations have taken place and the beam is at 4 GeV. The beam may be extracted at any of the four intermediate energies or the final energy and directed to all of the three end stations.

Each linac consists of twenty tanks 8.25 m long placed at a pitch of 9.6 m. Each tank, called a cryomodule, contains eight superconducting accelerating cavities 0.5 m long immersed in a bath of liquid helium at 2 K. The tanks are separated by a region of room temperature beam pipe with a quadrupole, beam position detector and two corrector dipoles placed on a common girder. The entire linac is contained in a tunnel 3.96 m (13 ft) wide by 3.05 m (10 ft) high; whose floor is 7.7 m (25.25 ft) from the surface, the tunnel floor slab is poured onto a rock-like material made of partially cemented shells known as marl. The tunnel concrete is enclosed in a membrane of vulcanized rubber and backfilled with no attempt to prevent complete immersion in the ground water.

The recirculating arc tunnels are the same size as the linac tunnel. The recirculating arcs undulate either side of an average 80.6 m radius in the semicircular tunnel. The stand

* Sponsored by the Department of Energy and the State of Virginia

with quadrupoles shown in the illustration of figure 7 is shown in the most extreme aisle squeezing position.

The element count is shown in Table 1. In general, all quadrupoles are supported on a girder along with their respective beam position detectors, corrector dipoles and vacuum apparatus. The quadrupoles are aligned on the girder with a three point support with respect to the beam position detector. Corrector dipoles are similarly positioned on the girder. The girder is then positioned on a three point support system described later. All other elements, such as the major dipoles, and septa are placed on their own three point supports.

Figure 2 shows the top and side views of the injector line consisting of 2 1/4 cryomodules, the relatively sparse positioning of the magnetic elements, and the intersection of the arc magnets (top view only).

Figure 3 shows the continuation of the injection chicane, the recombiner for the four recirculation arcs (at the injection end, five arcs are at the opposite end) and the start of the first linac.

Figure 4 shows a representative portion of the first arc (note the five beam lines). Note, quadrupoles have been placed over one another so common stands may be used for their girders. The stands for the dipoles will be slightly more complex.

Figure 5 shows a typical warm region stand intended for use between cryomodules. It illustrates the typical magnet placements on the girders and placement of the typical three point supports known as cartridges.

Adjustment Mechanisms & Stands

The cartridge, shown in figure 6, is based on a CERN design with simplification to accommodate our lighter loads and our access to the bottom for adjustment. We intend to place dial gauges on all cartridges to measure the six degrees of freedom while adjusting and locking. The cartridges will be placed in a pattern of two at the upstream end and one at the downstream. The two at the upstream will have cap adjusting screw orientations along the beam axis at the rear and perpendicular to the axis at the front. The cartridge at the downstream end has adjustment perpendicular to the beam axis. In this way, all degrees of freedom are constrained and adjustable.

This cartridge is also planned to be used in the recirculating arc stands shown in figure 7. Here a series of five quadrupoles in the first arc is shown. The stand has a single adjustor for the vertical direction at the base and a flexplate attachment to the tunnel at the top to accommodate vertical movement from adjustment and other motions. This feature allows direct adjustment for tunnel settlement of all five devices.

Tolerance Budget

Our tolerance budget is shown in Table 2. This is the total error budget and not only includes error in the placement of elements on the local beam line, but ambiguity in knowledge of the magnetic axis and error in fixation of the fiducials. The local beam line is defined as $\pm$ 25 m from the element. The DIMAD analysis which was used to develop these specifications assumed a Gaussian distribution with the tails truncated at $\pm 2\sigma$. (Smoothing of the beam line is assumed.) The accelerator remains robust up to twice these tolerances. This additional latitude is a provision for medium term settlement.

Alignment and Survey Plans

Our plans are to maintain both vertical and transverse monument networks in the tunnel which are not based on surface monuments. Provision has been made for going to such a network by means of four penetrations to the surface at the arc tangents and one in each end station.

We plan to use Geonet for data collection, storage, error check and analysis. We will use levels and inclinometers for survey and alignment of the vertical dimension. The transverse dimension will be surveyed with electronic theodolites and aligned with electronic dial gauges keyed to an electronic notebook. The ME5000 distance meter will be used for all distances down to 5 m. Jig transits and scales will be used for special cases. Fiducials on elements will be the stamped or machined surfaces that accept a fixture with exchangeable tooling balls and targets. Special elements will have integral tooling ball/target sockets.

Both the quadrupole and the dipole magnet measurement systems are built upon surface plates. We intend to verify the position of the fiducials, the measurement coils, and the pole faces at the time of measurement, by elementary metrology in an integrated operation.

Table 1

Element Counts

MAGNETS:	
Corrector Dipoles (< 32 cm $\times$ 1 kG)	1047
Major Dipoles (> 1 m $\times$ 1 kG; < 3 m $\times$ 7 kG)	390
Quadrupoles	707
Sextapoles	96
Septa	26
Lambertson SEPTA	1
TOTAL:	2267
CRYOMODULES	42 1/4 (338 Cavities)

Table 2

Tolerance Budget

Parameter	**Tolerance**	**Comments**
σ_x or σ_y	0.2 mm	(Dipole larger but not verified by calculations)
σ_z	5 mm	
σ'_z	10^{-3}	
σ'_x or σ'_y	set by σ_x or σ_y at both ends	for dipoles
Tx$'$ or Ty$'$	set by $\frac{\sigma_x}{l}$ or $\frac{\sigma_y}{l}$	for quadrupoles
Accelerating Cavity Exceptions		
σ_x or σ_y	1 mm	
σ'_x or σ'_y	4×10^{-3}	

- Tolerance Includes
  - Ambiguity in knowledge of magnetic axis
  - Error in fixation of fiducials
  - Error in placement of element of local beam line
- Local beam line is ± 25 m of element
- Assumes Gausian distribution with tails cut at $\pm 2\ \sigma$
- Accelerator remains robust up to twice the above tolerances — provision for medium term settlement

[apd.biallas]slacpaper.tex

MACHINE CONFIGURATION CEBAF

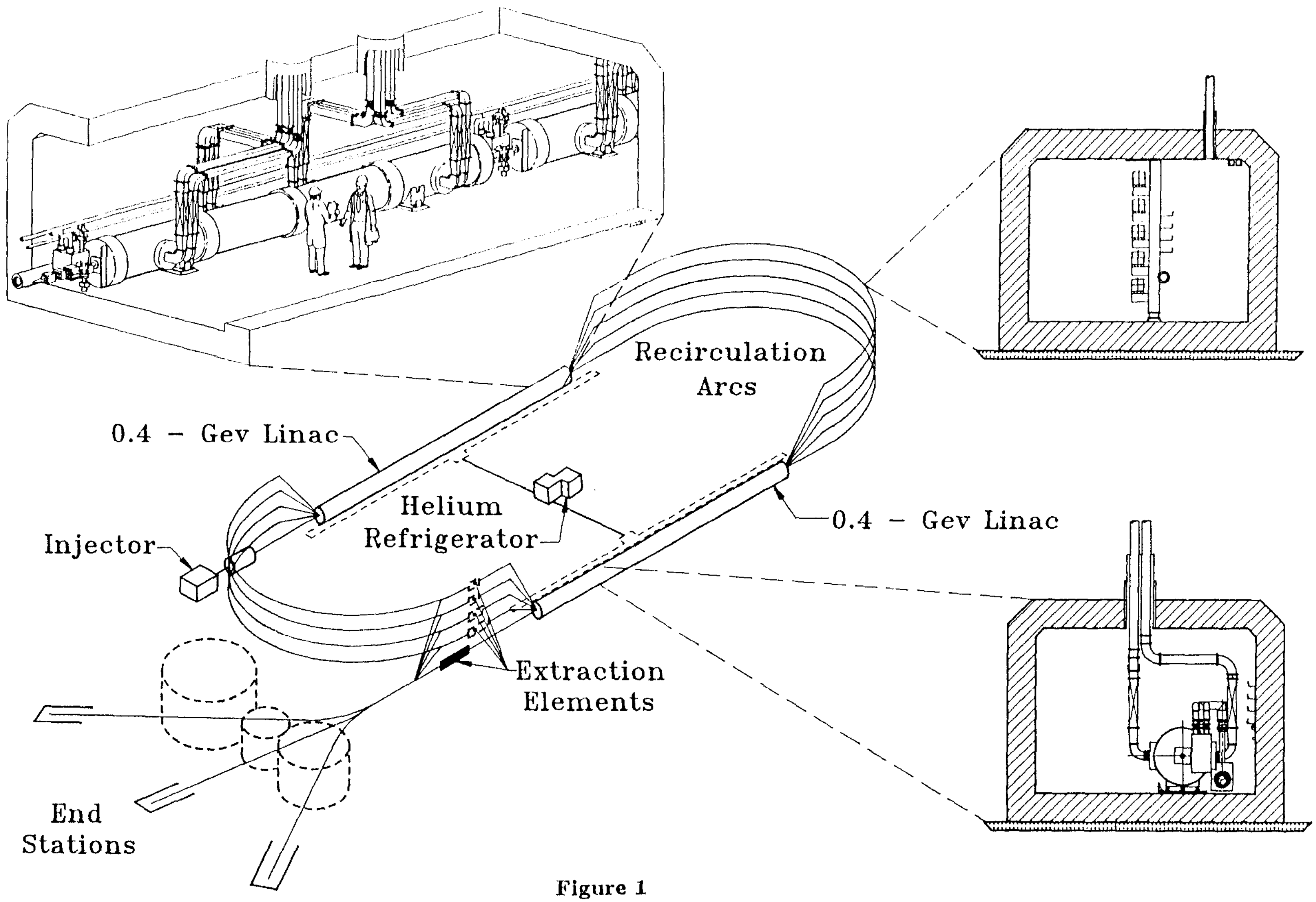

Figure 1

INJECTOR LINAC REGION

CEBAF

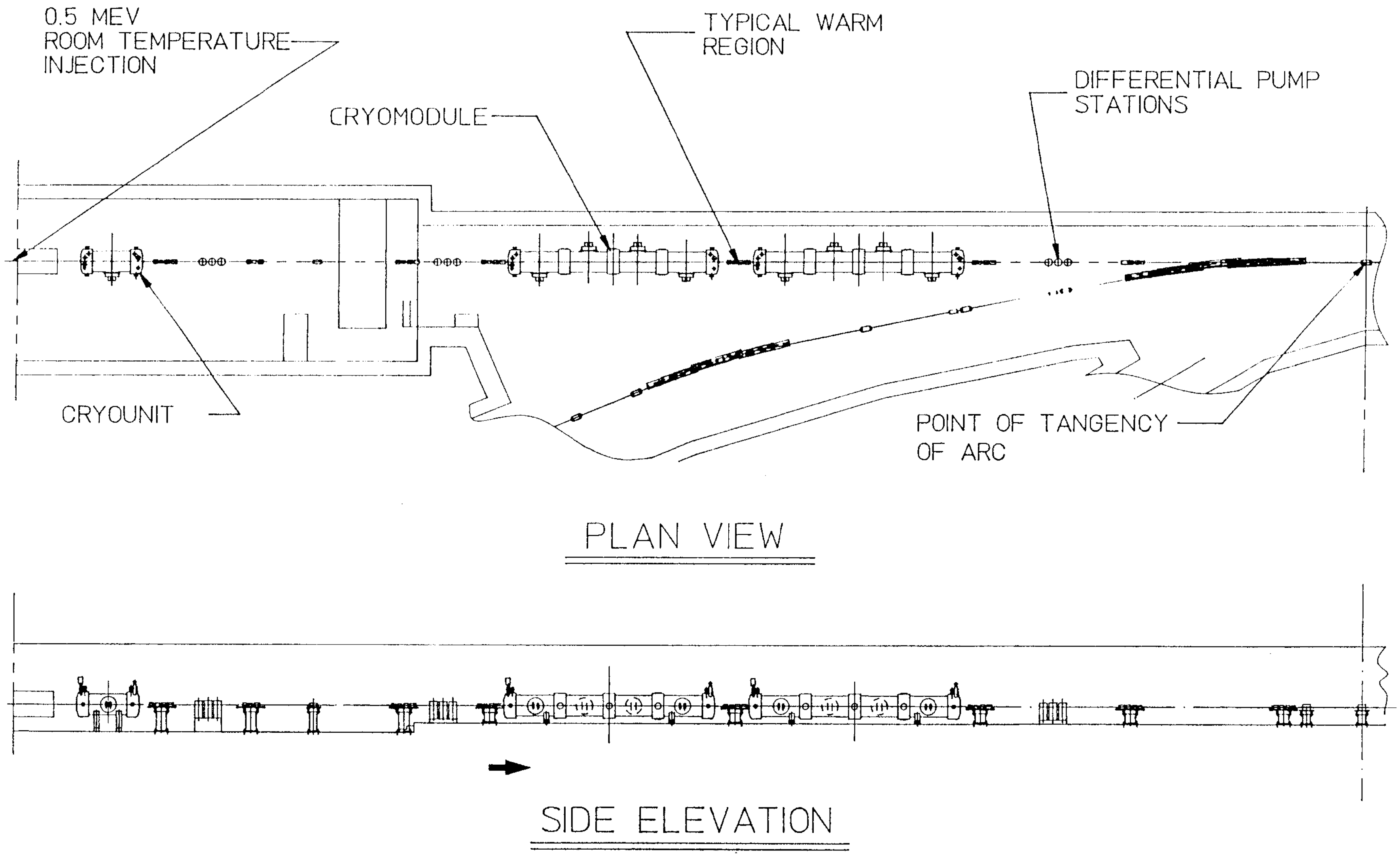

Figure 2

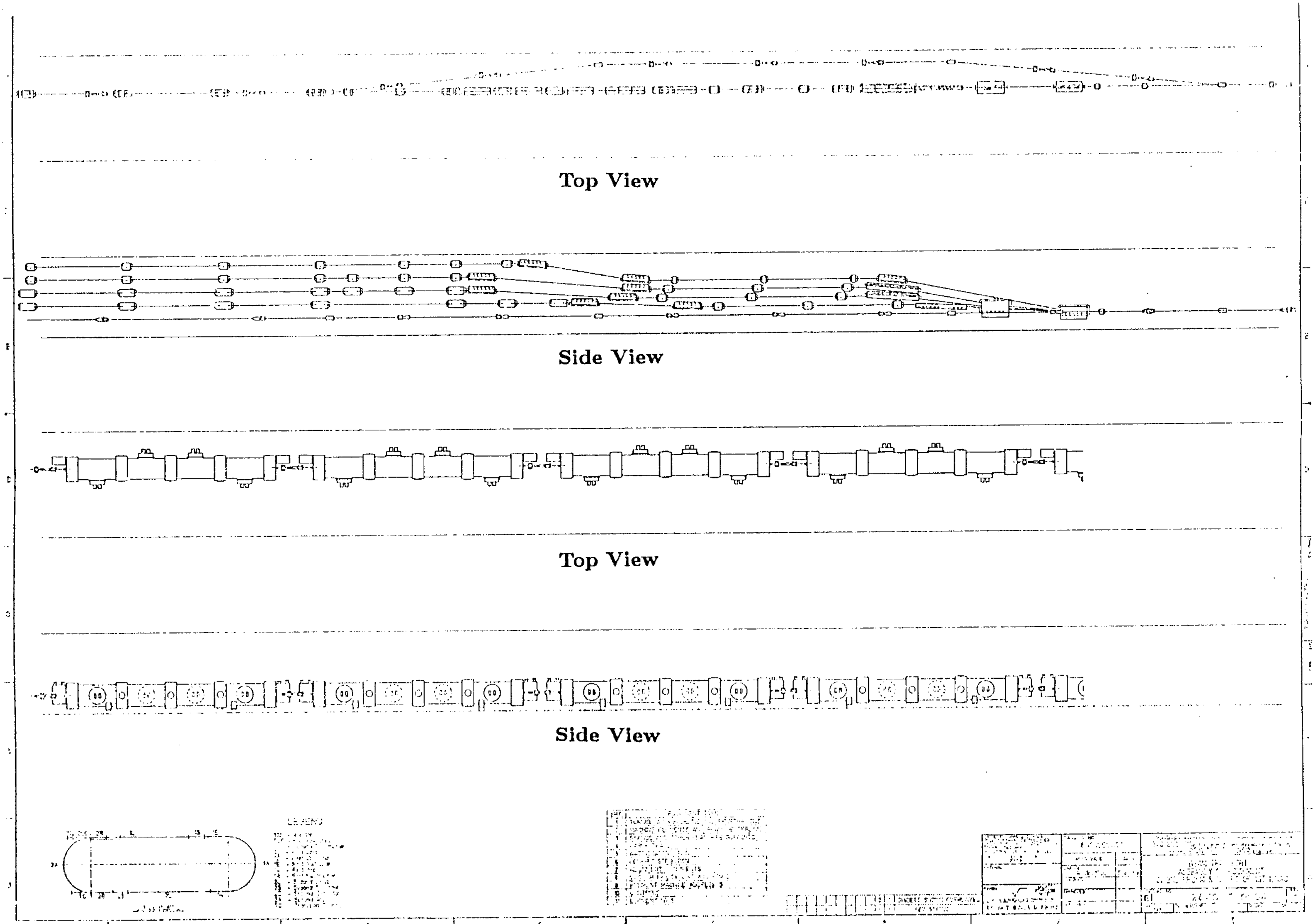

Figure 3

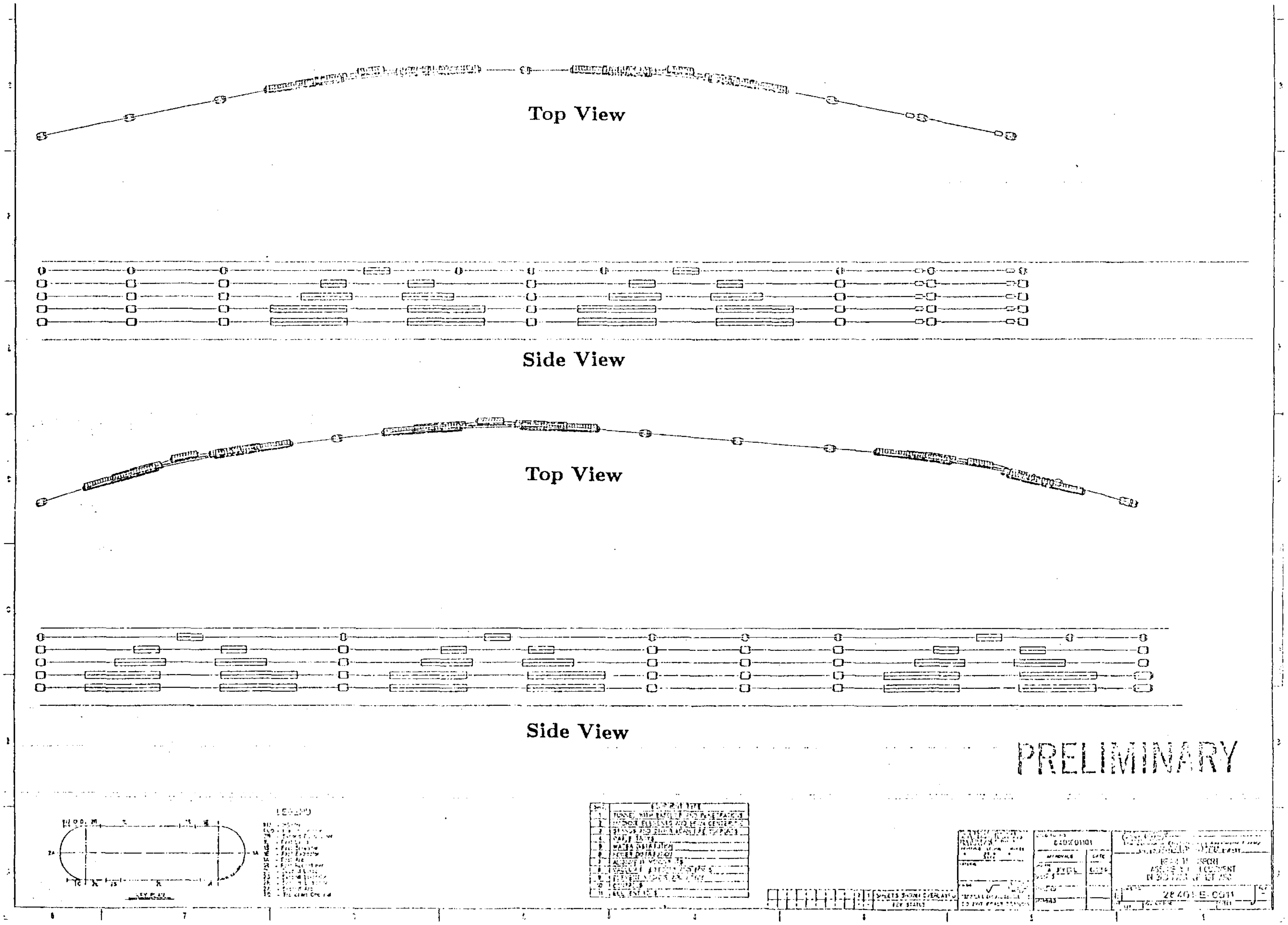

Figure 4

WARM REGION BETWEEN CRYOMODULES — CEBAF

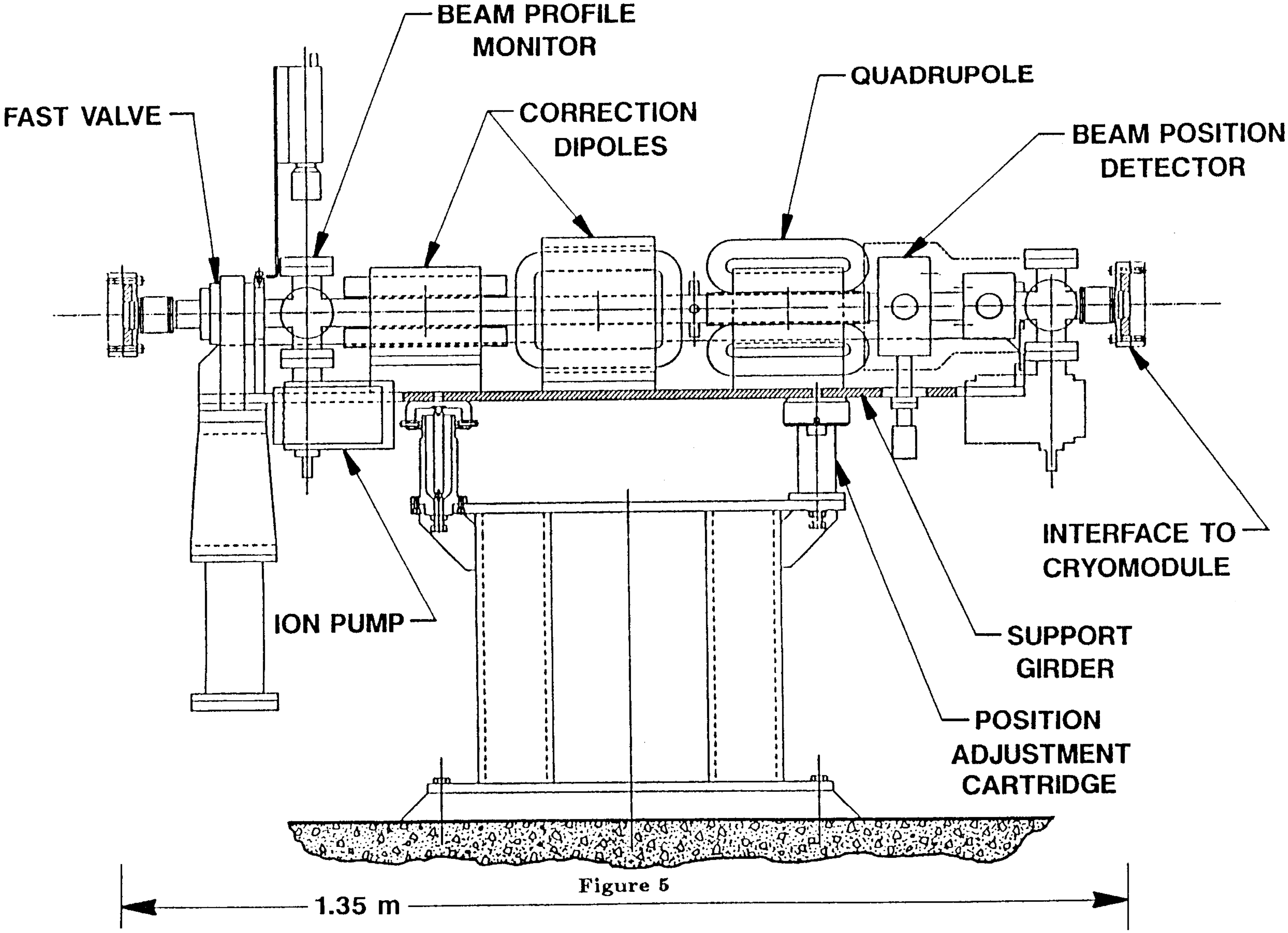

Figure 5

STAND ADJUSTMENT CARTRIDGE

CEBAF

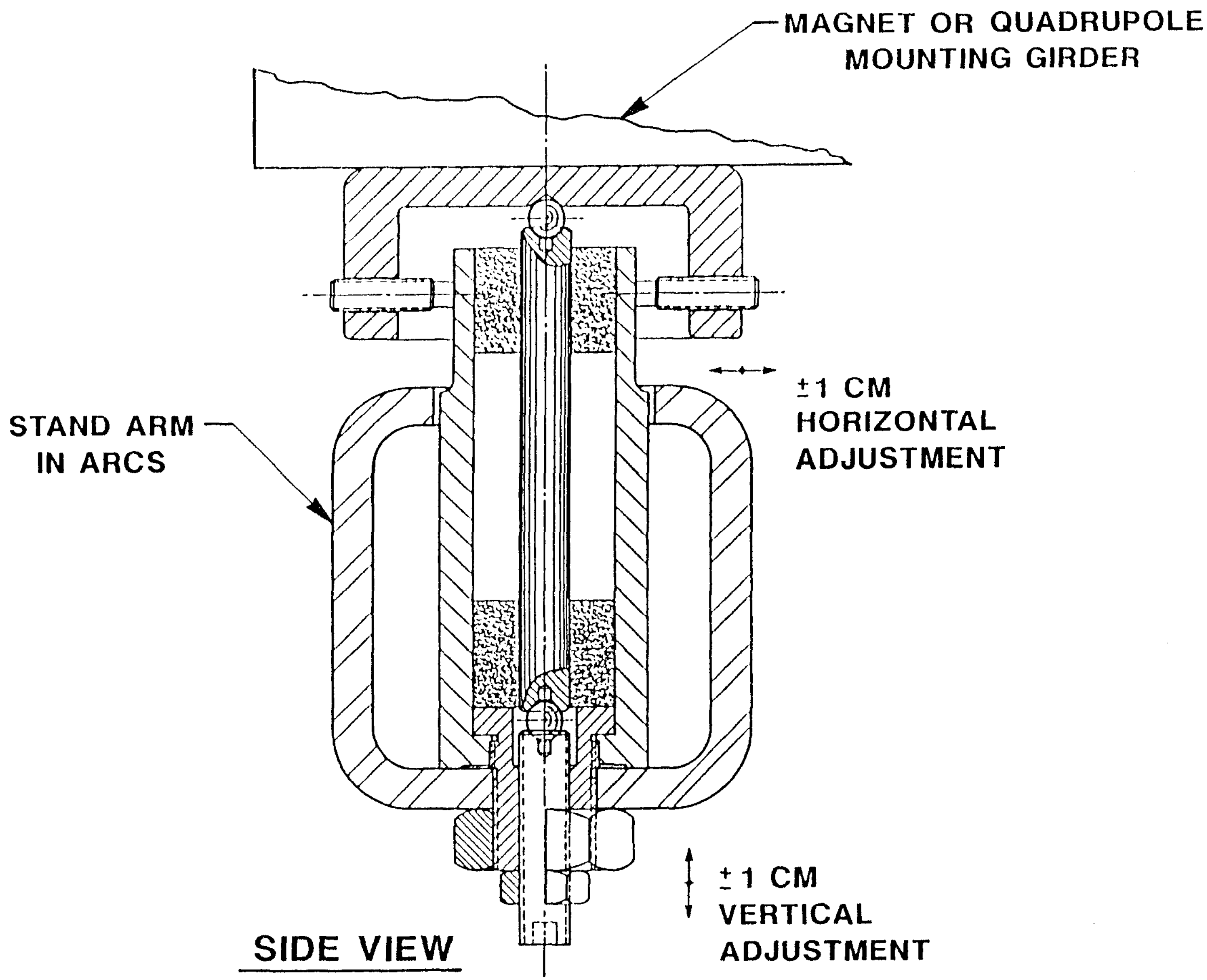

Figure 6

TYPICAL ARC CROSS SECTION SHOWING STACKED QUADRUPOLES

CEBAF

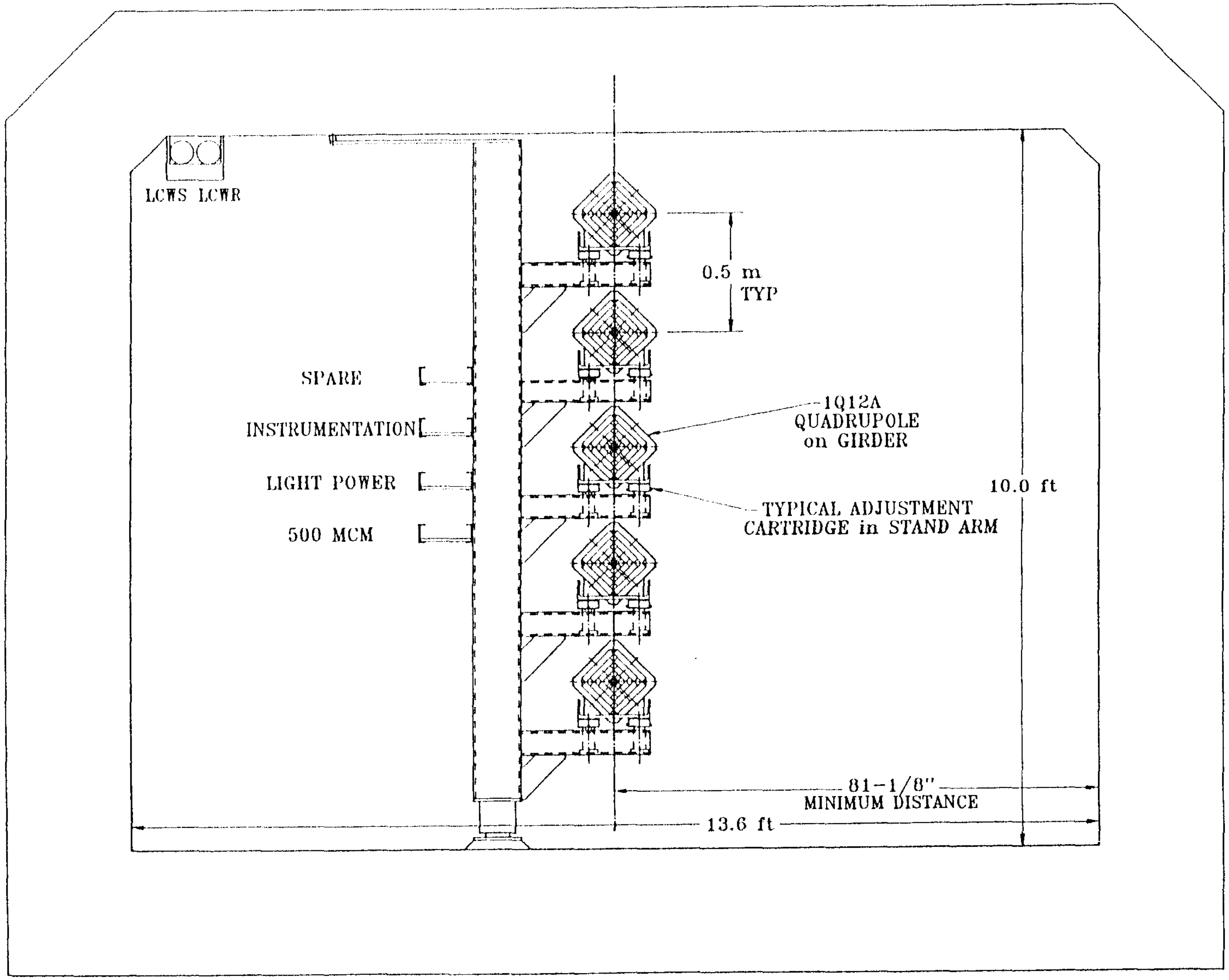

Figure 7

ALIGNMENT & GEODESY FOR THE ESRF PROJECT

D. Roux

European Synchrotron Radiation Facility

Grenoble, France.

INTRODUCTION

1. HOW DOES THE ESRF ALIGNMENT STAND WITH RESPECT TO OTHER MACHINES?

_1.1 Dimensions of the machine

_1.2 Parameters to be measured on this machine

_1.3 The objectives of the ESRF project.

2. WHICH SOLUTIONS FOR THE ESRF PROJECT?

_2.1 Standard Solutions for Standard Problems

_2.1.1. 'First order' geodetic networks for the ESRF

_2.1.2. Standardisation of the references and modular measurements.

_2.1.3. Instrumentation

_2.2 New, Modern Solutions for a Superior Storage Ring

_2.2.1. Hydrostatic Levelling System

_2.2.2. Servo-Controlled Jacks

_2.2.3. A Modern Calibration Base

CONCLUSION

TABLE OF DIAGRAMS

INTRODUCTION

New generation accelerators and storage rings for synchrotron radiation require ever increasing precision of alignment, precision which moreover must be preserved over a maximum length of time.

The use of ever smaller beam dimensions, and ever narrower vacuum chambers leads the magnet positioning tolerances to be reduced to a minimum. Thus, unlike in the past, annual realignment due to progressive deterioration of the ground stability can no longer be envisaged. Permanent monitoring of the ground stability must be guaranteed and its effects compensated, as soon as significant deterioration is recorded. It is this viewpoint that has dictated the choices made by ESRF in the field of alignment and monitoring.

1. HOW DOES THE ESRF ALIGNMENT STAND WITH RESPECT TO OTHER MACHINES?

1.1 Dimensions of the machine

The Storage Ring of the ESRF project is a separate-function machine. The beam is bent by means of dipoles, and focussed by quadrupole magnets. The 608 magnetic components[1] are to be installed along a circumference of 844 metres in a lattice reproduced 32 times in a machine which measures 270 metres in diameter Although this machine does not fall into the category of giant accelerators, it could be interesting to compare it with the SPS machine at CERN in order to show the density of the elements to be installed. This machine is also a separate-function machine with 1000 magnetic components distributed along a circumference of 7 km, i.e. five times more components per kilometre for the ESRF machine.

1.2 Parameters to be measured on this machine

The geometric parameters used in the orbital correction calculations are adopted as the precision criteria during the installation of the accelerator components. These parameters are as follows :

dr - radial deviation at a given point of the Storage Rings's circumference
dh - vertical deviation in relation to the horizontal reference plane
dt - deviation in the tilt of the magnets

1 64 dipoles, 320 quadrupoles and 224 sextupoles.

The dh and dt parameters are measured in relation to a horizontal reference plane and the dt parameter is defined in a relative manner from one point to another, i.e. in this project, from one quadrupole to another. It is interesting to compare these positioning tolerances with those of the old ISR machine in CERN , whose objective was also to maintain beam stability until its utilisation by the experimental scientists.

1.3 The objectives of the ESRF project.

Goals to be reached:

	CERN ISR[2] (radius 150 m) 1970		ESRF SR[3] (radius 135 m) 1990	
	Σt project	Σt results	Σt project	Σt expected
1) dt (mm)	0.15	0.08	0.10	0.08
2) dh (mm)	0.15	0.10	0.10	0.05 (with HLS)
3) dt (mrad)	0.2	0.02	0.2	0.02 (with HLS)

At a first glance, the goals of 1970 and those of 1990 do not seem to have evolved significantly. Indeed, the possibilities of high precision positioning have scarcely changed over the last twenty years within the range of measurements imposed by the accelerators (between approximately 0 and 50 metres). However, rapid developments within the field of electronics, the increasing reliability of computers and the development of automation today enable a number of solutions to be chosen, which ensure continuous monitoring of the machine in any given position, and the maintaining of this position to the same tolerances as those reached when the components were first installed.

If we consider the evolution of the ISR between October 1970 and August 1971, as shown in the graph below, we can see the deterioration of the magnetic components up to as much as 3 mm of amplitude in the vertical plane, over a period of 9 months on ground with a reputation for stability.

This graph enables us to highlight the difference between the two objectives from

2 *CERN 76-19 by J. GERVAISE, Geodesy and Metrology at Cern, A source of economy for the SPS Programme.*

3 *ESRF-SR/LAT 88-06 by L. FARVAQUE and A. ROPERT, Storage Ring Magnets Tolerances.*

1970 and 1990. The well-considered challenge for storage ring projects is to permanently maintain the sensitive components of the machine within the tolerances achieved when these components were installed. This means realigning the components at monthly intervals or even less in a record length of time according to the forecasted ground movements.

The ground settlement measurements[4], that have been carried out over the last six months on two experimental buildings of the *Institut Laue Langevin*, which mark the geographical limits of the ESRF project show a probable relative ground settlement near 0.6 mm/60 m/6 months. These results are quite comparable with those measured for the ISR machine at CERN: 3 mm/942 m/9 months.

Even if the ground under the ISR had a stabilisation age of only two years, instead of four years for our example an extrapolation shows:

ISR	3 mm/942 m/9 months
ESRF	2.8 mm/844 m/9 months

2. WHICH SOLUTIONS FOR THE ESRF PROJECT?

2.1 Standard Solutions for Standard Problems

2.1.1 'First order' geodetic networks for the ESRF[5]

The objective of these networks is to position the various installations of the project, buildings and machines and above all to enable a connection to be established between the PINJ, SYTU, SRTU' machines, transfer and beam lines.

There are precisely 3 networks at the present time:

a. External geodetic network, made up of about twenty points, its base is a regular octagon marked out over the Storage Ring Tunnel (diagram 2).
b. Internal geodetic network of the booster synchrotron, made up of a set of 48

4 *Protocol Measurement ESRF/ALGE 8903 , First elements for reflection upon the ground settlement on the ESRF site.*

5 *MAC Grenoble, June 29-30 1988, Alignment methods for the ESRF.*

pillars or wall brackets laid out according to the booster synchrotron lattice (diagram 3).

c. Internal geodetic network of the Storage ring, made up of a set of 64 pillars or wall brackets laid out according to the Storage Ring module (diagram 4).

2.1.2 Standardisation of the references and modular measurements.

Although the ESRF will be responsible for constructing the installations of the future, nothing can be gained by ignoring the innovations of the past. It is in this frame of mind that we have confirmed the choices made for previous projects (CERN, DESY, SLAC, ARGONNE) in the field of geodesic boring, essential for precision measurement (diagram 5 - 6), and in the division of the network into modules, well adapted to the instruments described below (diagram 7 - 8).

2.1.3 Instrumentation

In a previous paper[6], we report how we had hesitated between two instruments for measuring these networks. This dilemma of choice was solved by the results obtained on the interferometric base at CERN[7], which were recently confirmed by calibration measurements on a reference base carried out using the DISTINVAR[8]. We have chosen the most recent distancemeter on the market: the DI2000 manufactured by the Swiss company WILD[9]. The R.M.S. expected on the 'first order' external network with this distancemeter is less than ± 1 mm. Moreover, the pre-alignment installation of all of the components of the machine will be carried out with this instrument to ± 1 mm, which should allow us to succeed in aligning the machine in onepass only.

As far as the measurement of the 'first order' internal networks and the alignment of the orbit is concerned, we will use the DISTINVAR (diagram 9), which is the only instrument capable of measuring distances of 0 to 50 metres with a precision less than 0.05 mm, and the ECARTOMETER (diagram 10), which is the only instrument capable of measuring alignment offsets of 0 to 50 cm with a precision of 0.05 mm. These two instruments have been developed at CERN over the last twenty years, and have been available for the last four in an automatic version driven by micro-computer, thus rendering them more reliable and less fragile in the

[6] *MAC Grenoble, June 29-30 1988, Alignment methods for the ESRF.*

[7] *ESRF/ALGE Report 8805, April 1988 WILD DI2000 DISTANCEMETER CALIBRATION*

[8] *Protocol Measurement ESRF/ALGE 8906 February 1989, Base de reference INVAR*

[9] *This instrument will be demonstrated on the occasion of the visit to the ESRF02 building.*

What are the qualities of this instrument and why does it perform so well in comparison with its predecessors?

The limitations of systems available in October 1987:

a. Use of a contact sensor

b. Thermal problems connected to the high level of water used in the majority of the systems.

c. Condensation problems connected to the presence of water along the sight of the sensor in the existing systems.

Improvements made on the October 87 system by the ESRF prototype: (diagram 12)

a. The use of a non-contact sensor with a large integration surface avoids a whole number of problems caused by contact sensors (moistening, alteration of the touch point, meniscus effect, fluid vibration).

b. The use of an inexpensive and easy-to-use conducting fluid. The problem connected to its high factor of thermal dilation (2 µm/°/cm) is minimised by the use of a low level of water (3 cm) and a measurement of the vessel temperature to an accuracy of 0.1°C. This gives us a thermal error of less than 0.6 µm. This is possible because our machine is horizontal.

c. The presence of a radiator (small power transistor enabling the temperature of the sensor to be increased by 1°C in relation to the water).

What are the advantages of this instrument?

a. Replaces the encoders in the jacks with a quasi-similar precision, with a slight delay in the information due to the inertia of the system (less than 2 minutes),

b. The fact that it is installed in the support beams near the beam enables both the ground movements and the differential dilations of the supports to be taken into account (diagram 13 and 13 bis),

c. Enables the absolute level rise between the 96 elements and the transversal and longitudinal tilt of the support beams to be recorded,

d. The recordings are permanent and enable us to watch the machine "breathe" and consequently forecast defects due to the amplitude of to great a movement.

What are the improvements to be made to the prototype? (diagram 14)

These are manufacturing improvements that can be seen by comparing diagrams 11 and 12. No functional improvement is planned and the tender documents have been send on 22 June 1989.

The latest results presented during the MAC on 13-14 March 89 (diagram 15 to 18).

We had planned to maintain a load of 3.2 tonnes in a horizontal plane with a precision greater that 10 microns. This goal was reached. The experiment was carried out over a period of four consecutive days with a servo-controlled precision greater than 1 μm, and by moving the motors every thirty minutes. Parallel to this, a recording was made of the motor pulses and led us to fix the jacks in a range of $\pm$ 3.5 μm probably corresponding to differential movements on each jack provided by the effects of the thermal variations.(General variation provided by external temperature and local variation provided by internal temperature).This hypothesis was well confirmed by the analysis of the following results about the very long term measurement.(diagram 19 and 20)

The latest results presented during this workshop on 31 July to 3 August 89 (diagram 19 to 20).

We can now present a very long term measurement registered during 46 days.in, a semi-indusrial environment. In this experiment we have servo-controlled the jacks only when the movement was >= 20 μm always with an upward movement.

The main remarks to be made are :

_No variation registered as a function of the 5°C range of the experiment

_Small local variation of maximum 5um range connected with Civil Engineering Activities (The hypothesis of voltage variation during CW is suspected) but in any case there is no effect on the registered movement. (The effect should be controlled by an appropriate algorythm in the case of permanent servo-control) hands of less experienced operators.

N.B. A new possibility of R.M.S. measurement would seem possible with a new instrument called "The Lambda System", manufactured by the Dutch company APPLIED LASER TECHNOLOGY. This instrument based on the principle of laser measurement of distances without contact would enable the measurement of the distance of a tensioned nylon wire with a precision greater than 0.03 mm for an R.M.S. of 0 to 1 metres. It would present the advantage of removing the carrier control and of accelerating measurement input, in comparison with the CERN Ecartometer (the progress of this new instrument will be followed with great interest).

2.2 New, modern solutions for a superior storage ring

The large number of components (608) and the concern for distributing the loads over a limited number of supports, in order to minimise the number of measuring points and the number of adjusting jacks, has led us to decide on using 160 main support beams, 64 of which will support the dipoles, and 96 the quadrupoles and sextupoles (diagram 11 and 11 bis).

The first support beams will be equipped with standard, non servo-controlled jacks and the last support beams will be equipped with monitoring equipment and the servo-controlled jacks.

2.2.1 Hydrostatic Levelling System

This system was entirely developed by the ESRF and has been presented on two occasions. On the first occasion, the aim was to demonstrate its feasibility in October 1987 after functional and critical analysis of existing hydrostatic systems[10]. The second occasion was during the MAC of 11th and 12th November 1988[11], when it was presented in poster-form giving the first results obtained.

The following is a summary of the strong points of the system:

[10] *Conception d'un système de Contrôle altimétrique automatique et permanent pour le projet ESRF, ALGE 8703, Octobre 1987*
(Systems of EDF-France, CERN, ELWAAG001-Allemagne)

[11] *ALGE Report 8804 and 8806*

_Very good correlation between first and second curves.This means a perfect connection between HLS measurements and Stepping Motor Command.

_Small offset (maximum of 5 μm after an abnormal displacement or refilling of the system).

._Extraordinary correlation between the external temperature and internal temperature of the building and the heigh differences, readind by HLS with a noise lower than 1 μm as shown on the Zoom of the first seven days results

Even if it is difficult to quantify the part of each temperature effect (because it is a three dimensionnel problem connected with the exact position of each HLS on the marble in relation to the reference HLS on the wall of the building) it is very easy to qualify the two thermal effects on the ground movement registered by the 3 HLS installed on the marble.

_Reliability of the system. We have already recorded a year of operation without the slightest fault either in the capacitive system or in the hydraulic system (no purge of the circuit).

2.2.2 Servo-controlled Jacks

Considering the frequency of altimetric realignment which is expected (every month or more often) and of the duration of such an operation carried out manually (approximately eight days), the presence of jacks servo-controlled from the control room is now essential. This operation should take less than two hours by multiplexing the jack controls. Then a duration of thirty minutes would be sufficient to stabilise the totality of the hydrostatic system, and consequently contribute some final supplementary corrections.

The reliability of the prototype jacks that have been used for the past nine months without incident and with frequent displacements (they were never put out of operation for more than two days at a time), has convinced us of the use of this type of screw jack driven by stepping motor. These prototypes have been used as a reference for the preparation of the tender documents for the 288 jacks which will equip the Storage Ring.

A servo-control experiment has shown us the necessity of controlling the jacks on the upward movements, in order to completely eliminate the play which will now be less than 3 μm (see diagram of top and bottom controlling)

2.2.3 A modern calibration base

We have seen in the last chapters that numerous results presented in the last year have been carried out thanks to the calibration base at CERN, be it for calibrating the invar wires or modern instruments such as the DI2000, for example.

The large number of measurements to be carried out on our machines will require frequent calibration operations. These calibration operations should be rapid, reliable and well adapted to the instruments of today and tomorrow (especially as far as instruments using laser sources, and non-contactor sensors are concerned. At the present time the model base in this field is that of the *Polytechnicum de Zurich* , built in 1984, and the study of a similar base will be carried out in 1989. Its installation is planned as soon as the PINJ building is completed. It will be of use as soon as the installation of the first transfer line is underway and will be essential from the very first measurement taken of the Booster network.

CONCLUSION

A new generation of storage rings is coming into being, the solutions proposed by the ESRF in the domain of alignment are the first steps accomplished in the direction of a machine automatically controlled.

The solution adopted for the permanent adjustment of the quadrupoles in the vertical plane enable the amplitude of the corrections to be reduced by permanent maintenance of the machine within strict mecanical tolerances. The proposition to maintain the machine in a mean horizontal plane of ± 100 μm could evolve towards a value close to 50 μm or perhaps even less.

Parallel solutions may perhaps be found in the future for permanent adjustment of the beam in a horizontal plane, but the absence of an absolute referential (identical to that established by the H.L.S. in the vertical plane) limits its application to relative displacements based on monitor displays. The risk of causing the beam adjustment to diverge is great and this solution can not therefore as of yet be considered.

ISR . *Correlation between the vertical closed orbit and levelling of the magnets*

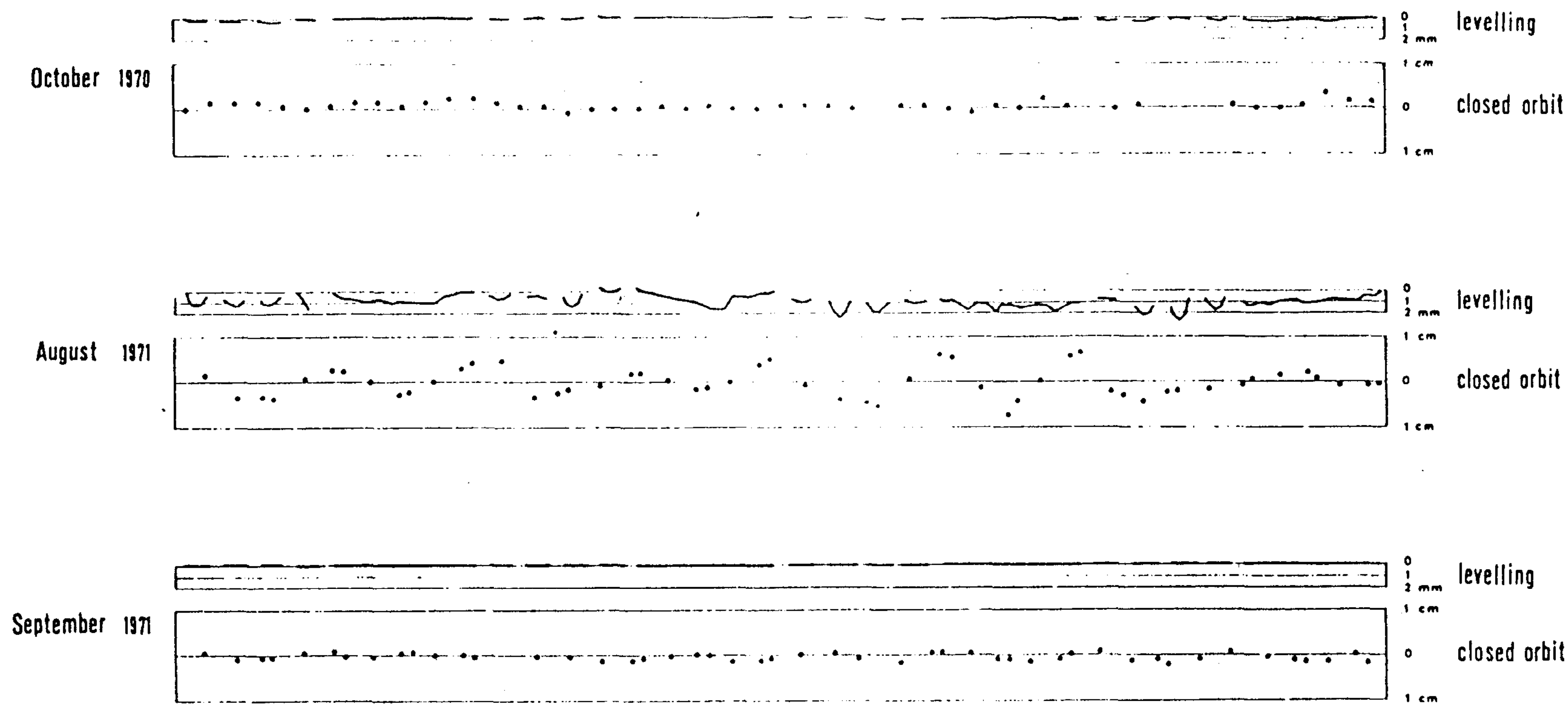

DIAGRAM 1

DIAGRAM 2

DIAGRAM OF EXTERNAL GEODETIC NETWORK

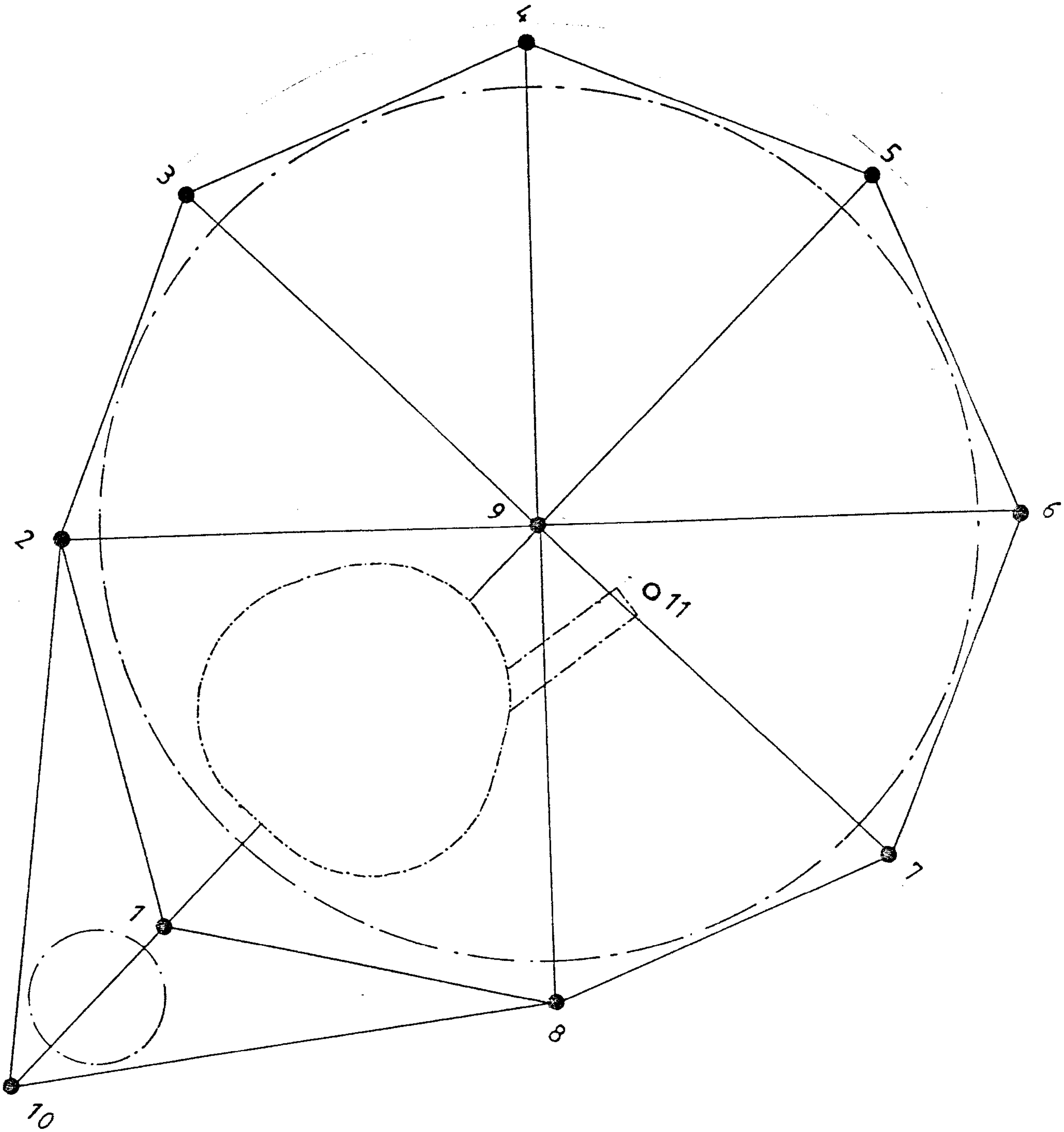

EQUIPMENT : ●	**11 Concrete pillars (Clear of frost)**

MEASURES
DISTANCEMETER 19 Measures of distances and THEODOLITE 10 Angular Stations
or DISTANCEMETER 27 Measures of distances

DIAGRAM 3

DIAGRAM OF SYTU GEODETIC NETWORK

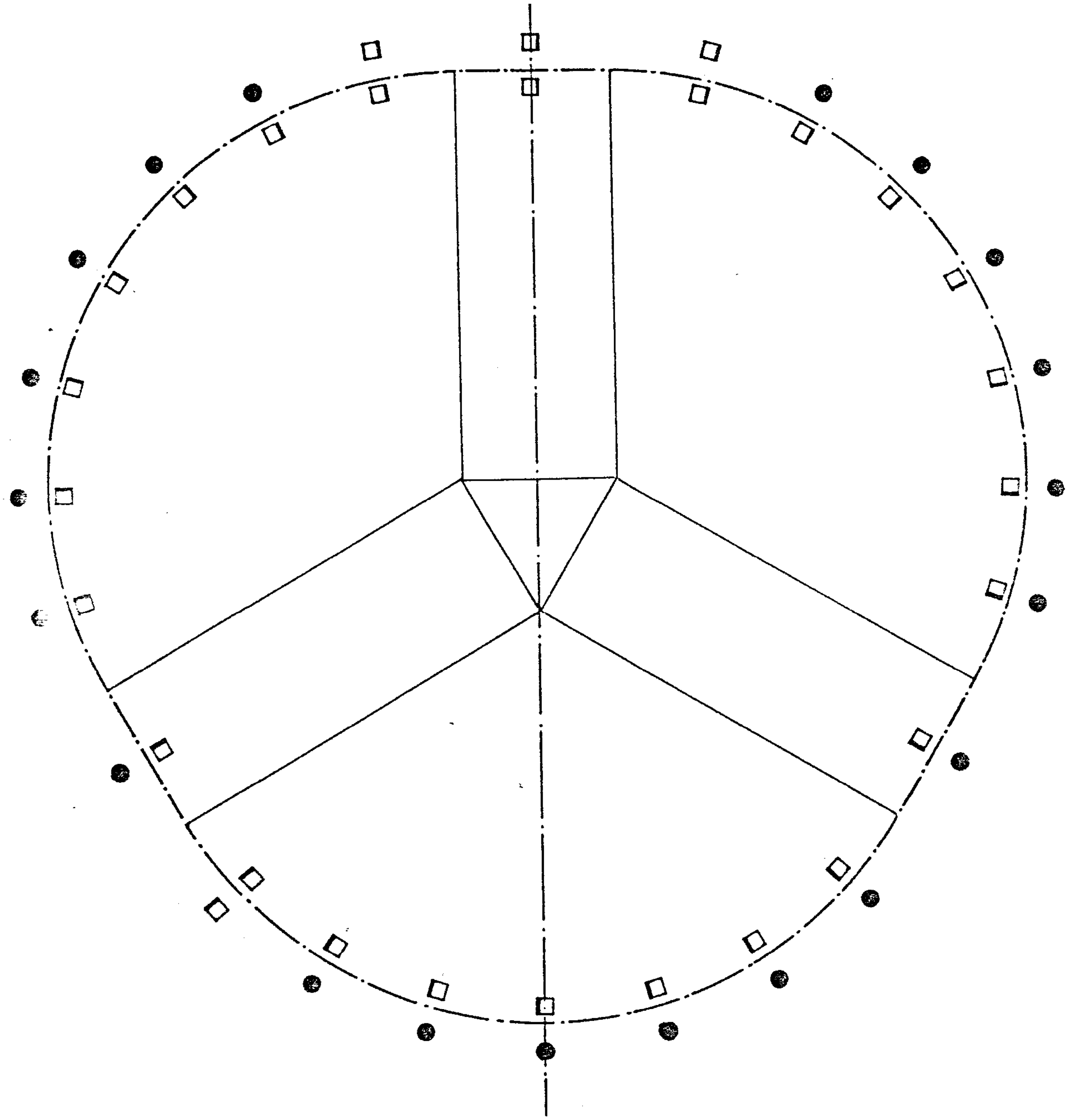

EQUIPMENT : □ 24 Concrete Pillars (Internal Ring)
□ 4 Concrete Pillars (External Ring)
● 20 Brackets on External Wall

MEASURES
DISTINVAR 147 Distance measurements
ECARTOMETER 30 Offset measurements

DIAGRAM 4

DIAGRAM OF SRTU GEODETIC NETWORK

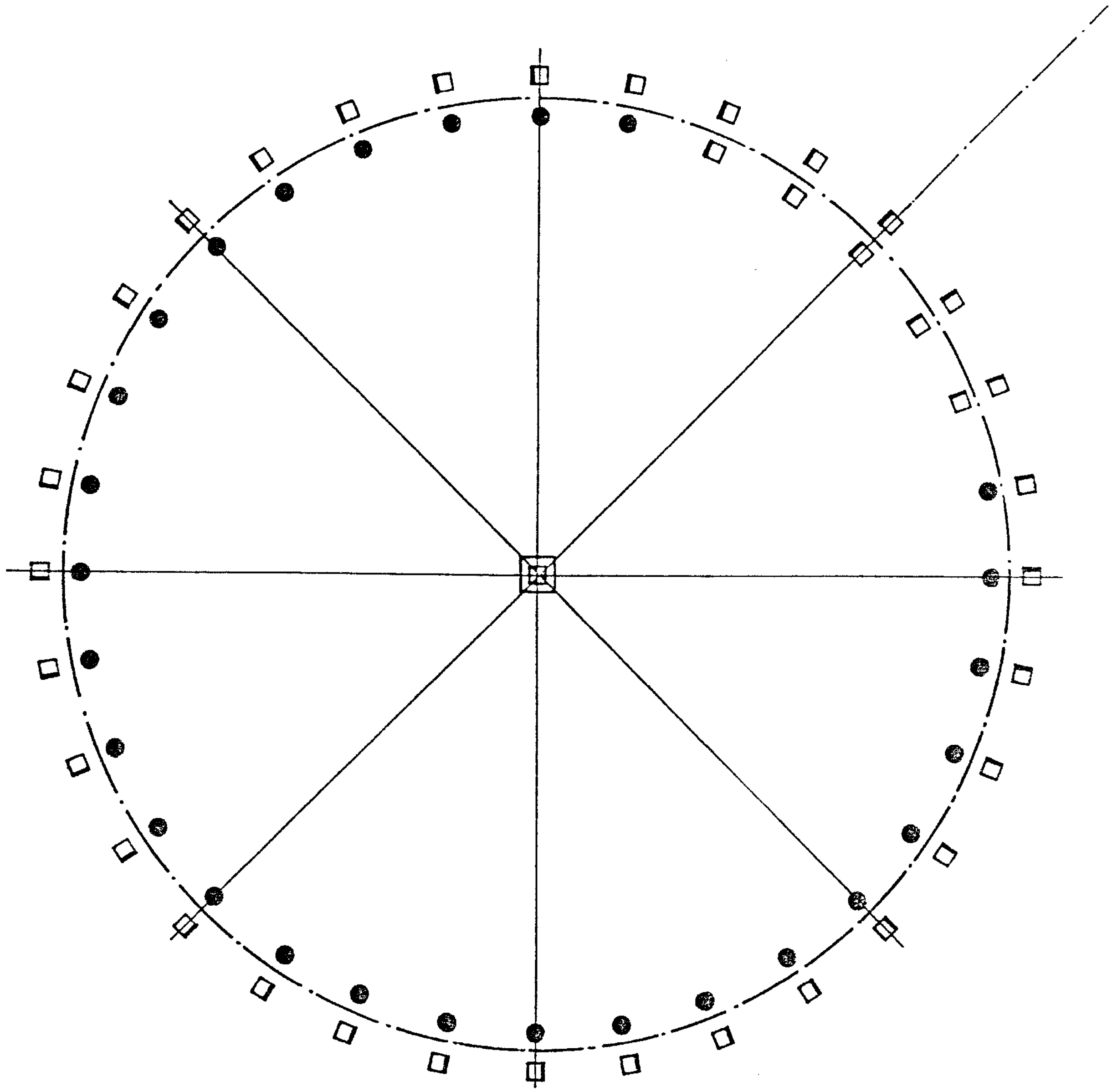

EQUIPMENT		
	⌷	32 Concrete Pillars (External Ring)
	□	5 Concrete Pillars (Internal Ring)
	●	27 Brackets on Internal Wall

MEASURES

DISTINVAR 128 Distance measurements

ECARTOMETER 30 Offset measurements

DISTANCEMETER 8 Radii measurements

DIAGRAM 5 REFERENCE MARK FOR QUADRUPOLE

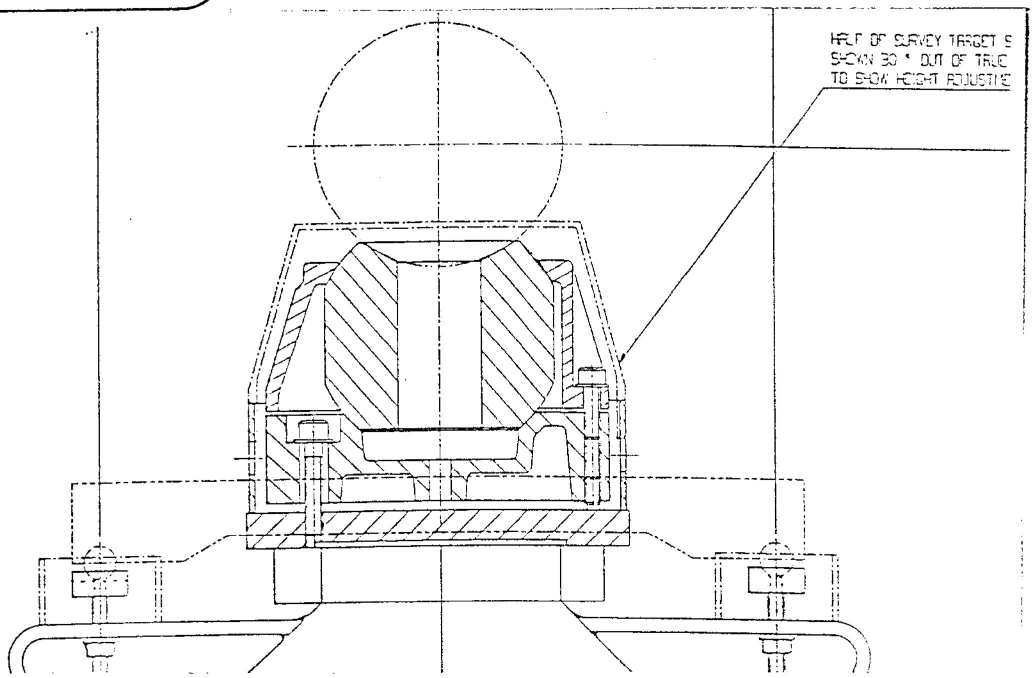

DIAGRAM 6 REFERENCE MARK FOR DIPOLE

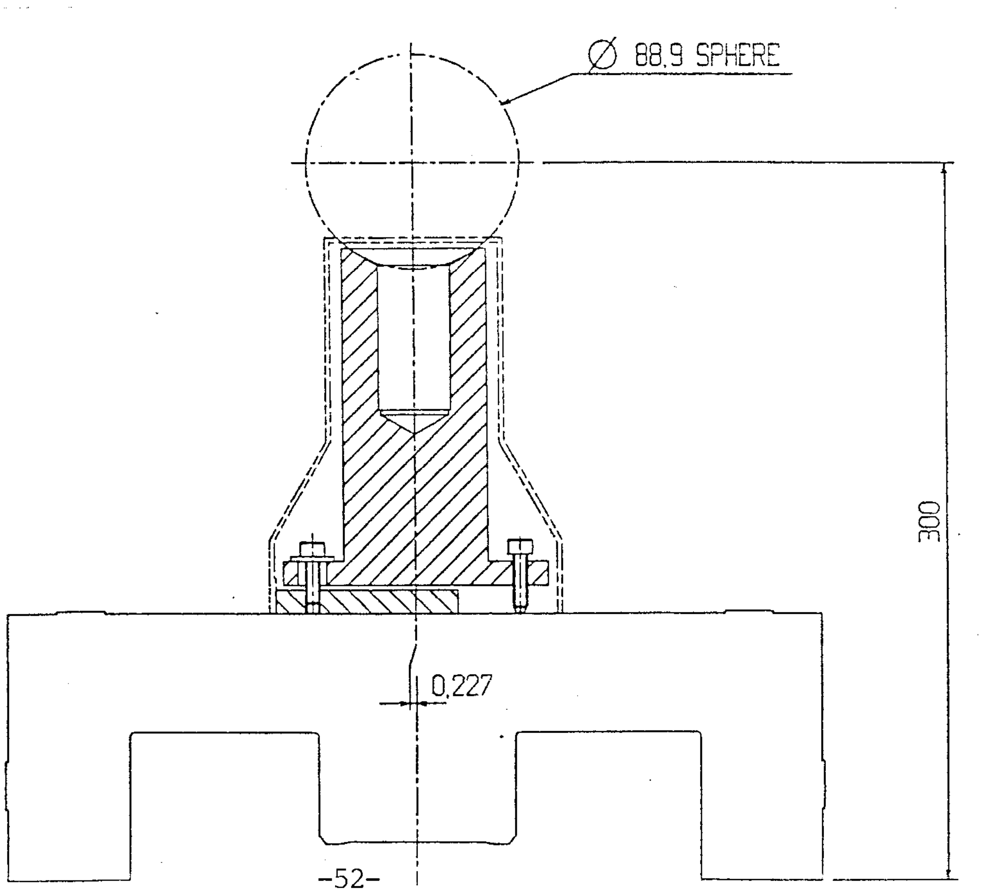

DIAGRAM 7 MODULES OF THE SYTU

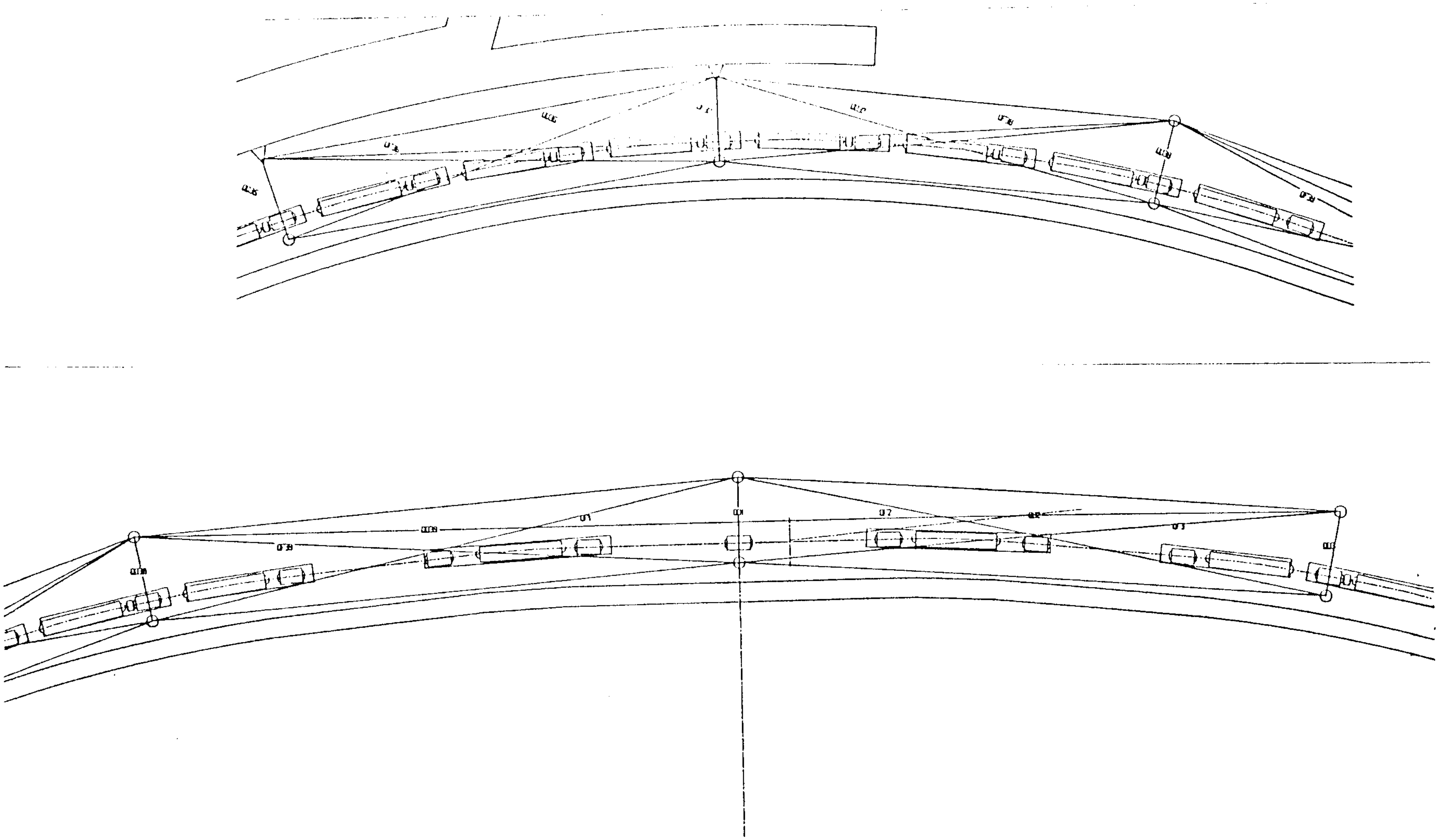

DIAGRAM 10 PRINCIPLE OF THE ECARTOMETER

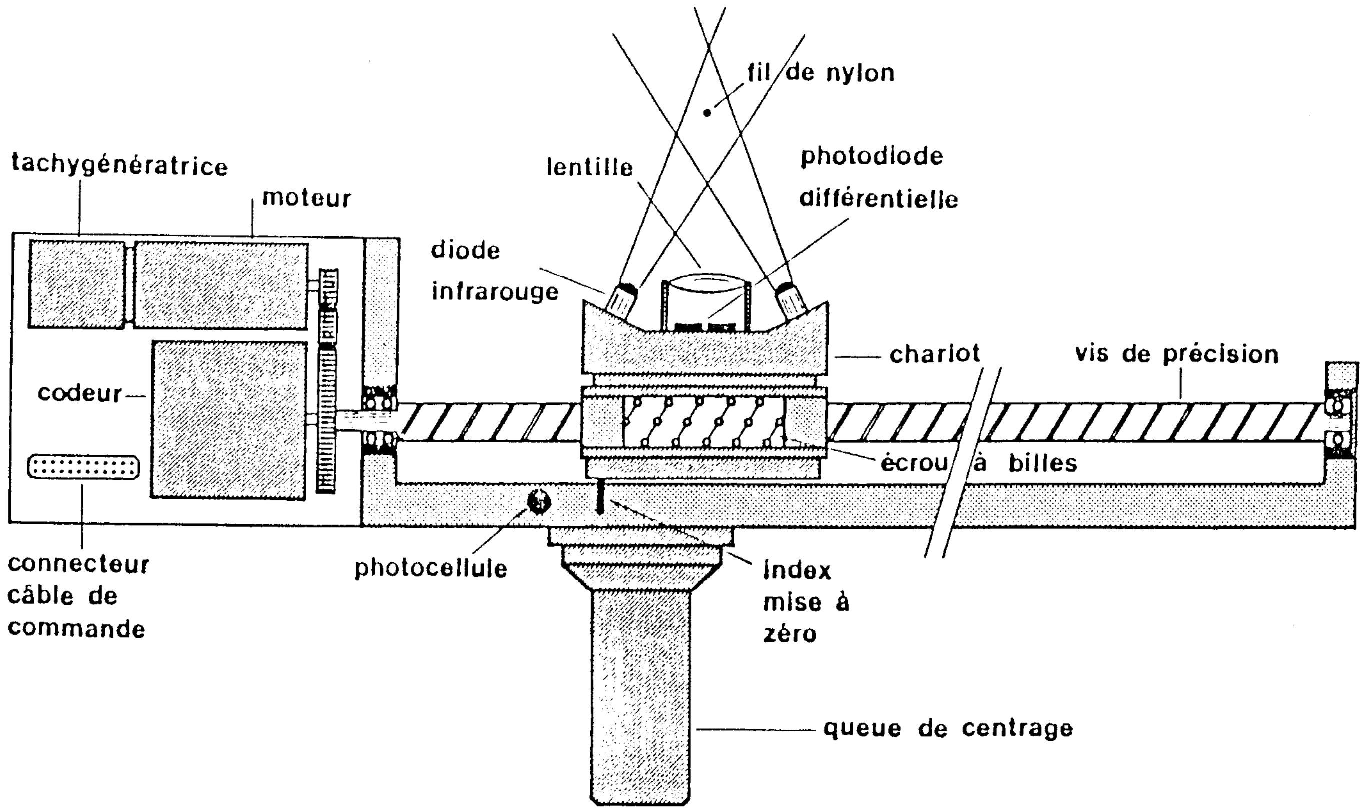

DIAGRAM 9 PRINCIPLE OF THE DISTINVAR

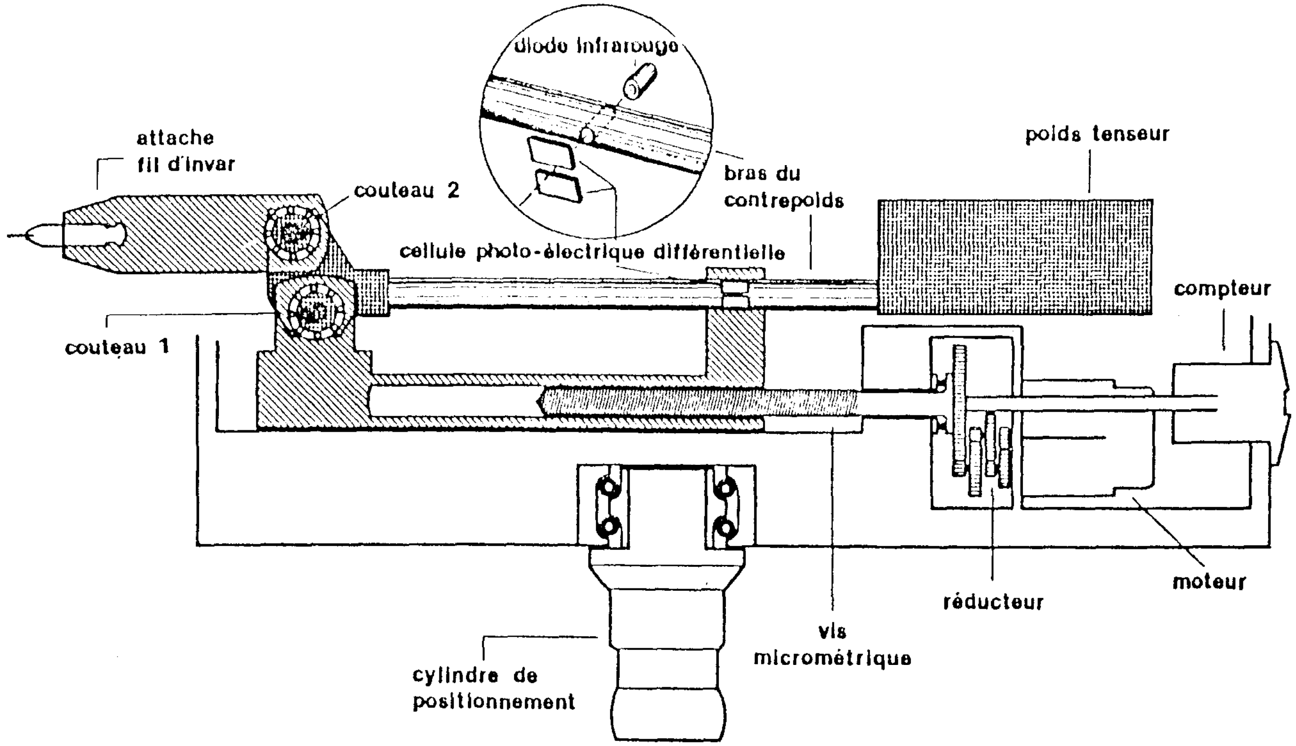

DIAGRAM 8

MODULE OF THE SRTU

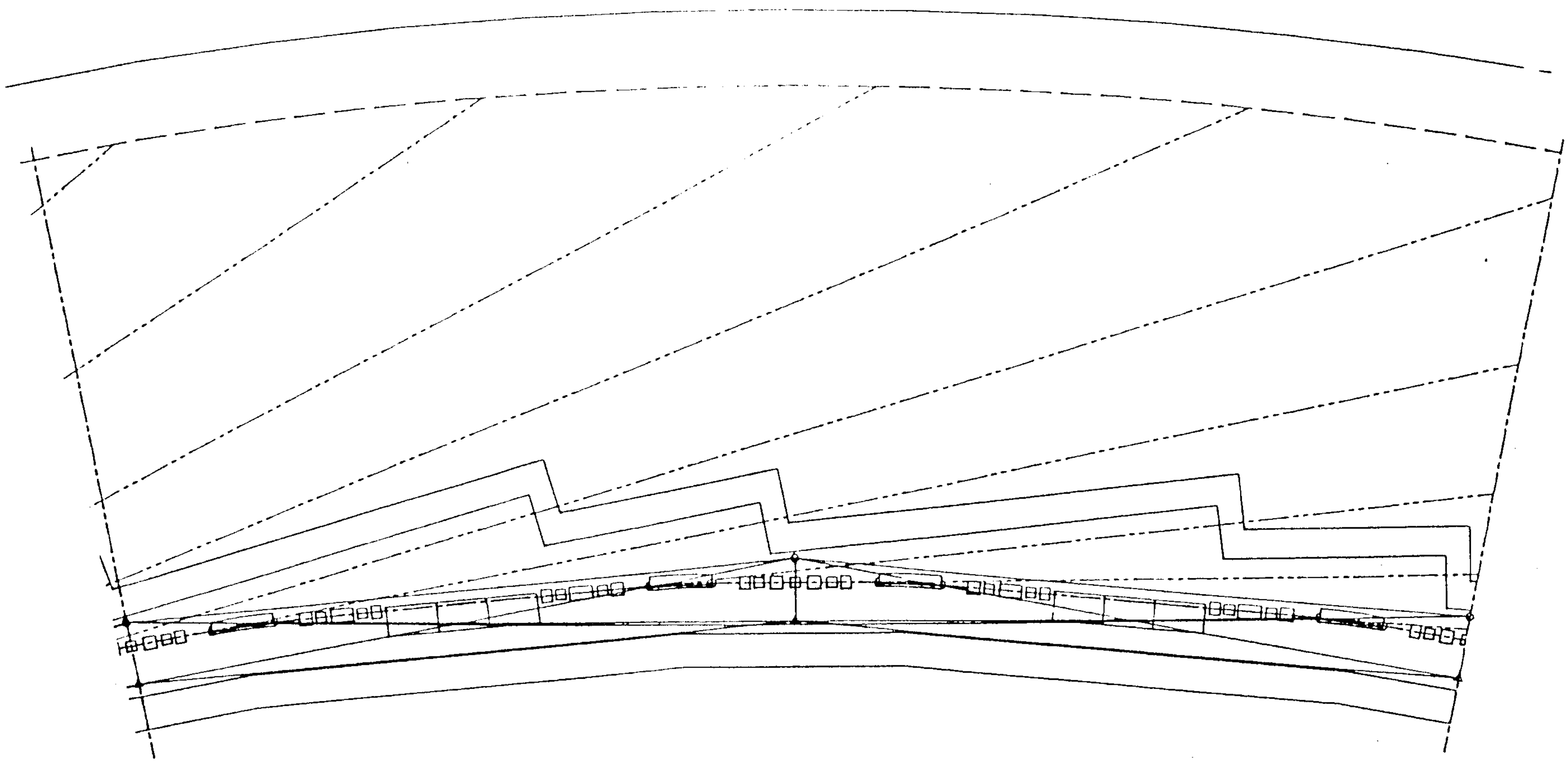

DIAGRAM 11

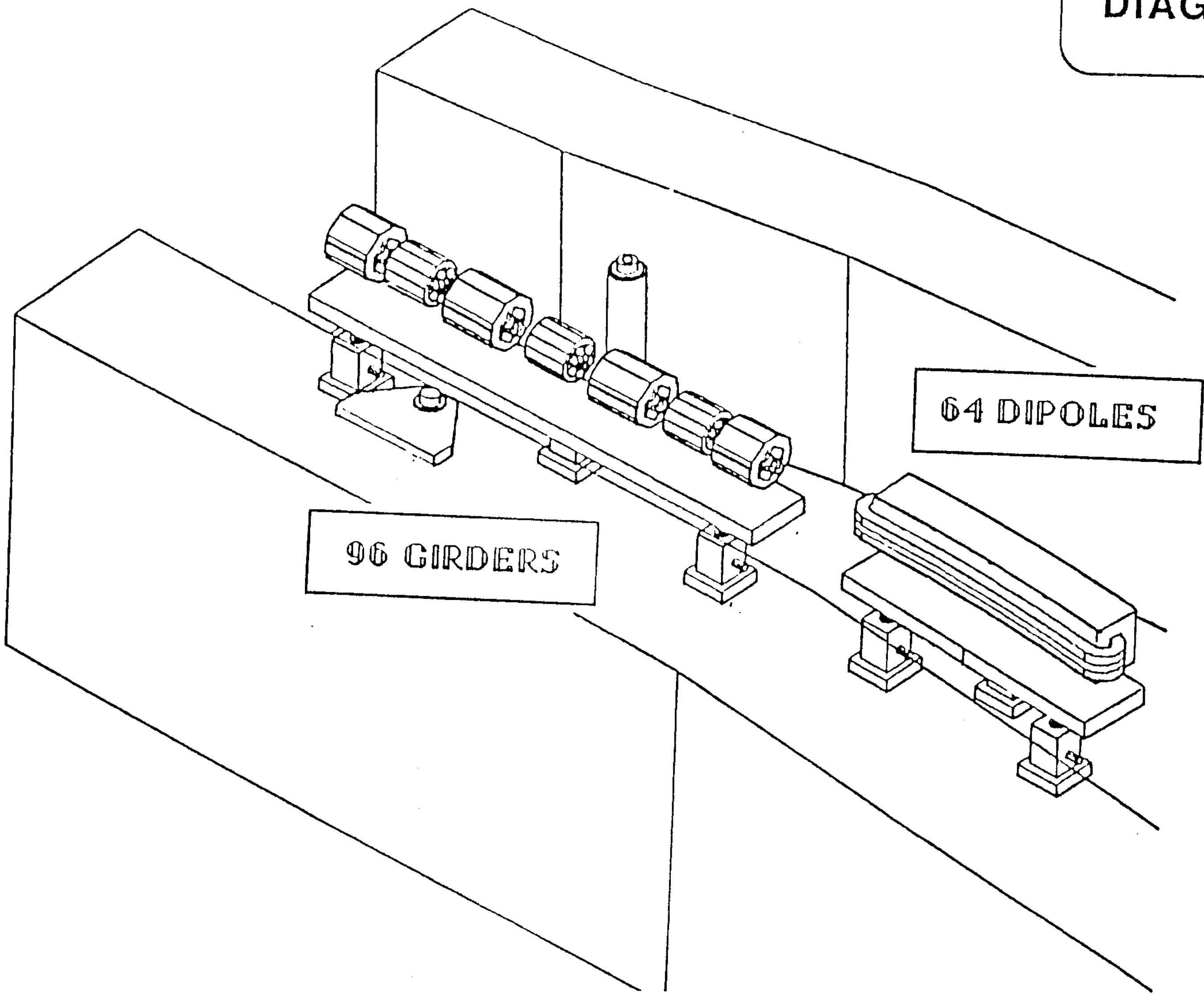

PROTOTYPE GIRDER (LONGITUDINAL VIEW)

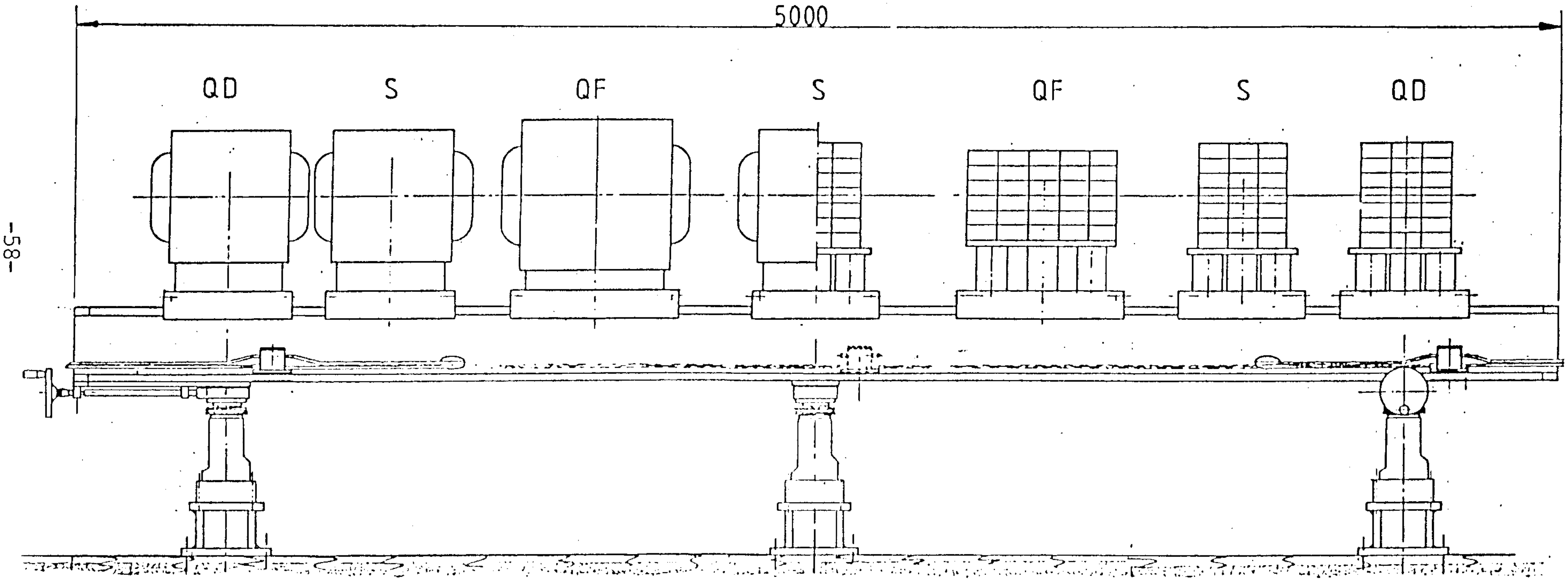

DIAGRAM 11 bis

DIAGRAM 12

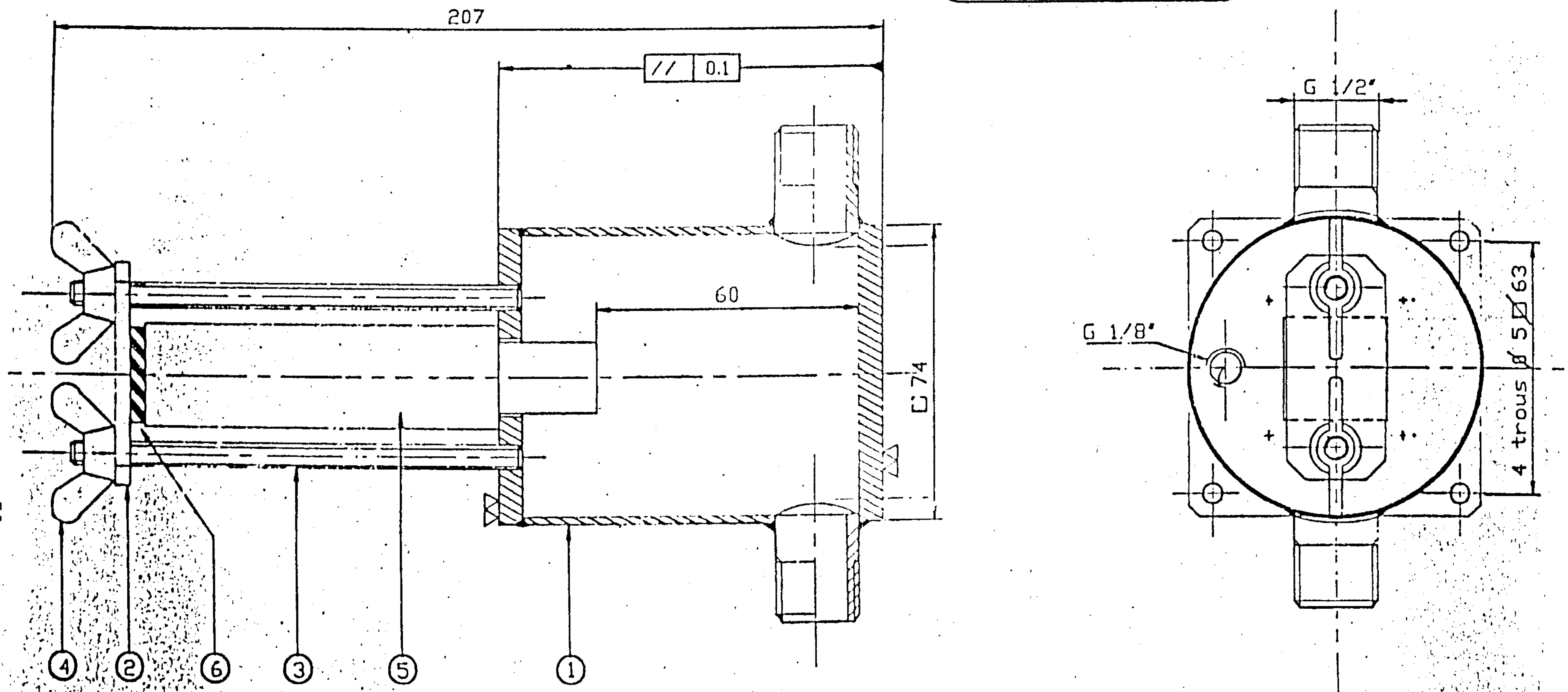

REP.	NB	DESIGNATION	MATIERE	OBS.
6	1	Rondelle ep. 4 mm	Caoutchouc	
5	1	Capteur de proximite capacitif		
4	2	Ecrou a oreilles M6	INOX	
3	2	Tige filetee M6 - long. 115	INOX	Frein filet fort sur (1)
2	1	Bride	INOX AISI 304L	
1	1	Pot de mesure	INOX AISI 304L	

Masse : environ 1 Kg (sans raccord ni capteur)

Plans annexes : 10511 , 10512 10513

NIVELLEMENT RADIER SYNCHROTRON

Pot de mesure - Ensemble

00

MISE A JOUR

Verifie : JG

Dessine : CH

Date :25/9/1987

ELECTRICITE DE FRANCE

DIVISION TECHNIQUE GENERALE
37, rue Diderot
B.P. 41 Centre de tri
38040 GRENOBLE Cedex Tel 76.04.44

ECH. 1

A3 D T G / T N N° 1 0 5 1 0 - 09

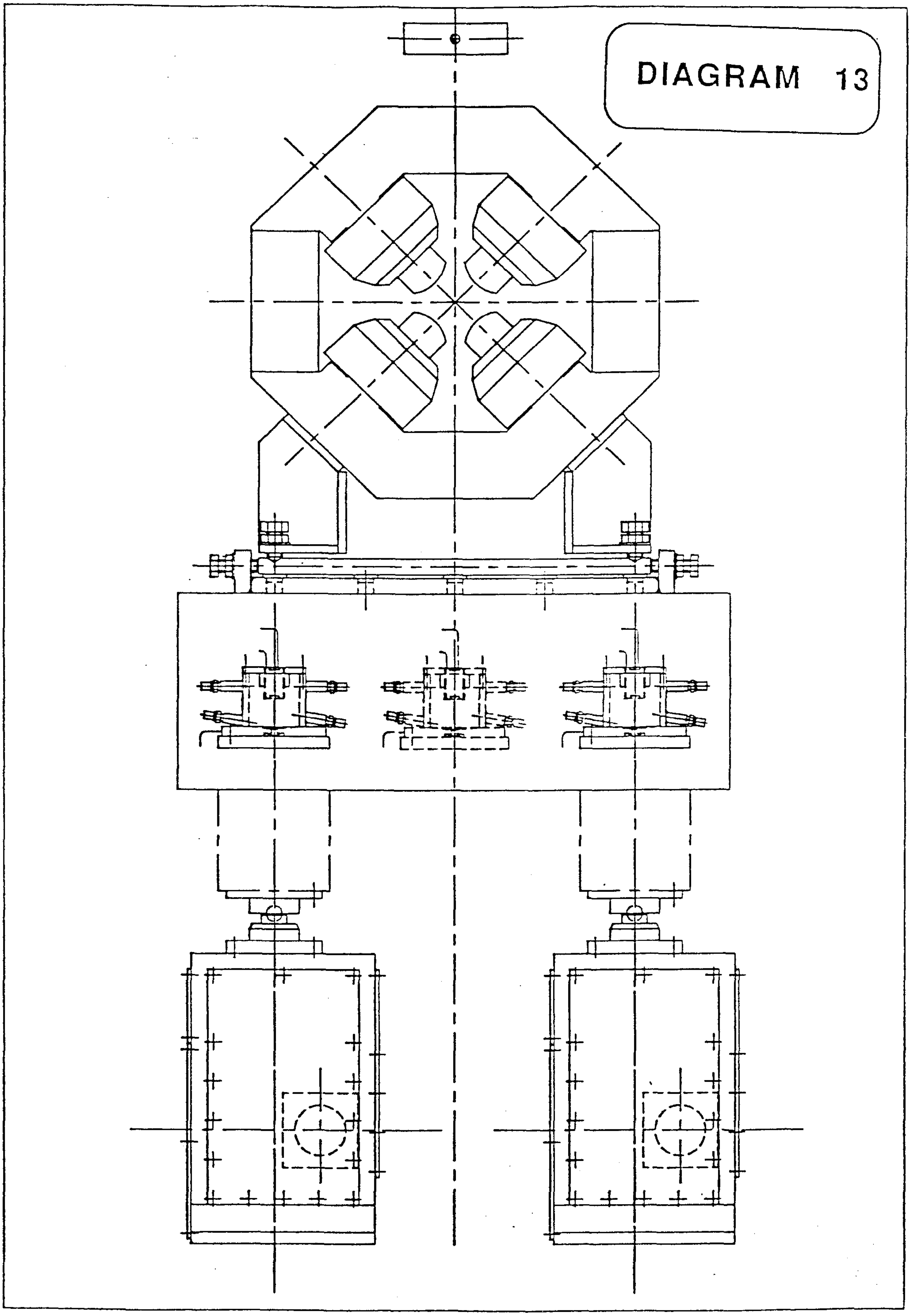
DIAGRAM 13

PROTOTYPE GIRDER (TRANSVERSAL VIEW)

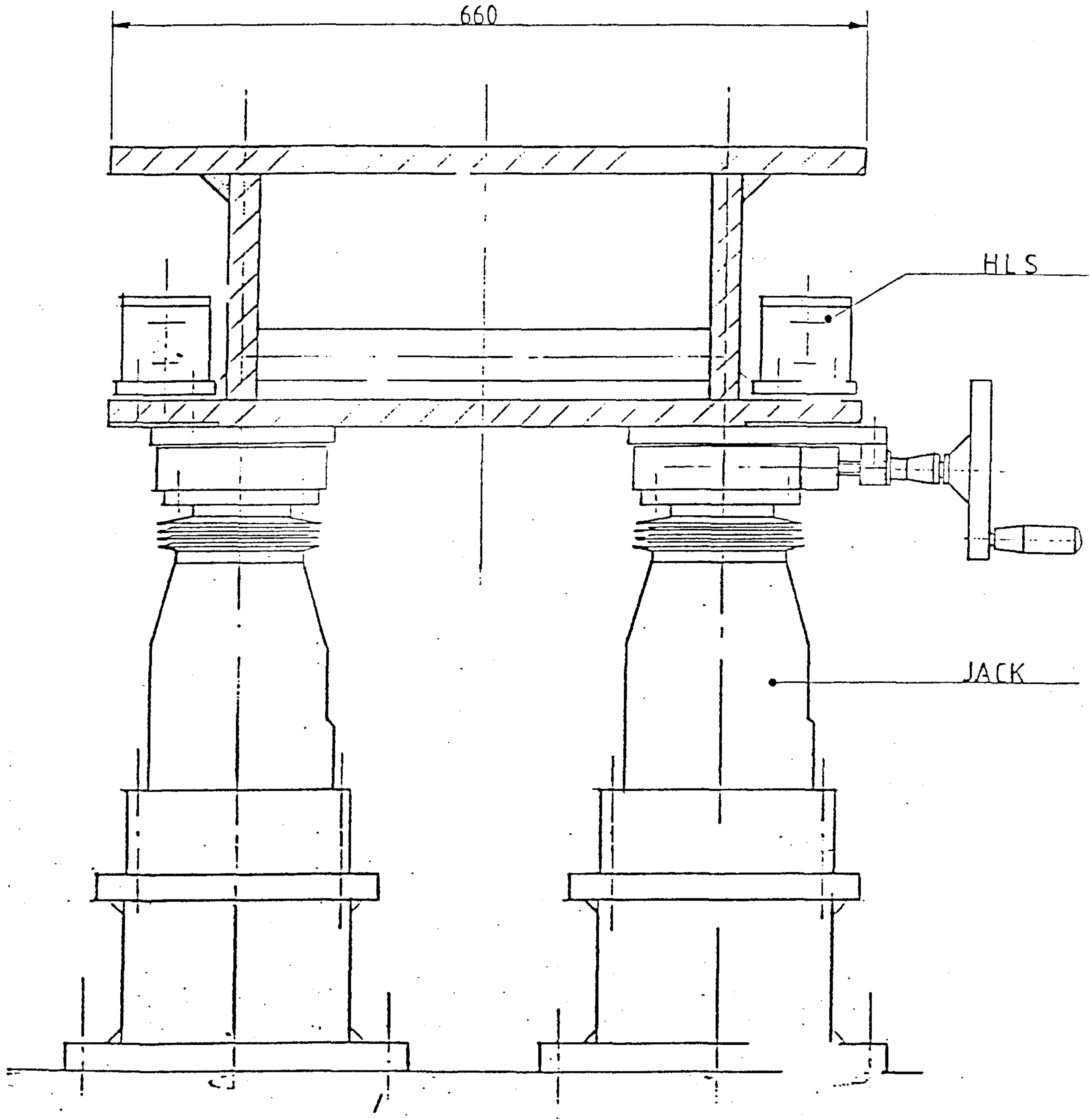

DIAGRAM 13 bis

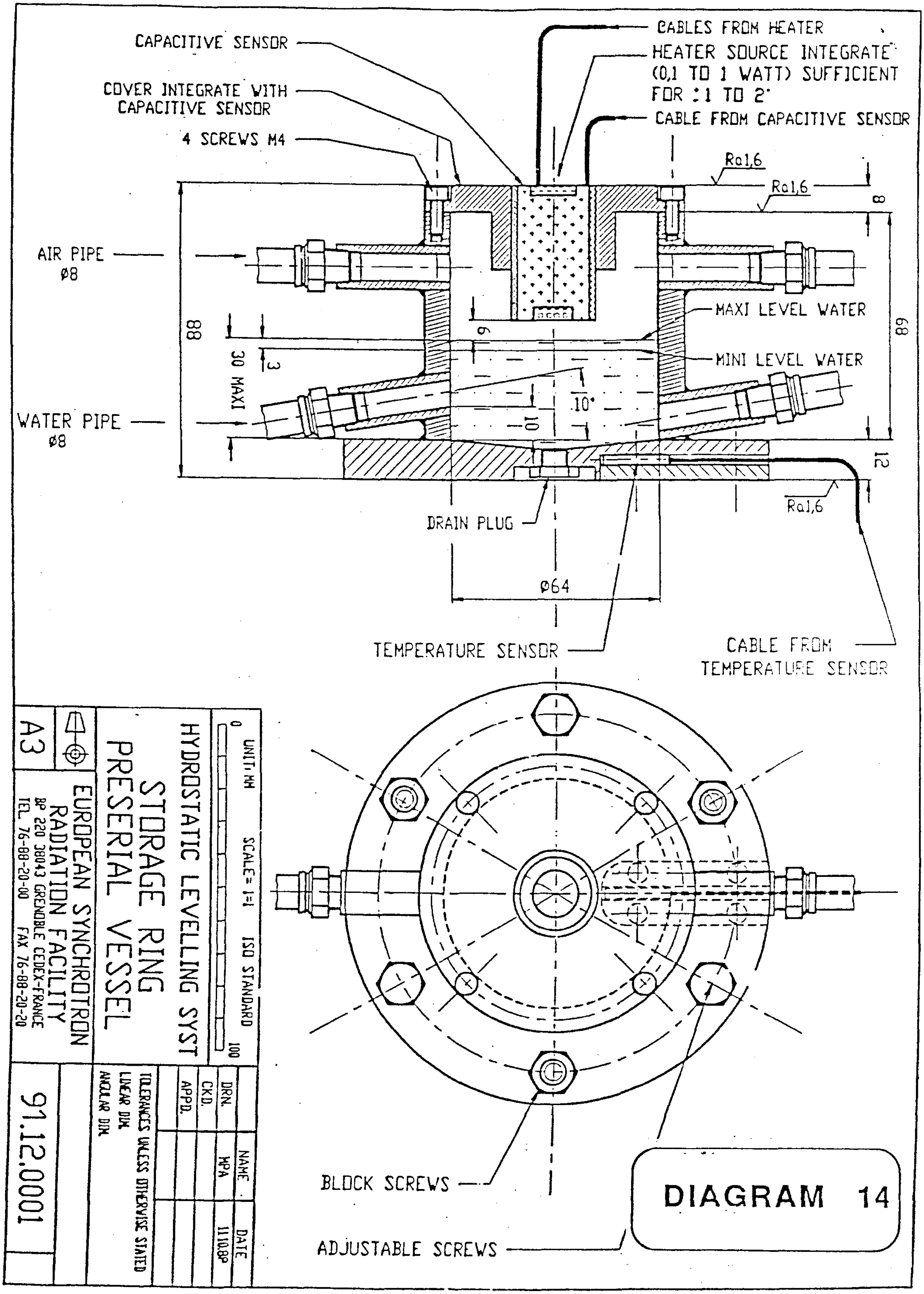
CABLES FROM HEATER
CAPACITIVE SENSOR
HEATER SOURCE INTEGRATE (0,1 TO 1 WATT) SUFFICIENT FOR :1 TO 2°
COVER INTEGRATE WITH CAPACITIVE SENSOR
CABLE FROM CAPACITIVE SENSOR
4 SCREWS M4
Ra1,6
Ra1,6
8
AIR PIPE ø8
MAXI LEVEL WATER
88
6
69
30 MAXI
3
MINI LEVEL WATER
10°
WATER PIPE ø8
10
12
Ra1,6
DRAIN PLUG
ø64
TEMPERATURE SENSOR
CABLE FROM TEMPERATURE SENSOR
BLOCK SCREWS
ADJUSTABLE SCREWS
UNIT: MM
SCALE= 1=1
ISO STANDARD
0
100
HYDROSTATIC LEVELLING SYST
STORAGE RING
PRESERIAL VESSEL
EUROPEAN SYNCHROTRON RADIATION FACILITY
BP 220 38043 GRENOBLE CEDEX-FRANCE
TEL. 76-88-20-00 FAX 76-88-20-20
A3
NAME
DATE
DRN.
MPA
11108P
CKD.
APPD.
TOLERANCES UNLESS OTHERWISE STATED
LINEAR DIM.
ANGULAR DIM.
91.12.0001
DIAGRAM 14

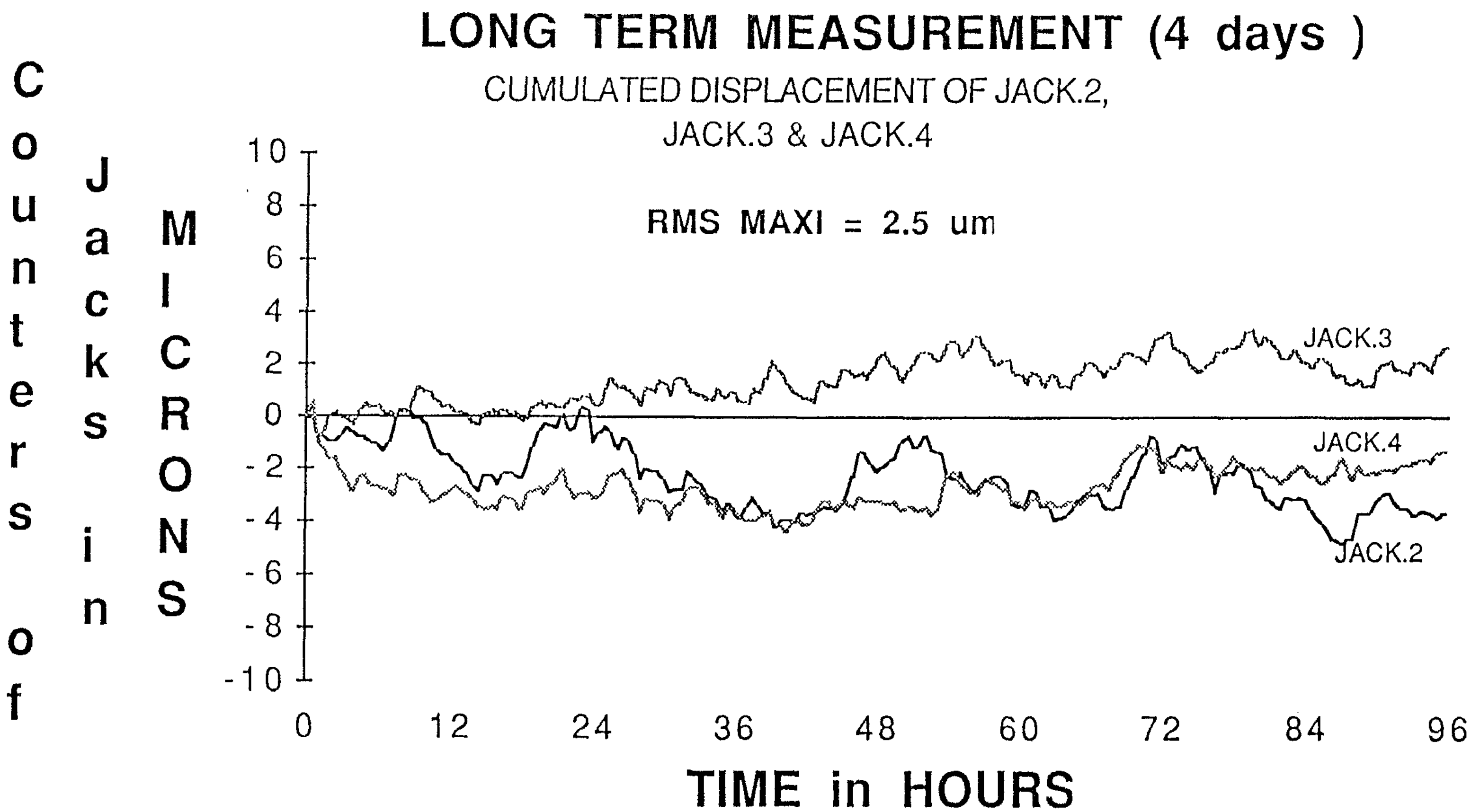
LONG TERM MEASUREMENT (4 days)
CUMULATED DISPLACEMENT OF JACK.2,
JACK.3 & JACK.4
RMS MAXI = 2.5 um
Counters of Jacks in MICRONS
10
8
6
4
2
0
-2
-4
-6
-8
-10
JACK.3
JACK.4
JACK.2
0
12
24
36
48
60
72
84
96
TIME in HOURS

DIAGRAM 15a

LONG TERM MEASUREMENT (4 days)

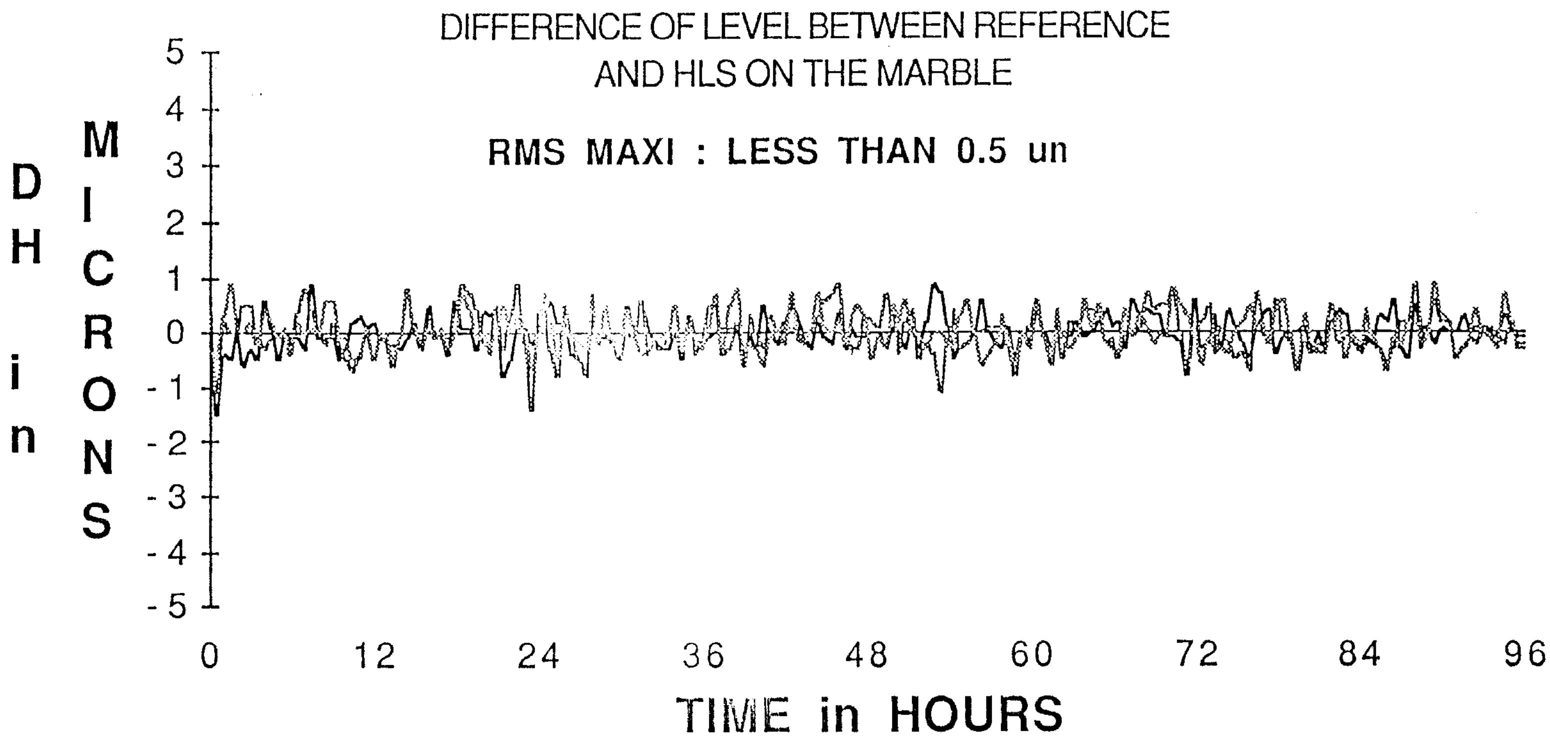

DIAGRAM 15b

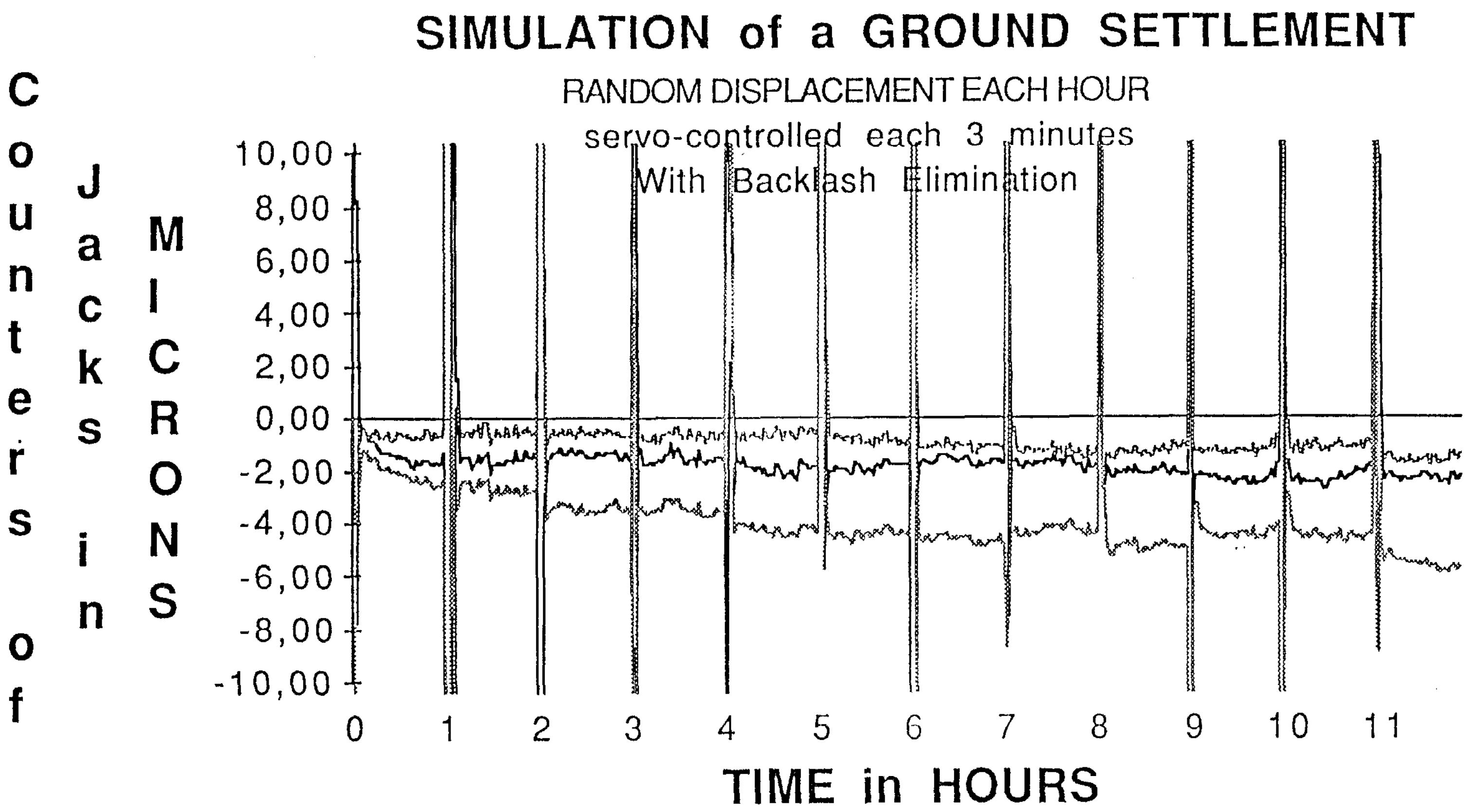
SIMULATION of a GROUND SETTLEMENT
RANDOM DISPLACEMENT EACH HOUR
servo-controlled each 3 minutes
With Backlash Elimination
Counters of Jacks in MICRONS
10,00
8,00
6,00
4,00
2,00
0,00
-2,00
-4,00
-6,00
-8,00
-10,00
0
1
2
3
4
5
6
7
8
9
10
11
TIME in HOURS

DIAGRAM 16a

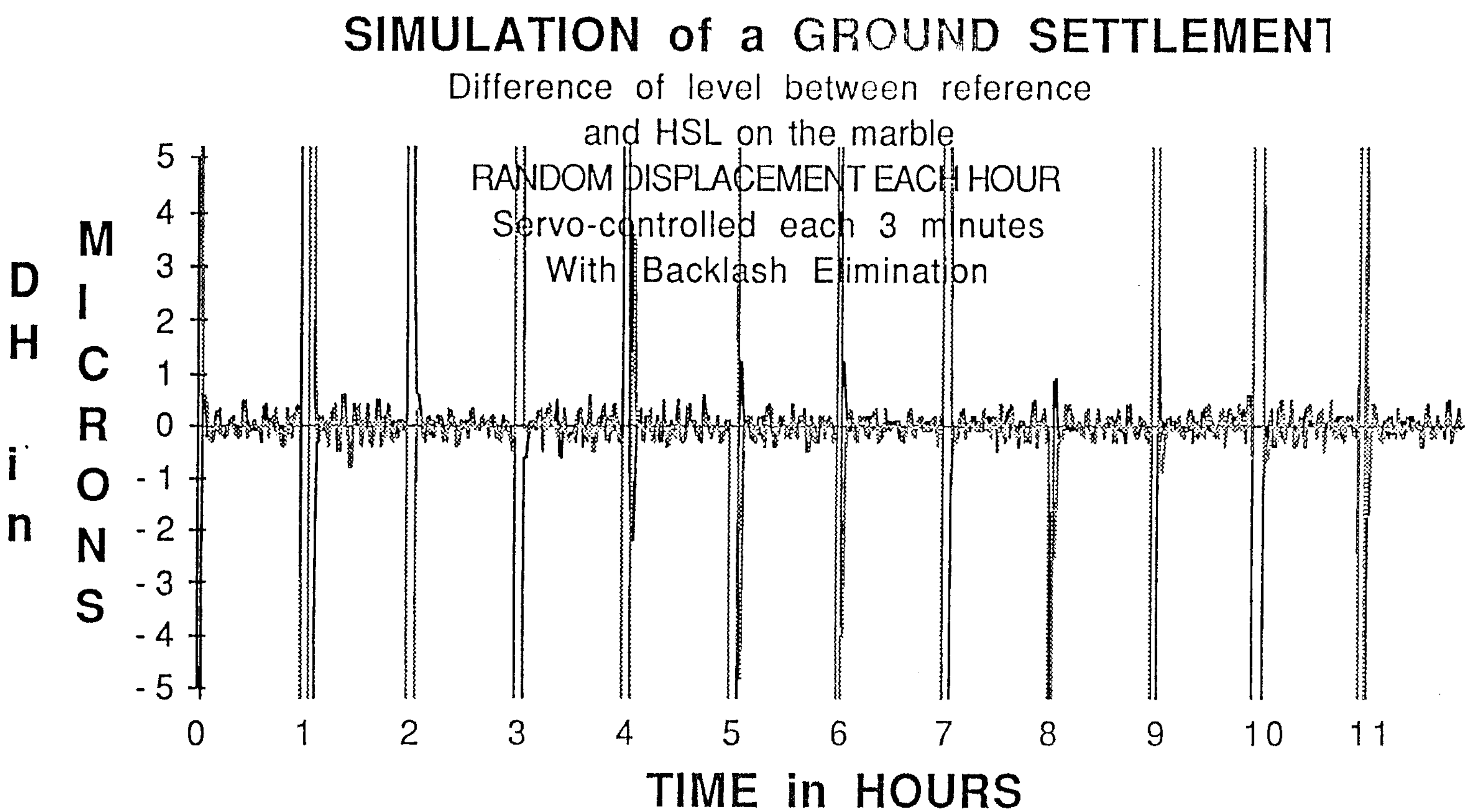
SIMULATION of a GROUND SETTLEMENT
Difference of level between reference
and HSL on the marble
RANDOM DISPLACEMENT EACH HOUR
Servo-controlled each 3 minutes
With Backlash Elimination
DH in MICRONS
5
4
3
2
1
0
-1
-2
-3
-4
-5
0
1
2
3
4
5
6
7
8
9
10
11
TIME in HOURS

DIAGRAM 16b

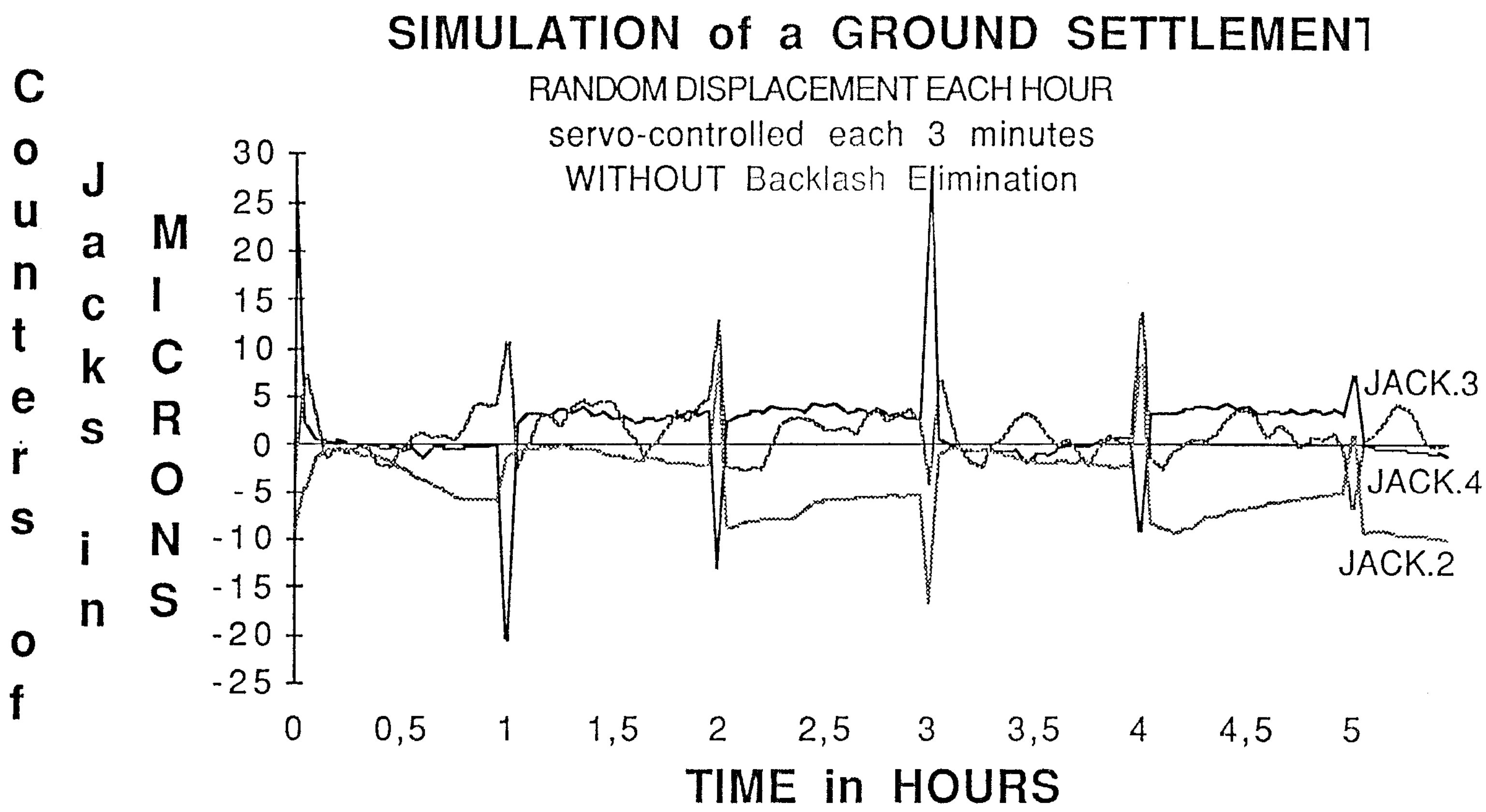
SIMULATION of a GROUND SETTLEMENT
RANDOM DISPLACEMENT EACH HOUR
servo-controlled each 3 minutes
WITHOUT Backlash Elimination
Counters of Jacks in MICRONS
30
25
20
15
10
5
0
-5
-10
-15
-20
-25
0
0,5
1
1,5
2
2,5
3
3,5
4
4,5
5
TIME in HOURS
JACK.3
JACK.4
JACK.2

DIAGRAM 17a

COUNTER.COMPJACK2

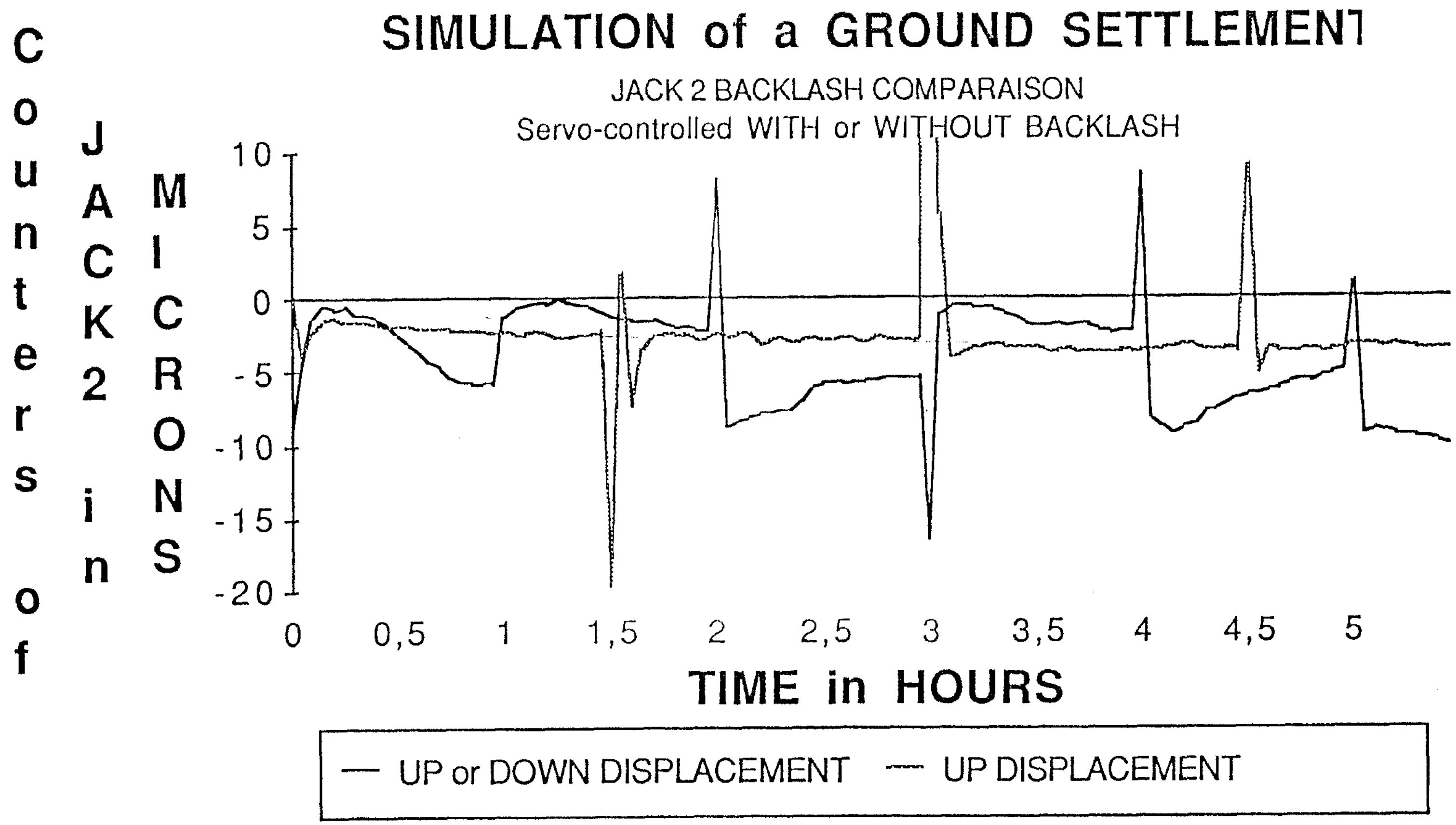

DIAGRAM 17b

ANALOGIC/DIGITAL CARD LIMITATION
MEAN = 2715.1

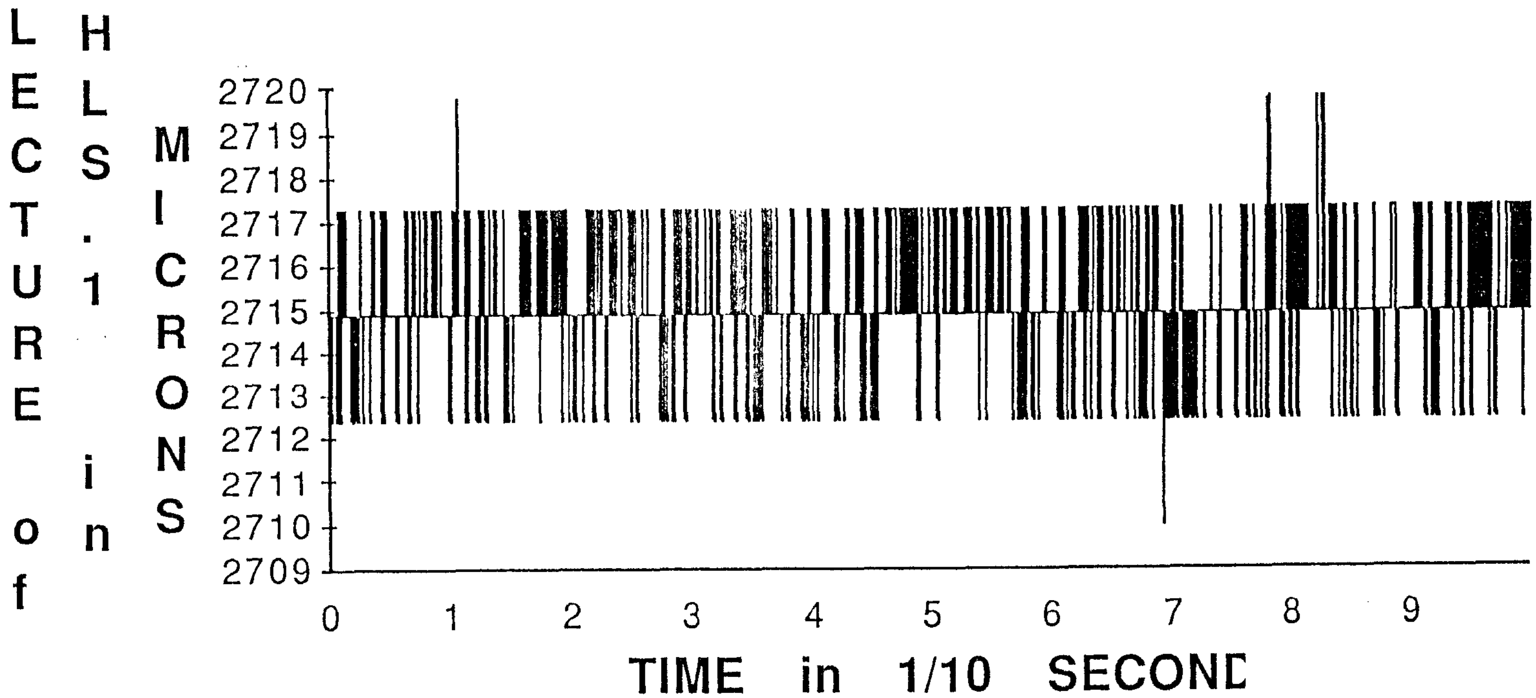

DIAGRAM 18

VERY LONG TERM MEASUREMENT (46 DAYS)

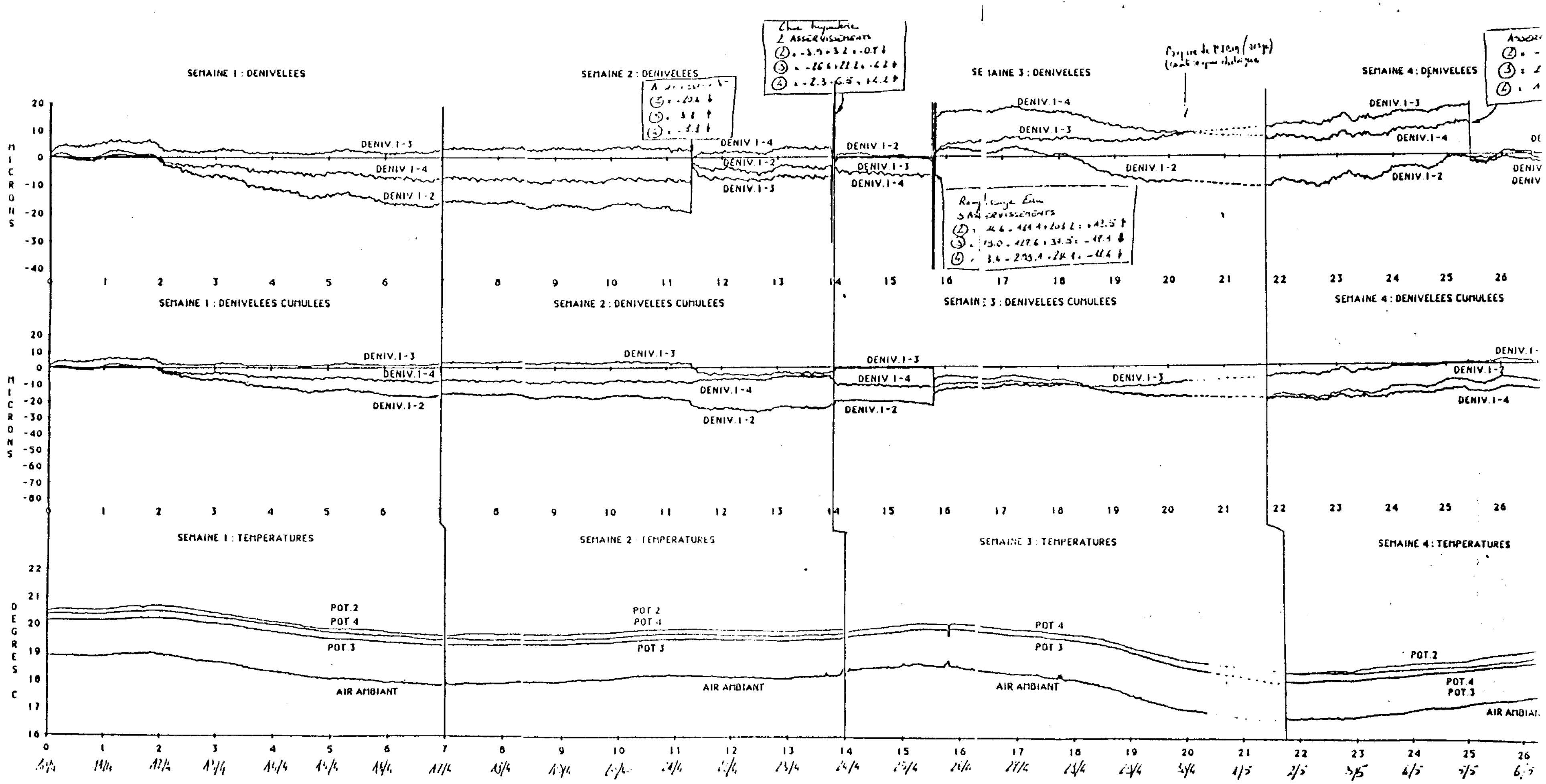

DIAGRAM 19a

VERY LONG TERM MEASUREMENT (46 DAYS)

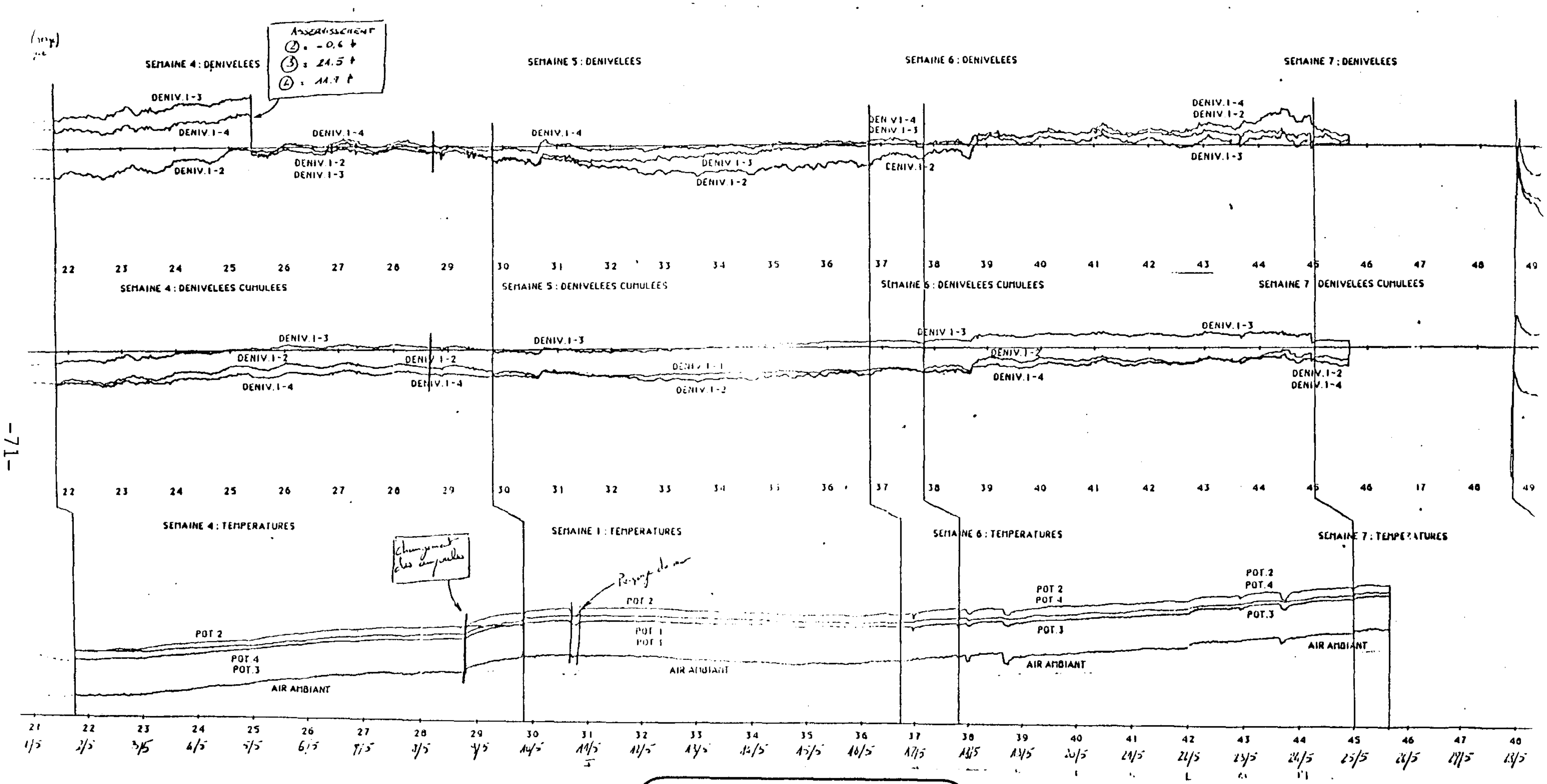

DIAGRAM 19b

ZOOM ON THE MOVEMENT OF THE SEVEN FIRST DAYS

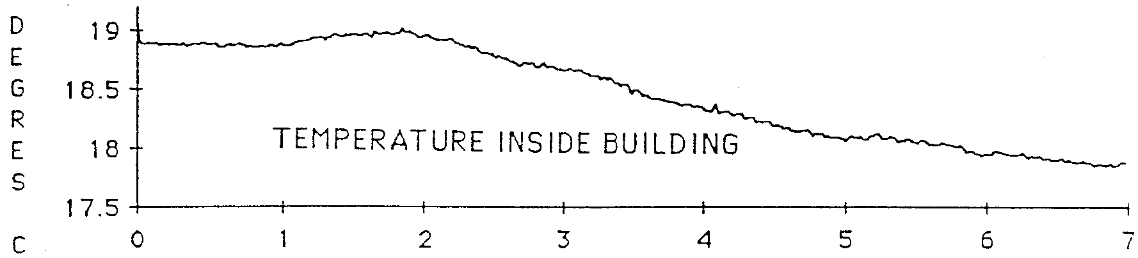

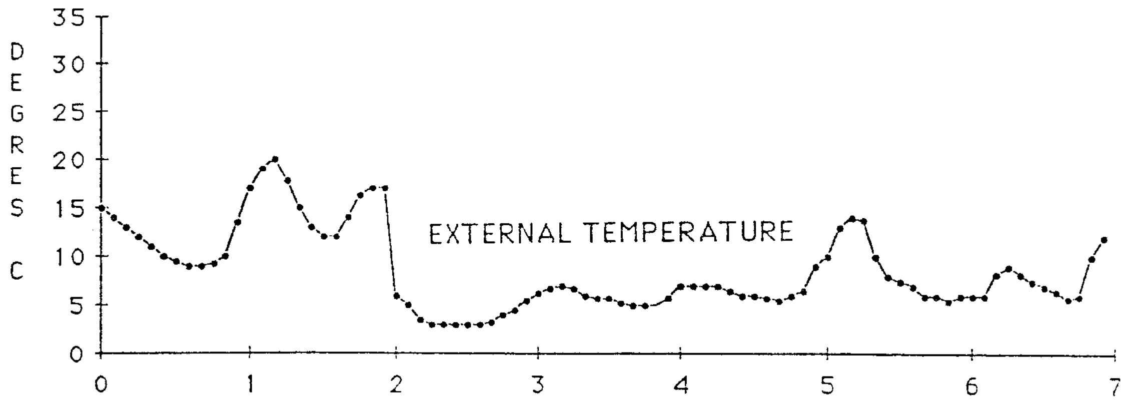

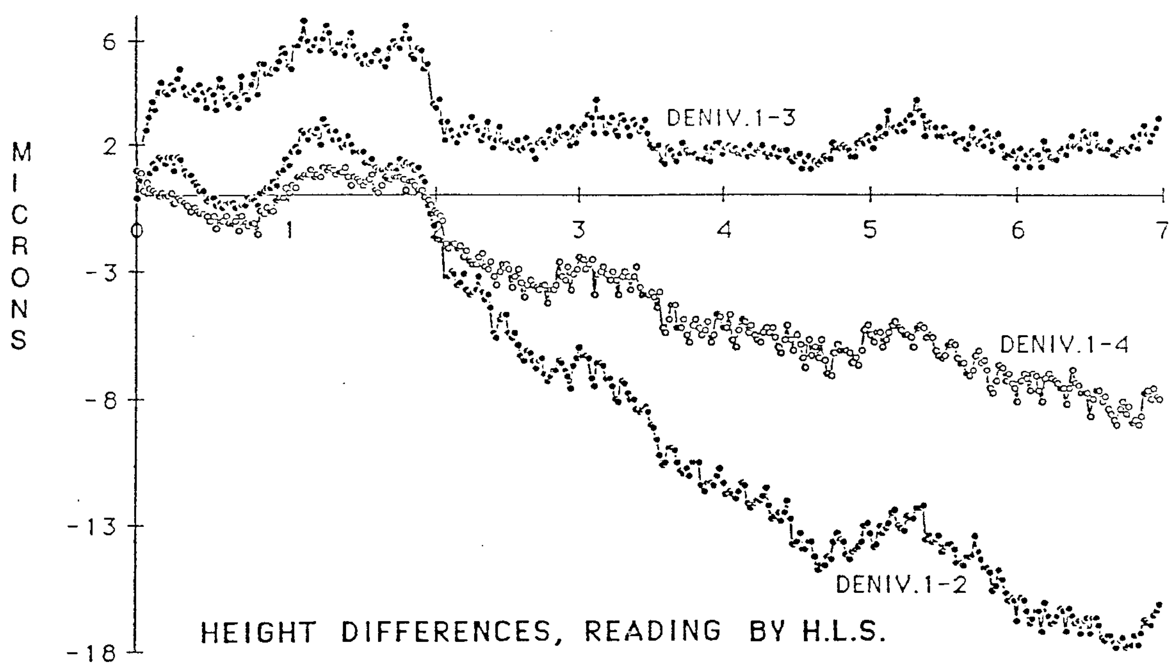

DIAGRAM 20

A TEST FACILITY OF ACTIVE ALIGNMENT SYSTEM AT KEK

N. Ishihara, S. Iwata, T. Matsui, H. Matsumoto,
H. Mizuno, S. Takeda, Y. Takeuchi, M. Yoshioka

National Laboratory for High Energy Physics, KEK
Ibaraki, JAPAN

K. Ishihara, S. Nakabayashi, K. Yasuda

Kawasaki Heavy Industries, Ltd.
Kobe, JAPAN

Abstract

A test facility with one control axis has been constructed at KEK to investigate a super-accurate alignment technique for the JLC (Japan Linear Collider) project. The facility consists of a stabilized laser system and a vibration control stage equipped with piezo transducers. Results of the first test show that the distance of about 28 cm is kept stable to 50 nm or better up to the frequency of 20 Hz, against the sine wave disturbance with a 500 nm amplitude.

Introduction

It is a common recognition that a sub-micron alignment system should be developed for the future e+e- collider like the JLC, since the vertical beamsize at the interaction point will have to be as small as 2 nm in order to get enough luminosity. On the other hand, the ground motion of the order of 100 nm should be expected even deep underground. For our information, the ground motion was measured at KEK site for two cases, one on a 16 m deep underground floor and the other at ground level. The results are shown in table 1. The data taken even deeper underground was reported elsewhere.[1] While the high frequency components are easily reduced by the conventional damping method, the lower components below 10 Hz are quite difficult to reduce. This is due to a low specific frequency of the passive vibration-proof table. Fig.1 shows the damping characteristics of the vibration-proof table employed in this experiment. In such a low frequency region, however, we can keep an object stable by means of the feedback method, called the active alignment.

We began a fundamental study last year to understand the control system using a laser interferometer and piezo transducers. The reason why such combination was selected is that the laser interferometer is the most accurate measuring device over long distances, and the piezo transducer seems to be the most convenient tool to move loads of many kg in the range of 10 μm.

In this report we will describe the facility components and the results of test.

Laser system

Since the initial goal of the present test facility is to keep the distance stable as accurately as 50 nm at the maximum length of 1 m, the wave length of laser is required to be stable to 5×10^{-8}. In the near future we will use the facility in vacuum vessels to avoid the effect of air turbulence. With this improvement in mind, we chose the separate-function laser system, called L-IM-10 (He-Ne laser of Tokyo Seimitsu Co.,Ltd.), in which the interferometer head is connected by fiber cables to the laser generator and to the fringe counter. We can easily install the head in the vacuum space by using a feed flange for fiber cables, without any beam alignment. At the present stage, the test has been made in the temperature controlled air of 1 atm.

The principle of the laser system is the Michelson type interferometer as shown in Fig.2.[2)] The laser beam coming from the generator is led through the fiber cable to the head and goes to the splitter. One beam goes to the built-in reflector and the other goes to the cornered cubic reflector mounted on the object which we want to measure the distance from. Beams coming back from both reflectors make interference fringes on the plane where four photosensors are arrayed. Each photosensor receives the light intensity given by

$$I(x) = 1 + \cos (4\pi x/\lambda + \alpha),$$

where x is the path difference of two beams, λ the light wave length ($\sim$633 nm) and α the initial phase. The phase difference from the next sensor is $\pi/2$, so the subtracted signals are

$$I_1 - I_3 = 2\cos(4\pi x/\lambda) \quad \text{and} \quad I_2 - I_4 = -2\sin(4\pi x/\lambda),$$

without dc component.

Since one cycle of the signal is divided into 16, the resolution is $\lambda/32 = 20$ nm.

Piezo transducer and position control stage

The piezo transducer should have low driving voltage to avoide possible discharge in the vacuum space, and to have good linearity to achieve fast response in the feedback system. The selected transducer is Model P-841.20 of Physik Instrumente Co., driving voltage of which is 100 V for the expansion of 30 μm. The transducer has a position sensor installed in the same casing. It is thereby possible to get as excellent linearity as 0.1 % of full scale.

The control stage made of stainless steel has a double structure, the upper and the lower stage with the same moving axis, as shown in Fig.3. An overall dimension of the stage is 180 mm x 160 mm x 42 mm, and movable parts of both stages have the same dimension of 100 mm x 100 mm and the weight of 1.2 kg. The typical loads of the upper and lower stages are 10 kg and 14 kg, respectively. Since the design value of spring constant is 1.47 x 10^7 N/m for both stages, the resonant frequencies are calculated to be 193 Hz for the upper stage and 163 Hz for the lower, using the relation

$$f = (1/2\pi) \cdot (K/M)^{1/2},$$

where f is the resonant frequency, K the spring constant and M the load mass. These frequencies are high enough in comparison with the operating frequency of less than 20 Hz.

In order to measure the real motion of the stages, a capacitance microsensor with the accuracy of 2 nm for 1 μm displacement has been also installed into each stage. Specifications confirmed by our tests are shown in table 2. The discrepancy of resonant frequency between the design value and the actual one is due to the larger spring constant of the actual stage.

Test

The block diagram of the test facility is shown in Fig.3. The corner cube is mounted on the upper stage and the interferometer head is located 28 cm from the corner cube as shown in Fig.4. The vibration-proof table supports the whole components. The lower stage gives disturbing movements to the upper stage with an arbitrary wave form. The laser system measures the distance between the interferometer head and the corner cube with the sampling time of 1 msec. The CPU of the controller calculates the counteraction required to keep the corner cube stable, and then drives the piezo transducer of upper stage. Results of the test are shown in table 3 and Fig.5 for sine wave vibrations with amplitude of 500 nm. One can see that the damping of 20 db or more is obtained up to 20 Hz. Especially for the vibration of less than 10 Hz, we can keep the stage stable within 30 nm amplitude.

Summary

Our first test has shown that the one dimensional position control system consisting of the laser interferometer and the piezo transducer is able to keep the distance stable around 30 cm with the accuracy of better than 50 nm up to 20 Hz of sine wave vibration of 500 nm amplitude. For tests at longer distances of several m or more, the laser beam path should be evacuated to avoid the variation of refractive index due to air turbulence. Now we are preparing for the test in vacuum. Next step will be the development of the active alignment system having multi control axes.

Acknowledgement

We would like to thank Prof. H.Sugawara, director general of KEK, for the encouragement of this work. Thanks are also due to Profs. Y.Kimura, K.Takata of KEK and Dr.T.Atsuta of Kawasaki Heavy Industries, Ltd. for their supports of this project. We appreciate the technical supports of KHI staffs.

References

(1) Y.Kimura, K.Takata and M.Yoshioka, Proceedings of the 1987 ICFA Seminar on Future Perspectives in High Energy Physics, BNL p.219

(2) T.Kurosawa, Y.Tanimura, K.Toyoda and T.Yamada, private communication

Table 1. Ground motion at KEK site.

(a) TRISTAN experimental floor, 16 m underground.

Horizontal (N-S)		Horizontal (E-W)		Vertical	
Amp.(nm)	Freq.(Hz)	Amp.(nm)	Freq.(Hz)	Amp.(nm)	Freq.(Hz)
159	196.0	162	196.0	220	2.5
147	194.0	146	2.5	157	196.0
115	2.5	136	194.0	145	100.0
113	100.0	113	191.5	144	194.0
114	191.5	86	183.5	113	191.5

(b) Assembly hall floor, above ground.

Horizontal (N-S)		Horizontal (E-W)		Vertical	
Amp.(nm)	Freq.(Hz)	Amp.(nm)	Freq.(Hz)	Amp.(nm)	Freq.(Hz)
896	2.5	783	3.0	806	3.5
453	5.5	473	5.0	480	5.0
255	196.0	222	193.5	469	9.5
185	194.0	220	189.5	290	46.5
180	148.0	212	196.0	280	13.5

Table 2. Specification of control stage.

Dimension (movable part)	100 mm x 100 mm
Movable range	21 μm
Yawing	< 0.2 sec
Resonant frequency	250 Hz
Response time	40 msec/μm
Position resolution	5 nm
Load capacity	20 kg

Table 3. Vibrations after the position control against the disturbance of 500 nm amplitude.

Frequency (Hz)	Amplitude (nm)	Damping (dB)
0.1	19	-28
0.2	18	-29
0.5	19	-28
1	18	-29
2	25	-26
5	27	-25
10	30	-24
20	52	-20
30	77	-16
40	97	-14
50	190	-8.6
60	210	-7.6
70	280	-4.9
80	370	-2.7
90	410	-1.7
100	470	-0.52

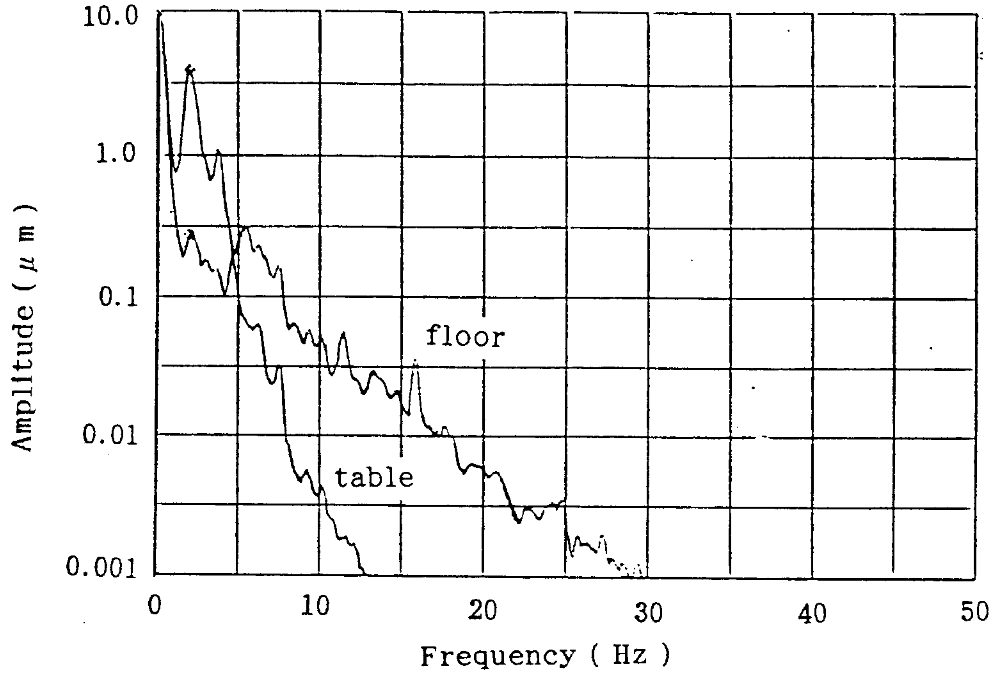

Fig.1 Damping characteristics of the passive vibration-proof table.

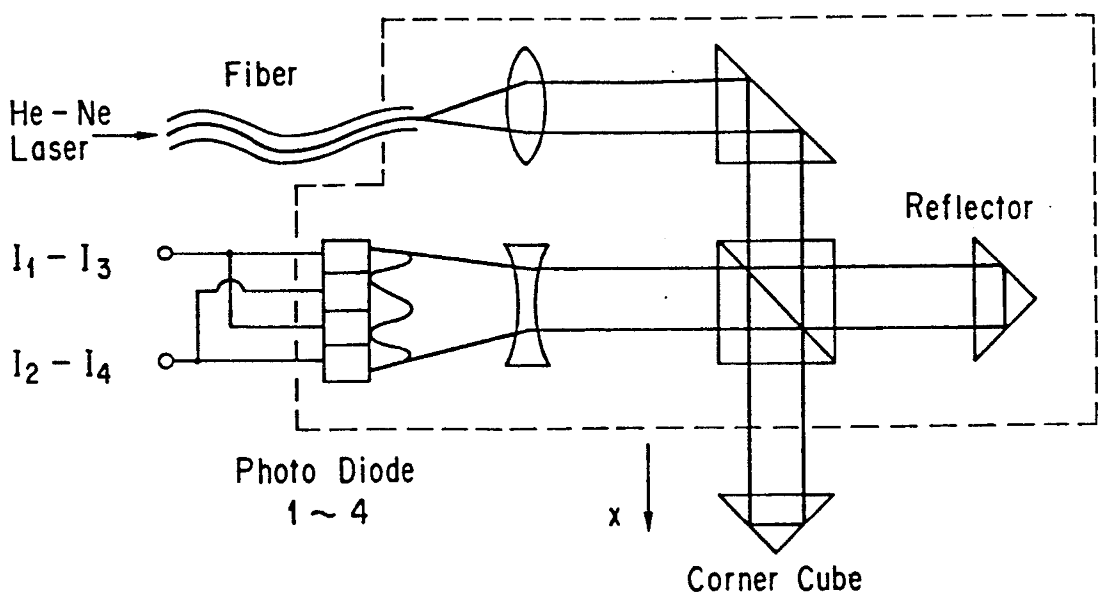

Fig.2 Conceptual drawing of the Michelson type laser interferometer, L-IM-10.

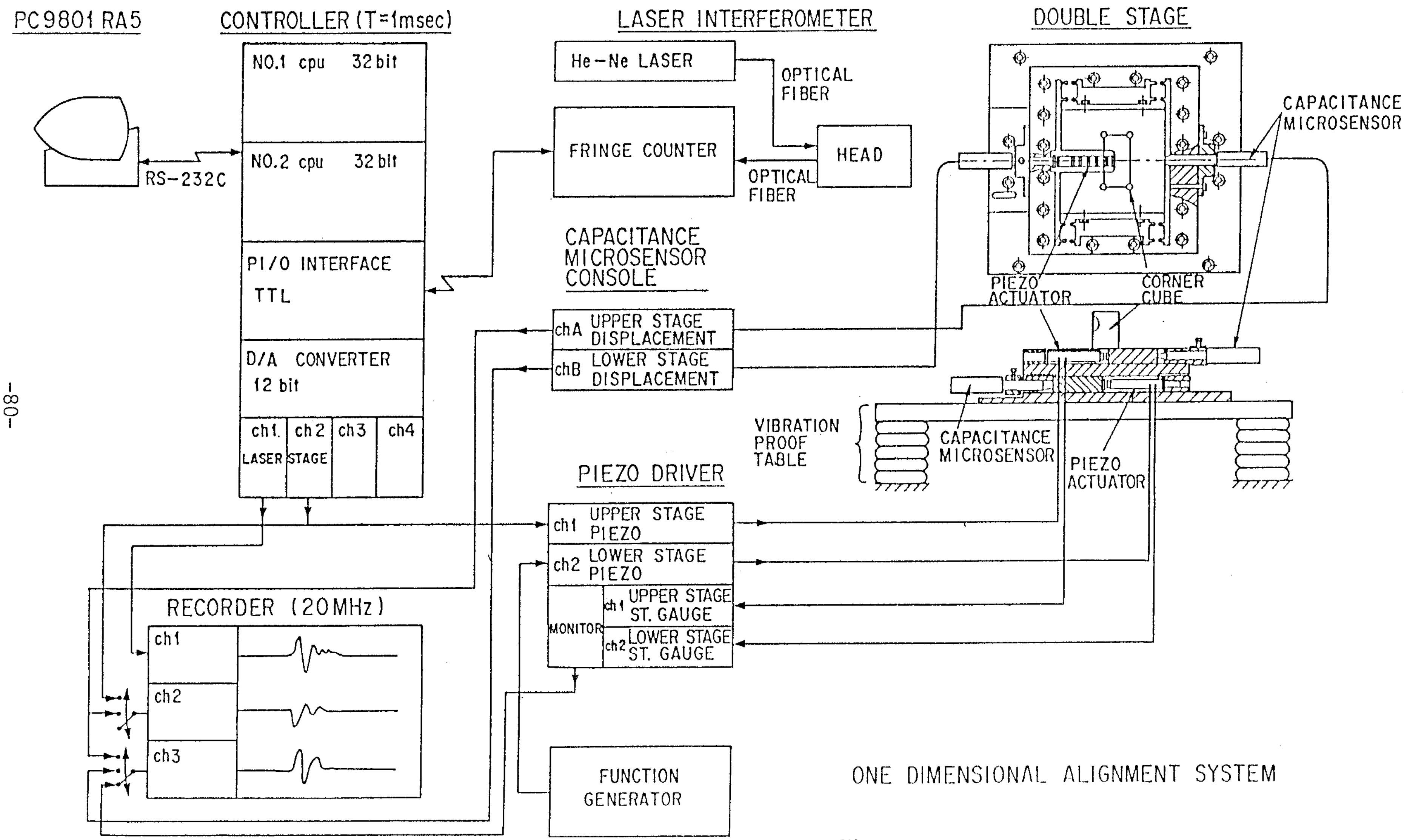

Fig.3 Block diagram of the test facility.

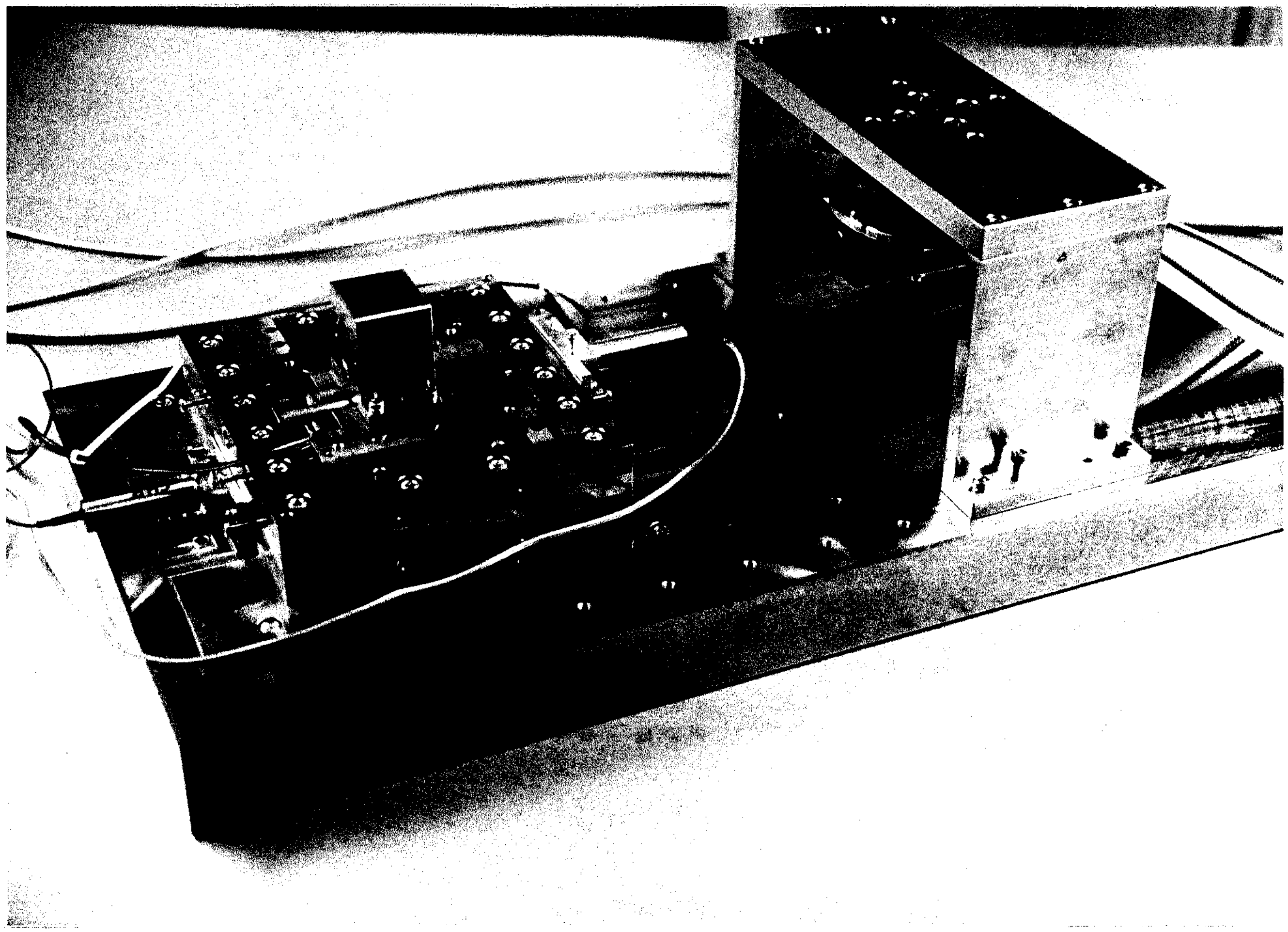

Fig. 4. Picture of the test facility.

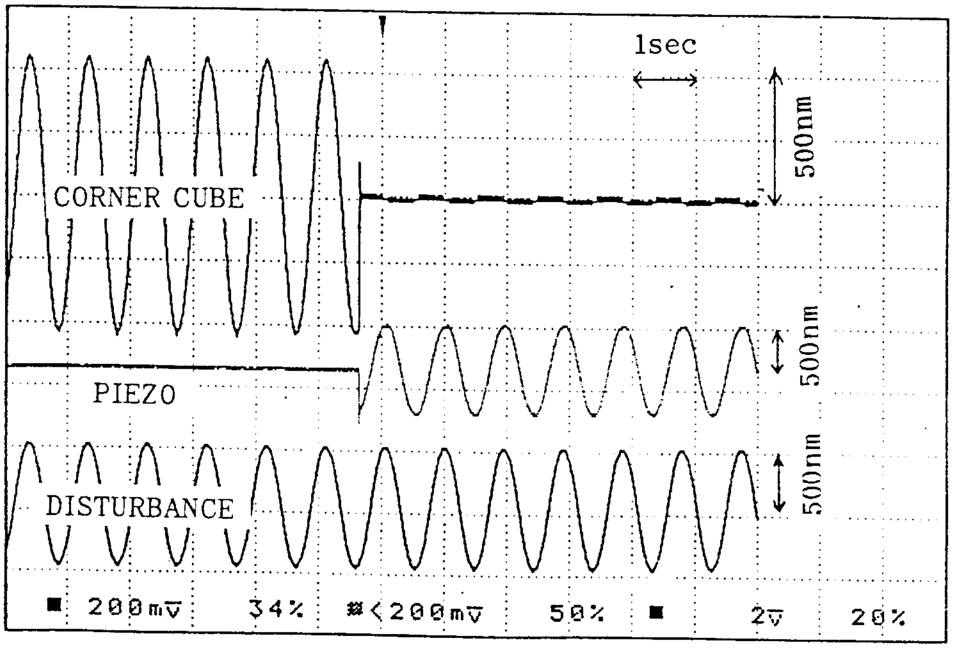

(a) 1 Hz

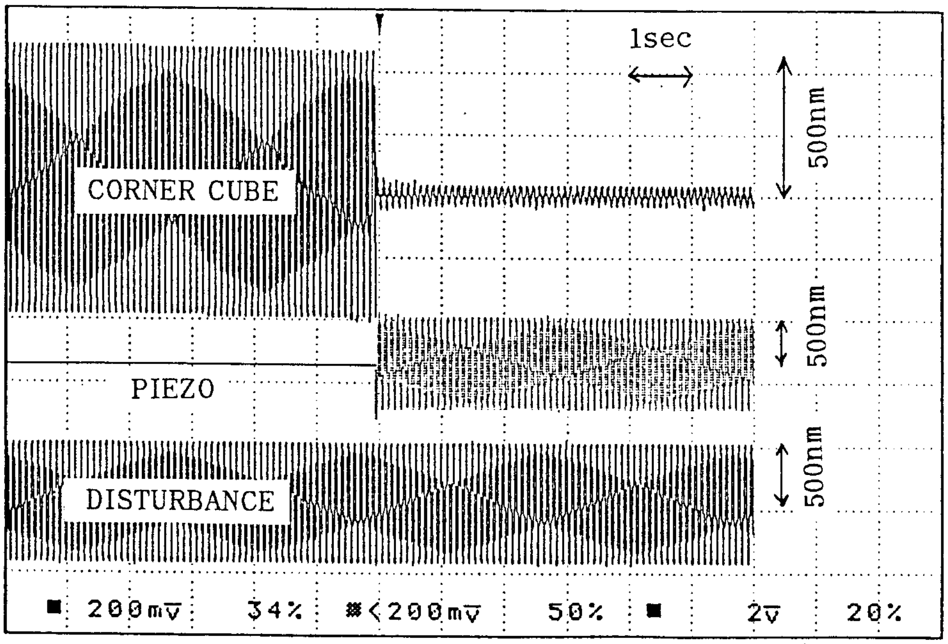

(b) 10 Hz

Fig.5 Typical damping feature on the oscilloscope. Disturbances of sine wave with 500 nm amplitude are added (a) at 1 Hz and (b) at 10 Hz.

THE MIT/BATES SOUTH HALL RING

W. WADE SAPP, JR.

Bates Linear Accelerator Center

Middleton, MA

ABSTRACT

The Bates laboratory is in the conventional construction phase of a project to build and commission a ring of 190 m circumference to store electron currents up to 80 mA at energies 0.3 - 1.0 GeV. Storage times of 1 msec to several seconds are planned for a variety of extracted beam and internal target physics experiments. The facility is briefly described and specific challenges in the areas of magnetic measurement, fiducialization, and survey and alignment are discussed. Transverse position precisions of approximately 100 microns and a total orbit circumference precision of 2 mm are sought.

1. INTRODUCTION

The laboratory (Fig. 1) is located about 25 miles north of the MIT campus near the top of a glacial drumlin with dense soil material which has a high test penetration resistance and a good presumptive bearing capacity (6 tons/ft**2). The present facility can produce 1% duty factor beams (600 Hz, 15 microsec) at energies between 50 MeV and 1 GeV; energies above 500 MeV are achieved by sending the beam a second time through the accelerator. The energy spread is 0.3% and the emittance at 500 MeV is 0.02 pi mm mr. There are two major experimental halls for pursuing a broad spectrum of primarily nuclear physics research: one hall contains a very high resolution 900 MeV/c magnetic spectrometer; the other contains three large magnetic spectrometers which are used primarily in various coincidence studies. A full-time staff of 95 supports users from over 70 institutions worldwide.

The ring now under construction and scheduled for beam tests in 1991 will provide stored beams for internal target experiments and extracted beams of high duty factor (above 80%). High intensity polarized electron beams are planned for 1992. The total estimated cost is $14.8 M plus $1.5 M for R&D; 69 PYE are budgeted for the project. (No experimental equipment is included in these numbers.) The Survey and Alignment budget is approximately $200 K; this does not include the cost of in-house manpower.

It is to be noted that even though both the laboratory and project are small compared to the others being discussed at this workshop, it nonetheless requires comparable alignment precisions and is above the threshold beyond which near-state-of-the-art equipment and methods are required. On the other hand, it is still below the threshold for having even one dedicated full-time alignment engineer. The author is a physicist who is in the process of learning enough survey and alignment technology to coordinate the efforts of a small engineering staff augmented by yet other physicists and technicians; over the years we have all developed millimeter habits which will have to be broken to install a 100 micron facility.

2. THE ALIGNMENT CHALLENGES

A more detailed plan view of the ring is shown in Fig. 2. The northeast quadrant is an exposed, poured concrete structure; except for the portion which passes through the existing experimental hall, the remainder of the ring is covered with earth more than five feet deep. The component list for the ring alone is given in Table I. The most demanding tolerances specified by the accelerator physicists are for the quadrupoles (Table II).

Table II. Ring quadrupole position tolerances

Coordinate	Initial	Stability
dx	0.1 mm	0.01 mm
dx'(pitch)	40 mr	10 mr
dy	0.1 mm	0.01 mm
dy'(yawl)	30 mr	1 mr
dz	1.0 mm	
dz'(roll)	1 mr	1 mr

Calculating the effects of various alignment errors is an ongoing activity of the accelerator physicists and is expected to continue even after the ring is commissioned. The latest calculations actually indicate that the tolerances in Table II. are somewhat conservative.

An additional set of challenges is presented by the ring dipoles, which are surplus from the Princeton-Penn Accelerator. These 30 ton magnets are much taller than the nearby multipoles, effectively preventing long sightlines in the arc regions. Figure 3. shows the approximate positions of just the multipoles in one of the more crowded sections between ring dipoles. The situation is reminiscent of the difficulties in the final focus region of the SLC, alluded to elsewhere in these proceedings by R. Ruland. The current proposed solution is simply to have a higher density of floor monuments in these regions and to use instrument stands high enough to provide sightlines one foot above the upper surface of the ring dipoles or just over 7 feet above the floor.

3. CURRENT STATUS

The concrete pouring is nearly complete; most of the temporary ceiling supports should be removed by mid-September; backfilling will be completed and all construction supports removed by mid-October. Preliminary field measurements of the ring dipoles have been underway for several months; "production" measurements and fiducialization should begin about one month from now. We have been extremely fortunate that NIST was able to make available to us the core components of a large XYZ mapping system; the X and Z motions are automated. The quadrupoles have been ordered, and the RFQ for the sextupoles should soon be ready. A flip-coil multipole harmonic analyzer, designed and built at Chalk River (Canada), is in shipment. Specifications for the harmonic analyzer and the XYZ mapping system being used with the dipoles are given in Table III.

Table III. Magnetic measuring equipment specifications

FIELD MAPPER SYSTEM (NIST)

(Probe Positioning)

X range		91	cm
Y range		7.6	cm
Z range		178	cm
X and Z drive min. step		32	microns
X and Z drive max. speed (typically 4 points/min.)		10	mm/s
X and Z measurement resolution		13	microns
Accuracy of X scale	+/-	13	microns
Accuracy of Z scale	+/-	20	microns

HARMONIC ANALYZER (Chalk River)

Bobbin length		80	cm
Bobbin diam. (std.dev.)	59.9712 +/-	0.0025	mm
Bobbin bowing		60	microns
Variation in groove depth	+/-	55	microns
Sensivity/Reproducibility to centroid of quadrupole	+/-	10	microns

We continue to rely heavily on the experience and advice of other laboratories (in fact, several of our advisers are in the room at this time):

for magnetic measurements --

Chalk River Nuclear Laboratories

FNAL

LAMPF

CEBAF

Francis Bitter Nat. Magnet Lab. (MIT)

LBL

for survey and alignment --

SLAC

LBL/ALS

University of Bonn

CEBAF

University of Saskatoon

We also have a formal collaboration with NIKHEF (Amsterdam), which is building a very similar ring on almost the same time scale. At this time NIKHEF is proposing to adapt their version of the Fresnel zone plate system for ring alignment whereas we are proposing to use the SLAC/GEONET system.

4. OPEN ISSUES

What follows is a time-ordered partial list of the issues which we are facing which are related to survey and alignment. I should thank the workshop organizers at this time for including discussions of almost all of these issues in the formal agenda.

-- connection of the new network to the existing beam switchyard: It has been requested that "no steering" be required along the straight line from the object point of the beam switchyard to the ring injection line, a distance of about 80 meters. (A misalignment of 0.05 mr between these two lines should be tolerable.) The beam line passes through three massive walls and one very narrow passageway. We propose to vacuum-bore-sight the line, with the complication of having to shoot through a 1 cm diameter aperture at the 40 m point and a 2 cm diameter aperture at the 70 m point. Extending the survey another 20 m to the output of the accelerator would require passing through another 1 cm diameter aperture at the 80 m point. The Z coordinate will be fixed by the present location of the spectrometer pivot on Beam Line "B".

-- magnet fiducialization:

ring dipoles - because the tolerance is +/- 1/2 mm, we expect to be able to use the mechanical center as the magnetic center and use either GEONET or SIMS to do the transfer to the survey targets.

multipoles - we will use a precision spindle to center the multipole magnet on the axis of the flip-coil bobbin bearing and use the measured deviation between the magnetic axis and the mechanical axis to correct the data set. We are concerned about the uniformity and smoothness of the poletips in these laminated core magnets as it affects spindle centering and error analysis.

superconducting solenoids - we have only just begun to worry about these devices.

-- magnetic field coupling: we are unaware of any useful rules of thumb for estimating the field distortion caused by neighboring magnets and, therefore, plan to measure the coupling between the ring dipoles and nearby multipoles as well as between neighboring multipoles. The combinations are too long for the harmonic analyzer so will be measured with the XYZ mapper.

-- adjustment stands: in many cases there are close-packed combinations of magnetic multipoles whose relative adjustment range is only +/- 1 mm (restricted by the vacuum pipe); to save money, we would like to learn of any designs which may be less expensive by virture of having a small range.

-- beam location w.r.t. fixed coordinate system: the accelerator physicists have asked for the ability to locate the center of the beam to +/- 1/4 mm (typical beam diameter is <1 mm). We will use fiducialized wire scanners, but there are only three planned for the entire ring. We will vary selected quadrupole fields and measure steering effects with downstream beam position monitors. We have thought about using synchrotron light from near the ends of the ring dipoles and seek advice from anyone with experience with shallow-depth-of-focus TV cameras and alignment and calibration schemes.

I am looking forward to both the formal presentations and informal discussions in this workshop and would like to take this opportunity to congratulate and thank the organizers for arranging an agenda which promises to be extremely useful for our development.

FIGURE CAPTIONS

Figure 1. Plan view of the Bates Linear Accelerator Center showing the South Hall Ring, which is currently under construction.

Figure 2. Detail plan view of the South Hall Ring

Figure 3. Approximate positions of magnetic multipoles in one of the more crowded sections between ring dipoles. Not shown are vacuum pumping ports at each end, a beam position monitor and one steering corrector set.

ACKNOWLEDGEMENTS

This work is supported in part by the U.S. Department of Energy under contract DE-AC02-76ER03069.

TABLE I. SHR COMPONENT LIST

ELEMENTS	NUMBER	LENGTH	GAP	MAX FIELD	SPECIAL FEATURES
	#	m	mm	at 1GeV	
Dipoles	16	3.59	76	3.7 kG	PPA Dipoles
Quads	79	0.30	65	5.5 kG	
Sextupoles	32	0.10	70	0.4 kG	
Corr. Sextupoles	2	0.10	70		
Octupoles	2	0.25	70	10 kG	

Ramped Air Quad	5	0.30	70	0.05 kG	Air Core
Ramped Dipole	1				0.1 mr deflection
Steer Corrector	32H, 32V				1 mr deflection
Corr. Octupoles	4				Air Core
Skew Air Quad	8				Air Core

Kickers	2	1.5	40		2 mr deflection
Mag Septa	3	1.0	14	2 kG	0.04 Gauss at Ring
Elec Septa	2	1.0	20	50kV/cm	

BPMs	31H,31V				10 @0.1mm, 1mm, 0.25μsec
Synch Monitor	16				Fiducial and digitize
View Screens	10				Smooth pipe
Curr Monitor	6				1%
Profile Monitor	3				Vacuum; smooth pipe

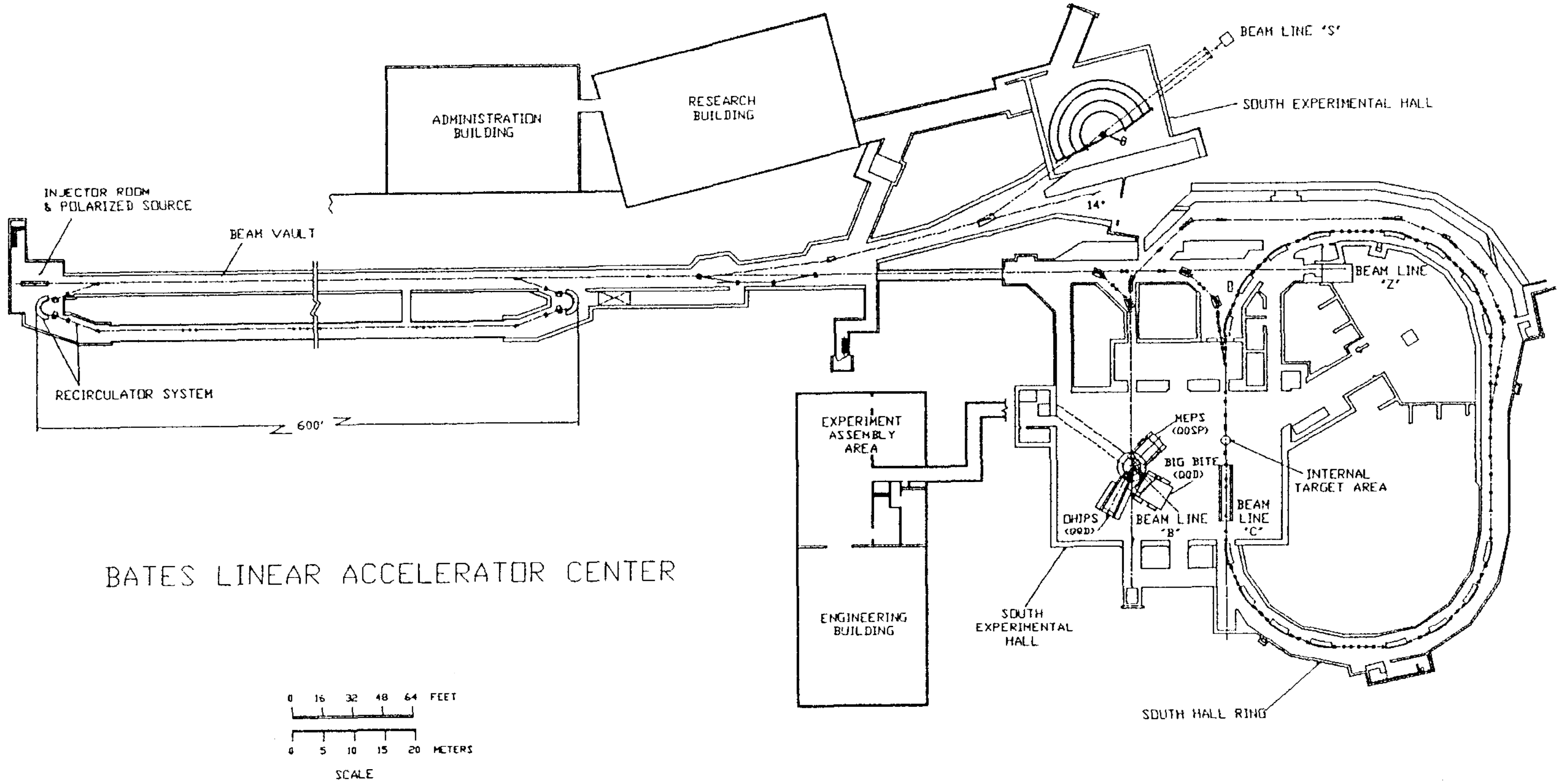
BEAM LINE 'S'
SOUTH EXPERIMENTAL HALL
RESEARCH BUILDING
ADMINISTRATION BUILDING
INJECTOR ROOM & POLARIZED SOURCE
BEAM VAULT
RECIRCULATOR SYSTEM
600'
14°
BEAM LINE 'Z'
EXPERIMENT ASSEMBLY AREA
MEPS (QQSP)
BIG BITE (QQD)
OHIPS (QQD)
BEAM LINE 'B'
BEAM LINE 'C'
INTERNAL TARGET AREA
ENGINEERING BUILDING
SOUTH EXPERIMENTAL HALL
SOUTH HALL RING
BATES LINEAR ACCELERATOR CENTER
0 16 32 48 64 FEET
0 5 10 15 20 METERS
SCALE

Fig. 1

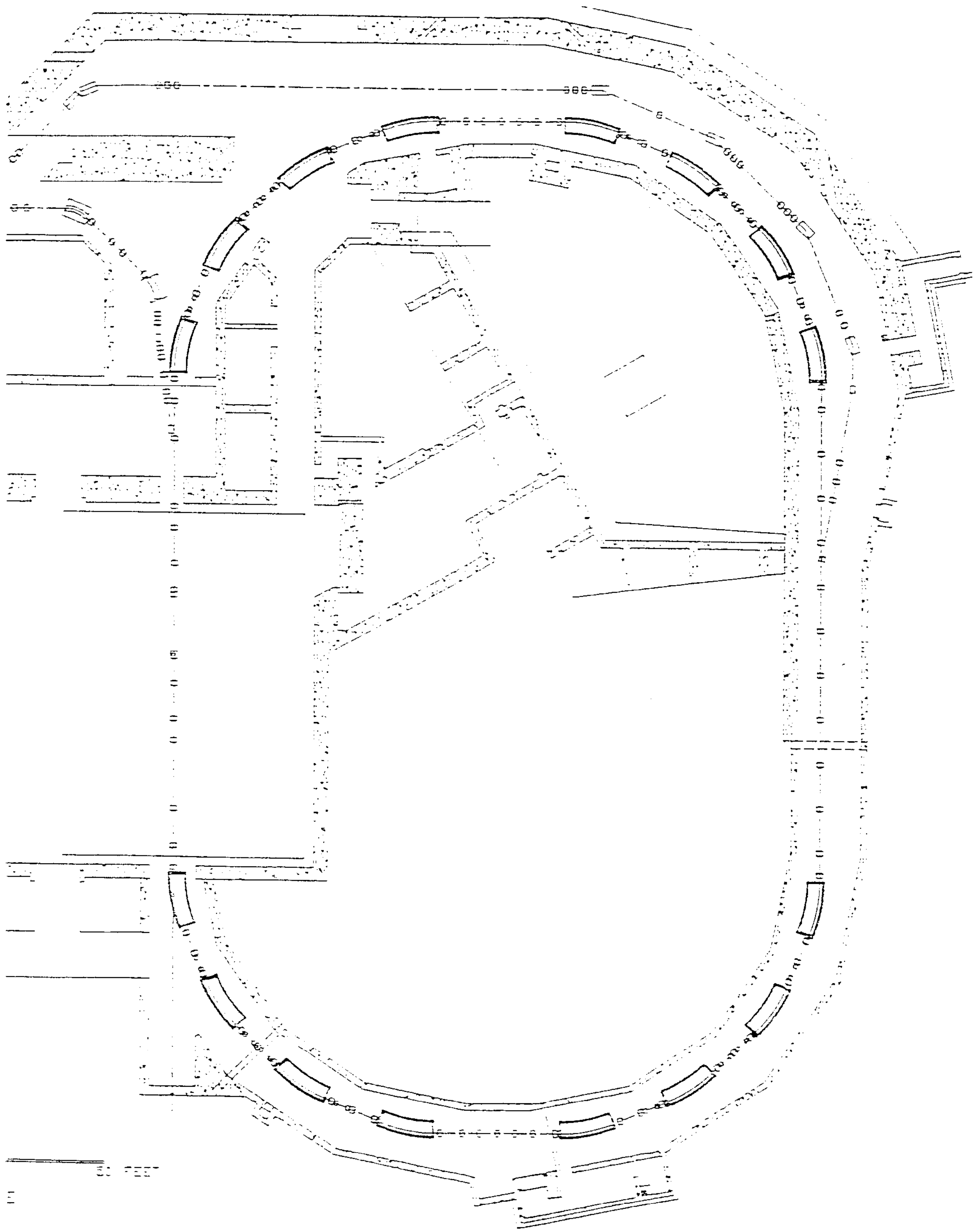

Figure 2.

THE TRIUMF KAON FACTORY

GEORGE S. CLARK

TRIUMF, University of British Columbia
Vancouver, British Columbia

TRIUMF is Canada's National Meson Facility. The TRIUMF site is hidden in a rain forest on the campus of the University of British Columbia in Vancouver, British Columbia. TRIUMF's current research program uses a cyclotron to accelerate 100 micro-amperes of protons to 500 MeV. The protons are directed along 0.1 km of beam lines to fixed target stations where the properties of muons, pions, and other particles are studied.

TRIUMF has proposed to the Canadian Federal and Provincial Governments that TRIUMF be upgraded to 100 micro-amperes at 30 GeV. To house the proposed 5-ring accelerator complex the TRIUMF site will expand from 10 acres to about 70 acres. Figure 1 shows the KAON Factory site plan. Negative hydrogen ions will be extracted from the cyclotron at 452 MeV and transferred to a booster complex. The booster complex will house a 452 MeV proton storage ring (A ring) and a 50 Hz 0.452-3 GeV synchrotron (B ring). The circumference of these rings is 215 meters. Figure 2 shows the Booster Tunnel cross-section, and that we intend to stack the rings one above the other. To isolate the storage ring from any vibration caused by the very fast cycling synchrotron, the A ring magnets will have separate supports from the B ring.

After the Booster synchrotron has accelerated the protons to 3 GeV, they are transferred to a 3 GeV proton storage ring (C ring) in the main accelerator tunnel. The main tunnel houses the C, D, and E rings. The D ring is a 10 Hz 3-30 GeV synchrotron and the E ring is an extender/storage ring to allow slow extraction at 30 GeV. These rings have a circumference of approximately 1.1 km. Figure 3 shows the Main Tunnel cross-section. The C ring will be mounted directly above the D ring, while the E ring will be offset horizontally to protect the C and D rings from slow extraction losses. Again we will try to isolate the storage rings from any vibration generated by the fast cycling synchrotron.

The status of the KAON Factory Project is that we have received $11 million for technical studies and to investigate interest from other countries in funding the project along the lines of the HERA project. Full funding is hoped for in mid-to-late 1990. TRIUMF currently is practicing alignment at the ± 1 mm level with only one full-time surveyor. With 3.7 km of rings with alignment tolerances about 0.1 mm and a further 1.3 km of beam lines, TRIUMF will have to learn about the world of precision surveying. We will learn from other labs such as CERN, SLAC, and DESY where this work is currently being done.

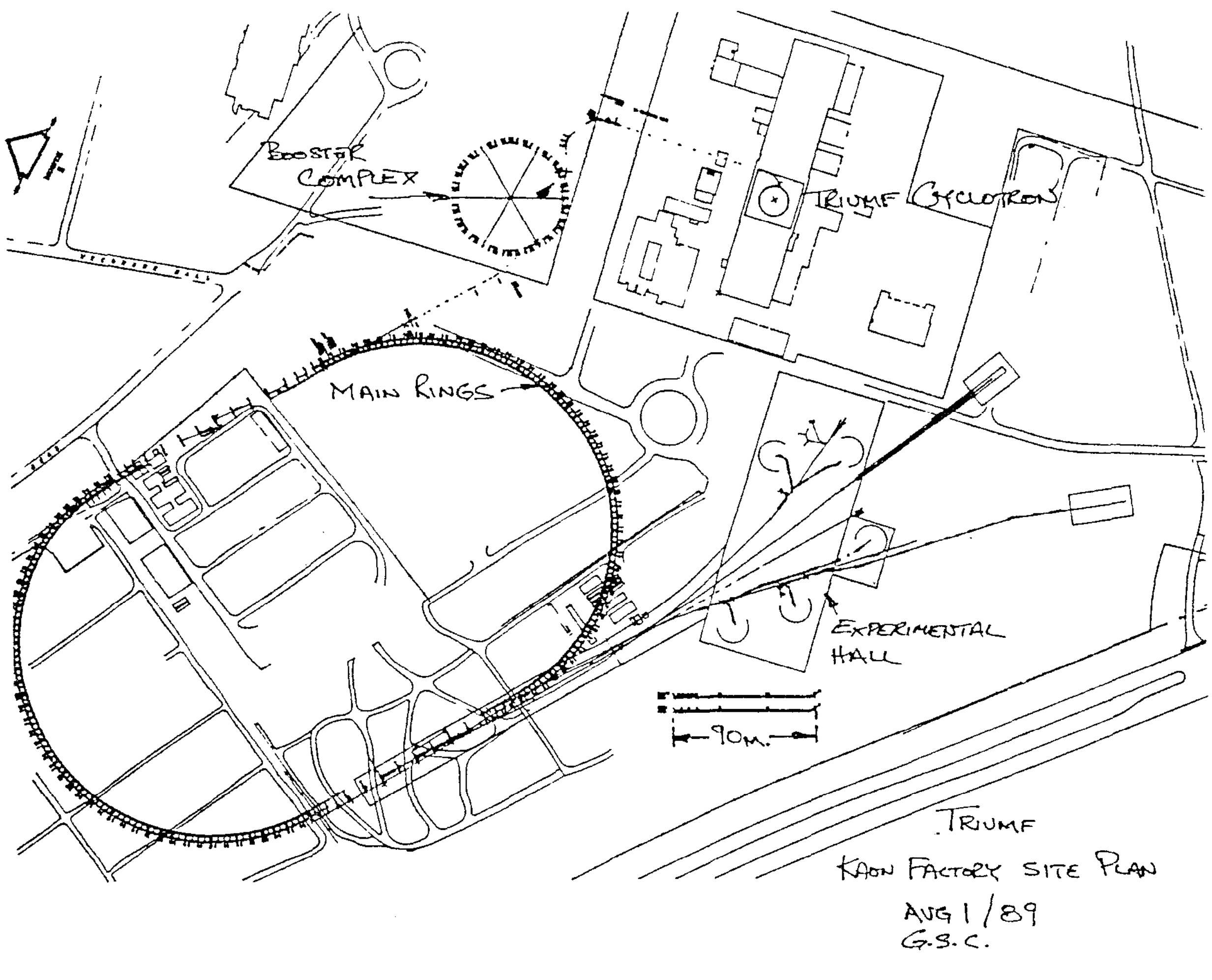

Figure 1.

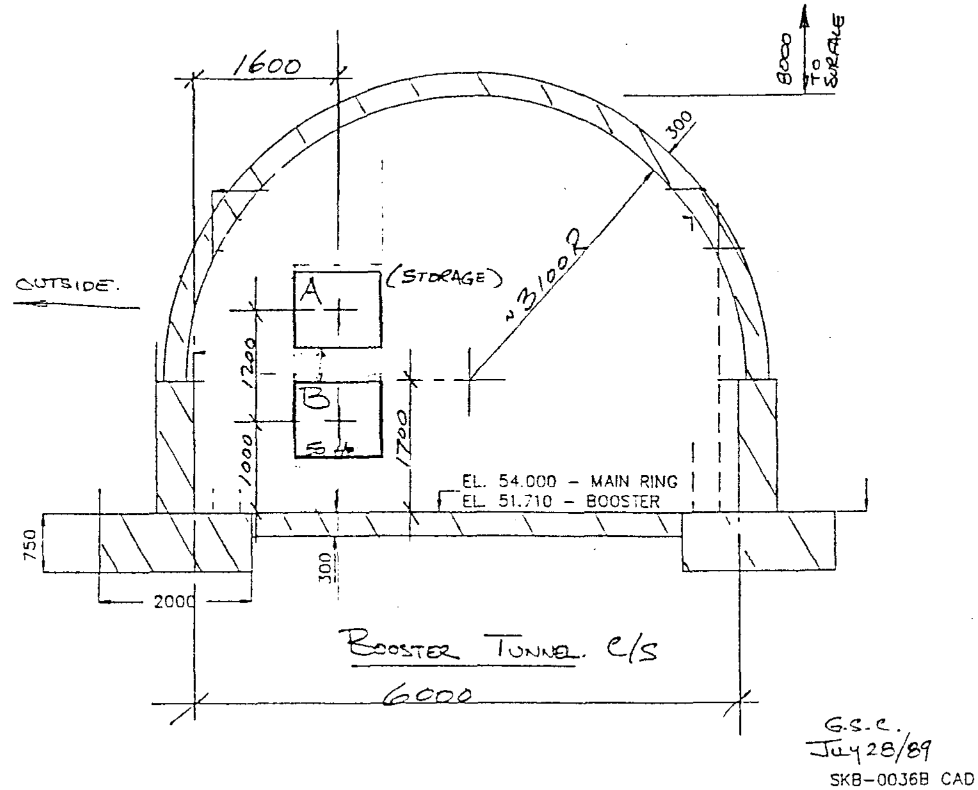

Figure 2.

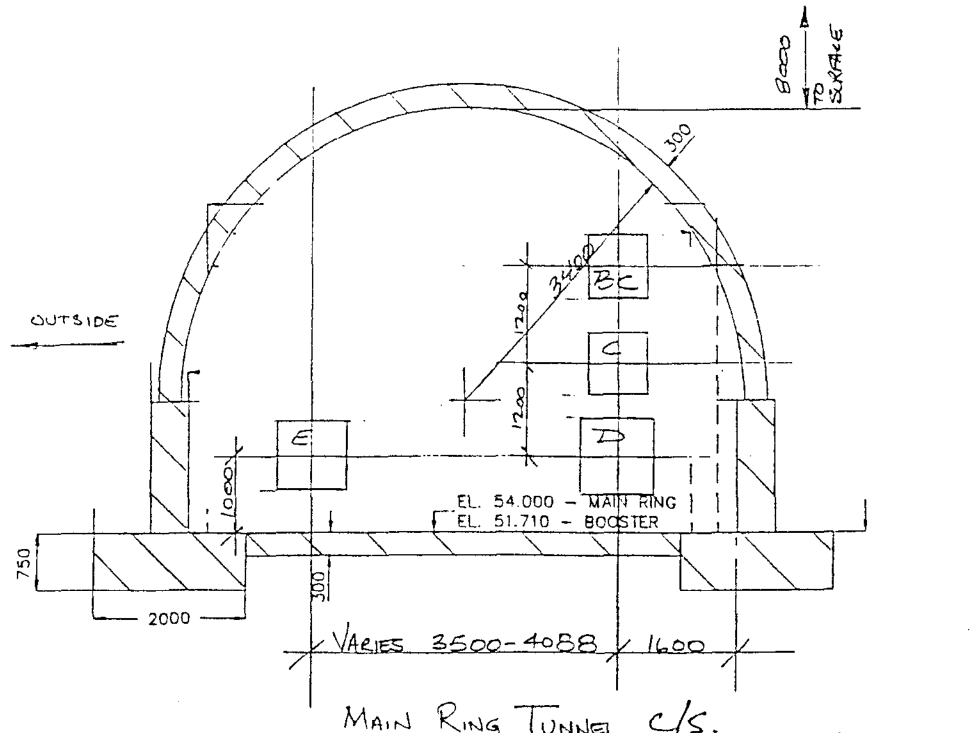

Figure 3.

A TEST FACILITY OF SUPER-ACCURATE ALIGNMENT SYSTEM FOR A LINEAR COLLIDER

N. ISHIHARA, S. IWATA, T. MATSUI, H. MATSUMOTO, H. MIZUNO,
T. SUMIYOSHI, S. TAKEDA, Y. TAKEUCHI, M. YOSHIOKA

National Laboratory for High Energy Physics, KEK

K. ISHIHARA, S. NAKABAYASHI, K. YASUDA

Kawasaki Heavy Industries, Ltd.

Japan

Abstract To develop an alignment system for Japan Linear Collider (JLC), a test facility consisting of a laser interferometer and piezo transducers has been constructed at KEK. The fundamental test using the sine wave disturbing vibration shows the distance between the interferometer head and the corner cube has been kept stable within an accuracy of 50 nm up to 20 Hz by the feedback technique, called active alignment method. The experiment with the random frequency disturbance suggests this system can be extended to the possible super-accurate alignment system.

INTRODUCTION

In the design study of JLC,[1] the beam size is calculated to be about 2 nm at the final focusing region, so the usual ground motion with the amplitude of the order of 100 nm becomes a serious problem for the alignment of final focusing magnets. While the high frequency components are easily reduced by the conventional damping method, the lower components below 10 Hz are quite difficult to suppress owing to a low specific frequency of a passive vibration-proof table. One thus needs tables or girders which are actively controlled to keep their relative positions stable against low frequency disturbances.

We have constructed a test facility to understand the girder control system using a laser interferometer and piezo transducers. In this report we will describe the facility components, the frequency dependence obtained by sine wave experiment and the test results using the white noise (random frequency noise) as the disturbing microtremor.

TEST FACILITY

Since the initial goal of the present test facility is to keep the distance stable as accurately as 50 nm at the maximum length of 1 m, the wave length of laser is required to be stable to $5x10^{-9}$. We also use the facility in a vacuum vessel to avoid the effect of air turbulence. From these points of view, we chose the separate-function laser system, called L-IM-10 (He-Ne laser of Tokyo Seimitsu Co.,Ltd.), in which the interferometer head is connected by fiber cables to the laser generator and to the fringe counter. We can easily install the head in the vacuum space by using a feed flange for fiber cables without any beam alignment.

The piezo transducer should have low driving voltage to avoid possible discharge in the vacuum space, and to have good linearity to achieve fast response in the feedback system. The selected transducer is Model P-841.20 of Physik Instrumente Co., driving voltage of which is 100 V for the expansion of 30 μm. The transducer has a position sensor installed in the same casing. It is thereby possible to get as excellent linearity as 0.1 % of full scale.

The control stage made of stainless steel has a double structure, the upper and the lower stage with the same direction of moving axis. In order to measure the real motion of the stages, a capacitance microsensor with the accuracy of 2 nm for 1 μm displacement has been also installed into each stage. It was found by the actual measurement that the yawing angle is less than 0.2 sec, resonant frequency 250 Hz, response time 40 msec/μm and load capacity 20 kg. The resonant frequency is high enough in comparison with the operating frequency of less than 20 Hz. Details of the test facility are described elsewhere.[2]

TEST

The block diagram and the picture of test facility are shown in Fig.1 and 2, respectively.

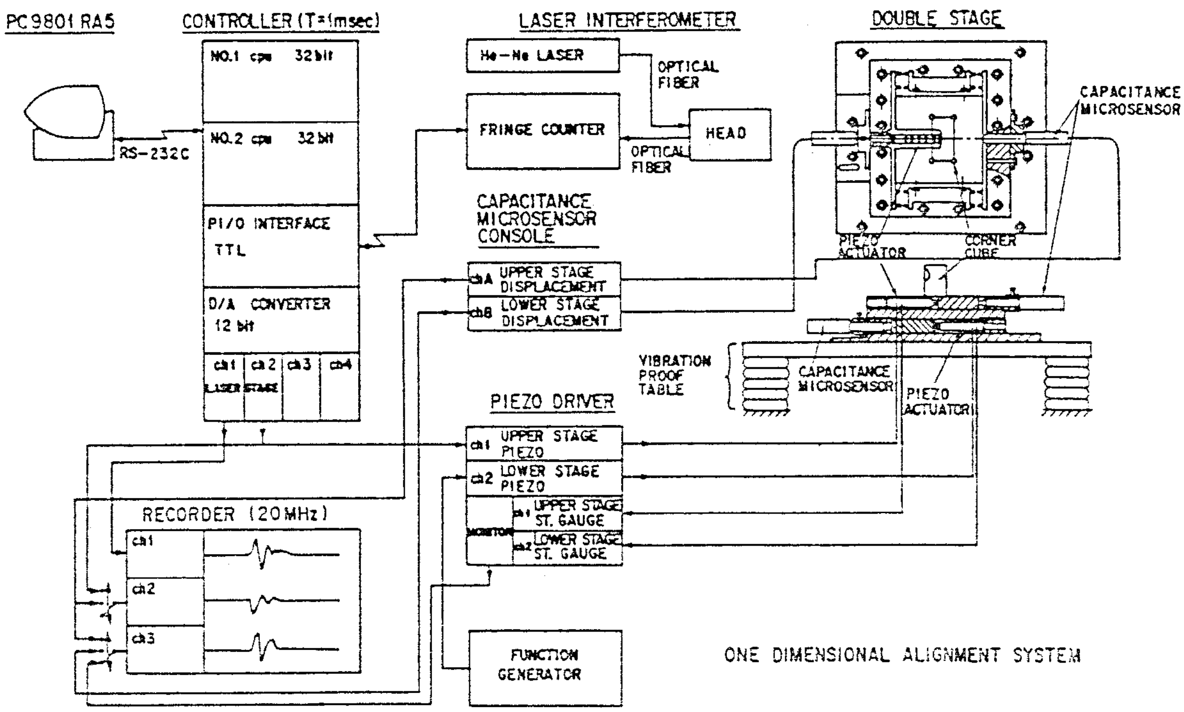

FIGURE 1 Block diagram of the test facility.

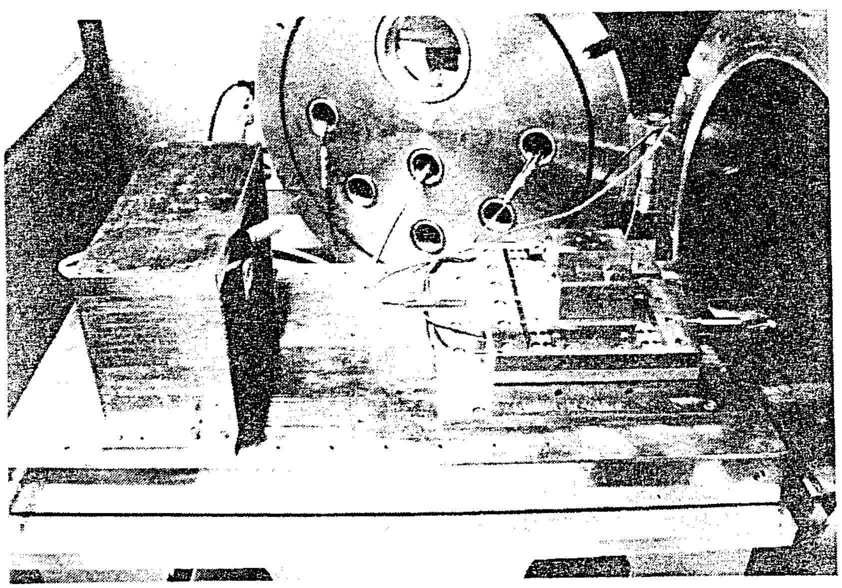

FIGURE 2 Picture of the test facility.

The corner cube is mounted on the upper stage and the interferometer head is located 28 cm from the corner cube as shown in Fig.2.
The vibration-proof table supports the whole components. The lower stage gives disturbing movements to the upper stage with an arbitrary wave form. The laser system measures the distance between the interferometer head and the corner cube with the sampling time of 1 msec. The CPU of the controller calculates the counteraction required to keep the corner cube stable, and then drives the piezo transducer of upper stage. Results of the test at 1 atm are shown in Table I for sine wave vibrations with amplitude of 500 nm.

TABLE I Vibrations after the position control against the disturbance of 500 nm amplitude.

Frequency (Hz)	Amplitude (nm)	Damping (dB)
0.1	19	-28
0.2	18	-29
0.5	19	-28
1	18	-29
2	25	-26
5	27	-25
10	30	-24
20	52	-20
30	77	-16
40	97	-14
50	190	-8.6

One can see that the damping of 20 dB or more is obtained up to 20 Hz. Especially for the vibration of less than 10 Hz, we can keep the stage stable within 30 nm. Figure 3 shows the typical damping feature observed on the oscilloscope, when a 10 Hz sine wave of 500 nm amplitude is added as disturbance.

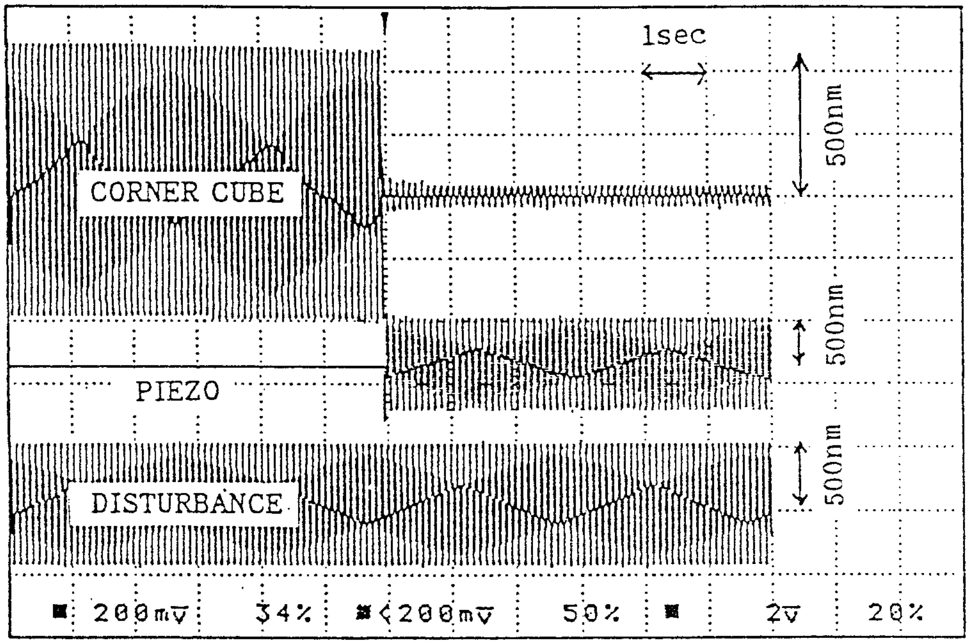

FIGURE 3 Typical damping seen on the oscilloscope against the disturbances of 10 Hz sine wave with 500 nm amplitude.

To investigate the response to the random frequency vibration, white noises with different cutoff frequencies are added as disturbances. Results are shown in Table II.

TABLE II Vibration damping against the white noise disturbances.

Cutoff Freq. (Hz)	Noise Amp. Max.P-P (nm)	Controlled Amp. Max.P-P (nm)	Damping (dB)
3	1380	50	-28.8
10	1920	100	-25.6
30	2220	300	-17.4
50	1980	630	-10.0

Figure 4 shows the typical display on the oscilloscope for the damping response against the white noise of 10 Hz cutoff frequency. The test in vacuum was performed without the capacitance microsensor, and we have obtained the same results.

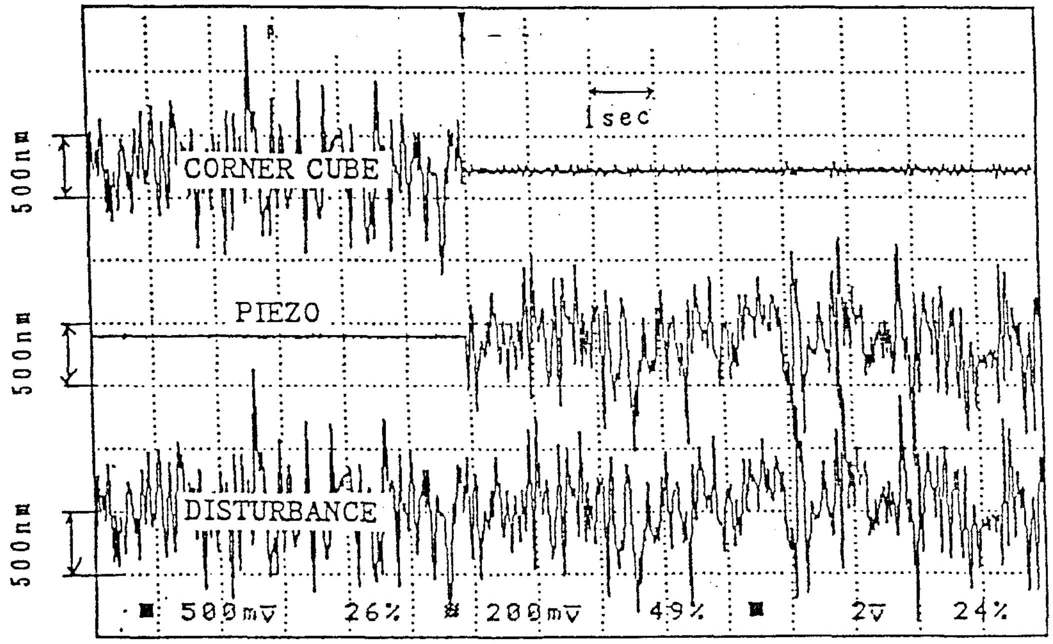

FIGURE 4 Typical display of the damping response against the white noise with 10 Hz cutoff frequency.

SUMMARY

The first test of the single axis active alignment was performed with a combination of laser interferometer and piezo transducer. Against sine wave vibration of 500 nm amplitude, the position has been controlled to better than 50 nm for frequencies up to 20 Hz. It has also been demonstrated that the damping is strong enough against the random frequency noise when the frequency components higher than 20 Hz are reduced by other methods.

ACKNOWLEDGEMENT

We would like to thank Prof. H.Sugawara, director general of KEK, for the encouragement of this work. Thanks are also due to Profs. Y.Kimura, K.Takata of KEK and Dr.T.Atsuta of Kawasaki Heavy Industries, Ltd. for their supports of this project. We appreciate the technical supports of KHI staffs.

REFERENCES

1. K.Takata and Y.Kimura, this conference.
2. N.Ishihara et al. Presented at the First International Workshop on Accelerator Alignment,SLAC July 31 1989

THE GEODETIC APPROACH FOR HERA

F. LÖFFLER, W. SCHWARZ

Deutsches Elektronen Synchrotron
Hamburg, West Germany

Abstract

At DESY in Hamburg the electron-proton-collider HERA is under construction. The demanded relative accuracy of some tenths of a millimeter can be achieved by specific alignment techniques and survey equipment. Methods and first results are described.

1. Introduction

HERA is a high energy accelerator, which is presently under construction at DESY in Hamburg. It consists of two independent storage rings designed for 30 GeV electrons and 820 GeV protons (Fig. 1). The counter-circulating beams collide head on in interaction regions, which are located in three of the long straight sections. In the regions close to the interaction points protons and electrons are within the same vacuumpipe. Then they are separated. While the electrons are kept in the e^- plane, the protons are brought to a higher level. At the end of the straight sections the height difference between electron and proton beam reaches 0.81 m and is then kept constant in the arcs of HERA, so defining the plane of the proton machine. The circumference of HERA is 6.335 km. All magnets for the e^- ring are normalconducting. The magnets of the proton ring are normalconducting in the straight sections, but superconducting in the arcs.

For the operation of HERA the other DESY-machines are used as preaccelerators. Electrons as well as protons are generated in linear accelerators (Linac I, Linac III). Then they are preaccelerated in the synchrotrons DESY II and DESY III respectively up to 7 GeV and transferred to the storage ring PETRA for further acceleration, the electrons up to 14 GeV and the protons up to 40 GeV. With these energies the particles are injected into HERA, the electrons clockwise, the protons anticlockwise.

Fig. 2 gives an overview of the area of Hamburg, where HERA is located. In the foreground the DESY-laboratory is shown surrounded by the PETRA-ring and private residential areas. In the center the HERA-ring is outlined with its four experimental halls. Only one is located within the DESY-site. The others were constructed on public ground. The HERA-tunnel lies in the western and southern regions beneath the DESY-laboratory and the residential areas. The rest of the ring is located predominantly under a large city park.

The HERA-machine-planes are not horizontal, but have an inclination of 1%. Therefore it was necessary to introduce a three-dimensional coordinate system to define the position of the accelerator components. These coordinates have to be projected to a reference sphere before they can be used for geodetic measurements.

Fig. 3 shows the dimensions of HERA with respect to the surrounding area and the orientation of the coordinate system. The sketched diameter gives the direction of the maximum inclination.

2. The Geodetic Network on the Surface

For the construction of the tunnel/2/ and the alignment of the machine a geodetic network on the surface was installed as shown in Fig. 3. Four points of this network were already given by the PETRA-system/1/. Three more had to be built especially for HERA. Near hall North a survey tower more than 20 m high was constructed. Another point was installed on the staircase-building of the "Volkspark-Stadion." The third is situated on a building near hall South.

All distances between the monuments are measured by the high precision electronic distance measuring instrument KERN ME 5000/3/, the height differences by precision leveling. The coordinates of the survey points then result from a least square fit of the observations.

Fig. 4 gives the results of several measurements of the combined PETRA-and HERA-network. The changes in position are not more than 1.5 mm. Since they include the actual movements of the monuments the achieved accuracy is sufficient for the alignment of the accelerators. Fig. 5 shows one of the PETRA-monuments, Fig. 6 the survey tower near hall North.

Additional survey monuments were built on top of the HERA-halls. Vertical steel pipes (diameter 0.4 m) were inserted in the ceilings and protected by concrete jackets. On top self-centering KERN-datums were mounted, as used for the other survey points at DESY/1/. In this case the datums are equipped on the underside with a target, which can be illuminated and seen from below. Each hall has one point. Its coordinates can be derived from distance and angle measurements from the neighboring monuments of the HERA-network (see Fig. 3). Fig. 7 shows the concrete pillar on top of hall South.

3. The Reference Traverse in the Tunnel

Special survey datums were developed for the tunnel. As Fig. 8 shows we chose steel plates with a well-machined surface and a centering bore. They are inserted in the concrete wall of the tunnel, which is used as a trail for the transport vehicle. Auxiliary pillars of aluminum can be mounted onto these plates. A pivot, which fits into the bore, gives the centering, a machined baseplate defines the vertical adjustment of the pillar, which can be attached by clamps onto the survey plate. On top of the pillar we again find the proved self-centering KERN-datum. It defines the actual survey point, so that reductions with respect to the baseplate are not necessary.

Over all we have 44 survey datums in each quarter of HERA, which have a distance of 35.2 m from each other. The underground system is completed by four plates, which are mounted on concrete platforms in the corners of each hall, and two auxiliary points in front of the tunnel mouths. The line of sight from these points to the adjacent corners of the hall pass through openings of the shielding wall, so that the connection of adjacent tunnel arcs is possible even when the experiment is in its final position (Fig. 9).

One of the four survey plates in the corners of each hall is located vertically below the pillar on the surface. A steel shaft is led through all floors, so that the illuminated target on top of the hall can be pointed at from below. By measuring zenith angles from the aluminum pillar in the hall to the surface point it is possible to determine the difference in x and y between the two points, once the height difference between theodolite and target has also been determined. The angle measurements have to be performed in two vertical planes, which are perpendicular to each other and orientated toward one of the adjacent survey points. The obtained accuracy for this coordinate-transfer from the surface to the tunnel level is better than 0.8 mm for height differences up to 32 m. We can use these points as reference points for the survey on one tunnel quadrant.

We have a basic traverse with distances of about 35 m and overlapping lines of about 70 m length. From each pillar the directions to the two preceding and the two following points are measured. The corresponding distances are determined from every second standpoint to minimize the observation time. In addition all necessary observations are done, which give the connection of the traverse with the reference points in the hall. For the angle measurements, we use precision theodolites KERN E2 (Fig. 10). The observation data is directly registered and analyzed by a handheld computer HUSKY-HAWK. The targets for the angle measurements have been used for many years in our other accelerators (Fig. 11). The distance measurements are carried out with the KERN ME 5000 (Fig. 12).

The complete position survey of one quadrant is performed in about 7 hours, when angle and distance measurements are made by two separate survey-teams. The standard deviation of the direction measurement is 0.1 to 0.2 mgon, that of the distance measurement better than 0.1 mm. The coordinates of the traverse points are obtained by a least square fit of our redundant measurements, where the reference points are used as fixed points.

4. Alignment of the Electron-Accelerator

In the arcs of the e^- ring the bending magnets and the preceding quadrupoles and sextupoles are fixed as one unit. The focusing magnets are mounted on a girder, which is connected with the dipole. They are aligned in the workshop with respect to the dipole.

In the tunnel the module rests on a support, which is arranged underneath the quadrupole. The dipole-end is placed on two screws of the following clockwise module for vertical adjustment. One of these screws fits in a groove, which allows an azimuthal movement of the dipole, while the radial position with respect to the following module is fixed. The height and inclination of the quadrupole side can be adjusted by two screws of the girder, which rest on hardened steelplates on top of the support. Radial and tangential corrections can be done by guide rods, which connect the girder and the support. Fig. 13 shows in side view the principle of the e^- configuration and also the protonmagnets above the electron machine. Fig. 14 gives details of the alignment mechanism.

For the positioning of the modules only one survey datum is necessary. Because of the inclined machine plane it has to define the position as well as the height. That was achieved by using the center of a sphere resting on a conical base, which is mounted on an aluminum platform. This then has to be attached to the side of the quadrupole and is centered by feet, which fit into grooves of the laminated iron. Additionally it carries a polished steel bar, which defines the radial inclination of the module. Fig. 15 shows this platform with a coincidence level.

The sphere used is of the CERN-type. The axis of its precision bore can be adjusted vertically with the help of a precision level at any position of the ring. Then it has to be locked in order to keep the vertical position during the subsequent measurements. Therefore a bearing cage has been developed, which in conjunction with a screwcap provides a fast lock and unlock procedure. In the precision bore of the sphere, with the use of an adapter, targets for angle measurements can be inserted as well as index marks for distance measurements or leveling rules for height measurements (Fig. 16).

With this equipment the alignment of the e^- modules was performed in two steps. First was a basic alignment of the magnets by polar measurements with respect to the reference traverse in the tunnel (Fig. 17). Since the survey points of the traverse are located directly opposite the reference sphere of each third quadrupole the azimuthal position of these spheres was achieved first by angle measurements with a very high precision. Simultaneously the radial position was corrected by reading a precision rule. Then the two adjacent quadrupoles were aligned by the given directions with respect to the reference traverse and the distances, which were measured with a tape from the magnet next to the traverse point. Necessary corrections of the inclinations and heights of the magnets were performed during the position alignment, using coincidence levels and precision leveling instruments. The reference points for the leveling procedure are inserted in the concrete wall beside the traverse plates. Their height was derived from precision levelings of the HERA-circumference.

Parallel to the adjustment of the quadrupole the dipole-end of the module had to be set to the correct value for height and inclination. Thus we used another platform which refers to the surface of the laminated iron of the dipole. Like that for the quadrupole it carries a steel bar for the inclination measurement. For the height control a special sphere is used.

Since the dipole-end of the module rests on the girder of the following clockwise module, the alignment procedure had to follow the ring counterclockwise. So there was no influence on the magnets, which has been adjusted before.

The accuracy of this basic alignment was about 2 mm. Since the final value in radial position and in height should be within some tenths of a millimeter, a second alignment procedure had to follow. Thus we performed a continuous position survey directly from the survey-spheres of the quadrupoles with respect to the neighboring magnets. By measuring the directions from one reference sphere to the two preceding and the two following ones (Fig. 17) one gets a high relative accuracy for the radial offset of the quadrupoles, whereas it is not necessary to take care of the traverse points in the concrete wall anymore.

To achieve these measurements we copied an adapter of CERN, which allows the combination of a CERN-reference-sphere with the self-centering datum of KERN. Thus the use of the KERN-targets and theodolites for the horizontal-angle measurements was possible (Fig. 18). As for the measurements of the reference traverse the observation data was directly transferred to the computer, so that the complete survey of one arc of HERA (100 modules) could be accomplished in one day.

The calculation of the least square fit of the direction-measurements was done with the nominal values of the distances between adjacent quadrupoles. As reference coordinates the nominal coordinates of all quadrupole-spheres were used. From the differences between calculated and nominal coordinates finally the radial deviations were derived.

Fig. 19 shows the results of such a survey of an arc. The calculated deviations are liable to a systematic deformation, which might be caused by horizontal refraction during the angle measurements as well as by inaccuracies of the self-centering of the theodolites and targets. Since it is not important for the machine that the magnets are on their nominal position, but that they are aligned on a smooth line, it is possible to calculate a best fit curve and to define the radial deviations with respect to this curve. The necessary alignment was performed using dial gauges. Then a complete control survey was carried out. In our example (Fig. 20) the results of the alignment were sufficient: the deviations from the calculated function are within some tenths of a millimeter.

The procedure for the vertical alignment of the magnets is very similar to that of the radial component. To obtain the necessary accuracy until now the height differences between adjacent quadrupoles were measured directly by precision leveling and the corrections were made with respect to the best fit curve. In the future it will be possible to measure both components at the same time. By the development of a theodolite-support, which rests directly in the conical base of the survey-platform the CERN-reference-spheres with the complicated adjusting and locking procedure will then no longer be necessary. The support centers itself by the lower part of a reference sphere. The vertical axis of the theodolite can be adjusted by two screws of the support, while that of the theodolite are locked in a medium position. So the height of the line of sight of the E2-theodolite is well defined and constant. As targets Taylor-Hobson spheres will be used, which can be inserted directly in the conical bases as well. By one pointing to the target the horizontal direction and the zenith angle are available and can be read out by the computer. The height differences then can be derived from the zenith angle measurements. Fig. 21 shows the underside of the new support and the conical base on top of the survey platform for the proton magnets.

5. Mounting of the Proton-Machine

The electron-machine is complete and made its first successful test run in

August/September 1988. In the meantime began the mounting of the superconducting magnets for the proton ring. As shown in Fig. 13 the proton cell has two dipoles and one quadrupole. Each magnet rests on the jibs of two supports, which overhang the e^- machine (Fig. 10). The height adjustment of the dipoles is performed by four independent screws: two on each jib. From the four feet of the quadrupoles two are coupled by a brace with a central pivot point, so creating a three-point support. Radial and tangential corrections can be carried out by similar guide rods as used for the e^- machine.

Each magnet can be equipped with two survey platforms, which are similar to those of the e^- ring (Fig. 21). They are attached to the side of the magnet by a tension-screw with respect to a plane, which is defined by the ends of three radial screws. The position in height is given by two vertical screws, which the platform rests upon. In azimuthal position a finger from the survey platform is fixed by reference screws respectively. All these screws are adjusted with respect to the geometrical axis and the main planes of the magnets by the construction companies. After delivering to DESY the position and inclination of the survey platforms are controlled and corrected, if necessary. Then the magnets are cooled down for the magnetic field measurements, which finally provide the position of the two reference spheres and the inclination of the reference bars on top of the survey platforms with respect to the magnetic field. With these values the nominal coordinates of the spheres and the corresponding inclinations for the foreseen location of the magnets in the HERA-tunnel can be calculated.

To perform the magnet alignment we once more have to refer to the tunnel traverse. Because of the height difference between the aluminum pillars and the proton ring and the different azimuthal distribution of the survey platforms a slightly changed procedure compared to the e^- ring is applied. First the position and height of one survey platform of a dipole is determined by angle measurements with the E2-theodolite using the new equipment as described before (Fig. 22, Fig. 23). Spherical targets of Taylor-Hobson are also used for the auxiliary pillars (a special adapter has been constructed on this behalf). Their height is determined by precise leveling. The directions to adjacent traverse points and to the second reference sphere of the standpoint-magnet are read in both the horizontal and vertical plane (Fig. 24) and registered by a computer. At the moment we use a COMPAQ SLT 286. Later on we will change to the MS-DOS-version of the HUSKY-HAWK, which is more compact and has a higher battery capacity. Additionally the horizontal angles to a 1 m-scale-bar on top of the next traverse pillar are measured. From the stored data the computer calculates the three-dimensional deviations of the two magnetpoints from their nominal values as well as the horizontal and vertical directions to the targets on the two preceding and the two following magnets in their nominal position. The theodolite telescope has to be set on these directions, while the corresponding magnets have to be moved horizontal and vertical until the crosshair of the theodolite covers the center of the target. For the azimuthal corrections the use of a steeltape is sufficient, which is fastened at one end to a reference point of the survey platform with the theodolite and read at the other end with an indexmark. The value of the nominal distance is shown by the computer also. Simultaneously the nominal inclinations of the survey platforms have to be achieved. They are measured by two Schaevitz-levels. The deviations with respect to the nominal values are read out continuously by a HUSKY-computer.

When the alignment of the neighboring magnets is finished, that of the standpoint magnet has to follow. Therefore the theodolite is mounted on a nearby survey platform. The radial and vertical deviations are transformed in correction angles and the magnet is moved respectively. The tangential corrections are controlled by tape-measurements.

The final control of the alignment is achieved by angle and distance measurements from the survey platforms similar to the procedure for the e^- ring. On principle certain dipole platforms are chosen as standpoints, as shown in Fig. 24. The magnet traverse is determined by angle measurements between the two preceding and the two following standpoints and the corresponding distance measurements. Additionally all survey datums of the magnets between adjacent standpoints are pointed at with the theodolite, so that these spheres are taken into account at least twice. If necessary connecting measurements to the reference traverse are performed. Then the least square fit of the redundant observations is made with respect to the used reference points.

Up to now a string of seven protonmagnets was mounted completely, so that a first test of the described alignment and control procedure was possible. Fig. 25 shows this part of the HERA-tunnel during the control measurements, Fig. 26 the Schaevitz-level on top of the survey platform and the reading index for the tape measurements. The results of our test alignment were encouraging. The following control measurement showed radial and vertical deviations from the nominal values within $\pm$ 0.3 mm. A second control survey reproduced the values of the first one to better than 0.1 mm.

The achieved accuracy is sufficient for the basic alignment of the proton ring. The final alignment will be performed, when all superconducting magnets of one arc are mounted and pre-aligned. The overall control measurement then gives coherent results for the remaining radial and vertical deviations. As for the e^- ring connections to the reference traverse then can be relinquished. The least square fit will then refer to the nominal coordinates of the magnet spheres.

6. References

/1/ **Löffler, F.:** Geodätische Präzisionsvermessung des Groß-Speicherringes PETRA. Allgemeine Vermessungs-Nachrichten 86 (1979) 8/9, 301-305.

/2/ **Löffler, F.:** Vermessungsarbeiten beim Bau des Beschleunigertunnels für HERA. Ingenieurvermessung 88, Beiträge zum X. Internationalen Kurs für Ingenieurvermessung, Beitrag D5; Dümmlerbuch 7808, Bonn 1988, ISBN 3-427-78081-3.

/3/ **Maurer, W.; Schirmer, W.; Schwarz, W.:** Wirkungsweise und Einsatzmöglichkeiten des Mekometers ME 5000. Ingenieurvermessung 88, Beiträge zum X. Internationalen Kurs für Ingenieurvermessung, Beitrag A10; Dümmlerbuch 7808, Bonn 1988, ISBN 3-427-78081-3.

7. Figure Captions

Fig.1

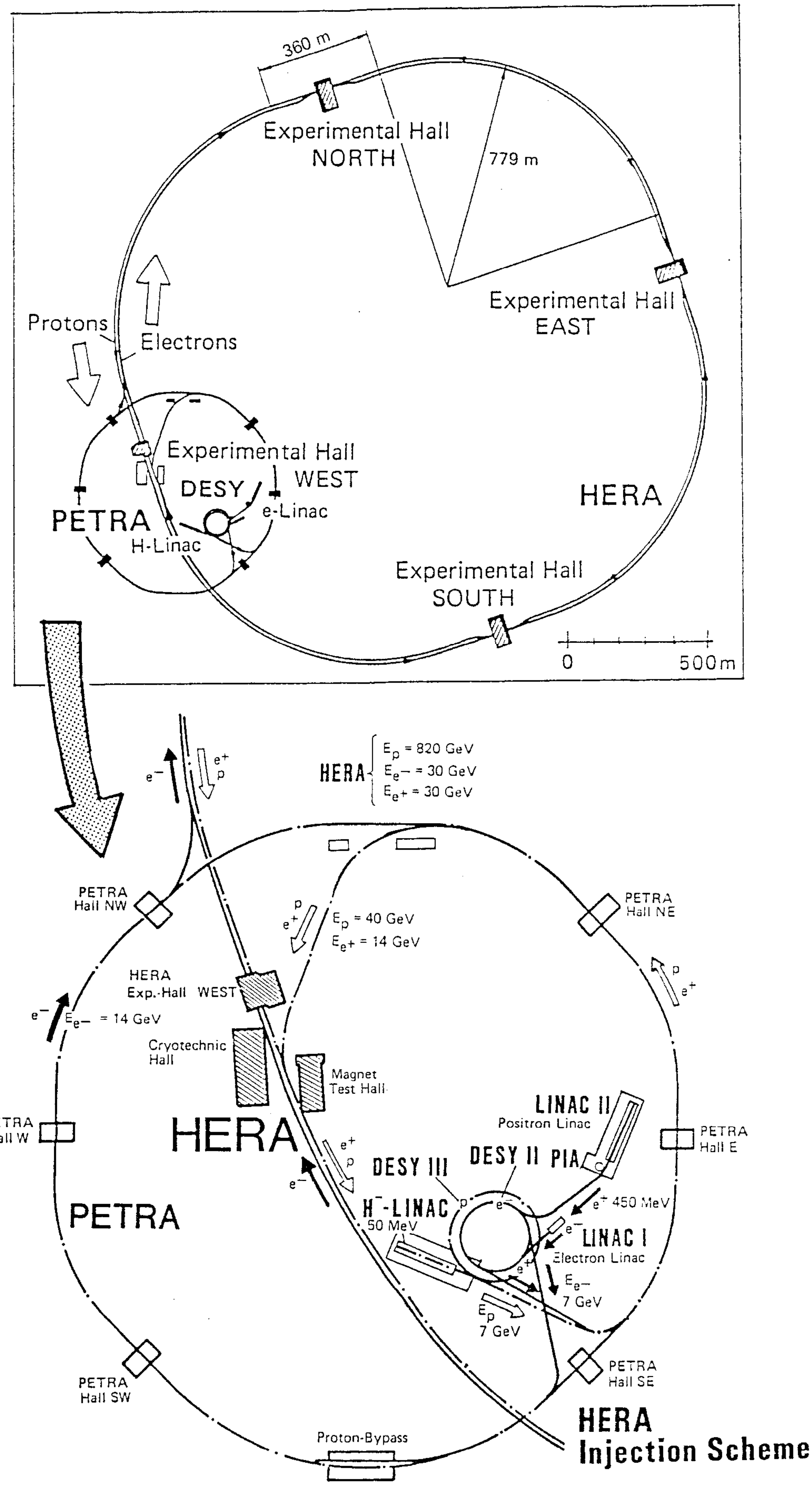

360 m
Experimental Hall
NORTH
779 m
Experimental Hall
EAST
Protons
Electrons
Experimental Hall
WEST
DESY
e-Linac
PETRA
H-Linac
HERA
Experimental Hall
SOUTH
0
500m
HERA
E_p = 820 GeV
E_{e^-} = 30 GeV
E_{e^+} = 30 GeV
PETRA Hall NW
PETRA Hall NE
E_p = 40 GeV
E_{e^+} = 14 GeV
HERA Exp.-Hall WEST
E_{e^-} = 14 GeV
Cryotechnic Hall
Magnet Test Hall
LINAC II
Positron Linac
PETRA Hall W
HERA
DESY III
DESY II
PIA
PETRA Hall E
PETRA
H$^-$-LINAC
50 MeV
e^+ 450 MeV
LINAC I
Electron Linac
E_{e^-}
7 GeV
E_p
7 GeV
PETRA Hall SW
PETRA Hall SE
HERA
Injection Scheme
Proton-Bypass

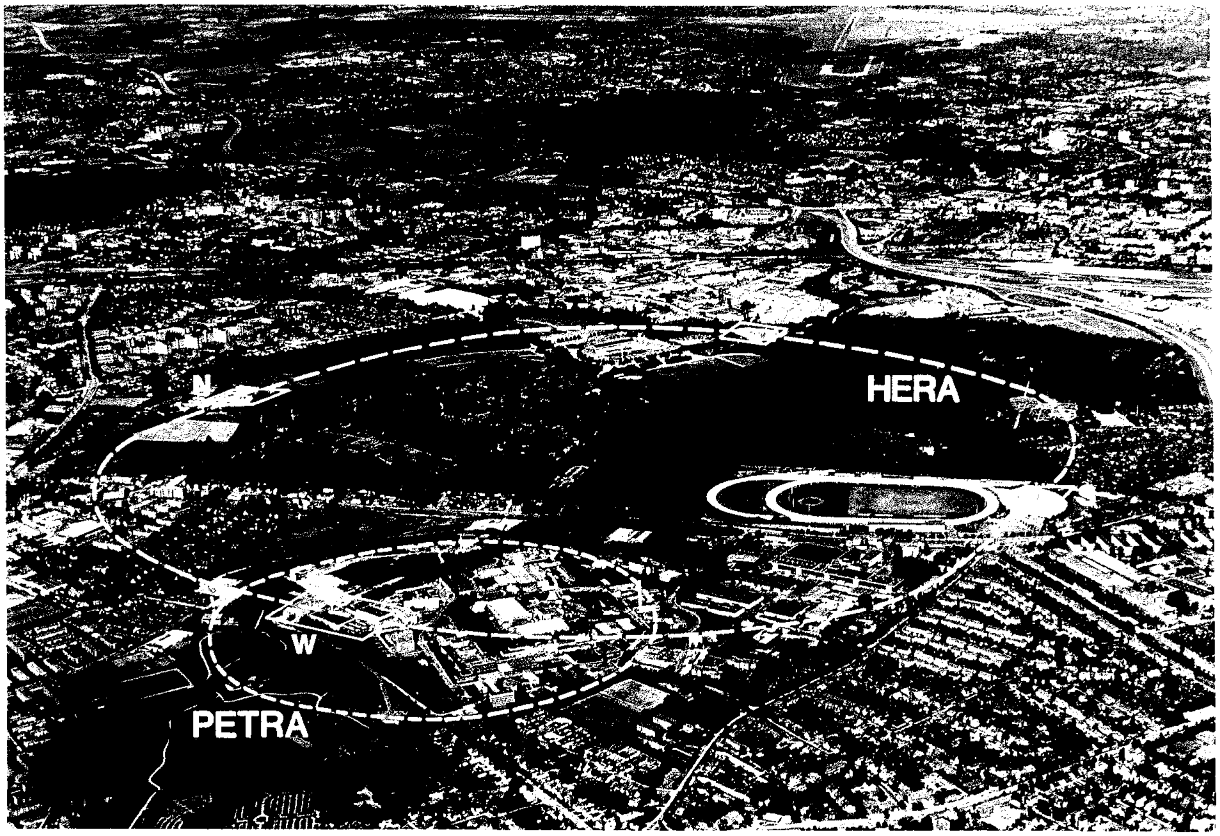

Fig. 2

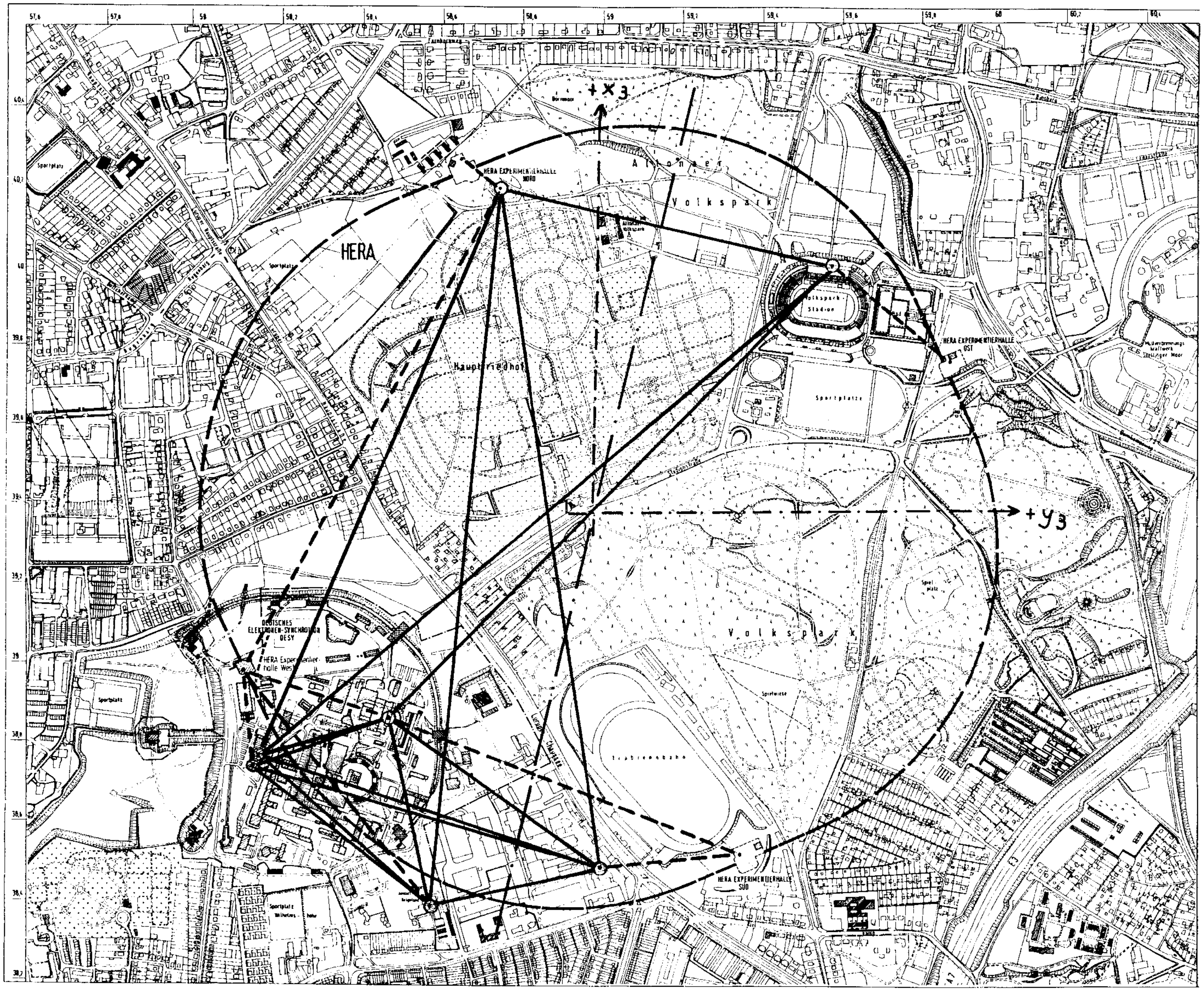
+x3
+y3
HERA
Volkspark
Hauptfriedhof
Sportplatz
HERA EXPERIMENTIERHALLE NORD
HERA EXPERIMENTIERHALLE OST
HERA EXPERIMENTIERHALLE SÜD
DEUTSCHES ELEKTRONEN-SYNCHROTRON DESY

Fig. 3

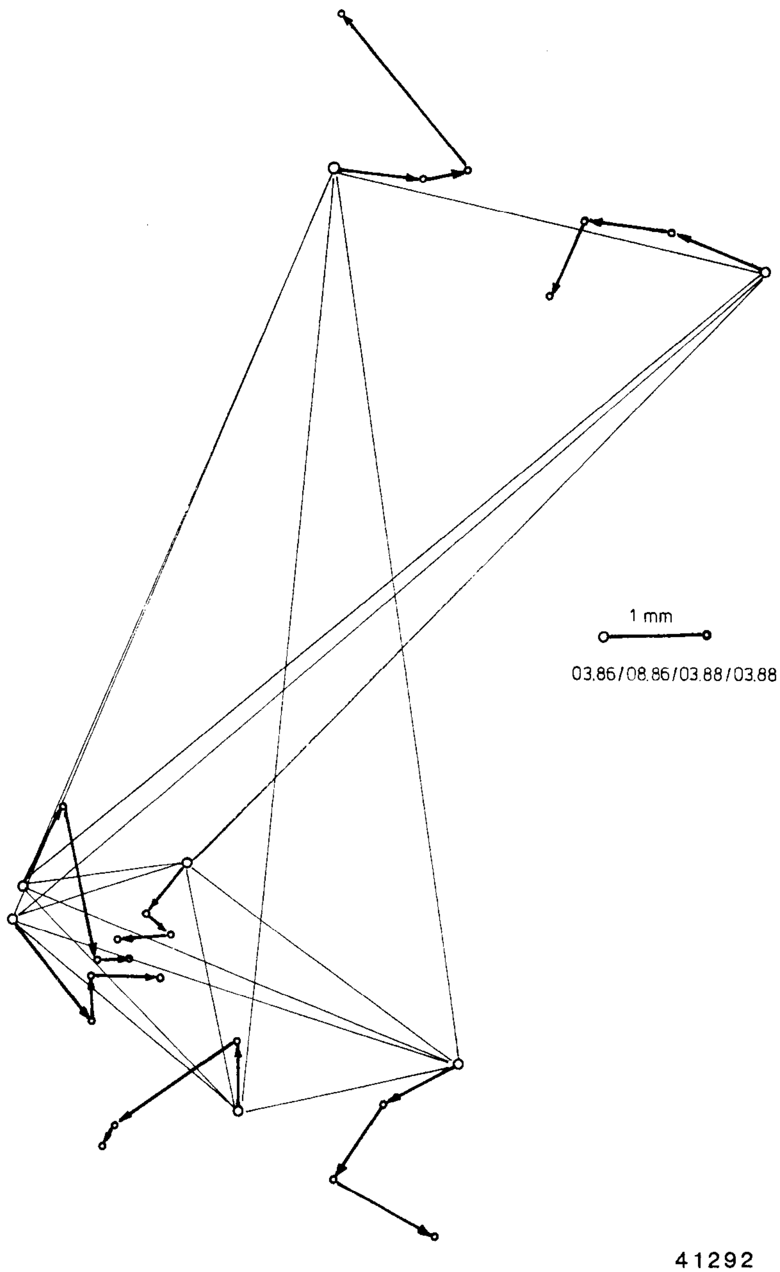

Fig. 4

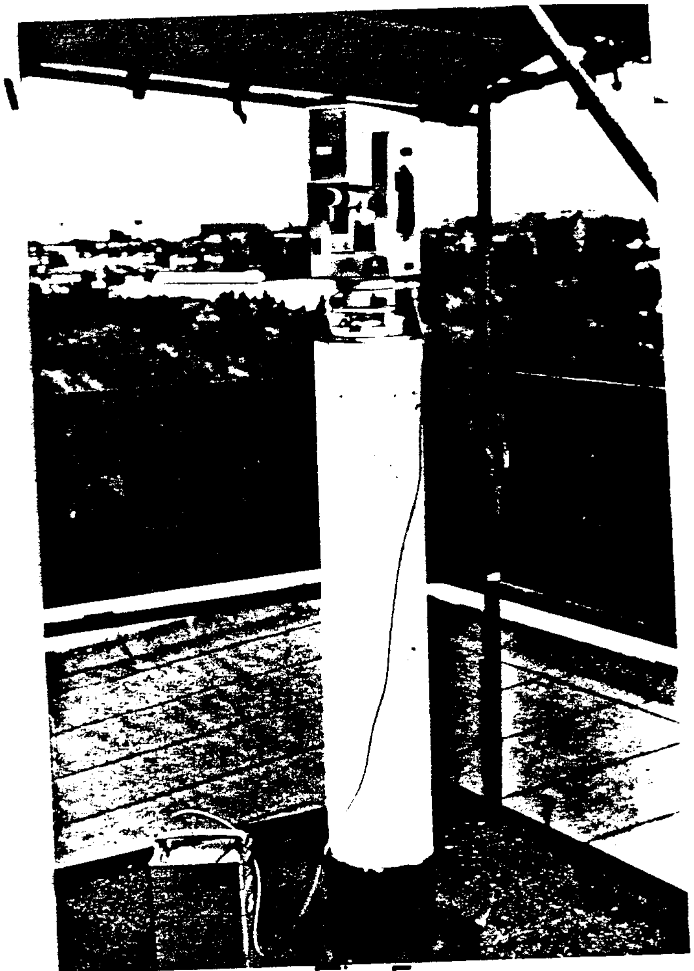

Fig. 5

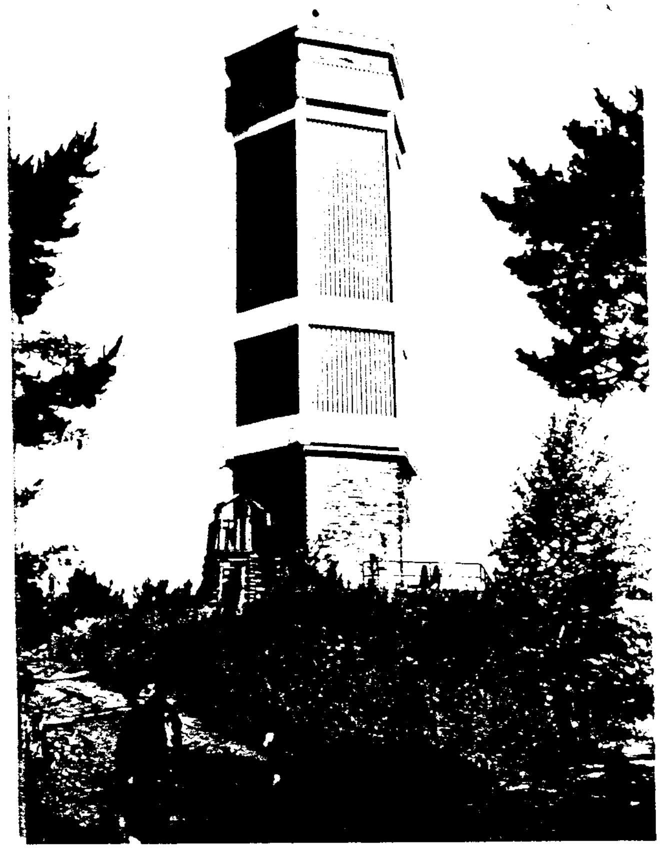

Fig. 6

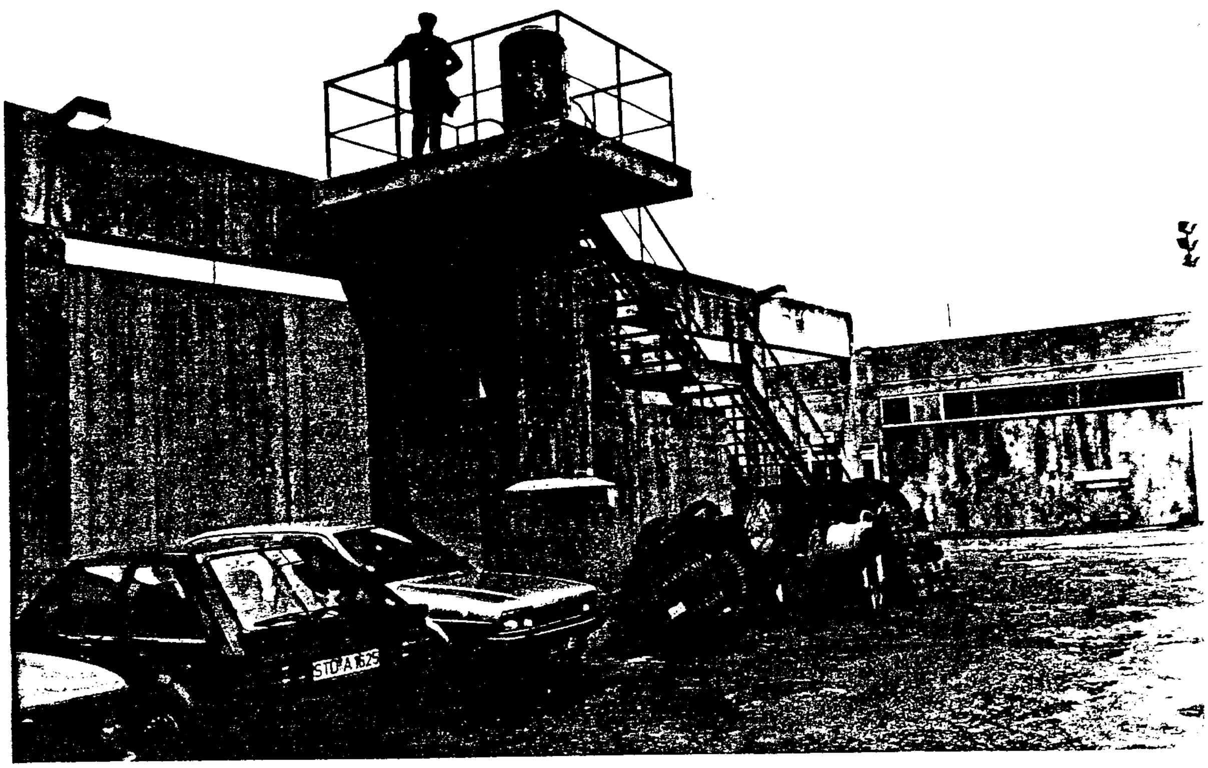

Fig. 7

Fig. 8

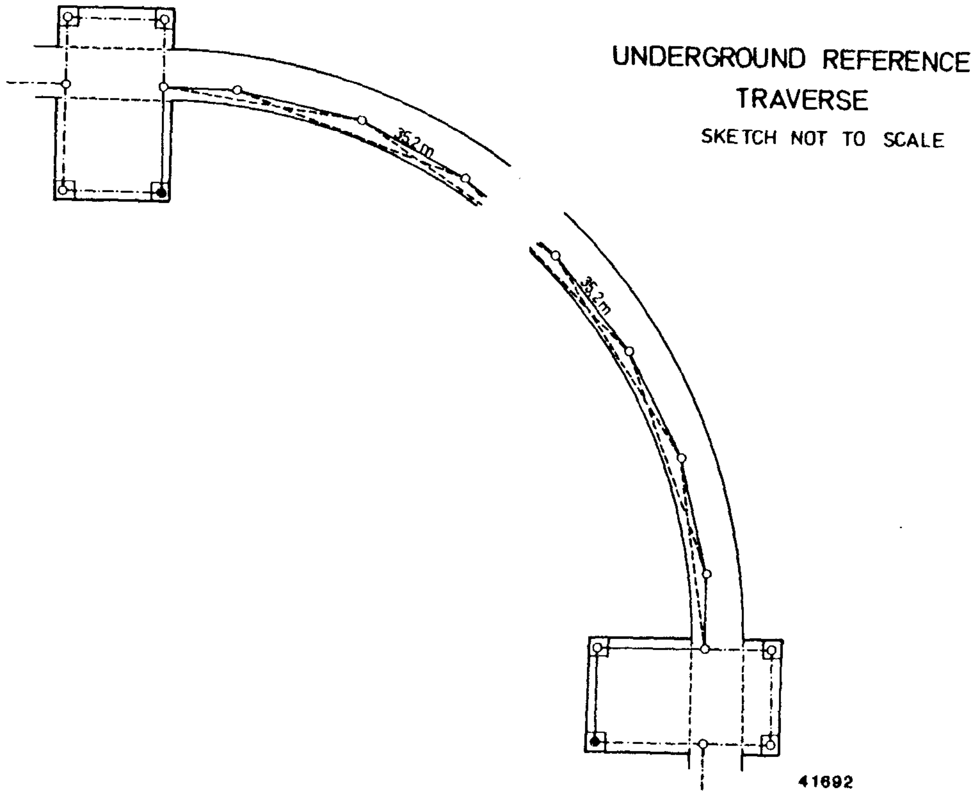
UNDERGROUND REFERENCE
TRAVERSE
SKETCH NOT TO SCALE
35.2m
35.2m
41692

Fig. 9

Fig 10

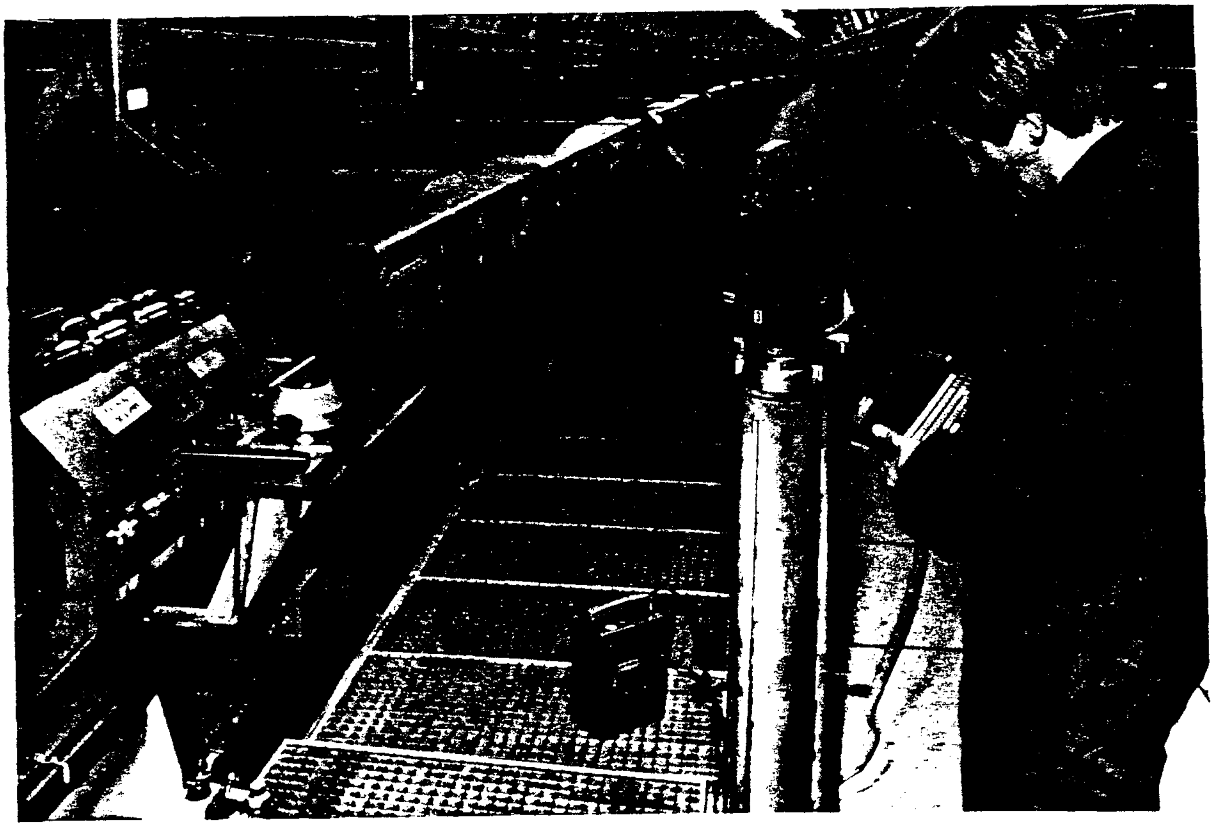

Fig 11

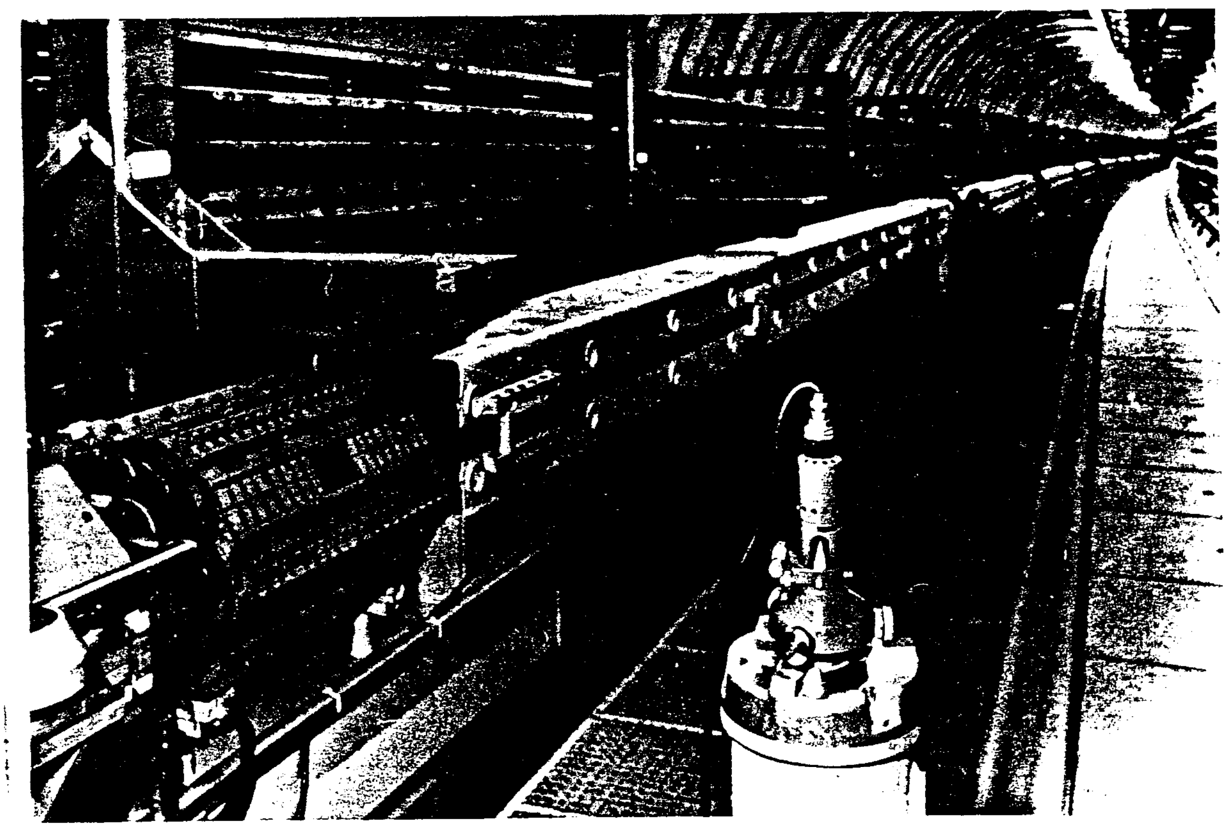

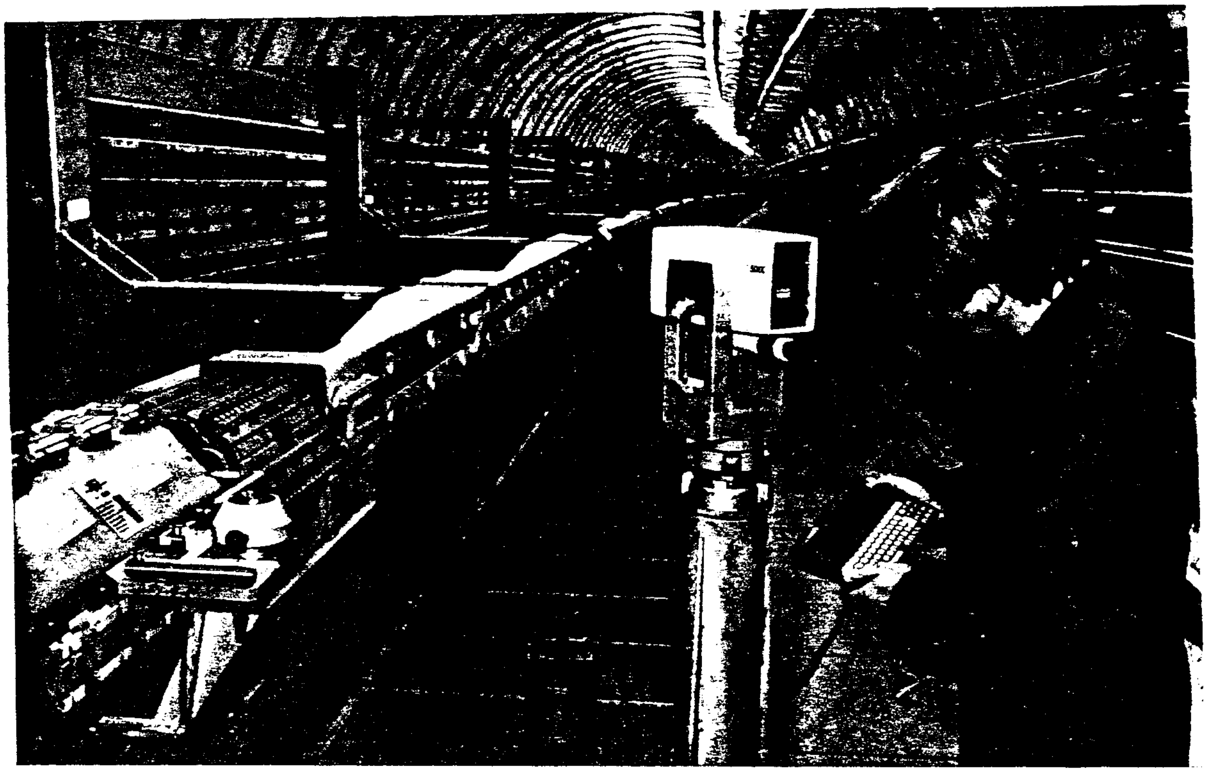

Fig.12

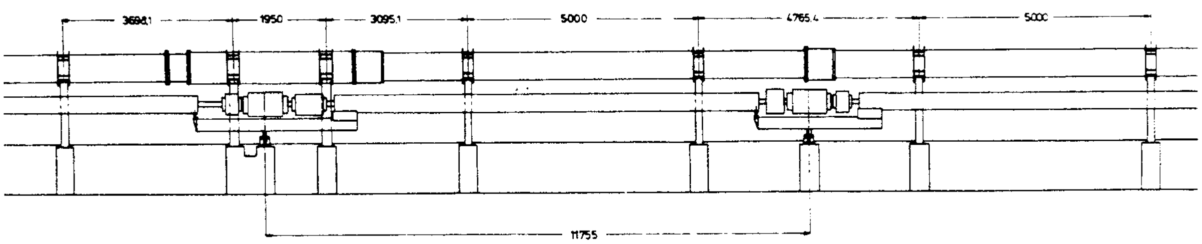

HERA - NORMAL - CELL

41693

Fig.13

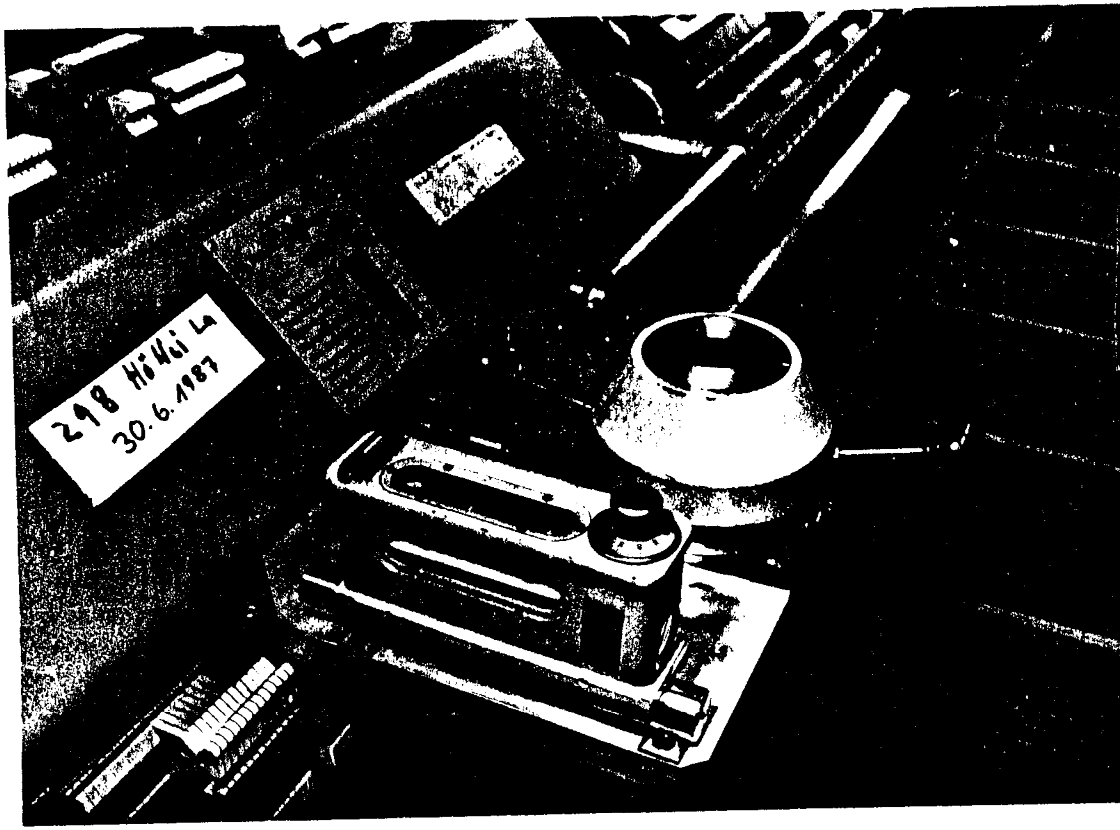

Fig.14

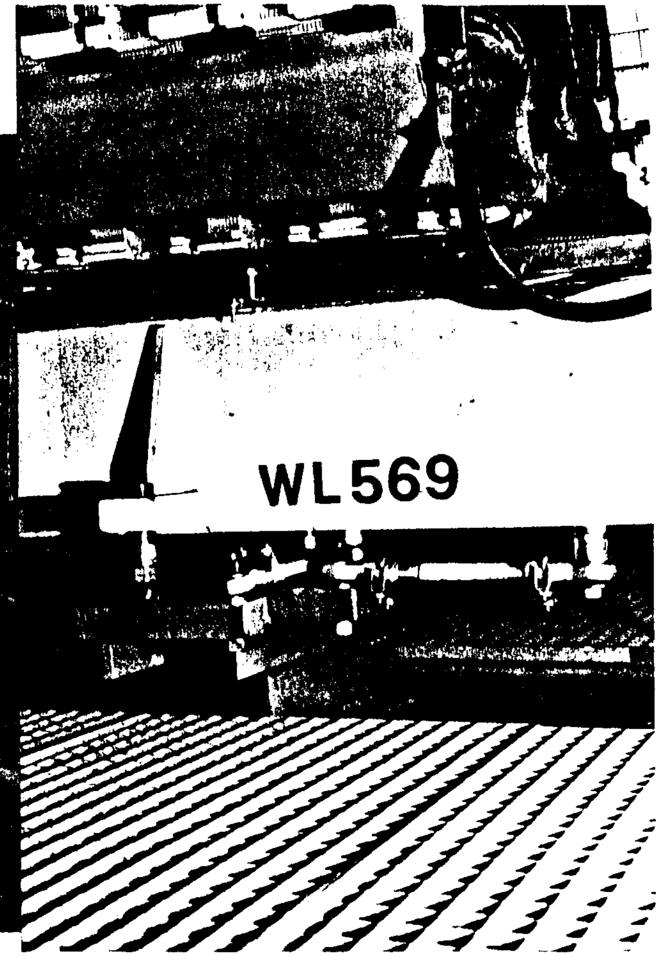

Fig.15

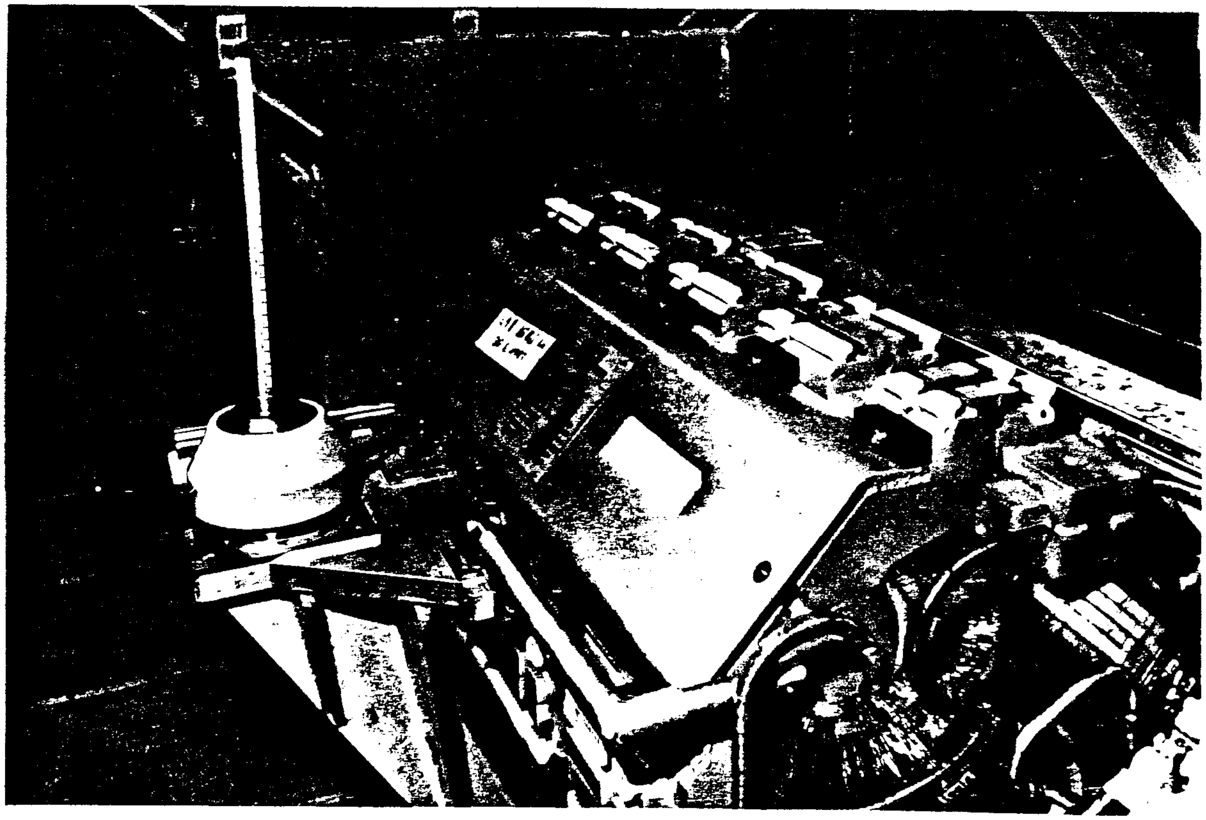

Fig.16

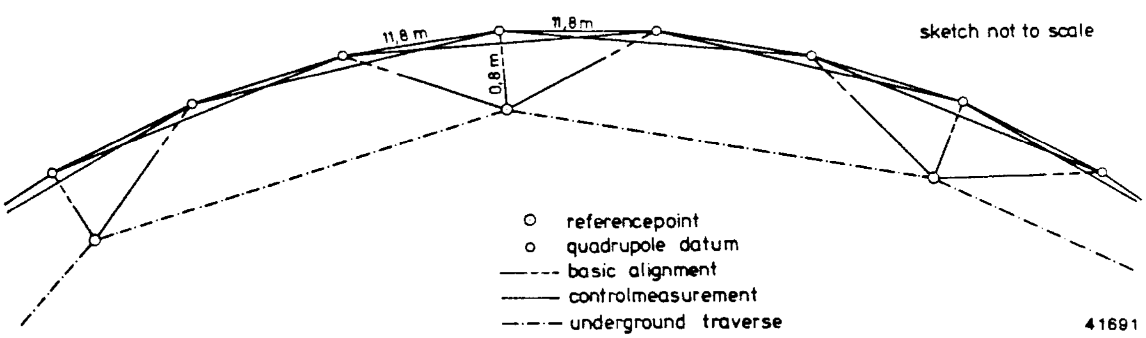
11,8 m
11,8 m
0,8 m
sketch not to scale
o referencepoint
o quadrupole datum
basic alignment
controlmeasurement
underground traverse
41691

Fig.17

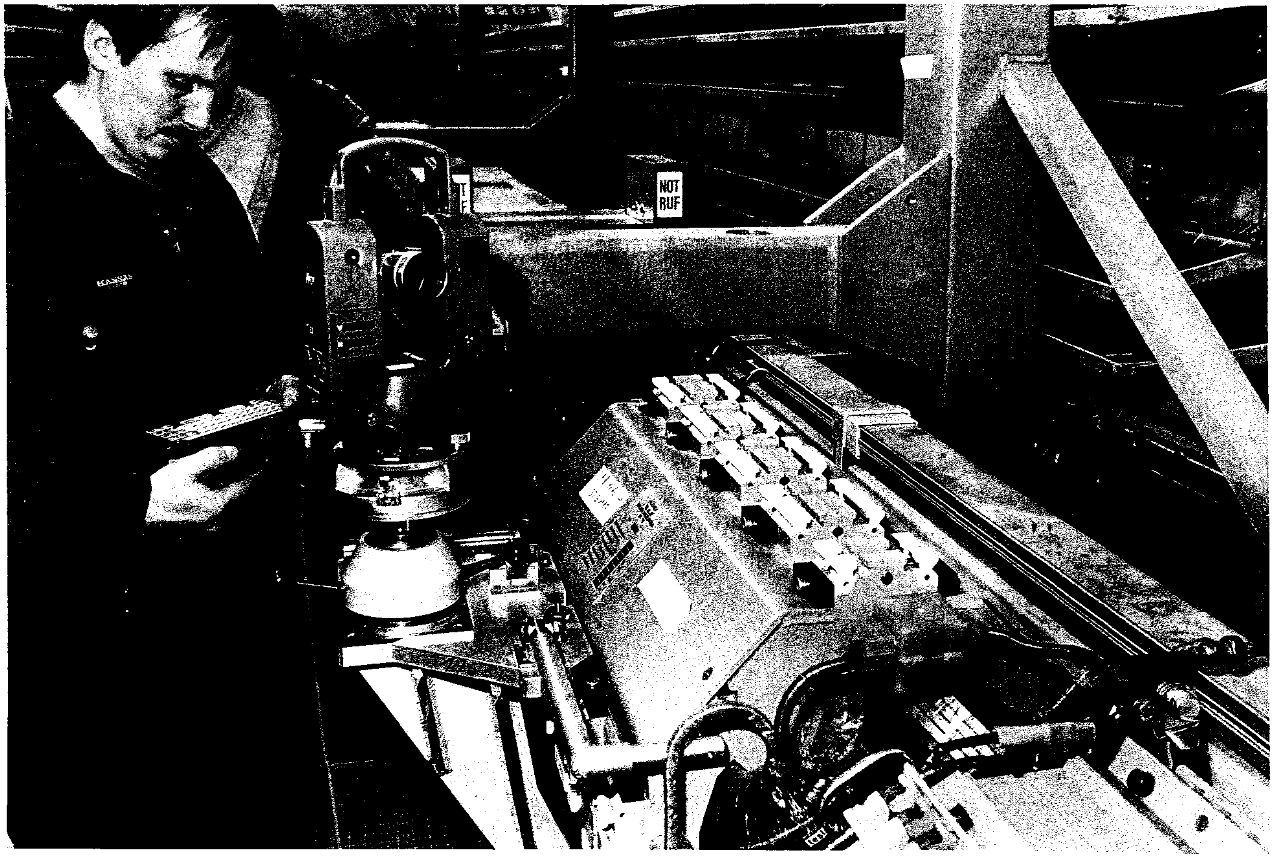

Fig.18

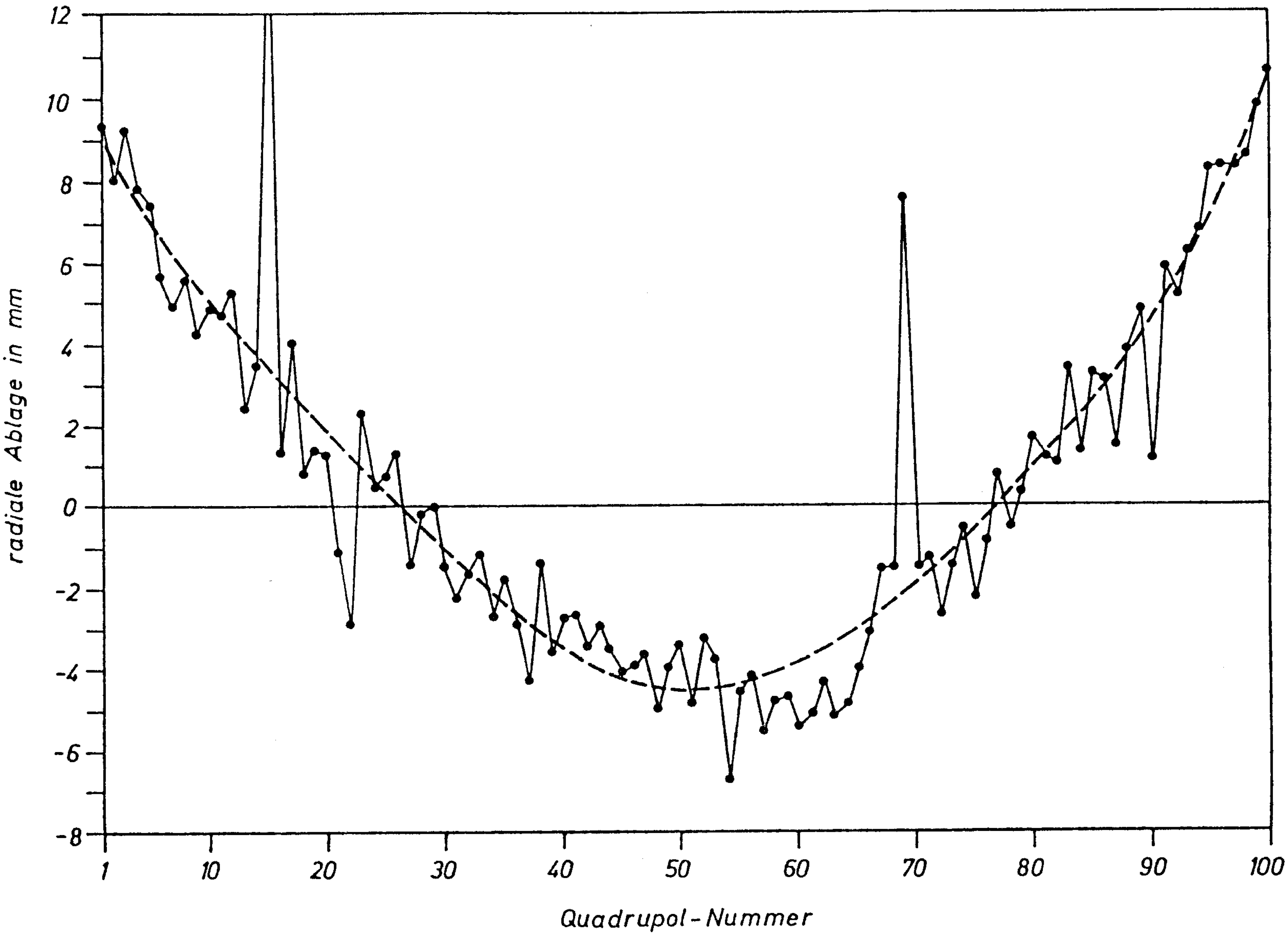

12
10
8
6
4
2
0
-2
-4
-6
-8
radiale Ablage in mm
1
10
20
30
40
50
60
70
80
90
100
Quadrupol-Nummer

Fig.19

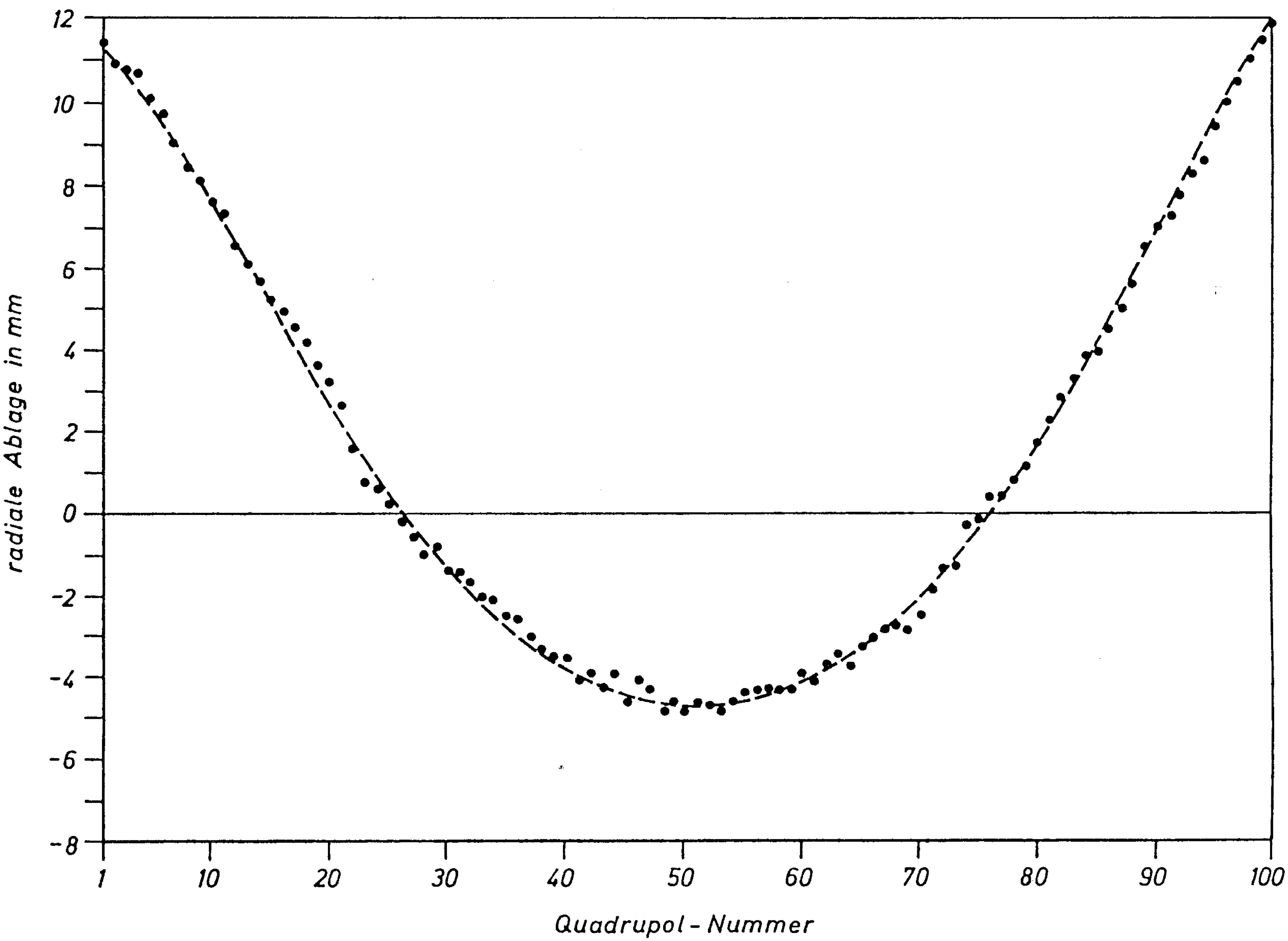
radiale Ablage in mm
12
10
8
6
4
2
0
-2
-4
-6
-8
1
10
20
30
40
50
60
70
80
90
100
Quadrupol - Nummer

Fig. 20

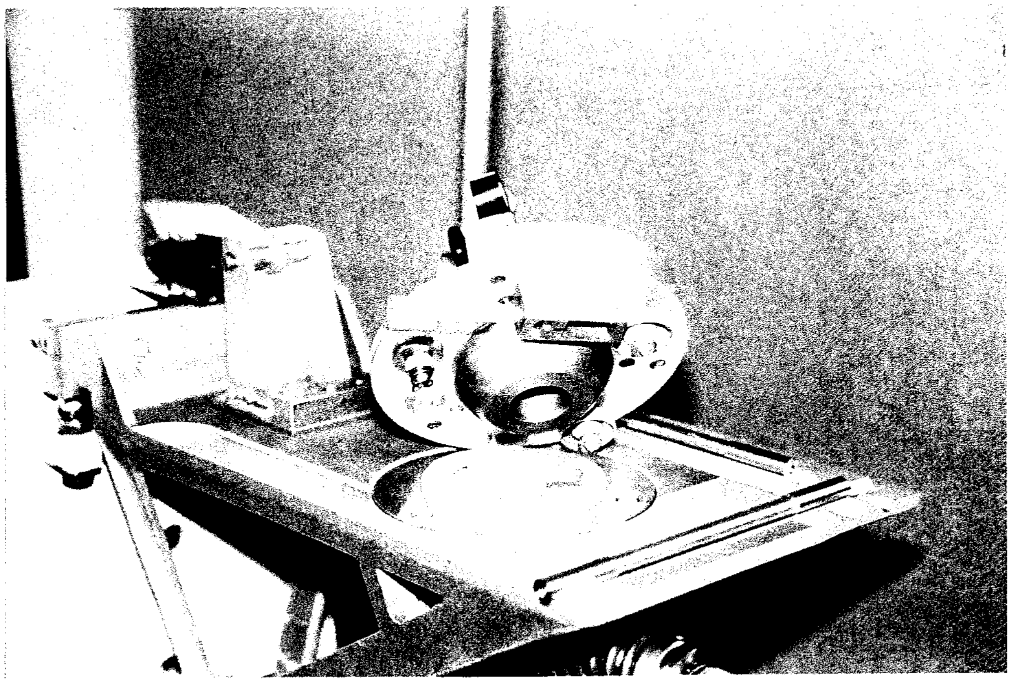

Fig. 21

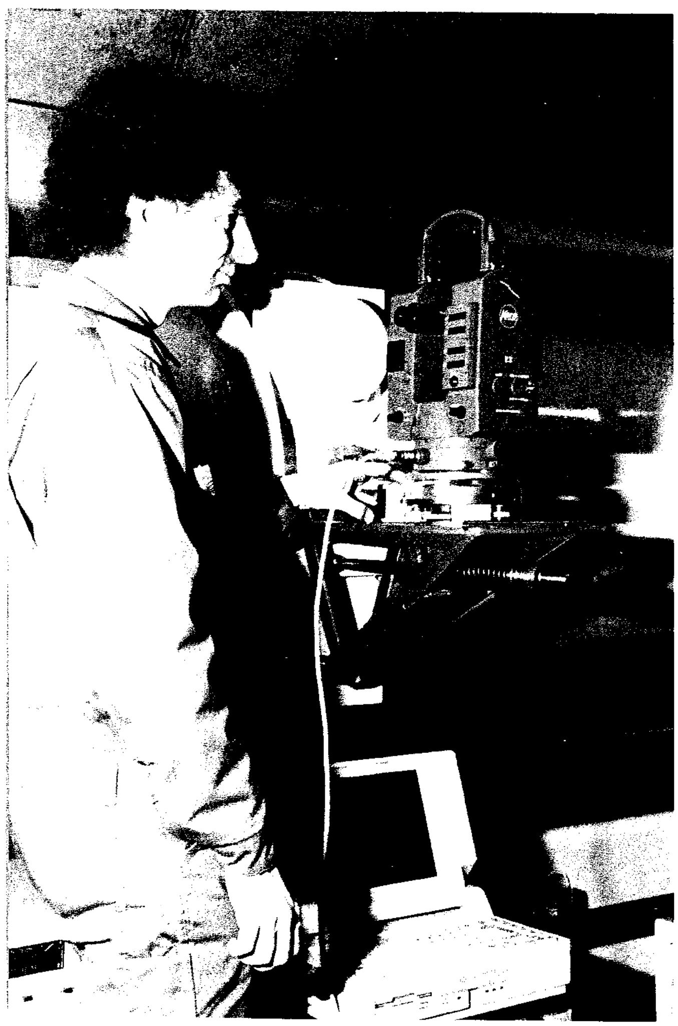

Fig. 22

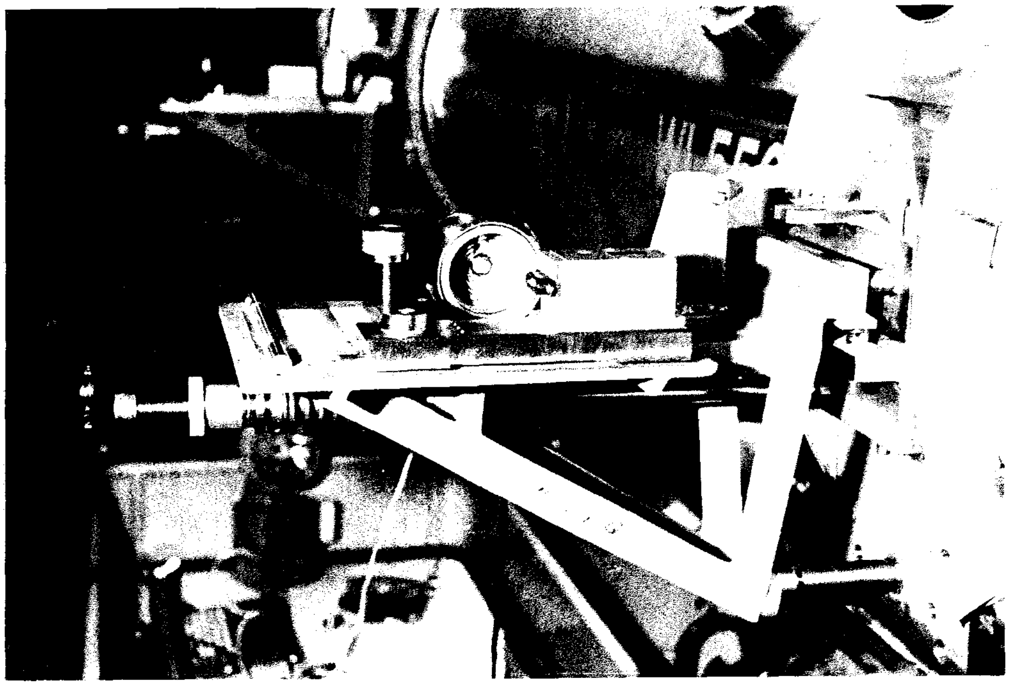

Fig. 23

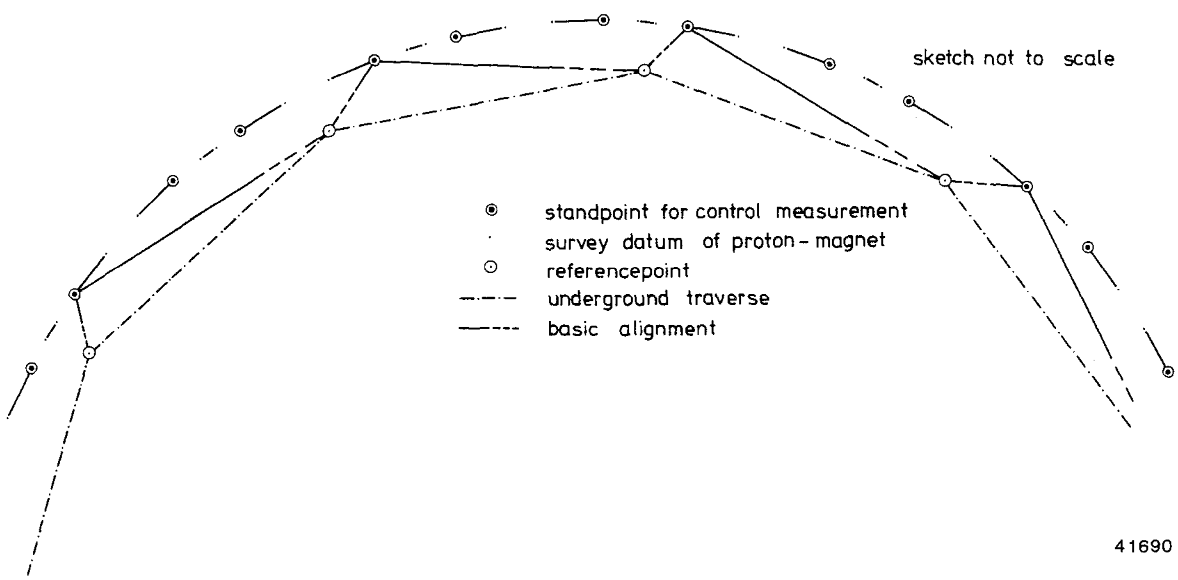

sketch not to scale
standpoint for control measurement
survey datum of proton - magnet
referencepoint
underground traverse
basic alignment
41690

Fig. 24

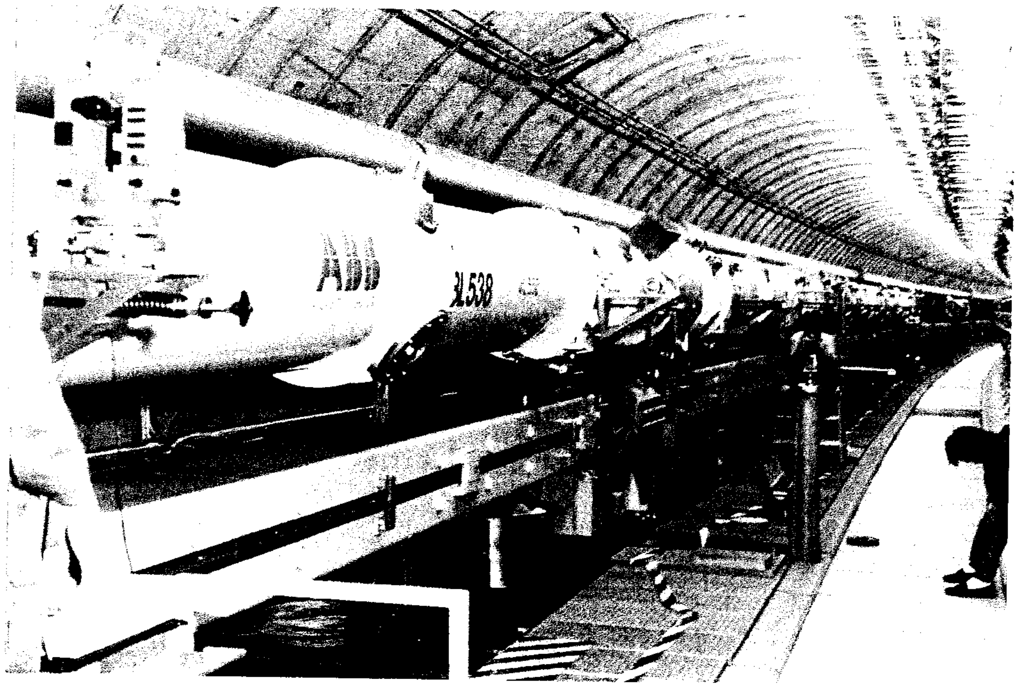

Fig. 25

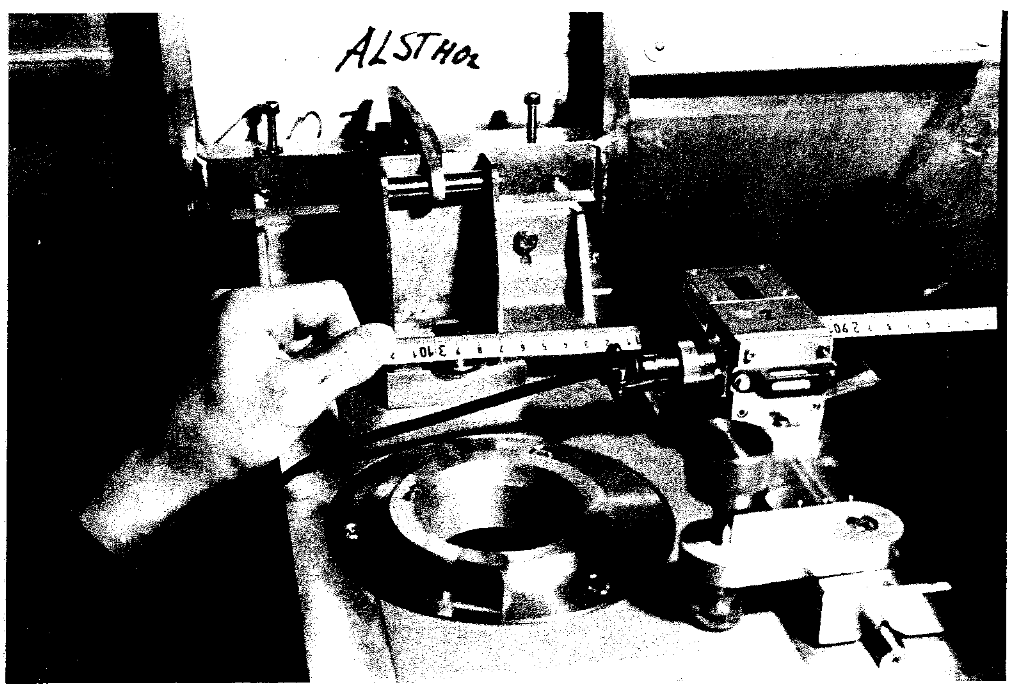

Fig. 26

GEODETIC METROLOGY OF PARTICLE ACCELERATORS AND PHYSICS EQUIPMENT

MICHEL MAYOUD

CERN - European Laboratory for Particle Research

Geneva, Switzerland

Abstract

This paper presents a review of the instrumentation, techniques and processing methods used at CERN for the metrology of large scientific equipment (from a few metres to several kilometres), the positioning of which requires high accuracy. Some specific features of tridimensional geodesy and comparative surveys of such objects are treated and illustrated.

I. INTRODUCTION

Since the construction of the first particle accelerator at CERN, in 1954, the Applied Geodesy Group has gained great experience in the metrology of large or very large objects. This initial machine was the largest in the world at that time, with its 200 m diameter. CERN has now built LEP (Large Electron Positron Collider), a new accelerator 27 km in circumference, for which the Geometrical tolerances have been tighter : a relative accuracy of 0.1 mm all along the machine and the best possible absolute accuracy with respect to the theoretical geometry.

To achieve such requirements, many specific devices and methods have been developed at CERN. Most of them have been widely described in various articles and the purpose of this paper is mainly to give a review of the more recent developments in instrumentation, techniques and processing methods, with emphasis on some particular problems related to the exceptional size of such machines. More detailed information on all these topics may be found in CERN bibliography.

II. GEODETIC METROLOGY OF LARGE OBJECTS

II. 1. PARTICLE ACCELERATORS

The search for accuracy in geodetic metrology demands that the processing of the data always remains rigourous, and takes into account any factor which can affect the exactness of the measurements or that of the results. For each project, the size of the new accelerator to be built has led to the reconsideration of several aspects of the methodology.

Major changes in geodetic concepts have been introduced in designing the SPS (2.2 km diameter) and LEP (8.6 km diameter) control networks.

First, in both cases, the computation of the theoretical XYZ coordinates of the machine has resulted in increasingly precise considerations of the geometry of the earth. For the SPS, a spherical approximation was sufficient to express the effects of the earth's curvature in computing the Z ordinates, correcting the vertical *descent* of geodetic points down the shafts or properly tilting the magnets, in order to obtain a real plane in space. With the LEP accelerator, which partly lies under the Jura mountains, a further step has been to determine the vertical deflections generated by gravity disturbances, and then to express the separation between a reference equipotential surface and a reference local ellipsoid (see IV.1). This knowledge provides the necessary corrective factors to convert measured altitude into ellipsoidal heights in 3-D computations (see IV.2), to correct the coordinates of bottom points from the effects of vertical deflections, or to reduce the gyro measurements.

One other change in the methodology is that repetitive measurements of the SPS or LEP control networks could no longer be thought of, and managed as, *absolute* surveys. For such long and flexible ring-shaped figures, the variations of the coordinates issued from different sets of comparable measurements have no physical meaning for the particles. The trajectory of a beam within an accelerator is mainly sensitive to short-range errors. Misalignments of the components are thus seen as local imperfections of the guiding magnetic field. Long-range errors have less effect but are not negligible. Thus, the major requirement for the geometry of an accelerator is that relative errors must be as small as possible. In other words, the figure must be smooth. This smoothing concept is fundamentally involved in a particular refinement process which is used for the first installation of a large machine and for any new partial or global survey when a re-alignment of components is to be done (see chapter V).

A further consideration is the fact that certitude in any accuracy problem cannot be acquired without a thorough knowledge of the stochastic behaviour of the measured networks. Although this statement sounds self-evident, it is in reality dependent on the method of estimating the actual errors and deformations which a network may undergo as a result of the random and systematic errors in the measurements. For this purpose, a simulation method has been developed at CERN on the basis of a statistical analysis under controlled perturbations (see IV.3.).

From another point of view, the considerable increase of accelerator size required an improvement in technical and economical efficiency of instruments, in-field measuring procedures, data logging, processing and data management.

For a 27 km long machine, with more than 4500 functional elements installed in a tunnel, about 32000 measurements have been carried out, collected and processed at different stages of the project. Such a tremendous effort, involving many people, must be thought of in terms of management and technically organized in a reliable and efficient process.

This consideration required the implementation of the best operational procedures, both for civil engineering controls and metrology of accelerators (see chapter III).

II.2. PHYSICS EQUIPMENT

Particle accelerators are very particular, due to their exceptional size. Physics equipment (Fig. 1), brings us back to more common dimensions and the following considerations may apply to other industrial objects.

The main characteristics - in relation to their metrology - of the new generation of experiments at CERN are :

- currently, 1000 m^3 and 10000 tons of equipment,
- complex structure, with concentric assembly of parts,

- sub-millimetric accuracies required,
- high density of connected elements (many masks),
- confinement in caverns, with a gas-like property to completely fill the available volume.

These features give a first idea of the technical and environmental difficulties of the task.

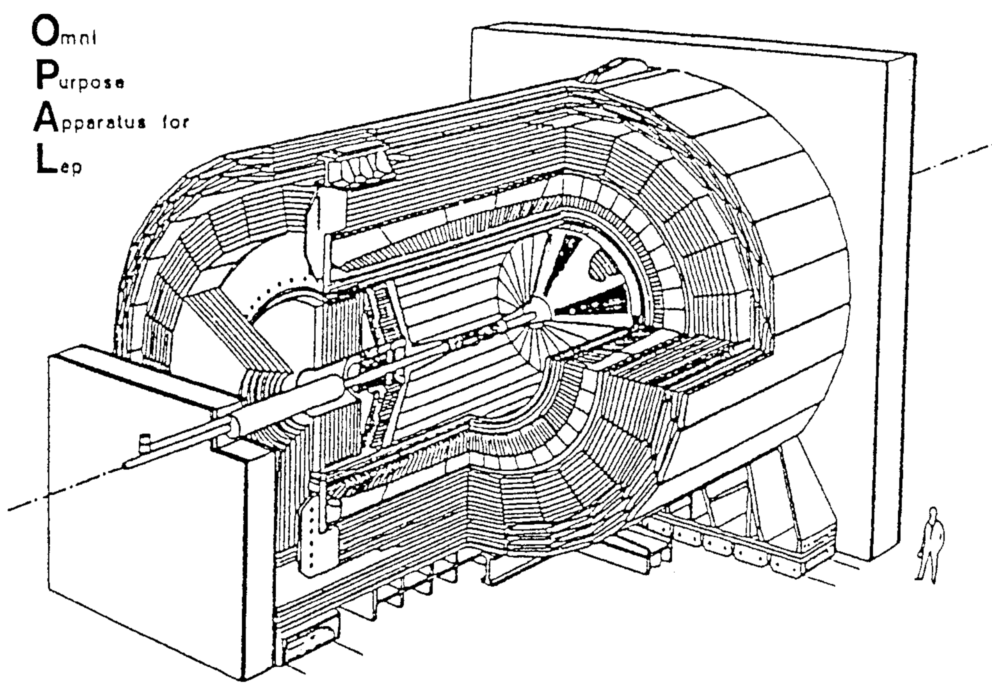

Figure 1 : Collider Experiment

One can describe modern experiments, specially the LEP ones, as a set of Russian dolls; each doll being designed to detect a certain physics phenomena. In order to obtain good results in the analysis of events (reconstruction of particle paths), a precise knowledge of detector positions, both with respect to the beam and respect to each other, is requested.

The modules are inserted one inside the other, the positioning relation being established geometrically. The biggest external one is the only one visible in the working position. The position of the smaller internal module can be reconstructed from the position of the largest, assuming that the geometrical relationship established during assembly is maintained. The assembly and positioning tolerances determine the precision to be achieved, the threshold being given by the most sensitive elements of the experiment.

To obtain the final coordinates of each detector of the experiment (alignment data base) a succession of survey operations is needed from the first availability of individual objects up to the data-taking position.

Each individual detector element is equipped with internal reference marks defined in its own coordinate system, with respect to a physical reference. In most cases, these internal marks are not convenient for surveying and special survey references must be installed. A first operation consists in realising a *link geometry* - by either geometrical, optical or mechanical methods - which is carried out in the laboratory, workshop or assembly hall. For that purpose, a complete and mobile micro-geodetic process has been developed. This system makes use of clamped tripods, invar measurements, micro-triangulation with up to three electronic theodolites

KERN E2 connected to a portable computer (HEWLETT-PACKARD IPC), distance measurements on the object itself with an accurate micrometric bar, inclusion of known mechanical constants between parts or marks. Observations are directly processed *in situ*, where it is needed.

Then, before being moved onto the beam line, the detectors are installed one by one in their definitive (relative) position. This lengthy stage is subjected to successive geodetic controls by means of an assembly network, materialised around the mounting location. During this *transformation geometry*, external (visible) reference marks of the detectors are surveyed, before being hidden by the next layer (Russian dolls problem).

The final stage of that complex geodetic process is carried out when the whole experimental equipment has been drawn and aligned on the beam line. There again, a control network is used for the determination of a sufficient number of the visible reference marks located on the *outer skin* of the object. This network must be carefully linked to the geometry of the accelerator and its coordinates, expressed in the CERN reference system, can be converted into *beam coordinates*. Hence, in a backwards and recurrent loop of successive 3-D transformations, the final coordinates of all fiducial marks of all detectors are at last determined in the beam reference system. The exact location and accurate geometry of the whole equipment are then known.

In order to open the scope of measuring facilities in such complex configurations, the tridimensional adjustment program is able to process many kinds of observations (see IV.2). Beside horizontal and vertical angles, orientations, distances, off-sets and levelling measurements, the following measurements are allowed :

- spatial off-sets in any plane of the object,
- theodolite off-sets, i.e. horizontal distance to a vertical plane (theodolite sight),
- vertical off-sets, i.e. horizontal distance to a vertical (nadiral or zenithal sight, plumb-bob).

These facilities may give a powerful means to provide appropriate and significant binding measurements, thus ensuring the homogeneousness and reliability of the metrology.

III. RECENT DEVELOPMENTS IN CERN INSTRUMENTS AND TECHNIQUES

III.1. UNDERGROUND CONTROLS

The tunnelling work, for a particle accelerator, must be carried out within very strict and tight tolerances. To avoid costly mistakes, conflicts or disputes, it is necessary to make controls at different stages of the construction, and to finally check the concrete lining of the galleries and caverns. For such a long and difficult task, the respective roles of firms and CERN surveyors were contractually defined and a close collaboration was established.

In that particular domain, some recent developments or refinements have been implemented, mainly in the vertical linking between surface and tunnel levels, the gyro measurements and profiling methods.

A convenient and reliable way to transfer points through deep shafts is shown in figure 2. This operation involves setting up three theodolites and their (calibrated) EDM, one MOM or WILD gyro, one WILD Na2 level and three special target or reflector holders(screwed on the pit curb-stone). All horizontal and vertical angles are measured, as well as distances, orientations and height differences. Observations are processed as a spatial block by means of the CERN 3-D adjustment program. Deflections of the vertical are taken into account to correct gyro measurements and to express the correcting vector due to the difference between the physical plumbline and the normal to the reference ellipsoid. For a pit as deep as 140 m, this correction can reach 6 mm. The accuracy of this operation is estimated to be $\sigma_{xy} \leq 1$ mm and $\sigma_H < 2$ mm.

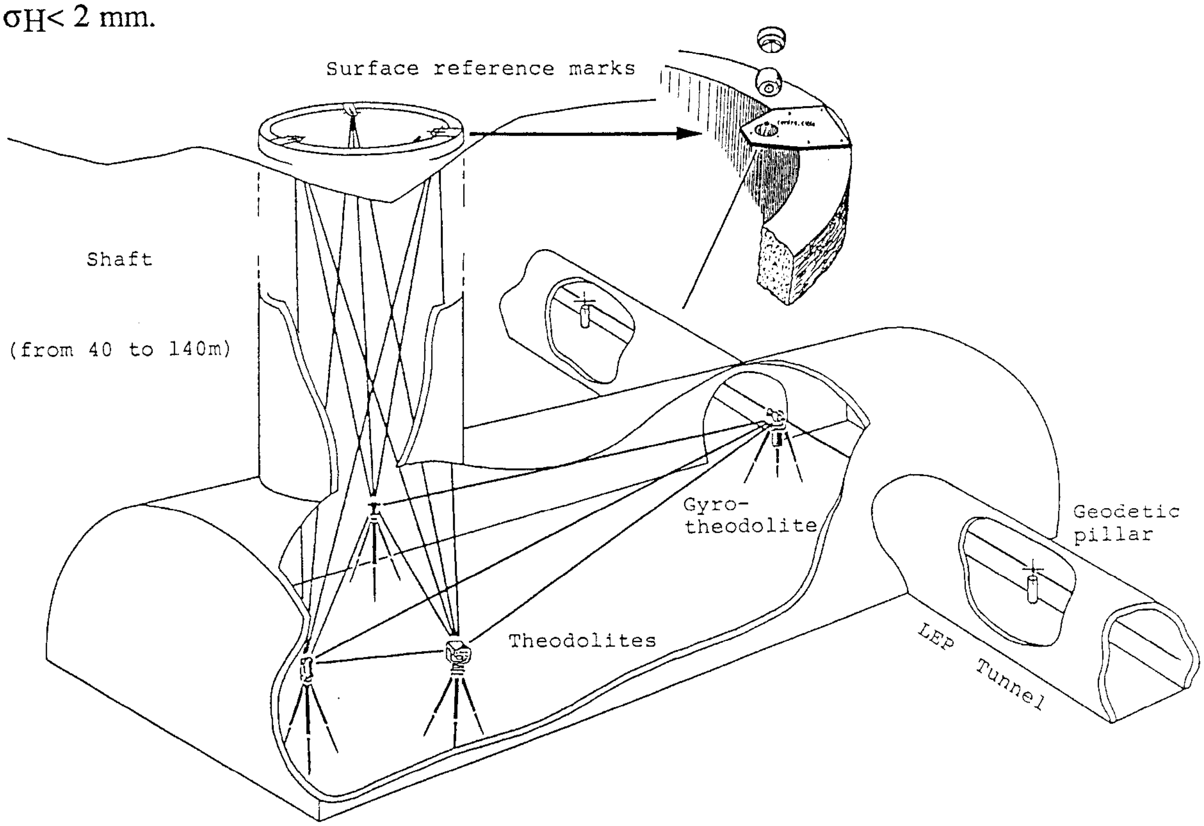

Figure 2 : Linking measurements at tunnel level

For the guiding of tunnels, after the experience gained for the SPS, LEP was a new challenge with its 27 km being cut in octants (3.3 km between control points). More than ever, gyro measurements were the only way to ensure minimum misclosures and a complete automation and computerisation of the WILD GAK1 Gyro has been undertaken, with a dedicated software for internal calibration, thermal corrections and North computations. The in-situ performances of the modified GAK1 vary from 11 to 18 cc (1 σ) in a ZP-MOTOR-ZP-MOTOR-ZP sequence, framed by two outdoor calibrations.

In parallel, very good results ($\sigma \cong 7$ cc) have been obtained with the MOM Gi-B11 gyro in long sequences of eight independent measurements, framed by calibrations.

The control traverses in the tunnel, are a combination of gyro observations, short and long-side angular measurements, invar distances between pillars, long-range EDM measurements, direct and indirect levelling data. Before computation, gyro measurements are corrected for convergence of meridians and for the effects of vertical deflections. All observations are processed in the 3-D adjustment program. Over the eight 3.3 km octants so bored and measured, the r.m.s. radial misclosure has been 10 mm (1 σ) only.

About the profiling of cross-sections of the galleries, it is only worth mentioning that very good performances have been obtained with analytic photoprofiles - accuracy better than 1 cm (1 σ) - along with fast production rates (two minutes for full data acquisition of one station and eighteen minutes per profile for observation, computation and plotting). For large caverns, where photoprofiling is not suitable, a FENNEL profile scanner has been tested and used, producing good results.

III.2. AUTOMATIC INSTRUMENTATION AND ALIGNMENT CONTROL

Without changing their basic principles, deemed still good, all CERN instruments have been fully re-designed in order to implement a computerisation of their functions and to make them able to work under digital control. The goal was to realize a complete computer-aided process for the measurement and alignment stages of the metrology of LEP.

The present range of automatic instruments is the following :

- Distinvar (counting unit 0.01 mm), for invar wire measurements from 0.40 m to 50 m;
- Laser interferometer with self-aligning reflector (counting unit 0.1 µm), for the in-situ calibration of invar wires with $\sigma \leq 0.01$ mm;
- Horizontal offset measuring device (counting unit 0.01 mm), with either a nylon wire or a laser beam reference line;
- Vertical offset measuring device (counting unit 0.01 mm) for direct geometrical levelling with a laser beam;
- Electronic inclinometer (counting unit 0.01 mrad) for the measurement of tilt angles.

All these instruments can be connected to a computer or a control box through a RS 232 line, and be digitally operated.

At the measurement stage, instrument control and data acquisition are made on small portable computers, like EPSON HX20 or PX4. Relevant Basic programs have been developed for each measuring procedure, guiding operations, collecting data, calculating statistics and formatting the data files.

For the alignment stage, a more powerful computer was required. Since no convenient one was available some years ago, it was decided to develop and build a field-computer, specially dedicated to this operation. Easily transportable, in a reasonable case, it is based on a MOTOROLA 68000 processor, can be powered by internal or external battery (or AC supply) possesses 1 Mb RAM and 1 Mb ROM memory, allows connection of five RS 232 lines, includes an additional support memory for 64 K RAM cartridges, has a 40 characters printer and incorporates digital transducers for temperature, humidity, pressure and battery control.

The computer-aided alignment of an accelerator component is conceived as shown in Figure 3. The control network is settled on plug-in tripods, and the coordinates of these reference points are derived from the previous stages of the metrology. The problem is then to carry out an accurate installation of an element - say a quadrupole magnet - at a pre-determined theoretical position.

A first pre-alignment step is realised, with help of an auxiliary hydraulic device, using a combination of length, offset, tilt and levelling measurements, controlled by the field computer. Then the quadrupole can be released on to its mechanical jacks, and the final positioning is carried out with, again, a full computer control of the operation. Real-time readings of all set up instruments permanently allows the program to compute the actual position of the quadrupole compared with theoretical coordinates and deduce the optimum moves to apply to the jacks.

Such computer-aided procedures have been repeated about 4500 times, around the 27 km of the accelerator.

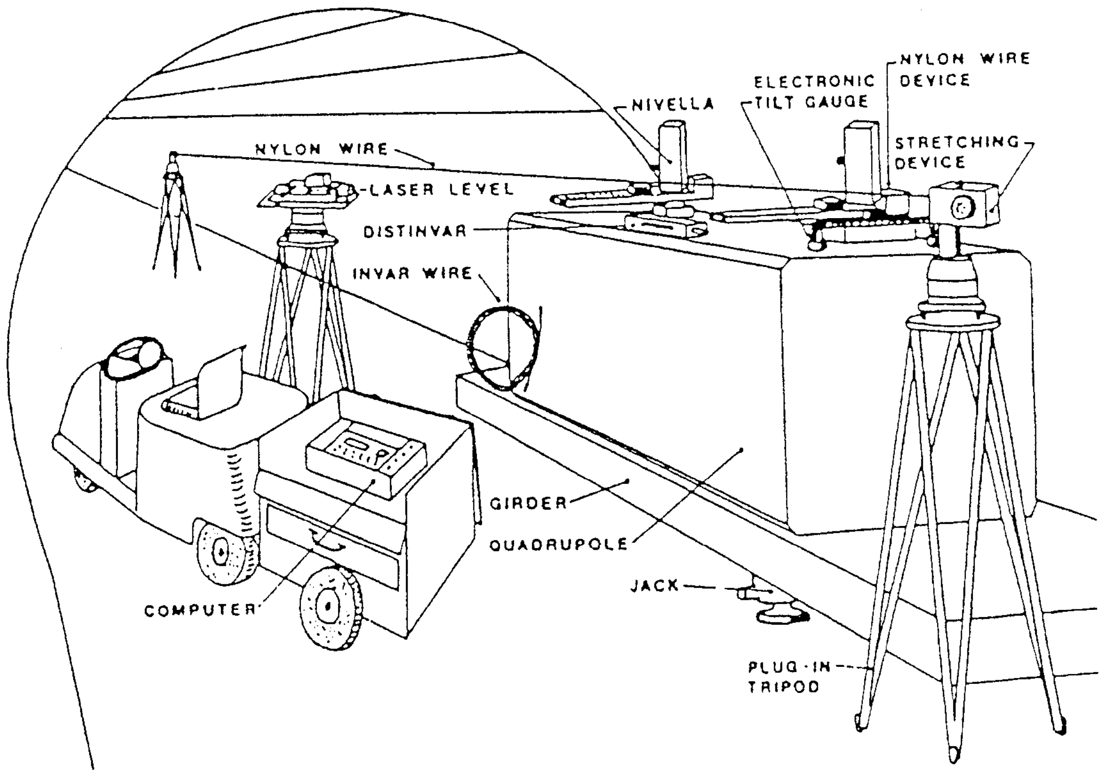

Figure 3 : Quadrupole alignment arrangement

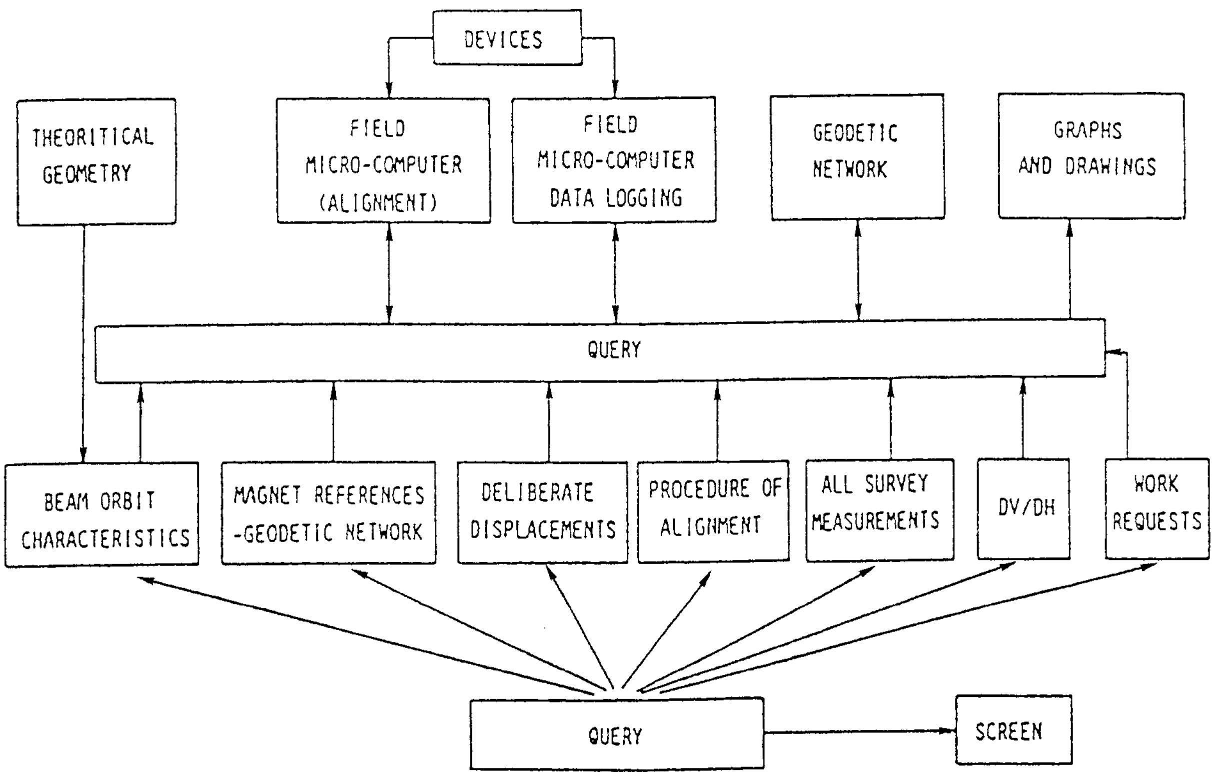

Figure 4 : Organigram

III.3. DATABASE MANAGEMENT

Beside LEP, other CERN accelerators and their transfer lines already represent more than 8000 elements laid along 20 km of beam lines. Each of them involves several metrological parameters : position of reference sockets, theoretical and actual coordinates, measuring procedure, use of special gauges, etc. Depending on beam orbit problems, they are regularly surveyed. Then some elements can be re-aligned due to local unstabilities, or they are deliberately displaced in order to act as correctors of the beam orbit.

To efficiently handle such a considerable amount of data, a specific database has been established with the Oracle system (Figure 4).

This development is now fully operational and it constitutes a very clear and powerful means to manage all stages of the survey process.

IV. DATA PROCESSING IN A 3-D LOCAL SYSTEM

IV.1. LOCAL EVALUATION OF THE GEOID

For the evaluation of equipotential surfaces under the area covered by LEP, CERN has made use of the large mass model (510 x 410 km) realised in Switzerland and completed with additional data.

Taking into account both the numerical integration in this mass model and several surface measurements of vertical deflections, the collocation program developed at Bern (Gurtner, 1978) allows the computation of equipotential surfaces at any altitude. A 10 x 10 kilometric grid has been used for the estimation of the Geoid and vertical deflections at different levels over the LEP area. All the data has been related to the local origin of the CERN system, in order to express the parameters of relevant corrections.

Starting from a method developed at Bologna (Achilli et al, 1982), CERN has also experimented with a computation of gravity components in a limited portion (70 x 50 km) of the mass model, restricted to the topography from level zero upwards. Although referred to the same local origin, the results show a kind of systematic gradient difference from those of the Bern program. The cause of this is probably the absence of any external constraint (no *absolute* surface measurement of ξ, η) and the non-consideration in the model of the remote influence of some high Alpine mountains. Expressed in vertical deflections, these differences range from -1.7 to 0.6 arc seconds.

Finally, in order to make an independent check on these estimated values, astrogeodetic measurements were carried out on eight points, using the zenithal camera of the Institute of Geodesy of Zurich (Burki et al, 1983). This camera, developed at the University of Hannover, has a 1 m focal length, two high-precision Talyvel automatic levels and its operation is fully computer-controlled. Six plates were taken per station and the measurements and computations have been made at the University of Hannover. The standard errors on computed geographic coordinates were quoted as 0.3 arc second (0.9 cc).

The comparison between the resulting *observed* values of the deflections and the predicted ones was remarkably good. The residuals are generally less than 1 arc second. The standard errors of this comparison are :

- $\delta\xi = 0.55''$ $\delta\eta = 1.03''$ for the Bern mass model,
- $\delta\xi = 0.57''$ $\delta\eta = 0.56''$ for the CERN limited mass model.

Being more confident in the BERN program, the results of the large model computations, combined with astrogeodetic measurements, were retained. The search for a surface fitting the 121 + 8 point estimates of the grid called for the following considerations :

- the prism spacing (500 m) of the mass model induces small relative errors;
- at such a large scale, an equipotential surface is more likely to be smooth than wrinkled;
- for sake of simplicity, a *light* parameterisation would be more convenient.

For these reasons, polynomials or piece-wise functions (like 3-D splines) were rejected and a canonical trend surface was looked for. The best least-squares fitting was a paraboloid limiting errors to less than 1 arc second in deflection, with respect to grid values.

IV.2. THE TRIDIMENSIONAL ADJUSTMENT PROGRAM

Many adjustment programs have been successively written to satisfy the geodetic needs for CERN accelerators : planimetric (XY) or altimetric (H) programs, tridimensional adjustment strictly limited to micro-geodesy, processing of large matrices, Helmert transforms, etc.

The size of the LEP project called for a new and rigorous computational tool, fully adapted to the processing of all kinds of geodetic data in a local system and whose main features are the following :

- local 3-D adjustment on the ellipsoid GRS80;
- altitudes are referred to the known local geoid and are subsequently converted into ellipsoidal heights;
- generalised least-squares processing of all types of available data, some kind being very peculiar to the metrology of experiments equipment;
- all angular measurements, observed relative to the local horizon, are re-expressed in the CERN cartesian system through an appropriate rotation matrix;
- direct levelling data is processed as vertical distances;
- various constrained/unconstrained computational cases are available;
- statistical and variance analysis of the results;
- generation of random and/or systematic perturbations for simulations;
- preparation of files for subsequent (weighted) Helmert transforms;
- free-formatting and intensive use of keywords for flexibility in data handling.

IV.3. THE CERN SIMULATION METHOD

Starting from the a priori standard deviations on measurements, derived from experience, the well-known tools of stochastic analysis are :

- unit weight variance : σ^2;
- covariance matrix : $C_X = \sigma^2 N^{-1}$, which gives expression of absolute and relative error ellipses;
- histogram of residuals, estimated accuracy of (groups of) observations, elimination or refinement methods;
- confidence intervals on estimates.

Nevertheless, this classical way of analysis may leave some interpretation problems on mixed networks. Significant distortions can occur on a posteriori estimates and it is difficult to appreciate the relative *strength* of each group of observations. Furthermore, no signal is given to detect the systematic errors, which are not modelled in this process. This kind of simulation does not give a clear view of the behaviour of a perturbated network and one must remain rather wary when interpreting the resulting statistical figures.

A pragmatic way to obtain a picture of the true situation is to simulate on a computer all the perturbations which can affect the geometry of a figure : Gaussian errors in measurement, artificial generation and addition of systematic errors, controlled constraints, etc.

For this purpose, the provisional coordinates (or theoretical ones for accelerators) are taken as ideal. Measurements are supplied in the input file as for a normal computation of the network. The program computes the ideal measurements and a gaussian generator adds random errors scaled on a-priori variances. The data is then processed as usual. Repeating these operations gives a *Monte-Carlo* generation of *'n'* sets of hypothetical measurements of the same network.

Empirical statistics carried out on the results give very interesting estimates to be compared with the known (and controlled) a priori values of the variance of each group of observation or, even, to allow a direct analysis of the effect of errors on the coordinates. Tests can also be made to appreciate the agreement of actual results with predicted values. Such a method gives a clear idea of the response of a complex network to random errors and provides some corrective factors to apply to the various estimates in order to make a correct scaling of the predicted errors.

When adding systematic errors and/or controlled constraints, the simulations also give a true image of the distortions suffered by the network. The effect of each constraint can then be evaluated. The resulting shifts of the mean values of the residuals, with respect to any selected systematic error in each group of measurements, gives an idea of the *warning lights* to watch for when actual measurements are to be processed.

This pragmatic method has been used for years at CERN and it is a very helpful tool for the engineer who needs a real knowledge of the network he has to design and optimize, and then observe and compute.

V. SMOOTHING AND COMPARATIVE SURVEYS

When installing the machine components, the first determination of the control network gives the displacement vectors between their actual *rough* position and their theoretical one. In fact, magnets are positioned around an unknown mean trend curve (one among an infinity) contained within the envelope of maximum errors. The polynomial degree of the curve depends on redundancy, overlap of measurements, and the bridge distance between control (fixed) points. The final relative errors are a quadratic combination of those of the network itself and those of the positioning, i.e. installation errors. Their statistical nature is essentially gaussian : the aligned elements are randomly and normally distributed around this mean trend curve (Figure 5).

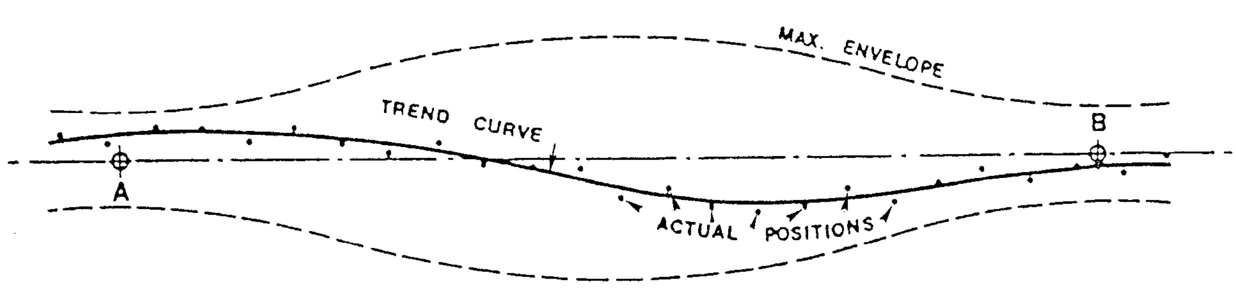

Figure 5 : Position of magnets with respect to theoretical orbit

As the major requirement for the geometry of an accelerator is that the relative errors must be very small ($\sigma \leq 0.1$ mm), an obligatory step for surveyors is to check the installation by measuring and - if needed - improving the smoothness of the machine alignment.

Another important consideration is that, when making successive surveys of long and flexible figures, absolute comparisons would be a nonsense. The difference between trend curves, corresponding to each survey, must be analytically eliminated without inducing systematic or harmonic errors, which are critical for an accelerator.

This mathematical problem is not trivial and different methods have been evaluated for the separation of absolute and relative discrepancies. Polynomials were rejected due to the inner constraints generated between data points when increasing their order. The Fourier decomposition was rather dangerous with respect to the harmonic sensitivity of beam orbits. Therefore, a special smoothing algorithm has been developed in order to process the local data in a purely relative way, e.e. without any absolute involvement in coordinates.

The smoothing process consists of a set of radial or vertical measurements (Fig. 6) which are treated in the following way :

$$(1/1+k)\ dRh - dRi + (K/1+k)\ dRj + St - Sm = vi$$

where :

H, I, J, are three successive points,
k = proj (HI) / proj (HJ) along HJ
dR = unknown radial discrepancy with respect to mean curve
St = theoretical sagitta in point I, with respect to HJ
Sm = measured sagitta
vi = residual of the measurements

Each point receives three overlapping measurements resulting in a good redundancy. Nevertheless, these measurements only cover six points (i.e. three quadrupoles) and the global system would be rather poorly conditioned if a determination of coordinates was required. But as the purpose is to get local and purely relative information, this fact is not critical if the normal system is solved under the double condition $||dR||$ and $||v||$ minimum.

The condition $||dR||$ minimum constrains the reference line of the ordinate dR to be the mean curve. This condition cannot be directly expressed in the adjustment. Neither can it be linearized since the differential increments, the unknowns dR, and the residual v are, nearly, of the same order of magnitude. The convergence would consequently be slow and the results uncertain.

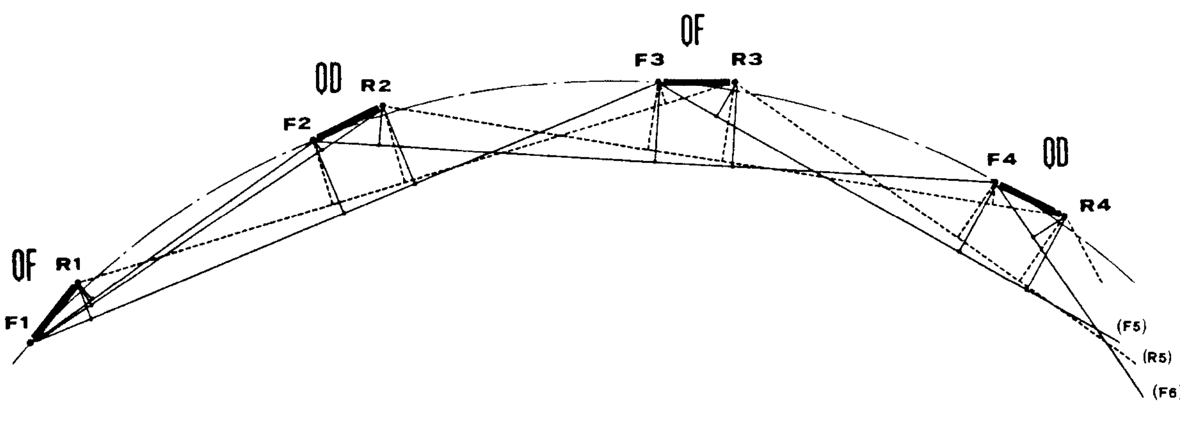

Figure 6 : Scheme of smoothing measurements

The only way which has been found for solving such a system is to move dRi onto the right-hand side of the equation, introducing for each central measurement on I a new observation equation :

$$1/\sqrt{3}\ (1/1+k\ dRh + k/1+k\ dRj + St - Sm) = dRi\ (+vi)$$

The weight $1/\sqrt{3}$ comes from the fact that each point receives three measurements.

The normalisation of these additional equations is equivalent to $\Sigma(dr + v)^2$ minimum, i.e. :

$$(\Sigma dr^2 + \Sigma vi^2 + 2\ \Sigma dR\ vi)\ \text{minimum.}$$

Σvi^2 is set to its minimum by the normalisation of the first equation, for each measurement. These residuals vi constitute a Gaussian distribution $[0, \sigma_m]$ and the radial ordinates dR are also expected to be a set of Gaussian variates with, of course, a zero mean-value. Σdr^2 will consequently be a minimum if the quantity (Σdr . vi) tends to zero, this being the case for two Gaussian samples of the same dimension N.

If the sample V has dimension n = N/3, this is more difficult to prove. But it can be checked easily with a program using the computer's Gaussian generator.

This global procedure is a kind of compromise, which is not quite rigorous but nevertheless satisfactory. Simulations and real computations have given acceptable results both for checking the first installation and for successive and comparative surveys of the machines.

For vertical positions, smoothing has been first made *visually* by drawing a mean curve on a plot of differences H measured - H theoretical. A similar procedure has been tried by generating pseudo-observations of vertical off-set values, derived from adjusted altitudes, with the same overlap. Results here are also satisfactory :

- unfavorable sign sequences are located,
- outstanding dR values can be pointed out.

VI. CONCLUSION

The very accurate instruments and sophisticated methods presented in this paper have been designed for obtaining the most precise knowledge of the shape, dimension and position of very large scientific objects. But it is also worth remembering that industrial and engineering surveys are performed in an industrial or scientific environment, where many topological problems occur in the installation of a very high density of various equipments.

For that purpose, digital cartographic systems - in connection with C.A.D. systems - are a powerful means to manage and maintain the survey data of complex and evolving industrial sites.

At CERN, a software package from INNOVAL (France) has been implemented for the complete management of the 1400 hectares of the site and the 500 000 m2 of building floors, laboratories, galleries, halls, etc. All topographical, technical, management and administrative data can be entered in the Site and Buildings Databases, constituted with the *Espace* package, through graphical and standard alphanumeric terminals. In addition to its cartographic performances, such a system provides a very efficient way to correlate management information with the topographical location of any kind of equipment.

BIBLIOGRAPHY

ACHILLI V., BALDI P. : Computation of local anomalies of the vertical deflections in geodetic networks, Survey Review No 205, Vol. 26, (1982)

GERVAISE J., MAYOUD M., MENANT E: : Système tridimensionnel de Coordonnées utilisé au CERN, CERN 76-03, (1976)

GERVAISE J. : Applied Geodesy for CERN Accelerators, Part I - Seminar on High Precision Geodetic Measurements, University of Bologna, (1984)

GURTNER W.: Das Geoid in der Schweiz, Institut für Geodäsie und Photogrammetrie, Mitteilungen Nr 20, Zurich, (1978)

MAYOUD M. : Programme de lissage radial, Note interne CERN/SU, (1974)

MAYOUD M. : Géométrie théorique du LEP, LEP Note No 456, (1983)

MAYOUD M. : Applied geodesy for CERN accelerators, Part II - Seminar on High Precision Geodetic Measurements, University of Bologna, (1984)

CERN ACCELERATOR SCHOOL : Applied geodesy for particle accelerators, CERN, Geneva, Switzerland, 14-18.4.1986, Proceedings CERN 87-01 (1987) :

COOSEMANS W. : Computer aided geodesy (II) - Instrumentation

FISCHER J.C., HAYOTTE M., MAYOUD M., TROUCHE G. : Underground Geodesy

GERVAISE J., WILSON E.J.N. : High precision geodesy applied to CERN accelerators

GURTNER W. & BURKI B. : Deviation of the vertical

HUBLIN M. : Computer aided Geodesy (I) - LEP installation procedure

ILIFFE J. : Three-dimensional adjustments in a local reference system

LASSEUR C. : Metrology for experiments

MAYOUD M. : Computing and analysis methods

QUESNEL J.P. : Data logging and management of geodetic measurements with a database.

– GEONET –

A REALIZATION OF AN AUTOMATED DATA FLOW FOR DATA COLLECTING, PROCESSING, STORING AND RETRIEVING*

Horst Friedsam, Robert Pushor and Robert Ruland

Stanford Linear Accelerator Center
Stanford University, Stanford, California 94305

ABSTRACT

GEONET is a database system developed at the Stanford Linear Accelerator Center for the alignment of the Stanford Linear Collider. It features an automated data flow, ranging from data collection using HP110 handheld computers to processing, storing and retrieving data and finally to adjusted coordinates. This paper gives a brief introduction to the SLC project and the applied survey methods. It emphasizes the hardware and software implementation of GEONET using a network of IBM PC/XT's.

* Work supported by the Department of Energy, contract DE-AC03-76SF00515.

INTRODUCTION

The Stanford Linear Accelerator Center (SLAC) is in the process of building a new particle collider, the Stanford Linear Collider (SLC) [ERIKSON, 84]. The tunnel which houses the SLC is about 3 Km long and contains approximately 1000 magnets. To do the precision alignment of these magnets nearly 400 control points are established. The positioning of the magnets in X,Y,Z, roll and pitch requires the determination of about 2500 fiducial marks [OREN, 85]. The accuracy requirement for the absolute positioning of each magnet is 1 to 2 mm while the relative positioning between adjacent magnets requested an accuracy better than 0.1 mm. All magnets have to be positioned using an iterative procedure from the rough layout of coordinates for the magnet support systems to the final smoothing of adjacent magnets [PIETRYKA, 86]. This leads to an estimated 50,000 to 60,000 coordinates which have to be determined during the construction time frame of 3 years. To control this huge amount of data an automated data flow from data collection to data processing and finally data storing is essential. Since none of several evaluated software packages [GRÜNDIG, 84] fulfilled our needs or matched the already existing hardware, the decision was made to write a customized data base program, GEONET. Figure 1 shows a finalized sketch of the data flow from the measurements to the coordinate database as it is implemented in GEONET [RULAND, 86].

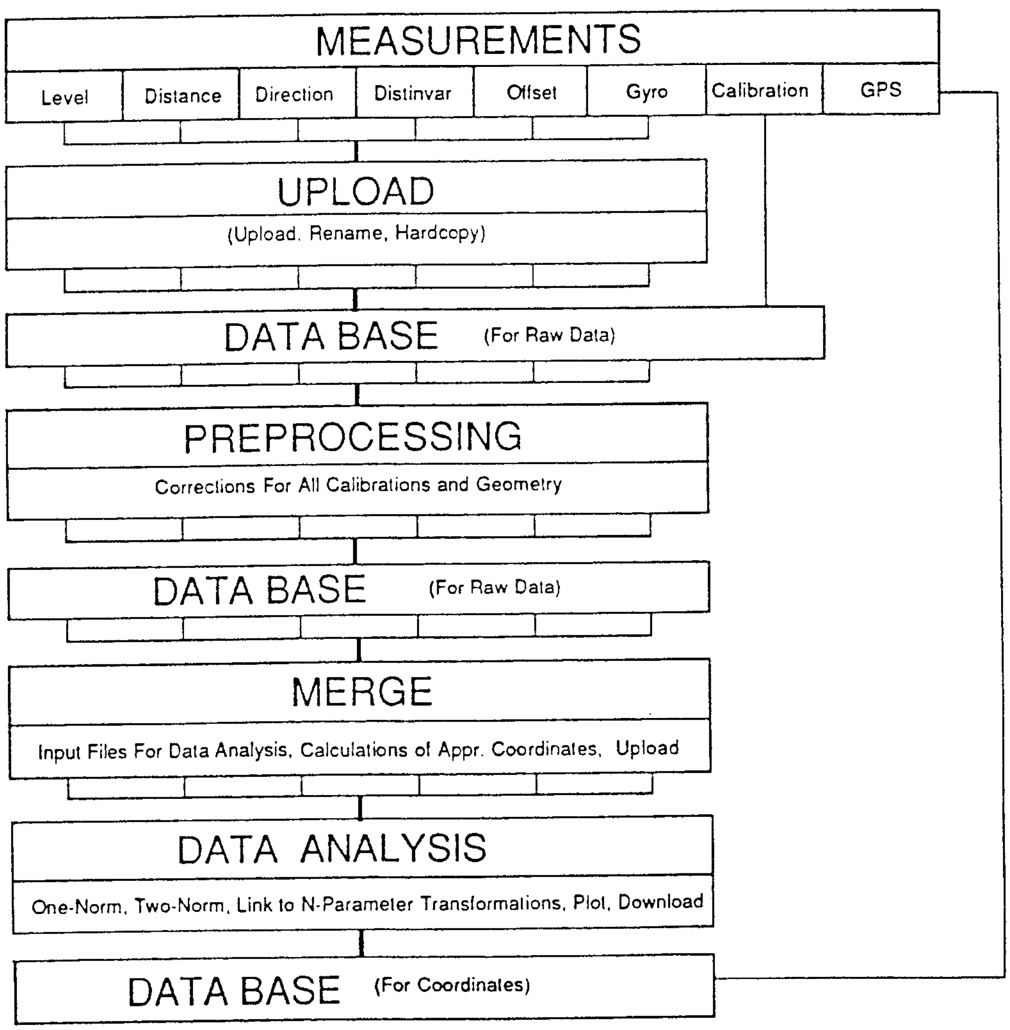

Figure 1 Data Flow Chart

HARDWARE CONFIGURATION

In order to establish a totally automated data flow procedure each step of the surveying process needed to be computerized as much as practical, beginning with the collection of observations in the field and carrying through to the final least squares adjustment of coordinates. The first step was to find a suitable data collector. After having evaluated several different hand held calculators for example the HP41CX, HP71B, EPSON HX20 etc., the HP110 portable microcomputer from Hewlett-Packard was chosen. Although the HP110 computer has the disadvantage of being heavier than most other available data collectors [DONAHUE, 86], its sturdiness, reliability, ease of data transfer, size of memory and the capability to write specialized data collection programs made it the best choice for a data collector.

The link between HP110's and survey instruments is accomplished using the RS-232 port built into the HP110. In the case of KERN E2 theodolites a SLAC designed interface box, able to serve up to four theodolites, is used to translate the signals from the E2 to the standard RS-232 levels. The communication between E2 and HP110 is bi-directional, making it possible not only to record data but also to send data such as horizontal and vertical angles to the E2 for display or to control its settings.

Two different concepts for the implementation of a geodetic database were considered. The first was to run the data handling and least squares adjustments on a mainframe, either an IBM 3081, VAX 750, or VAX 860 [GRÜNDIG, 84]. The alternative concept was to set up a system of Personal Computers, interconnected by a local area network. Each idea had certain advantages and disadvantages. The obvious advantages of the mainframe approach is its speed and virtually unlimited memory size. But the major disadvantages are the inability to have control regarding operation and maintenance hours and the difficulty to establish a connection to the field data collectors. These are tasks easily accomplished with a PC/XT. Consideration of the advantages of both the mainframe and PC/XT led to the decision to implement a hybrid system combining the best features of both approaches.

The first part of the hybrid system, the data management, is done using a cluster of PCs. The local PC workstations are interconnected by a 10 Mbit Ethernet local area network. Remote access is also possible using modems; this feature is used for the transfer of calibration data between the office and the calibration room, located several miles away from the server. Each PC is equipped with a co-processor, 640 Kbytes of memory, a 20 MByte hard disk and an accelerator board running at a clock rate of 10 MHz. The network permits sharing of a 35 Mbyte hard disk, an internal tape backup system and an HP LaserJet printer. In addition, plot facilities including A-size and E-size plotters are available. A sketch of the hardware setup can be seen in Figure 2.

To establish the connection between the HP110 data collectors and the network, each PC is equipped with an HP-IL interface board which lets the PCs look at the

HP110's as at external disk drives. The actual data transfer is done by using the DOS copy command. This link provides an easy, fast and reliable exchange of files in both directions.

The second part of the hybrid system involves the use of an IBM 3081 mainframe to process least squares adjustments. Input files, created on the individual PC workstations, are uploaded to the mainframe and result files are downloaded via an RS-232 communication port to the PC.

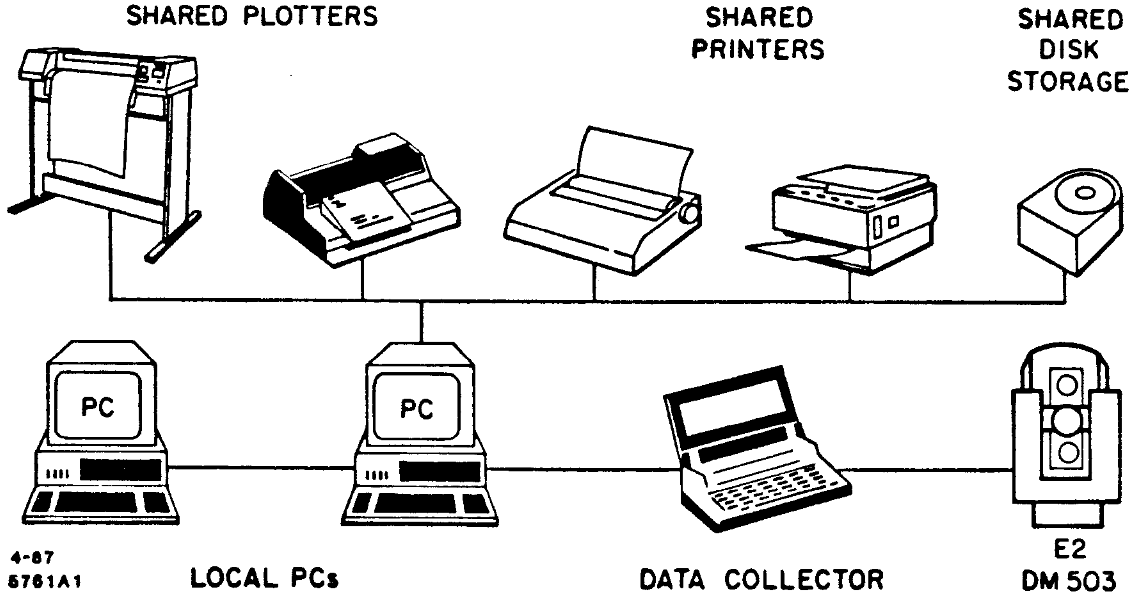

Figure 2 Hardware setup

SOFTWARE CONFIGURATION

Basic Structures

During a large scale survey project such as the construction of the SLC several different forms of data have to be managed. Among these forms are:

- recorded field data observations
- calibration data for various instruments used
- reduced measurement data
- and several different coordinate databases

GEONET provides data structures and programs to handle all of the above data forms.

GEONET takes advantage of the subdirectory structure provided by the DOS operating system on the PC. Each recorded field observation is transferred from the

HP110 data collectors to the PC and stored in a data file system. All data files are stored in a four level hierarchal structure and can be accessed via a menu by using a pathname of the following form :

$$\text{pathname} = \backslash \mathit{basename} \backslash \mathit{location} \backslash \mathit{type} \backslash \mathit{epoch}$$

where	*basename*	is the data file system identifying name.
	location	is the location of the points surveyed.
	type	is the type of survey data.
	epoch	is the survey epoch.

GEONET can handle more than one data file system at a time and it is possible to use up to 16 unique names for each of the location, type and epoch variables. The result files created by the reduction programs are stored together with the measurement data using the same pathname. Calibration data is stored in a similar form using a calibration file structure also of four levels. The coordinate database is defined as a two level subdirectory structure. In this case the pathname is created as follows:

$$\text{pathname} = \backslash \text{COORD} \backslash \mathit{location}$$

where	COORD	is the coordinate database identifying name.
	location	is the location of the points in the database.

Data Management System Function Menu

1.	Upload field data	2.	Process pending updates
3.	Data reductions	4.	Transfer to shared disk
5.	Generate Input file	6.	Perform Adjustment
7.	Coordinate database	8.	NSC800 operations
9.	Access server disk files	10.	Access calib data
11.	System configuration	12.	Archive subsystem
13.	Escape to DOS	14.	Exit Geonet

Enter function number:

Figure 3. GEONET Main Menu

The interaction between these various data forms is organized by the GEONET data management system function menu shown in Figure 3. It is presented after the user enters his password. Each password allows access to a unique group of GEONET functions depending on the user's privilege. The upload function for instance can be used by each member of the survey crew while the reduction of data is a restricted function only accessible for privileged users.

The following sections describe each of the options addressed in the data management system function menu in more detail.

Upload Field Data

The function "Upload field data" is used to transfer data collected, using the HP110, to the local hard disk of the PC and then to a shared temporary storage disk maintained by the server. Each individual data collection program creates its own filename and a unique filetype for each observation. For instance, the filename for a direction set is given by the station name and the filetype is defined as .DIR, thus simplifying the upload procedure by using wildcards for the file transfer. Other measurements such as EDM or Distinvar observations obtain a filetype .DST and .INV, respectively. During the upload procedure the filetype is replaced by the Julian date of the day the measurements were recorded. At the same time the filetype of the original data file still residing on the HP110 is changed to .999 thus eliminating the possibility to upload a file twice and making it an easy task to erase all uploaded files on the HP110 after the data transfer is done.

The upload program also accesses an index file stored in the same subdirectory as the recorded observations. It is always updated whenever a new observation file is added to a subdirectory. The index file is used by other programs, mainly reduction programs, to open and read each individual file of a specified subdirectory.

Currently, data collection programs for the following observation types exist:

- Direction measurements
- EDM measurements
  - DM503
  - Mekometer
- Distinvar measurements
- Level measurements
- Set-out of points [CURTIS, 86]
- Control of dial gauges

Most of these programs incorporate error checking routines which are performed in the field while measuring. For example the direction collection program checks for gross errors, such as pointing to the wrong target, and also performs a statistical analysis after three sets of direction measurements are completed. This analysis verifies for the user the reliability of the measurements made on a station by calculating the mean square error for the direction sets. In case the statistical check fails an additional set is requested by the program. If the statistical analysis still fails after the fourth set is measured, the station has to be remeasured completely. Another example of error checking is used while leveling. By using double scaled level rods it is possible to compare the difference of the left and right scale reading against the known offset between both scales and thus check for gross errors. An even number of setups within a level loop is required by the program, to eliminate the level rod offset when using two different rods.

Process Pending Updates

After uploading the recorded field data to the PC, the next step is to transfer these observation files from the shared disk to the actual database for permanent storage. This is done by function two of GEONET's main menu called "Process pending updates".

Data Reduction

Before the input files for a least squares adjustment can be formed, certain observations must be reduced for geometric or atmospheric corrections, while others have to be reformatted. Level lines, for instance, are reduced for the effects of the level rod calibration, as well as for the measured temperature of the rod tape during leveling [PELZER, 83]. Distances are reduced to a reference surface, in this case a Gaussian sphere best fitting the ellipsoid at the longitude and latitude of SLAC. Atmospheric corrections are also taken into account [BRUNNER, 84]. Direction sets are summarized and reformatted to their final form.

Reduction programs for the following measurements are currently available:

- Level measurements
- EDM measurements
  - DM503
  - MEKOMETER
- Distinvar measurements
- Direction measurements
- Offset measurements

After having evaluated the results of the reduction programs the user can move the result files from the local disk to the GEONET database using again option two "Process pending update". The next step will be to generate an input file for the appropriate least squares adjustment.

Generate Input File

The input file generation function creates input files for a group of geodetic adjustment programs used at SLAC [BURSTEDDE, 87]. These adjustment programs include 1–norm and 2–norm adjustments for 1, 2 or 3 dimensional networks. The datum of the network may be chosen as a unconstrained, minimal constrained, constrained or as a connected net bound to a superior net. The program for which the input file is required is determined using the menu shown in Figure 4.

Definition of the Program Name

Adjustment type	(OT)	=>
Network dimension	(123)	=>
Input data	(ERD)	=>
Orientation	(UATCF)	=>

Adjustment	Network	Input	Orientation
O...1 Norm	1...One Dimen	E...Error Prop.	U...Min. constrained
T...2 Norm	2...Two Dimen	R...Real Obs.	A...Constrained
	3...Three Dimen	D...Def Analysis	C...Connected
			F...Unconstrained

Figure 4. Definition of Adjustment Program Name

The program names are all four letter combinations where the first letter indicates the adjustment type, the second letter the network dimension, the third letter the input data type and the fourth the datum of the net. The user types one letter after each arrow on each line of the menu. These letters are then concatenated to form the program name .

Once the name of the program is known, the user is presented with a series of submenus which allow the user to specify which points to include in the adjustment, what types of observations are to be used and from which epochs the data should be taken. The data is then merged automatically into the input file in the format required by the adjustment program.

Perform Adjustment

Only 2 out of the 24 different possible adjustment programs running on the mainframe, were implemented on the PC network; a one-dimensional constrained adjustment (T1RA) for a level net with up to 60 benchmarks and a two-dimensional constrained adjustment (T2RA), which allows the adjustment of a net with a maximum of 40 points. All other adjustments are being processed on the mainframe after uploading the input file to the IBM 3081.

Coordinate database

Choosing this option takes the user to a sub-menu , which provides two options:

- Updating of an existing database
- Retrieving of coordinates from a database

In order to update a certain coordinate database, a specially formatted file, created by each least squares adjustment, has to be downloaded from the mainframe to the PC workstation. The coordinate database can then be updated using this function. An input file created for a later least squares adjustment then always picks up the most recent coordinates as approximate coordinate values.

The second option of the sub-menu can be used to retrieve coordinates of the coordinate database, thus providing a history of the movement of each survey monument.

NSC800 Operations

This option is provided for up and downloading programs and data files between the PC/XT and NSC800 micro processor controlled devices such as the SCHAEVITZ inclinomter, the hydrostatic level ELWAAG [THIERBACH, 79] and OFFSET measurement devices for the linear accelerator section of the SLC. The programs and interfaces which control these devices have been custom developed at SLAC.

Access server disk files

A privileged user is allowed to browse through the database, verify the contents of a selected subdirectory and print or edit certain files, by using this function.

Access calibration data

Similar to the previous function, this option enables one to browse through the calibration database.

System configuration

The system configuration option allows the user to create a new survey epoch for the data and calibration file system or to delete obsolete ones. The deletion of a survey epoch is only possible if the selected subdirectory does not contain any files.

A separate coordinate database can be assigned to each survey project. This option provides the possibility to create new coordinate databases using the standard basic structure described earlier.

Archive subsystem

Considering the fact that even the smallest files allocate 2 Kbytes of disk space, this function allows the user to combine several files into one file, in order to save disk space. This process is called data compression and is mostly used after the data reductions are done and the raw data is no longer used. Another part of this function allows one to archive obsolete data onto floppy disks in order to free up even more disk space. In both cases archived and compressed files can be retrieved and split into individual files at any time if necessary.

Escape to DOS

The escape to DOS function permits the user to temporarily return to the DOS command level while running GEONET. This is useful for examining the contents of the hard disk or performing a DOS command. To return to the GEONET session, the 'exit' command is used.

Exit GEONET

The Exit Geonet function terminates a GEONET session. It returns the user to the subdirectory from which GEONET was originally invoked.

CONCLUSION

The experience with GEONET has shown that the time it takes from recording measurements in the field to obtain adjusted coordinates is reduced tremendously by using an automated data management system. Without a system like GEONET it would have been impossible to align the Stanford Linear Collider in the given time frame of three years.

REFERENCES

1. Gründig L., Bahndorf J., 1984, *Optimale Planung und Analyse von 2— und 3— Dimensionalen Geodätischen Netzen im Ingenieurbereich — Programmsystem OPTUN* — in: Ingenieurvermessung 84 — Beiträge zum IX. Internationalen Kurs für Ingenieurvermessung, GRAZ, **pp. B2/1–12**.

2. Donahue, T., 1986, *The Building of a Total Survey System* in: Seminar for Surveyors and Civil Engineers FORESIGHT Newsletter & P.O.B. Publishing Co., Burlingame Appendix 3–A & B.

3. Burstedde I., 1987, *Das Programmsystem GEONET zur Ausgleichung geodätischer Netze* in: Allgemeine Vermessungs–Nachrichten, 3/87, **pp. 118–130**.

4. Burstedde I., Cremer, K., 1986, *Zur Ausgleichung geodätischer Netze nach der 1–*

Norm, in: Allgemeine Vermessungs–Nachrichten 6/86, **pp. 228–235**.

5. Pushor R., 1987, GEONET Data Management System User's Guide Version 3.00, Unpublished documentation, Stanford Linear Accelerator Center, Stanford University, CA.

6. Brunner F.K., 1984, *Modeling of Atmospheric Effects on Terrestrial Geodetic Measurements*, in: Geodetic Refraction, Springer Verlag, New York, **pp. 143–162**.

7. Pelzer, H., 1983 *Systematic Instrumental Errors in Precise Leveling*, in: Precise Leveling, Dümmler Verlag, Bonn, **pp. 3–17**.

8. Oren, W., Ruland, R. 1985, *Survey Computation Problems Associated with Multi-Planar Electron-Positron Colliders*, in: Proceedings of 45th ASP-ACSM Convention, Washington, D.C., **pp. 338–347**, SLAC-PUB-3542.

9. Curtis, C., Oren, W., Ruland, R., 1986, *The Use of Intersecting Lasers in the Alignment of the New Electron-Positron Collider at the Stanford Linear Accelerator Center* in: Proceedings of the 46th ASP-ACSM Convention Washington, D.C., **pp. 61–69**, SLAC-PUB-3837.

10. Ruland, R., Friedsam, H., 1986, *A Realization of an Automated Data Flow for Data Collecting, Processing, Storing and Retrieving — GEONET —*, invited paper, presented at the XVIII FIG Congress, Toronto.

11. Pietryka, M., Friedsam, H., Oren, W., Pitthan, R., Ruland, R., 1985, *The Alignment of Stanford's New Electron-Positron Collider*, in: Proceedings of the 45th ASP-ACSM Convention, Washington, D.C., **pp. 321–329**, SLAC-PUB-3543.

12. Erickson, R. (Editor), 1984, SLC Design Handbook, Stanford Linear Accelerator Center, Stanford University, CA.

13. Thierbach, H., 1979, Hydrostatische Mess-Systeme, Sammlung Wichmann Neue Folge Bd. 12, Wichmann Verlag, Karlsruhe, **pp. 72–75**.

14. Kernighan W., Ritchie M., 1978, The 'C' Programming Language, Prentice-Hall, Inc.

THE APPLICATION OF THE PRINCIPAL CURVE ANALYSIS TECHNIQUE TO SMOOTH BEAM LINES

H. FRIEDSAM, W. OREN

Stanford Linear Accelerator Center
Stanford University, Stanford, CA

Introduction

The smoothness of a beam line refers to the quality of the relative positioning of a number of adjacent beam guiding components. The fact that smoothness is of highest priority when positioning magnets can be seen in the local tolerances imposed by the beam optics. In the past, smoothing has been done by separating horizontal and vertical misalignments and then applying some sort of analytical or manual "feathering" technique. The Stanford Linear Collider (SLC) did not easily lend itself to this sort of smoothing because of the highly coupled nature of its pitched and rolled beam line. This paper will discuss an attempt to develop a repeatable method which is independent of the inconsistencies of human judgment and can simultaneously smooth in two or more dimensions.

Goals

Four major goals were defined for the smoothing algorithm used on the SLC alignment. The first, was to simultaneously model errors for both horizontal and vertical directions. Secondly, a smooth curve whose shape was suggested by the data and not by a predetermined model was implied by the fact that unknown systematic errors were being eliminated. Thirdly, this curve must be a reproducibly fit, independent of the inconsistent nature of human judgment. Fourth, the result of the procedure was to minimize the number and size of magnet movements to reach the final alignment criteria.

Smoothing The SLC Beam Lines

The alignment tolerances set out for the SLC show how smoothness is more important than absolute positioning for beam transport. For this machine a global positioning envelope is set to ± 5 mm for every arc magnet, while the relative alignment of three adjacent magnets must be within ± 0.100 mm (Figure 1). Probably the biggest enemies in achieving this last tolerance are unmodelled systematic measurement errors.

The pitched and rolled sausage-link beam line formed by the arc magnets makes this modeling particularly difficult. The absolute design shape of the path is a series of curves and straight sections in pitched and rolled planes. This form does not readily lend itself to fitting with polynomials or splines. The large coupling of X and Y motions also prevents the separation of smoothing operations into two components.

Solution

The complication of an irregularly shaped beam line was eliminated by subtracting out the actual size and shape of the beam lines, leaving a series of residual misalignments for a string of magnets. Figure 2 shows an example plot of X and Y residuals which now must be modeled. This plot indicates a highly systematic trend which can be explained by unaccounted systematic errors inherent in the measurement procedure. These errors cause a strain or bowing when the observed network is adjusted, using least squares, holding the endpoints fixed at their ideal coordinates.

Principal curve analysis was chosen to simultaneously pass a one dimensional curve through the X and Y residual misalignments mapped out along the Z-axis.* This curve will pass through the middle of the data set such that the sum of the squared errors in all variables are minimized. If the procedure were allowed to iterate many times the curve would approach almost all the data points thus creating a form which may or may not be considered smooth. This presents a problem of determining what is smooth.

The 0.1 mm local alignment tolerance suggests a calculatable smoothness criteria. Figure 3 shows how a 0.1 mrad angular offset of one magnet direction to its neighbors will result in a 0.1 mm transverse offset at beam line. If this threshold is exceeded, the curve is defined as no longer being smooth.

One of the goals of smoothing was to minimize movements of the magnets to a smooth curve. However, if an outlier from the trend curve exists, it may artificially bias the fitting routine and draw the curve away from the general neighborhood trend. For this reason a robustness estimator is included in the modeling program to weight out these points.

The end result has been a series of transformation programs which standardize the measured magnet misalignments to a common reference line where they can be modeled. A one dimensional principal curve which passes through the middle of the multidimensional data set is then fitted. This curve is non-parametric with its shape suggested by the data. Through robustness estimators and physics defined smoothness criteria, the curve is reproducibly fit to the trend of the alignment

⋆ "Principal Curves and Surfaces" by Trevor Hastie; SLAC Report - 276, 11/84.

data. What results is a table of movements to be applied to the magnets to align them to the smooth trend curve.

Observation Plan and Adjustment

The horizontal network consists of a series of direction sets measured from stations directly on the magnet reference points. The observation plan is designed so that each point including the positions occupied by the instrument is sighted at least three times. What results is an extremely long and narrow network made up of directions. To strengthen the network in the beam direction, distances between reference points are measured with the Distinvar. These observations are then adjusted in a least squares routine where the endpoints of the network are held as knowns. This constraint often causes the bowing seen in the residual misalignments plotted in Figure 2.

The vertical network is built up through overlapping leveling runs which span the same reference points observed in the horizontal measurements. This network is also reduced by holding fixed the same end points of the total level line. The residual misalignments in Y as shown in Figure 2 tend to be more random due to the lack of unmodeled systematic errors encountered in leveling.

Example

At first this technique was applied only to arc magnets ignoring junctions between the arcs and the special sections of the beam line such as the final focus. This was done because evenly spaced magnets with a homogenous observation plan were easy to describe and model. However, this homogeneity was broken when one proceeded into the final focus where magnets were irregularly spaced and each had multiple reference points for the alignment. The following example was the first attempt at smoothing the transition between the south arc and the final focus.

Figure 4 shows the misalignments in X and Y which must be modeled. Figures 5 shows the step by step fitting of the data in the Y direction. The X direction is also being smoothed during the same operation but is not shown here. Note the application of the robustness measure on the data points part way down the beam line. Figure 6 shows the final fitted curve in the X direction. The "rough" look to the plot results from the uneven scale on the horizontal axis verses the vertical axis (60,000 mm verses 1.2 mm). Table 1 summarizes the final movements to be applied to the magnets. All changes of 60 microns or greater are flagged for adjustment. Finally, Table 2 shows the results of a check measurement of the same area. The only remaining adjustments are ones caused by mechanical modifications to the magnets after the initial alignment.

Further Improvements to the Technique

Two immediate improvements are suggested through our experience. The first involves the weighting of points in the smoothing routine so that a small area of magnets can be "patched in" to existing elements. This would enable one to force the direction of the beam line if movements of one section were not desirable. The second improvement is not quite as straight forward. It involves the definition of what is smooth. How does one stop the iteration process on sections of a beam line where the alignment tolerances are not as well understood as they are for the arcs. If this problem can be solved a general smoothing algorithm for any beam transport line could be developed.

Conclusion

Through the application of principal component analysis a successful smoothing procedure was developed for the highly coupled SLC beam line. The routine allows for a flexible yet repeatable fitting of data which may be superimposed with with unmodeled systematic measurement errors. A smoothness criteria was developed which reflected beam alignment tolerances and still allowed the number of magnet adjustments to be minimized. The technique still needs improvement to make it a general smoothing program but its application to the SLC has already been highly successful.

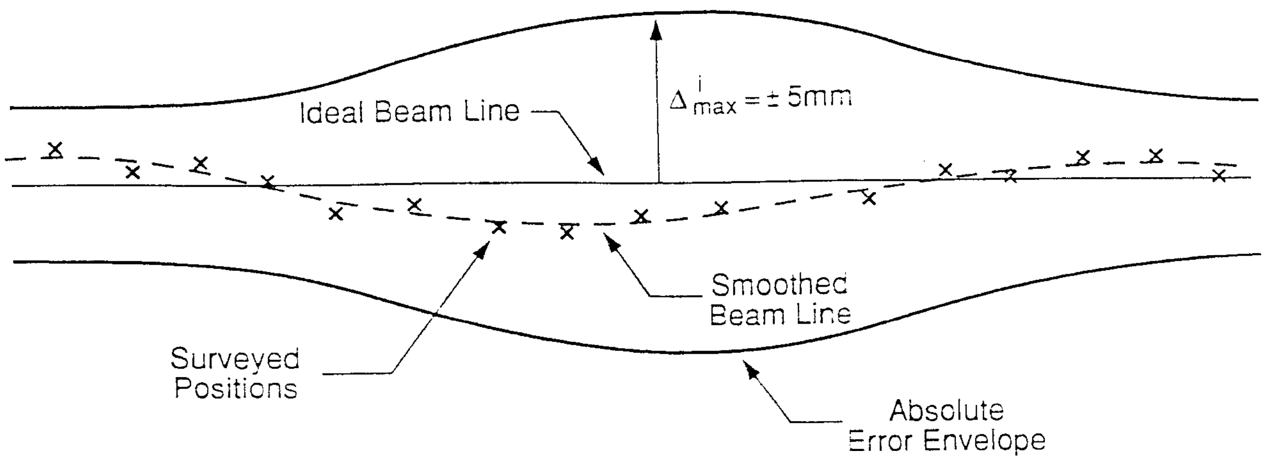

Figure 1. Global Positioning Envelope

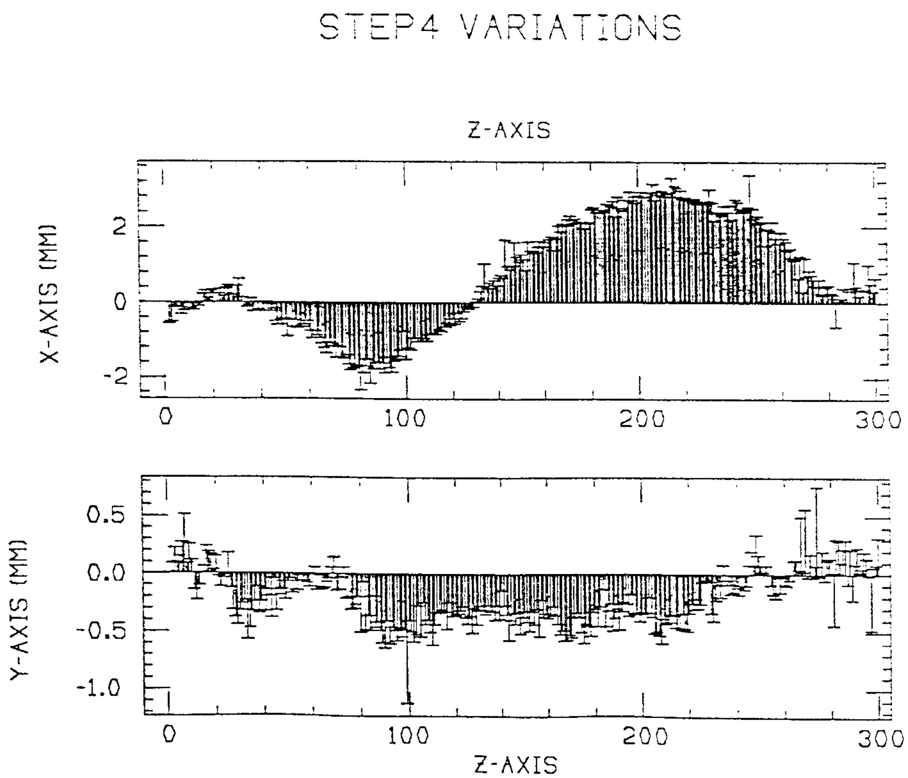

Figure 2. X and Y Residuals

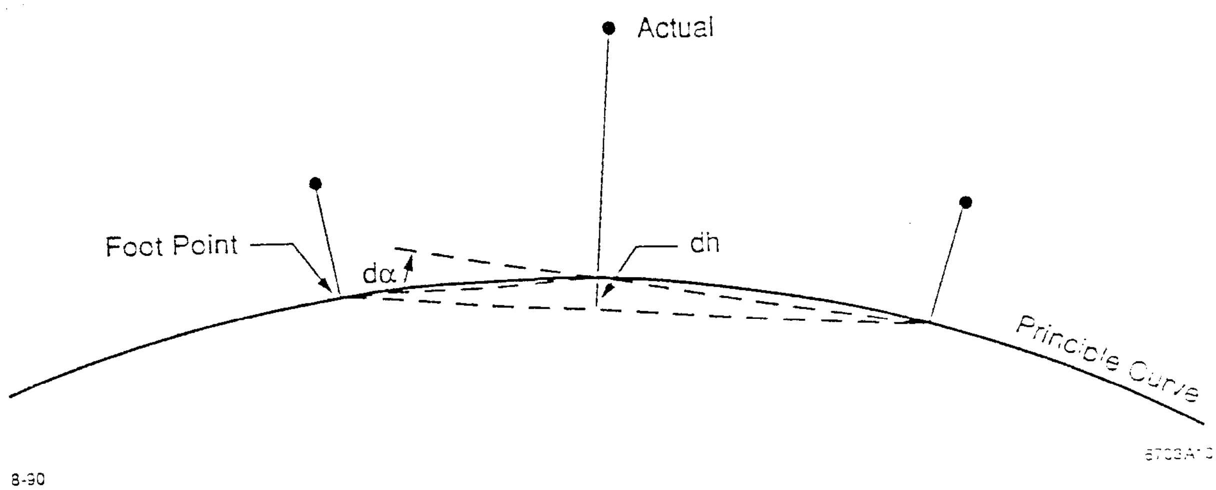

Figure 3. Smoothness Criteria

$d\alpha \leq 0.1$ mrad
dh 0.1 mm

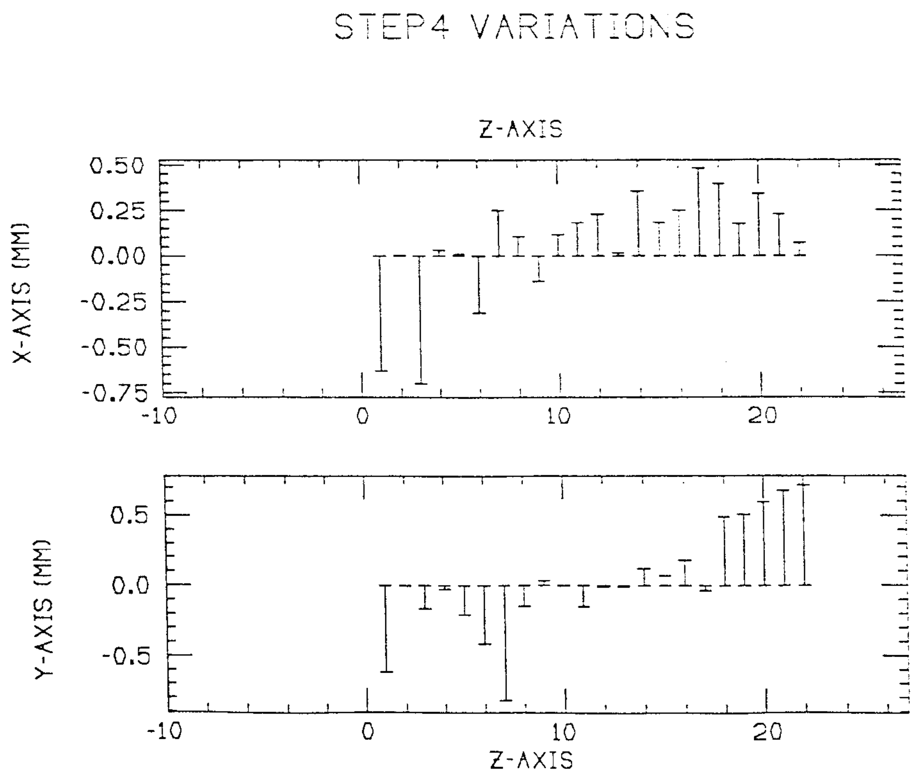

Figure 4. X and Y Residuals

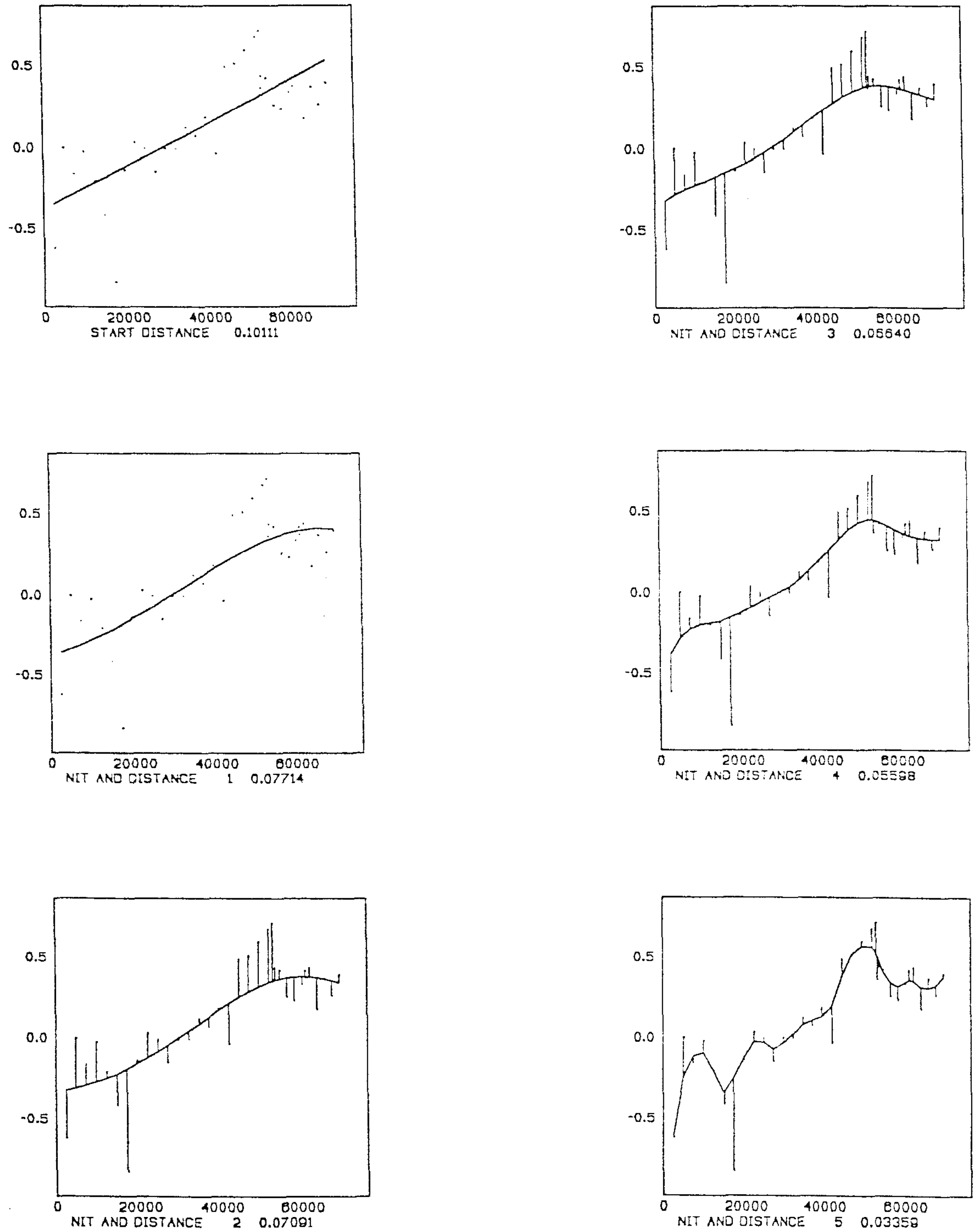

Fig. 5. Step-by-Step Fitting of a Smooth Curve in Y Direction

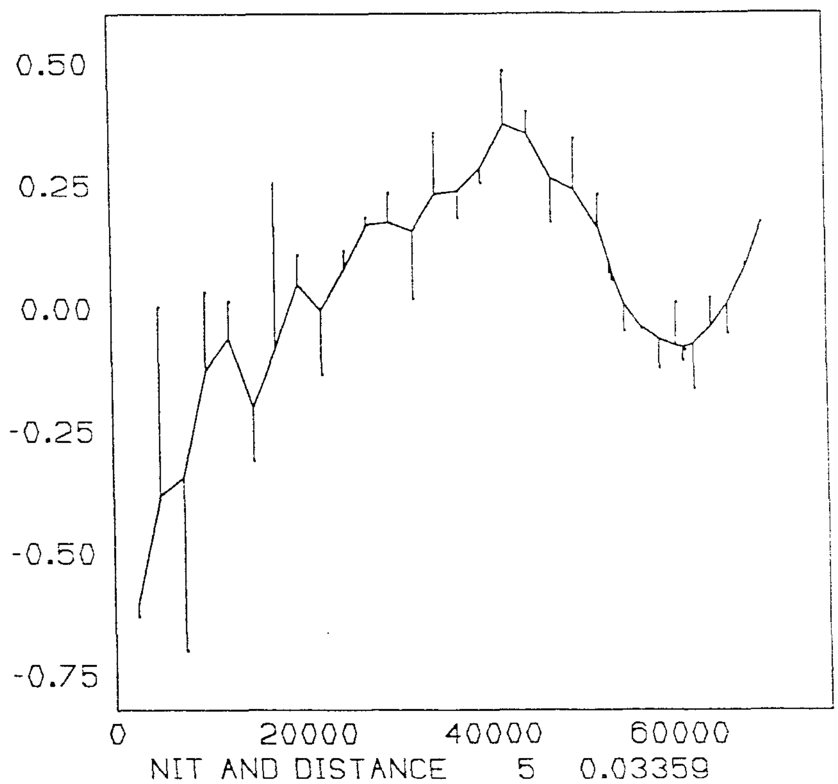

Fig. 6. Final Fitted Curve in X-Direction

STEP4 DIAL GAGE ADJUSTMENTS - 02-04-89 - 10:36

NAME	Z[mm]	X[mm]	Y[mm]	
XS2301FF	0.01081	0.13784	0.23016	* *
XS2302FF	-0.01273	-0.37920	-0.28359	* *
XS2303FF	-0.00280	0.42136	-0.06511	* *
XS2304FF	-0.00719	-0.23363	-0.17675	* *
XS2305FF	0.00058	-0.15426	0.01493	* *
XS2306FF	0.00852	0.21948	0.23377	* *
XS2307FF	0.02288	-0.30323	0.66675	* *
XS2308FF	0.00039	-0.11449	0.01219	*
XS2309FF	-0.00389	0.17062	-0.12944	* *
XS2310FF	-0.00170	-0.03913	-0.06088	*
XS2311FF	0.00300	-0.06695	0.11618	* *
XS2312FF	0.00005	-0.07959	0.00205	*
XS2313FF	0.00085	0.16814	0.03980	*
XS2314FF	-0.00088	-0.14156	-0.04550	*
XS2315FF	0.00099	0.05692	0.05766	
XS2316FF	0.00012	-0.00191	0.00801	
XS2317FF	0.00372	-0.22948	0.29115	* *
XS2318FF	-0.00177	-0.15982	-0.16799	* *
XS2319FF	-0.00106	0.04017	-0.12900	*
XS2320FF	-0.00102	-0.17158	-0.16960	* *
XSFF01FF	-0.00103	-0.11324	-0.23440	* *
XSFF01RF	-0.00120	0.02223	-0.27376	*

MEAN AND VARIANCE FOR Z X AND Y

ZMEAN:	0.00075663 ZVAR:	0.00680846
XMEAN:	-0.04324045 XVAR:	0.18852785
YMEAN:	-0.00287997 YVAR:	0.21795110

Table 1.

Magnet Movements After the First Iteration

STEP4 DIAL GAGE ADJUSTMENTS – 02-10-89 – 16:58

NAME	Z[mm]	X[mm]	Y[mm]	
XS2301FF	0.00003	0.00039	0.00062	
XS2302FF	-0.00103	-0.01428	-0.02283	
XS2303FF	0.00802	-0.30181	0.18715	* *
XS2304FF	-0.00001	-0.00246	-0.00024	
XS2305FF	-0.00038	0.00092	-0.00983	
XS2306FF	0.00047	0.00876	0.01287	
XS2307FF	0.00052	-0.00364	0.01501	
XS2308FF	-0.00038	0.01081	-0.01174	
XS2309FF	-0.00009	-0.02333	-0.00305	
XS2310FF	-0.00023	0.00609	-0.00808	
XS2311FF	0.00030	0.00893	0.01178	
XS2312FF	-0.00009	-0.02992	-0.00382	
XS2313FF	0.00069	0.02967	0.03198	
XS2314FF	-0.00048	-0.03095	-0.02498	
XS2315FF	0.00020	-0.00269	0.01184	
XS2316FF	-0.00004	0.04543	-0.00285	
XS2317FF	-0.00004	-0.03912	-0.00333	
XS2318FF	0.00001	-0.04687	0.00112	
XS2319FF	0.00005	-0.00008	0.00615	
XS2320FF	-0.00053	0.08747	-0.08847	* *
XSFF01FF	-0.00024	-0.10377	-0.05333	*
XSFF01RF	-0.00003	-0.11914	-0.00660	*

MEAN AND VARIANCE FOR Z X AND Y

ZMEAN:	0.00030547	ZVAR:	0.00176313
XMEAN:	-0.02361905	XVAR:	0.07592055
YMEAN:	0.00178909	YVAR:	0.04824993

Table 2.

Magnet Movements After a Second Iteration

SIMS: The SLAC Industrial Measurement System

BERNARD BELL

Stanford Linear Accelerator Center
Stanford University, Stanford, CA 94309

1. Introduction

The development of electronic sensors and of small powerful computers, and their integration together have led to the development of what has come to be known as Industrial Measurement Technology (IMT). Industrial Measurement Systems feature one or more electronic sensors and a computer with powerful software. The software has three essential components: data collection, data reduction and data analysis. In the field of industrial surveying, the IMT system is the automated theodolite system, but other systems such as the laser tracker are on the horizon.

2. History of IMS at SLAC

Kern was the first survey company to market an Industrial Measurement System when it released ECDS (Electronic Coordinate Determination System) in the mid-1980s. Originally written for the PDP-11, a version was later released for the PC (ECDS-PC). SLAC purchased this system in 1986 and immediately began to use it for the alignment of the SLC (Stanford Linear Collider). Although ECDS enabled us to perform tasks with a speed never before achieved, we experienced limitations in the software. Since Kern proved unresponsive and we were unable to purchase the source code for any amount of money, we set about writing our own portions of code. We first wrote a system of menus tailored for our specific alignment tasks, and disabled much of the ECDS menu structure. Due to dissatisfaction with the ECDS bundle adjustment program, we wrote our own bundle adjustment in 1988. A further step toward having our own complete IMS was to develop a data capture program, a task which has been underway since the beginning of this year. We do not yet have data analysis features that are fully integrated, but we do have stand-alone packages that have been written at SLAC. When we first started tinkering with ECDS there was no intention of developing a complete system, but we now have all the elements of such a system – SIMS, the SLAC Industrial Measurement System.

This paper describes the features of our system and some of the uses we have made of it.

1. SIMS Described

1.1 Hardware

The sensor used in SIMS is the Kern E2 electronic theodolite, our workhorse of the past few years, but it is planned to expand SIMS to handle Wild T3000 theodolites. Our choice of computer is the Compaq III portable because of its convenient size, but any 286 machine can be used. A 287 co-processor is advisable, but not essential, for the heavy-duty number-crunching software modules. The hardware is housed in a wooden crate mounted on the back of a small electric cart for easy portability around the laboratory. This crate contains the computer, a printer, and the power supply for the theodolites. Space is provided for other devices, such as an inclinometer interface box which is usually housed in the bottom. A panel on the outside of the crate provides receptacles for the cables to the theodolites as well as to other instruments such as the inclinometers. The panel has four E2 ports but more theodolites can be connected by using little mutliplexer boxes built at SLAC.

1.2 Software

In order to avoid retraining operators and to maintain consistency with old ECDS data sets, the SIMS programs were originally designed in a style similar to ECDS. As time has gone on, though, and SIMS has evolved into an entity totally distinct from ECDS, the two IMS systems have diverged in their looks and functionality.

Whether the measurement tool be a theodolite, a laser tracker or a CMM, IMS software has three major components:

(*a*) *Data Capture:* The software to control the measurement heads and record data from them. Elementary error checking should be included.

(*b*) *Data Reduction:* The software to calculate coordinates from the raw data, preferably using rigorous least-squares methods.

(*c*) *Data Analysis:* Software to analyse and evaluate the computed coordinates. Capabilities should include coordinate transformations and geometrical fits (*e.g.*, circles, planes).

The SIMS software is written in Microsoft C and Microsoft Fortran to run under DOS.

1.2.1 Data Collection

The data capture program offers all the functionality of ECDS with the addition of several features that we have found necessary for our work at

SLAC. It was because ECDS did not offer these features that we developed our own data capture program. Some of these features have become available in later versions of ECDS, but they were not available when we had need of them.

1. *Direct and Reverse Measurements.* ECDS allowed observations on only one face. A measurement job in the summer of 1988 required vertical angles exceeding 50°. By taking measurements on both faces a substantial improvement was obtained in the strength of the bundle adjustment. Since then our standard measurement procedure has been to measure all points on both faces, no matter what the vertical angle. For steep sights the mean of direct and reverse measurements eliminates certain instrument and set-up errors. For all observations, the mean of direct and reverse measurements eliminates collimation errors. With electronic theodolites the collimation error can be corrected electronically, but we have had problems with these correction values drifting significantly over time. It is our recommendation that all measurements for industrial survey be two-faced, something that has been ingrained into us in school for good reason.

2. *Re-initialization of any theodolite at any time.* For a large object, or even for a small one in which one cannot see all points from one set-up, the theodolites are moved to new locations for further measurements. In ECDS this required exiting the program and starting all over again with the re-initialization of all instruments. Often it is not desirable that all instruments be moved. SIMS has therefore been written to allow any instrument to be moved and re-initialized at any stage in the program without disturbing the other instruments or the program.

3. *On-line checking of observations against nominal coordinates.* For much of the work for which SIMS is used, nominal coordinates are available for the points being measured. This is so when the task is to align elements into their design locations, or to undertake an as-built survey to check conformity with design coordinates. It is possible in SIMS to measure the control points on an object, exit the program to run the bundle adjustment and any necessary coordinate transformations, and return to the data capture program in the same place but now with known coordinates for the theodolites in the object coordinate system. This permits on-line checking for the consistency of observations with the nominal coordinates of the points. For each measurement point a check is made of the control file. Points in the control file can be identified as fixed or approximate, and separate tolerances can be applied to these two types of points. This feature is useful in trapping blunders such as misnamed points or sighting on the wrong point, something

that can frequently happen if there are a lot of closely-spaced points.

4. *Non-sequential instrument addresses.* The address switch on the Kern E2 theodolites can be set from 0-9, but ECDS required the instruments to be numbered sequentially from 1. Since our theodolites are identified by the address switch, the number being assigned in the order of their acquisition, this forced us to change the numbers, making it difficult to keep track of which physical instruments were used for a particular survey. SIMS has been written to handle any addresses from 0-9 and they can be non-sequential. The only requirement is that two instruments not have the same address. This enables us to know exactly which physical instruments have been used.

1.2.2. Data Reduction

The data reduction part of SIMS consists of 3 programs:

(a) MEAN: calculates the mean of the direct and reverse measurements and prints this to the output file, together with the horizontal and vertical differences between the observations. Differences greater than 5 mgon are flagged.

(b) INTER2: computes approximate coordinates for the theodolites and for the object points, using data in the control file.

(c) 3DCD: the bundle adjustment, which is a rigorous, iterative least-squares adjustment (Gaunt, 1988). The 3DCD print-out contains not only the final coordinates, but also the residuals in the observations, standard errors for the object points and theodolite stations. Relative errors between any two points can be optionally requested in the input file. The residuals are in angular units, unlike the ECDS bundle adjustment which gave residuals as the perpendicular distance offset from the observed point; this is of little value since it is as dependent on the distance between the instrument and the point as it is on the angular accuracy of the observation.

There are two versions of 3DCD, one on the PC the other on the mainframe computer. The programs are identical except for the number of observations and points they can handle:

	Theodolite Stations	Object Points	Observation Pairs
PC version	10	70	700
Mainframe	25	350	8750*

1.2.3. Data Analysis

The data analysis part of SIMS exists as a set of stand-alone programs, mostly on the mainframe, that have not yet been integrated with the suite of

SIMS programs on the PC. There is not a pressing need for this integration since it is usually more convenient to do the data analysis back in the office while the field crew continues to record data. The programs used most often are the 7-parameter coordinate transformation package and the plane and circle fit routines.

2. Use of SIMS at SLAC

2.1 SLC Manget Junctions

The two arcs of the SLC are each about 1400m in length and contain about 460 magnets, divided into sets of 20, each set being known as an achromat. Although the tolerances on the absolute position of each magnet are tight, it is the relative alignment of each magnet relative to its neighbors that is especially critical. Due to topographical restrictions of the site, the SLC arcs undulate up and down as well as being curved in the horizontal plane. As a result, each magnet is pitched and rolled out of the horizontal by up to 10° in pitch and 15° in roll. The change in pitch and roll from magnet to magnet is small, except at the achromat junctions where there can be an abrupt change in attitude. Because of these large discontinuities in magnet orientation across achromat junctions, it proved impossible to develop a mechanical jig for the alignment of the adjacent magnet ends. It was for the alignment of these junctions that we first used ECDS, and it quickly proved its worth. The method was to survey the fixed end of one magnet and then, having performed the necessary coordinate transformations, measure the adjacent adjustable end of the next magnet in the coordinate system of the fixed end. Although ECDS proved itself useful for data collection and for the bundle adjustment, its shell was cumbersome for SLAC's needs. Consequently we wrote our own shell program, tailored specifically to the project, and incorporated only such parts of ECDS as were needed (Oren, 1987). In addition our shell contained interfaces to databases of magnet calibration values and of ideal coordinates as well as interfaces to other electronic equipment such as inclinometers and electronic digital indicators.

Thus was started our history of dabbling in ECDS, a process which eventually led to the development of a completely independent system, though this was not envisaged at the time.

2.2. Fiducialization of Beamline Components

The standard feature that is used as a reference or fiducial on beamline components is the quarter-inch tooling socket. Prior to installation, coordinates must be determined for these sockets in a coordinate system based upon the magnetic or geometric centerline of the part. Small parts are taken offsite to a contract measurement service with a Coordinate Measuring Machine (CMM). Parts too large for this CMM have been measured at SLAC using SIMS. In this case, SIMS is operating like a large but portable CMM.

2.3. Alignment of Detector Components

SIMS has proven useful as an alignment tool in the construction phase of SLD components. The Čerenkov Ring Imaging Detector (CRID) is built inside a cylinder 3.5 m in diameter and 7 m long. The various subassemblies of CRID lie on planes and circles at various distances from the centerpoint. It was easy then to fit circles and planes through measured points, using the residuals from these best-fits to bring the parts into their ideal locations. Several iterations were made to bring the points within tolerance.

Due to its size, the assembly of CRID did not lend itself easily to optical tooling, but SIMS proved its worth as an alignment tool.

2.4. As-built Surveys of Detector Components

In the past year a couple of projects have been undertaken which have proven very stretching both for our survey crews and for the SIMS software. At the same time, they have been excellent an proving ground for SIMS, and the current state of the software owes much to needs and ideas that arose during these projects.

Both projects required the measurement of a large number of points in as-built surveys of components for the SLD detector. No alignment was required, only XYZ coordinates in the coordinate system of the relevant chamber.

2.4.1. The End-Cap Drift Chambers

The SLD detector has four end-cap drift chambers, two large chambers 3.5 m in diameter and two smaller chambers of 2 m diameter. All four chambers are approximately 30 cm thick and contain three layers of wires, rotated 60° with respect to one another. The task was to measure the location of each wire terminator block. Visibility was relatively poor because the blocks were recessed inside the layers and because the direction of the blocks on one layer was 60° or 120° different from the other layers. As a result it required many instrument set-ups to measure each chamber, even with four instruments in use. The most instrument stations used was 43 for one of the large chambers. The resultant data set was too large even for the mainframe version of 3DCD and was broken into two sets, of 27 and 16 stations. It was for this project that it was helpful to have software that facilitated the movement and re-initialization of any theodolite at any time. An interesting feature of this project is that it was easier to rotate the chambers than to move the instruments to see a new set of blocks. The X-axis of each chamber was marked on the top so that the theodolites could be pointed in the right direction during initialization.

2.4.2. The Central Drift Chamber

The SLD Central Drift Chamber (CDC) is a cylinder 2 m long and 2 m in diameter with 40,000 wires stretched end to end. The wires are held in 640 terminator blocks in each end cap. We were requested to measure not only the location but also the attitude of each of the 1280 blocks. To determine the plane of each block required the measurement of at least three points on the target fixture. Including the fiducial points and blocks that were re-measured after being replaced, over 4000 points were measured, each with direct and reverse observations from three theodolites. The geometry and measuring conditions were excellent, but the task of making 25,000 separate measurements imposed a strain on both the operators and the software. Through the course of this project a number of suggestions were made and implemented to streamline the SIMS software. Since there was no need for the simultaneous least-squares adjustment of all the points, the data was reduced in sets of up to 200 points as the work progressed.

The CDC was also rotated as the measurements progressed while the instruments stayed in place, but unlike the end-cap chambers which were rotated in the horizontal plane, it was rotated in a vertical plane about its horizontal axis. Consequently, there were times when the theodolites were "upside-down" in the object coordinate system. In order for the bundle adjustment to run successfully it was necessary to enter the approximate orientation of the theodolites in the input file.

Neither of these projects would have been feasible just a couple of years ago. It is the development of IMS that has rendered such large surveys possible. Nor would the projects have been feasible with ECDS because the clumsiness of the software would have rendered the project prohibitively expensive in manpower requirements. Having proven our capability in handling such projects we expect requests for further as-built surveys. SIMS will be used unless the project lend itself to photogrammetry and funding is available for such.

3. Conclusion

SIMS has been developed from ECDS to suit the measurement tasks specific to SLAC. There is no pretence that it is the most suitable package for all industrial measurement needs. ECDS or the Wild MANCAT package may indeed be more suitable for more conventional tasks, but SIMS is adapted to the specialized requirements of accelerator alignment. It has been beneficial to develop our own in-house system. A particular advantage of this is that we have our own source code onsite so that new features can be incorporated as the need arose. SIMS has been evolving for the past three years and will surely continue to evolve to meet the ever-growing challenges of survey and alignment at SLAC.

4. References

1. Gaunt, J.M., Bundle Adjustments and Tri-dimensional Coordinate Determination, 1988, SLAC-PUB-4717.
2. Oren W., R. Pushor & R. Ruland, Incorporation of the Kern ECDS-PC software into a project orientated software environment. *Proc. of the 47th ACSM-ASPRS Convention*, SLAC-PUB-4141.

5. Addendum

Since this paper was presented in August 1989, SIMS has been further enhanced and developed. Wild T3000 theodolites have been fully integrated, so that it is now possible to use Kern instruments alone, Wild instruments alone, or both simultaneously. Due to the different protocols of the two types of instruments, they are addressed over separate serial ports. SLAC does not use electronic theodolites from other manufacturers, but there is no reason why it would not be possible to expand SIMS to include such instruments.

A Compaq III 386 portable computer with 387 processor is now used. The increased speed is especially noticeable in the data reduction programs, but has little effect on the data capture program which is limited by operator input and by the fixed speed of the theodolite electronics. The PC version of the 3DCD least-squares adjustment program has been compiled under the NDP Fortran compiler which breaks the 640kB limit on the size of a Fortran program under DOS. This has allowed the PC version to be enlarged so that it is now identical with the mainframe version.

A small portable AC power supply has been built which provides power for the theodolites and interfacing and multiplexing capabilities. The unit has ports for four Wild theodolites and four Kern theodolites. Two serial ports are provided for direct connection to the computer.

CAN THE KERN ME5000 MEKOMETER REPLACE INVAR MEASUREMENTS?

RESULTS OF TEST MEASUREMENTS WITH THREE MACHINES

T. W. COPELAND-DAVIS

Stanford Linear Accelerator Center
Stanford University, Stanford, California 94305

ABSTRACT

The use of the Kern Me5000 as a 'stand alone' instrument is restricted to a minimum measurement distance of approximately 20m (Kern internal 'low range' program), with a display readout to the nearest 100µm. Using an external program, it is possible to extend both, the display resolution to 10µm, and the range down to distances well below 20m. This paper attempts to explain Kern's reasoning behind the original limitation of approximately 20m, and presents the results from testing three Mekometer Me5000 instruments. Their similarities, differences, and accuracies are assessed for distances below 25m providing a comparison against the use of invar wires.

INTRODUCTION

For most of the accelerator research centres, the primary range of distance measurement is less than 200m. Below 50m invar wires are used to determine the required networks within the accelerator tunnels for installation and verification of the accelerator components. With the advent of the Kern Mekometer Me5000 an alternative solution to the measurement of quasi-linear (machine and transfer lines) or three-dimensional (experimental areas) networks using invar wires is offered.

The use of the Kern Me5000 as a 'stand alone' instrument is restricted to a minimum measurement distance of approximately 20m (Kern internal 'low range' program), with a display readout to the nearest 100µm. Using an external program, it is possible to extend both, the display resolution to 10µm, and the range down to distances well below 20m.

This paper attempts to explain Kern's reasoning behind the original limitation of approximately 20m, and presents the results from testing three Mekometer Me5000 instruments. Their similarities, differences, and accuracies are assessed for distances below 25m providing a comparison against the use of invar wires.

Starting with the basic equation for distance measurement :

$$D = (N \times L) + A \qquad (1)$$

Where

N x L = the number of Standard Wavelengths.

A = fractional part of **L**.

The standard-length is a light wave modulated with constant frequency **F**. The half wavelength **L** of the modulation is :

$$L = \frac{c}{2 \times F}$$

So with the light velocity in a vacuum C :

$$c = \frac{C}{n}$$

Where

c = light velocity in the medium (ie. air).

n = index of refraction of the medium which is a function of temperature, pressure, humidity, etc...

To improve the resolution of the fractional part of **L**, the modulation is applied on the polarization of the light beam. Schematically (see figure 1), the optical path is : from the source, the light passes through the modulator and is sent to the reflector, returning to a phase detector which compares the polarization with the internal reference beam. The difference of phase is then transformed into a fraction of **L**. In relation (1) above, the unknowns are **N** and **D**. All electro-optical distance meters use two or more frequencies to find **N** but can be separated into two distinct groups due to their method of measuring the fractional part of **L**, namely, **A**.

The first group of instruments which include the Kern Dm502, AGA Geodimeters, Mekometer 3000, and Wild Di2000, use discrete, fixed frequencies to measure the phase difference between the reference and return beams via an electro-optical process.

An alternative method, adopted by the second group, is to vary the frequency until the fractional part is effectively nulled. The Terra Technology Terrameter and Mekometer Me5000 (see figure 1) belong to this group and have the advantage that they are not affected by cyclic errors.

For the Me5000, which uses a Helium-Neon laser (approximate wavelength 0.6m), Kern designed a system incorporating a quartz oscillator coupled together with a light modulator. This produces a working frequency range of 460MHz-510MHz.

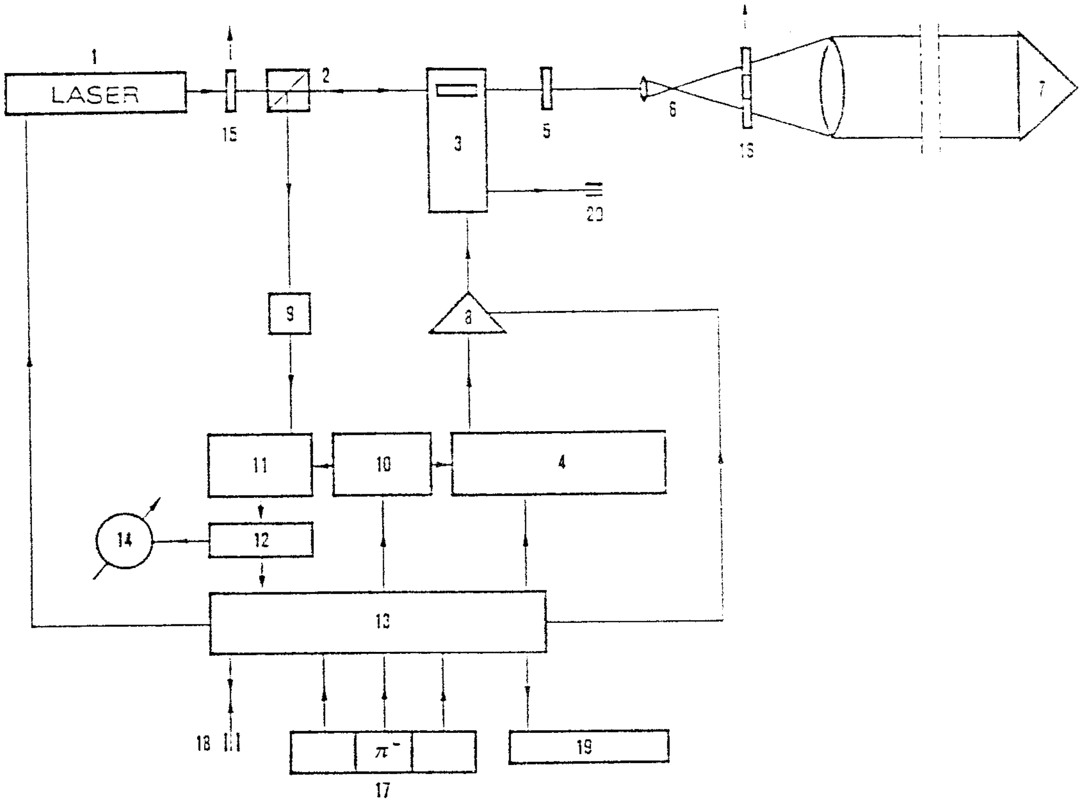

1	Laser	11	Lock-in amplifier
2	Polarization beam splitter	12	A/D converter
3	Modulator	13	Controller
4	Frequency synthesizer	14	Indicator
5	λ/4 plate	15	Attenuator
6	Telescope	16	Aperture
7	Reflector	17	Control switches
8	RF-amplifier	18	Data I/O
9	Light detector	19	Display
10	Sweeper (Wobbler)	20	Frequency output

FIGURE 1 Schematic diagram of the Me5000 (from [1]). A Helium-Neon laser (1) emits continuous linear polarized light of wavelength, 632.8nm. The light ray passes unaffected, through a polarized beam splitter (2) into the modulator (3) to give a polarized modulated frequency of approximately 500Mhz, the frequency being set by the synthesizer (4). The beam continues to the λ/4 plate (5), which serves as the temperature compensation for the modulation crystal, and through the telescope (6). The telescope widens the beam before it travels over the measurement path and returns from the reflector (7). In the reverse direction, the contracted beam passes back through the λ/4 plate, where now, the electro-optical crystal acts in reverse to demodulate the light wave. If at the entry and exit points, given by the amplifier (8), the phaselag of the modulated signal is balanced, then the original linear polarization is restored. In this case no light passes onto the light detector (9), the zero point always occuring when the distance is a multiple of 1/2 the modulation wavelength (approximately 30cm).

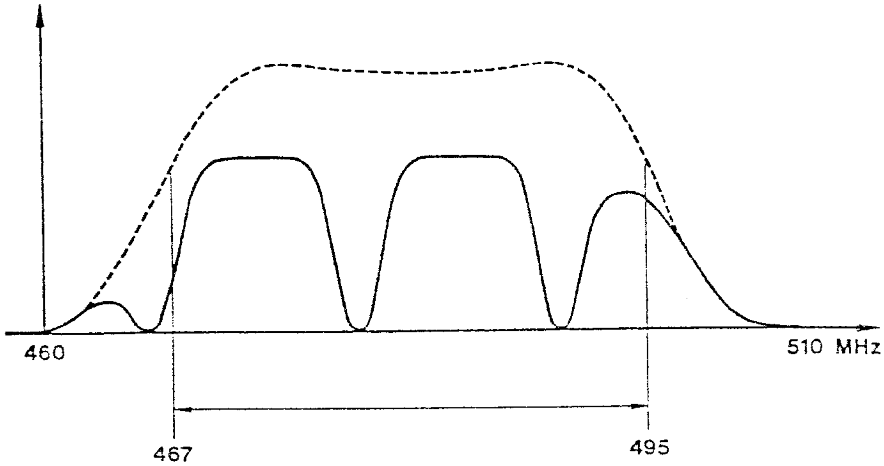

FIGURE 2 Frequencies and minimums (from [1]). The dashed line represents the modulation frequency curve throughout the working range of the instrument obtained during internal calibration of the crystal (plotted against the intensity). The solid line shows an example of how this curve is affected during the measurement process (the minimums occuring where the phase difference between the reference and return beams approaches zero). Although three minimums are shown, the first one is outside the usable range, having a low definition due to the modulation efficiency. The other two are within the optimum band width and would exhibit a good result (notice that both of these appear where the modulation frequency intensity is at a maximum; as the intensity decreases the definition of the minimum is reduced).

However, the actual frequency range used for measuring is reduced from this to an optimum band-width of 470MHz-490MHz; this range varying slightly between instruments due to the uniqueness of each crystal used (see figure 2).

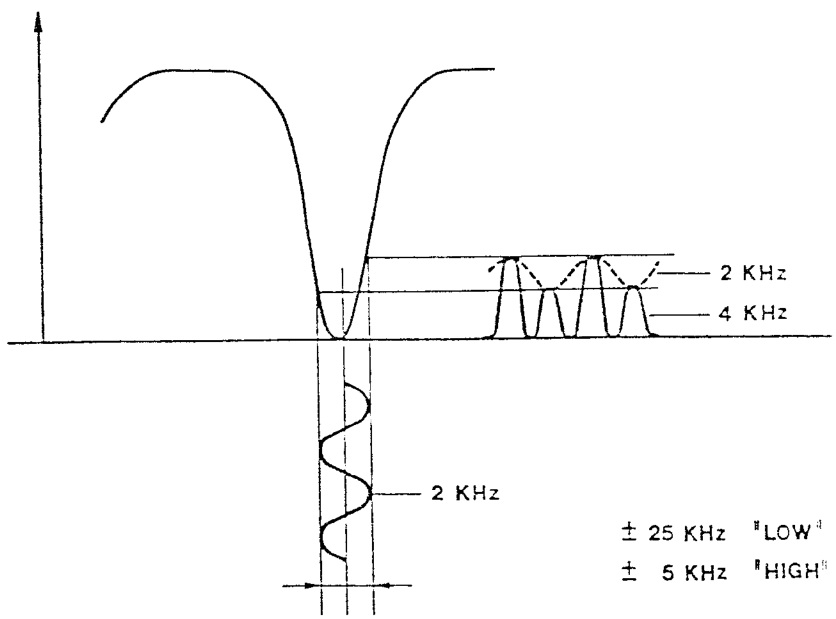

FIGURE 3 Search of a minimum (from [1]). To determine more accurately a frequency at the zero point, the modulation signal is changed by a wobbler, (10) in figure 1, with a sine wave of 2Khz and a shift of either ±5Khz or ±25Khz (dictated by the selection of 'low' or 'high' range). In the case of zero phase difference, the detector diode actually receives a frequency of 4Khz. Additionally, the amplitude difference, with a frequency of 2Khz, is measured in the lock-in amplifier, (11) in figure 1, and sent to the computer via an A / D converter. The zero point is found by changing the synthesizer frequency in steps of 0.3ppm.

In order to measure a distance, the Me5000 varies the modulation frequency to search for minimums within the optimized band-width (ie. where the superimposition of the returned and internal reference beams are exactly in opposite phase. see figure 3). These places are referred to as minimums because residual background prevents the complete suppression of light.

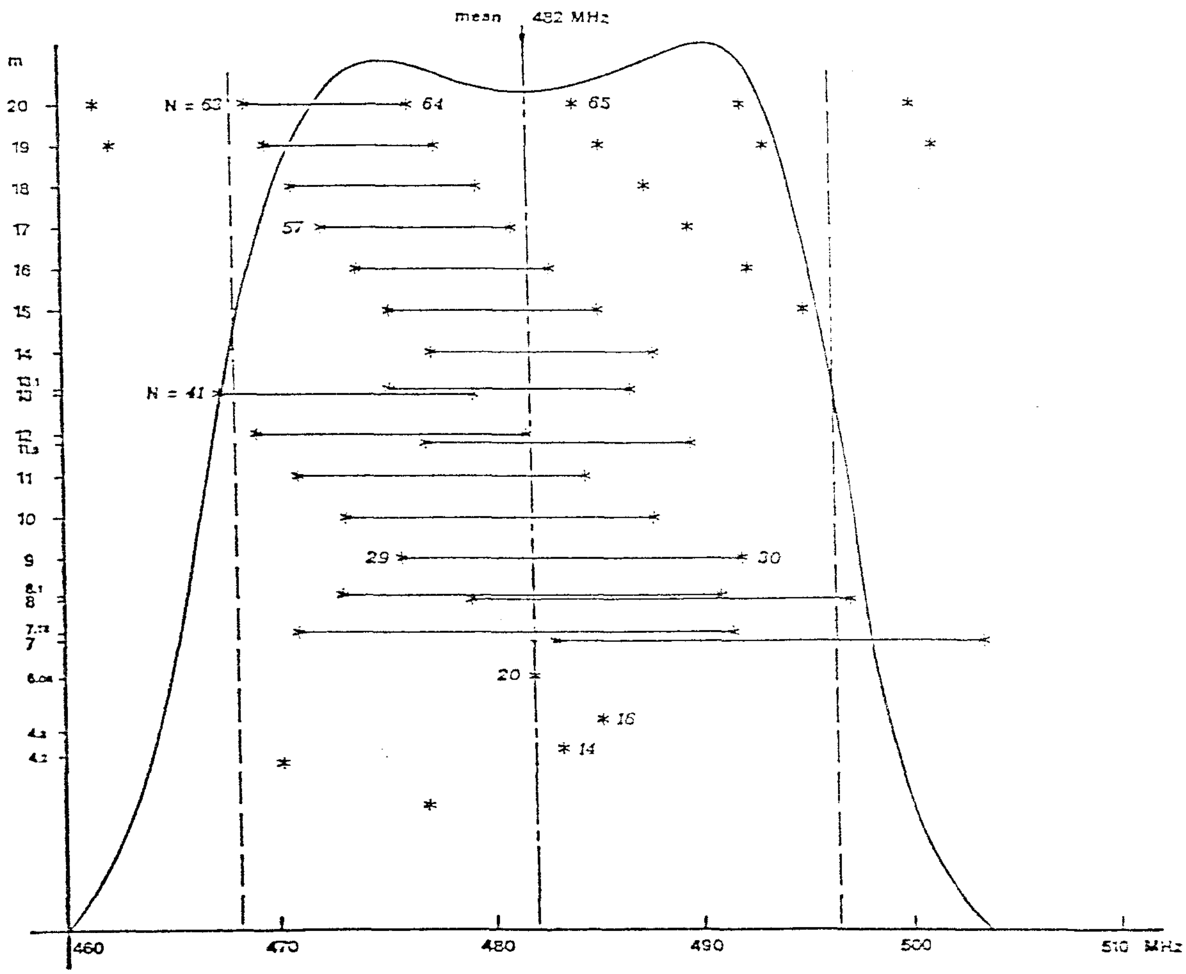

FIGURE 4 Distances, frequencies, modulation efficiency and minimums. This figure illustrates several characteristics of the Mekometer 5000. As in figure 2, the frequency curve is displayed with the extended band-width limits of 467Mhz-495Mhz. Following a horizontal line across from the distance axis the location of minimums (number and spacing) is depicted, each asterisk corresponding to a minimum. The general trend can be seen; the spacing of the minimums increase as the distance decrease, but the difference, in Mhz, between adjacent minimums, for any given distance, remains identical (e.g. if the second minimum is 5Mhz higher than the first, the third will be 5Mhz higher than the second). Therefore, knowing two frequencies, it is a simple computation to determine if any others exist within the extended range of the instrument without any further searching. This leads to the logic, that for distances greater than 25m, where more than four minimums exist, the minimums used for the distance calculation are chosen to be the first, last and median ones (the median minimum being the closest to the centre of the band-width). The cut off point between finding two frequencies, or only one frequency, within the range is not precise (e.g. only one frequency is found at 8m, but two occur at 7m).

Depending on the distance measured and the available frequency band-width, there are a varying number of possible minimums for the determination of D. This number increases from 4 frequencies at 20m as the distance is extended (in its normal mode as a stand alone instrument). When the distance is reduced below 20m, the number of frequencies decrease until only one

Before a calibration was conducted using an HP interferometer as the reference standard, the position of the windows present for each machine were calculated from the extended modulator range. The distances set during the tests included positions at the edge of windows as well as the centre, from table 2 we can see that due to the smaller range of machine B, there is approximately a 30% reduction in the size of the measurement windows between 4 and 5 metres and hence an approximate distance is required sooner than for the other instruments (notice the reduction in window size as the distance is decreased with all of the instruments).

Instruments A and C				Instrument B			
Position of Measurement Windows (metres)		Percentage of measurable distances per metre		Position of Measurement Windows (metres)		Percentage of measurable distances per metre	
lower limit	upper limit	Distance (metres)	(%)	lower limit	upper limit	Distance (metres)	(%)
2.984	3.083	0 - 1	11	2.904	3.033	0 - 1	8
3.197	3.405	1 - 2	30	3.208	3.350	1 - 2	20
3.501	3.728	2 - 3	54	3.513	3.668	2 - 3	40
3.804	4.050	3 - 4	71	3.817	4.985	3 - 4	50
4.108	4.373	4 - 5	88	4.122	4.303	4 - 5	58
4.412	4.695	5 - 8000	100	4.427	4.620	5 - 6	75
4.715	8000			4.731	4.938	6 - 7	90
				5.036	5.255	7 - 8000	100
				5.340	5.573		
				5.645	5.890		
				5.949	6.208		
				6.254	6.525		
				6.559	6.843		
				6.863	8000		

TABLE 2 The range of distances measurable (in metres) translates into the given percentages per metre. It was found that machines A and C exhibited virtually the same windows, instrument B losing a large percentage of measurable distances. This affects the performance of B in two ways; namely, a need to enter the approximate distance at longer distances due to only one frequency being available, and a greater restriction to the distances possible to measure.

CALIBRATION SETUP

Prior to calibration of the instruments, a series of tests were conducted to compare the dispersion characteristics of the standard Kern Me5000 reflector against the HP interferometer prism. Although a slight increase in dispersion was observed the overall differences when using the mean of three measurements were considered insignificant.

Using a 30m calibration bench, a Mekometer was positioned just off the end of the bench on a separate rigid stand at the interferometer beam height. By using two HP interferometer prisms 'back to back' on the bench, the following observational errors were eliminated:

1) all measurements were taken at the same height eliminating the need to apply height reductions later,
2) by not using the standard Kern prism, problems due to height differences between the Interferometer and Mekometer laser beams were avoided.

Therefore, all measurements recorded led to the calibration the instruments for relative distances (ie. the absolute distances were not compared).

minimum can be found in the optimized band-width, here an approximate distance is required to compute N in the above equation. However, minimums may also occur outside the optimized band-width and still within the modulator limits of 460MHz-510MHz. Where this situation occurs, it is still possible to obtain a distance but the reduced efficiency of the modulator can lead to a loss in definition of the minimum, causing a drop in the attainable accuracy. Eventually, as the distance is shortened even further, the only minimum found occurs outside the optimized range of the modulator so that the resulting distance may be less accurate or even wrong (e.g. it locates a point of inflexion rather than a minimum). Finally, where the only (theoretically) possible minimums occur outside the working range of 460MHz-510MHz, no measurement is possible. This situation is referred to as outside the measurement window (see figure 4).

With this design, the primary operating range from 20m to 8000m was chosen by Kern so that no approximate distances would be required (as at least 2 minimums are locatable in the optimum range of the modulator). Incidentally, the problem of finding the minimums is reversed at very long distances (greater than 8000m) as the minimums get closer and closer it becomes difficult to change the frequency by small enough steps so that a minimum is not missed.

SHORT DISTANCES

For distances less than 18m it is necessary to have a separate measurement procedure via an external program in order to initialize the parameters of the instrument prior to any measurement. This is required to optimize the instruments sensitivity for minimum detection, the primary influences being the frequency sweep range and the signal interruption characteristics. In fact, the design range of 20m to 8000m is also split into high and low range, selectable via a switch on the instrument display, to give optimum frequency sweep band-widths from approximately 20m to 1000m and above 1000m.

The original versions of the Me5000 provided a short distance capability by using only the optimized band-width. In an attempt to further extend the measurement range at short distances the band-width used was increased to 3/4 of the light intensity (465MHz-495MHz corresponding to a maximum and minimum half wavelengths of 320.9mm and 302.7mm respectively). This effectively extended the window size and so reduced the need for approximate values until much shorter distances (ie. two frequencies are found at shorter distances). However, a trade-off in accuracy can be noticed when using a frequency not within the optimal band-width.

The first indication of a difference between the three machines was noticed by looking at the variance of the modulator working range when the instruments are warm. Table 1 shows the ranges for the three instruments (instruments warm), giving an indication that their capabilities are related directly to the uniqueness of the quartz crystal used.

Variance of Modulator Working Range (MHz)			
Instrument Range	A	B	C
Normal	472.8-487.6	474.8-489.6	472.1-486.2
Extended	464.7-493.6	472.1-492.3	464.0-493.0

TABLE 1 Variance of the modulator working range (Mhz). This table clearly shows the basis of the difference between the three machines. Instrument B has a much steeper slope on the left hand side of the modulator curve (unlike the curve shown in figure 2), resulting a restriction of measurement possibilities in comparison to A and C.

The modulator band-width actually shifts very slightly as the instrument warms up. This change does not influence the results obtained in the normal use of the instrument, but there is a corresponding shift in the measurable windows implying a small variation in distances measurable below approximately 10m.

OBSERVATIONS

Starting at a distance of approximately 25m, a series of three measurements were recorded and corrected for meteorological influences, the mean being used for the Least Squares regression fit. The distance was then reduced by regular intervals until 10m, below which, each distance measured corresponded to either, a minimum located within the centre of the band-width, or a minimum at the lower edge of the extended band-width. To obtain the required distances measured by the Mekometer, the correct distance change using the Interferometer was pre-calculated and implemented. The range selected for each measurement was chosen as specified within the program; for example, below 20m, the selection chosen used the 'very short' distance option parameters, and above 20m the normal distance parameters were implemented.

The time taken for a particular measurement varies depending on whether one or two zeros are present and the location of the point within the band-width. It is also dependent on the distance; experience has shown that the definition of the zero becomes worse as the distance decreases.

Using the short distance modes, below approximately 16m, the final distance is computed from either two frequencies obtained or a single frequency plus an approximate distance given by the operator. This coarse distance must be known to an accuracy of ±0.1m in order to compute the number of nodal points, (N). Experience has shown that, if entering the approximate distance prior to the search, it is always better to err on the higher side of the actual distance (i.e. +0.1m) so as not to initiate the search after position of the minimum (the starting position is pre-calculated from the median frequency within the band-width). Should the coarse distance be greater than ±0.1m, an incorrect result will be calculated as the wrong nodal number will have been computed. Within the range where measurement windows are present, the required approximate distance must be determined to greater accuracy for the search to detect a minimum (to 2mm depending on the location of the frequency). The necessity for mm accuracy stems from the change in frequency due to a change in distance; the longer the distance the smaller the change in frequency.

In addition to the variance of measurement windows for each instrument, it was noted at very short distances, usually less than 5m, that two frequencies (minimums) may be located, in contradiction to the theory stated previously. This anomaly is possible because as the distance measured decreases, the definition of the minimums also reduces until the instrument mistakes a point of inflexion for a minimum. Should this incorrect frequency not be rejected, the ensuing reductions to obtain the distance will yield the wrong result. Usually, the incorrect frequency can be disregarded by verification of each frequency with the coarse distance measured to an accuracy of 1mm.

Another observation which affects the instruments only within the range of the measurement windows (below 6m), is the variance of the working frequency range of the modulator. As the machine warms up there is a noticeable shift in the frequency band-width downwards by usually 0.5MHz, which corresponds to a shift in the position of the measurement windows. Although this always occurs during the warm up, it is transparent at distances above the measurement windows and can be ignored.

For all distances measured, the final distance determined by the Mekometer was the mean of a series of three individual measurements. In virtually all cases, from the experienced gained, the dispersion of individual measurements should not exceed 120μm. The exception to this occurs at extremely short distances where poor minimum definition leads to an increase in dispersion.

RESULTS

Based from this theory, the results, shown in the individual graphs, were obtained for machines A and B and C. For the these graphs, the regression line parameters and overall standard errors can be seen in table 3. The overall standard errors, in the worse case (160μm-instrument B), are still within Kern's quoted accuracy of ±200μm. The measurement range was taken from 25m down to the minimum feasible distance for each instrument This minimum feasible distance being defined as the point where windows account for less than 50% of the distances per metre.

RESIDUALS FROM LEAST SQUARES REGRESSION FIT

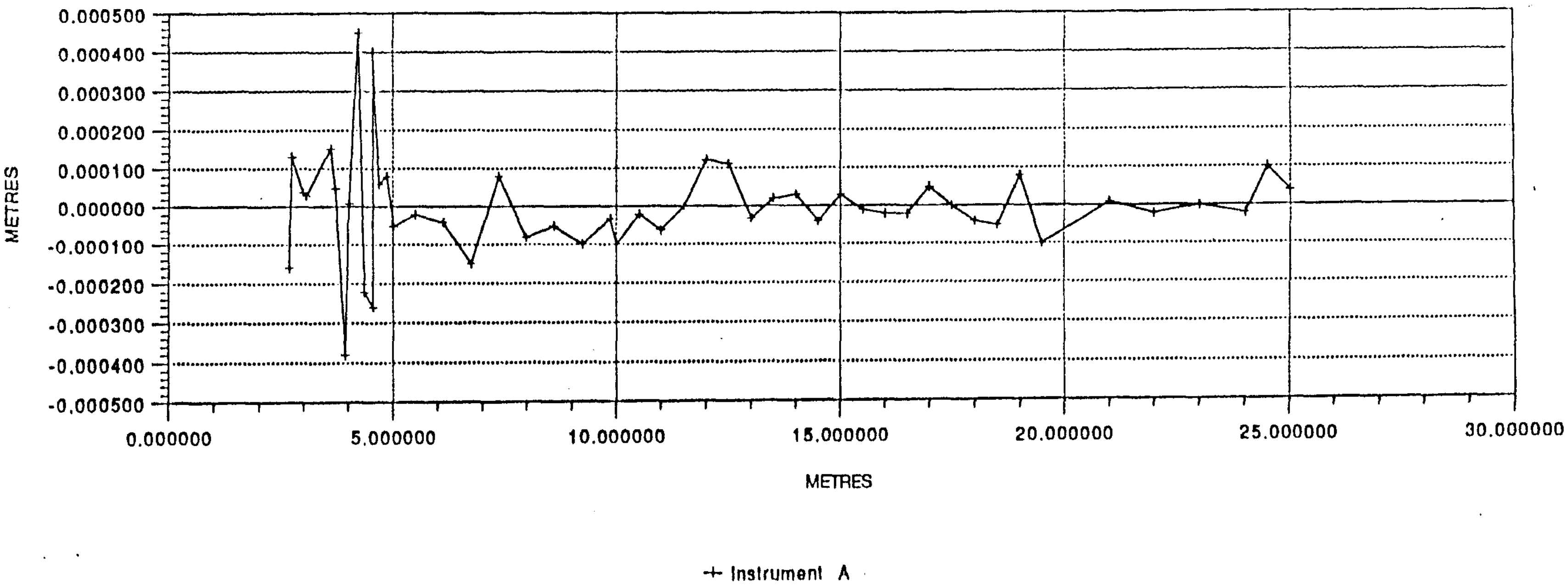

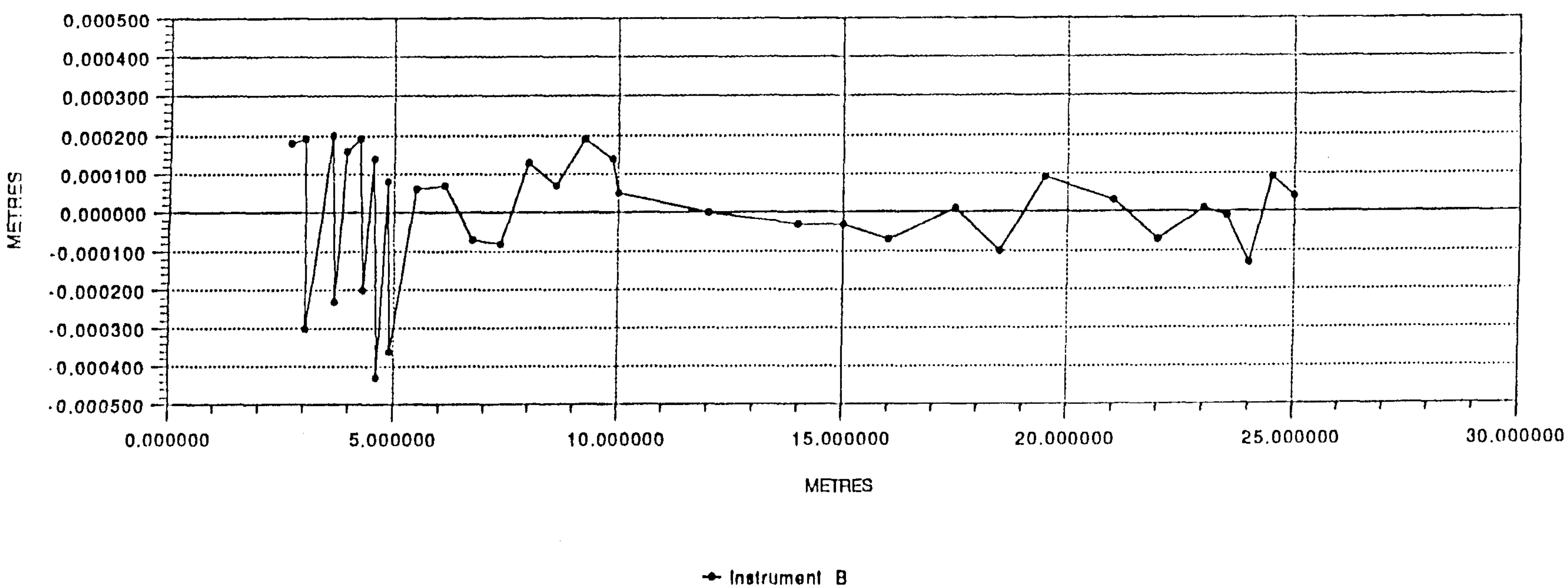

Although the measurements were not made exactly at distances which were an integral number of 1/2 wavelengths (approx 30cm), in general it appears that the distance is more accurate when this condition has been met (this usually does not apply in the normal range as other influences become of greater concern).

Regression fit for a line **a**X + **b**Y = **r**			
Instrument	A	B	C
	Metres	Metres	Metres
a	0.000018	0.000129	0.000393
b	1.000002	1.000016	0.999994
r	1.000	1.000	1.000
Overall Standard Errors			
	Metres	Metres	Metres
σ_o	0.000100	0.000160	0.000134
σ_a	0.000024	0.000048	0.000037
σ_b	0.000002	0.000004	0.000003

TABLE 3 **The overall standard errors and regression line parameters obtained for the three machines**. The measurement range was taken from 25m down to the minimum feasible distance for each instrument. This minimum feasible distance was defined as the point where windows account for less than 50% of the distances per metre.

However, there may well be a basis for optimization of the short distances when in the initial planning stages of a survey. As can be seen from these individual graphs, the residuals increase noticeably below 5m for all three instruments.

Regression fit for a line **a**X + **b**Y = **r**			
Instrument	A	B	C
	Metres	Metres	Metres
a	0.000126	0.000202	0.000330
b	0.999996	1.000012	0.999997
r	1.000	1.000	1.000
Amended Standard Errors			
	Metres	Metres	Metres
σ_o	0.000066	0.00080	0.00059
σ_a	0.000029	0.000041	0.000027
σ_b	0.000002	0.000003	0.000002

TABLE 4 **The amended standard errors and regression line parameters obtained for the three machines**. The measurement range was taken from 25m down to 5m.

Table 4 indicates the significant reduction in the standard errors when the cut off point is raised to 5m. Combining the three graphs together shows further the various consistencies between the three instruments. Effectively, this graph may be subdivided into 4 sections in order to explain the variations:

RESIDUALS FROM LEAST SQUARES REGRESSION FIT

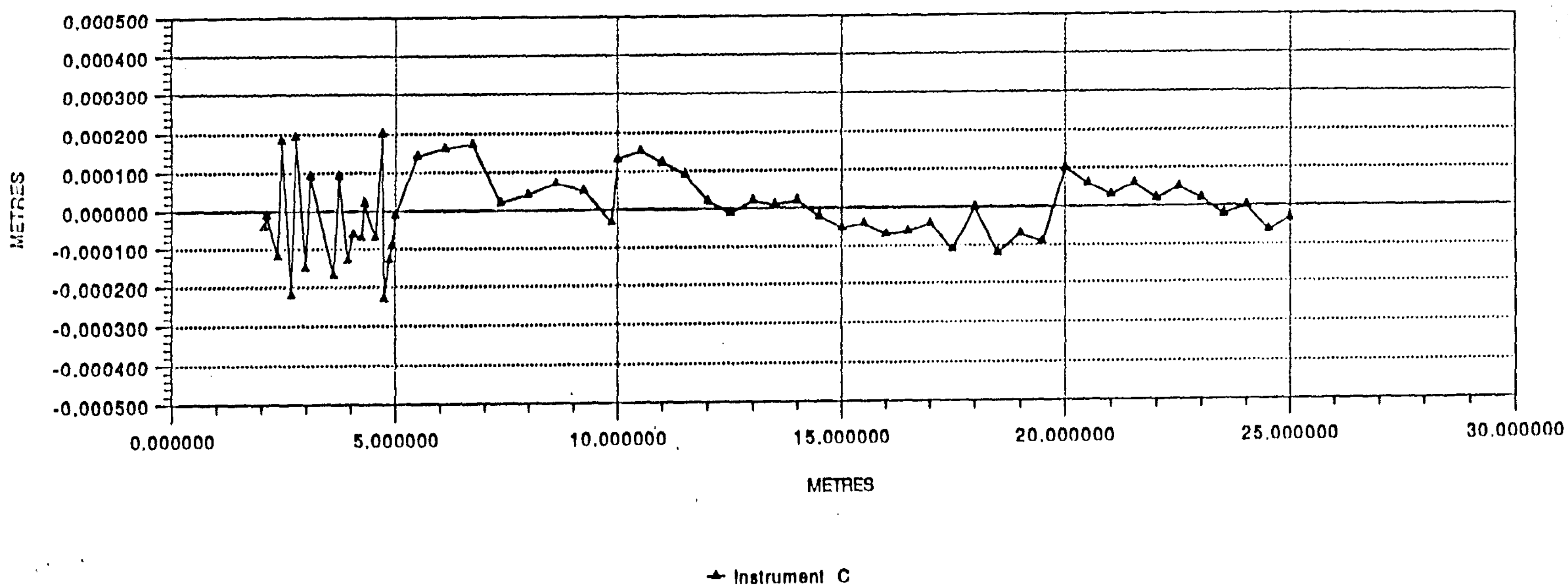

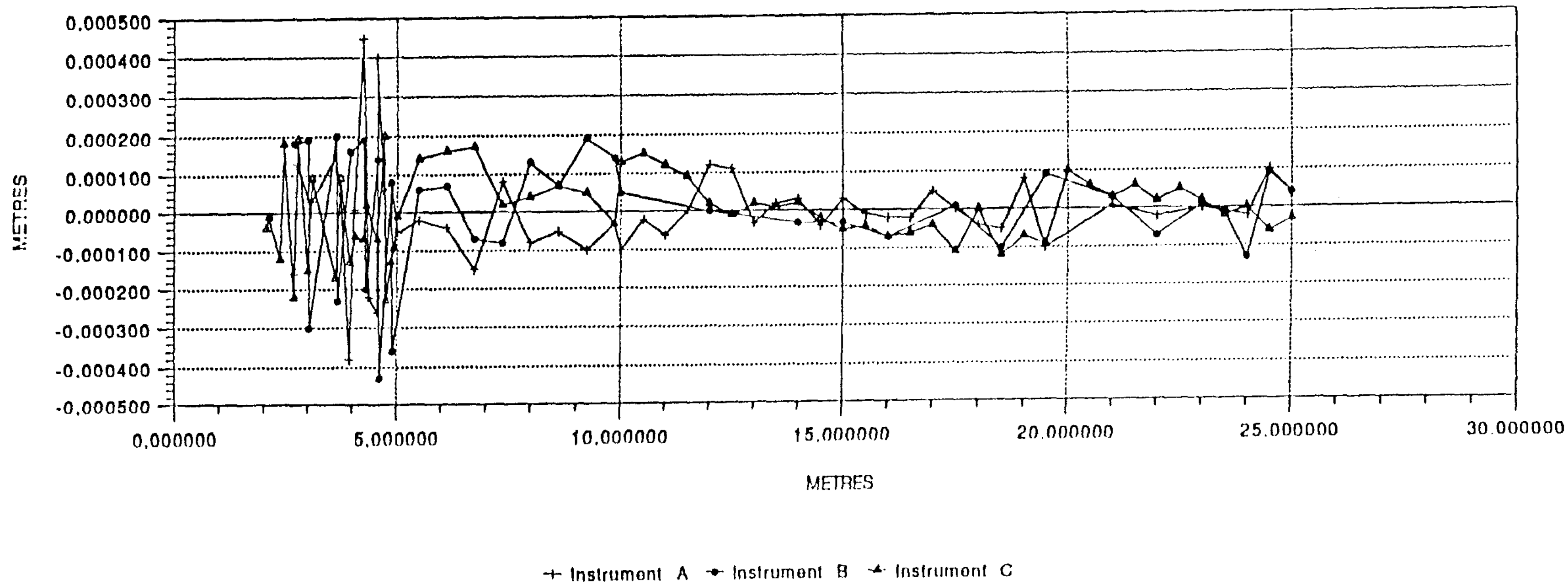

1) **Below 5m**. Only one frequency is located and, as a small change in the distance will correspond to a large change in the frequency, the resolution of the minimum will be reduced leading to a decrease in accuracy.

2) **5m to 12.5m.** Here, two frequencies are found, with a strong possibility that one of them occurs outside the optimum band-width. Although, the accuracy is less than at longer distances, because the final distance is a reduction from two zero points, the accuracy remains greater than when below 5m.

3) **12.5m to 20m.** In this region, most of the time, the minimums will be within the optimized band-width coupled with the correct initial parameter set for the range (for example the low and high range selector for 'normal' distances).

4) **Above 20m**. This gives a good indication that the instrument is reaching the limit when the low range initial setup parameters are used. As the region is an overlap between the very short distance and the lower end of the low range settings, perhaps an increase in accuracy may result in using the same option as with the section 12.5 to 20m.

It should also be noted that the HP interferometer prisms are much smaller than the standard Kern Prism and therefore may exhibit slightly different results. However, within the restrictive tunnel environment, it becomes preferential to employ a smaller prism due to limited lines of sight.

CONCLUSION

With the Mekometer Me5000, Kern has produced an excellent instrument of sound design and construction incorporating the best possible choice of crystal modulation range, plus an ability to access the internal Eprom, via special commands, for utilization with a portable computer. In fact within its usual working range the limiting factor tends to be the instruments sensitivity to atmospheric conditions. Additionally, to extend the instruments normal working limits it is essential to have good software. To this end, a complete software package has been developed at SLAC to directly incorporate measurements into the GEONET environment.

In order to make a direct comparison against invar measurements a 3-dimensional trilateration network consisting of 33 distances (8 less than 5m, 16 between 5m and 10m, and 8 more than 10m) was measured at SLAC (in the collider hall of the SLC) using both the Me5000 and Distinvar. The ease of using the Me5000, especially as these distances varied from 3.3m to 13.9m, was clearly demonstrated against the use of invar wires. However, as the original network was setup primarily for invar measurements two distances within the network could not be measured by the Me5000 due to line of sight difficulties. Therefore, the two corresponding invar distances were appropriately weighted and added to compensate the Me5000 network After reduction via least squares, the final results for the Mekometer and Distinvar measurements yielded standard errors of 0.178mm and 0.143mm respectively, in a 95% confidence limit. However, from the calibration results presented in this paper, the accuracy of the Mekometer drops significantly when measuring distances below 5m, indicating that the results would probably be closer to the adjustment via invar if distances below 5m were avoided.

Another illustration of the results attainable can be seen from a three-dimensional 'ring' traverse typical of the type required for small accelerator rings. The network was measured entirely by trilateration using the Me5000 together with geodetic levelling and consisted of 38 distances varying from a minimum of 2.6m to a maximum of 13.4m (the majority lying within the range 5m-9.2m). The final standard error computed via least squares was 0.18mm in a 95% confidence limit.

Although the Distinvar is not commercially available in its automated form, it is still used extensively for network measurements at accelerator research centres. This system requires a prior knowledge of distances to within 5cm so that the invar wires may be cut and calibrated both before and after the survey. Certain distances may not be measurable with the Distinvar such as, steep slopes or where access to enable suspension of the wire between points is difficult. For longer distances, such as a linear traverse, typical within a tunnel environment, the Me5000 has be used to compliment the use of the Distinvar, for example, to check for propagation of errors.

'Can the Kern Me5000 Mekometer replace invar measurements' does not yield a straight forward answer. For short distances below 5m the Distinvar will give better results. However, the Mekometer does offer a viable alternative for measurement between 5m and 25m, as indicated by table 4, against the usual standard error of 70µm for the Distinvar. Above 25m, the Me5000 would be the instrument of choice, a distinct advantage being its ease of use over a larger measurement range. Full application of this range, from a minimum feasible distance to 8000m, would enable surface and tunnel networks to be measured using the same distance measurement system.

REFERENCES

[1] Das Mekometer Me5000 - Ein neuer Präzisionsdistanzmesser. D.Meier and R.Loser. KERN, Aarau, Switzerland. 1986

[2] Kern Mekometer Me5000 and short distance measurements. E.Menant and T.W. Copeland-Davis. CERN LEP/SU, Switzerland. 1989

INSTRUMENTATION OF THE NINETIES

R. LOSER, D. MEIER, T. SCHOLIAN

Kern & Co. AG

Switzerland

1. Introduction

Technological progress, changed measuring tasks and steadily increasing accuracy requirements necessarily lead to the new and continued development of measuring instruments. The following article is intended to provide an outlook on future instruments, this topic being considered from two viewpoints:

1. New development of instruments that will be commercially available in the near future.
2. Publication of some investigation results which provide information about the technical capabilities of measuring principles and methods that might lead to the development of new instruments.

From the viewpoint of new instruments, only the precision inclination meter NIVEL 20 will be briefly described, since the Laser Tracking System also to be expected in 1990 is presented in a separate publication.

A second part describes the technical possibilities for the further development of distance meters based on the measuring principle used in the Mekometer ME 5000. In particular, we will report on the possibilities for the development of a two-color distance meter and a distance meter for short distances (2 m - 200 m) with accuracies in the area of 10-20 μm.

2. Precision Inclination Meter NIVEL 20

2.1 Design and Operation

NIVEL 20 is a high-accuracy sensor for the measurement of deflections of the vertical in two dimensions. The magnitude and the direction of a deflection of the vertical can be determined with one setup of the sensor. The inclination-sensitive element is a liquid in a closed container. The liquid's surface is perpendicular to the direction of the vertical, independently of the sensor's orientation. The inclination of that surface relative to the sensor is measured by optical means. All the optical components needed for that purpose are fastened to the underside of a flat glass plate. The plate also forms the bottom of the container with the transparent liquid. By means of the optical components, the luminous surface of an LED is imaged in a position-sensitive photodiode. The light from the LED is guided from below through the flat glass and the liquid, is totally reflected at the liquid's surface, and then passes again through the liquid and the flat glass. Finally, the photodiode detects the position of the impinging light spot relative to the zero position which was adjusted and calibrated in the horizontal configuration (see Fig. 1).

The flat glass plate, serving as a component and simultaneously as the support for the actual sensor element, is clamped into a trough-shaped metal base. The sensor is set up on three hardened and ground circular support surfaces on the underside of this base. The support surfaces have through holes for M4 screws in the center. On the metal base is placed the printed circuit board with the analog amplifiers and, optionally, a CPU card with a serial interface. The sensor is covered with a plastic hood. The plastic serves primarily as a thermal insulator which is meant to prevent external heat effects from causing nonuniform thermal expansions in the interior of the NIVEL 20 and consequent measuring errors. A temperature sensor is also installed to monitor the sensor's temperature. The direction of the measurement axis X is established by a stop edge on the metal base. The measurement axis Y is perpendicular to it. A bubble level is used for rough determination of the horizontal. The values of inclination in the X and Y directions and the sensor temperature are available as measurement values. The standard version of the NIVEL 20 has and RS-232 or RS-485 serial interface, the latter having the capability of operating up to 32 NIVEL 20s in the same network. A NIVEL 20 with analog outputs is provided for special applications.

1 LED
2 Imaging optics
3 Liquid
4 Liquid container
5 Biaxial position detector

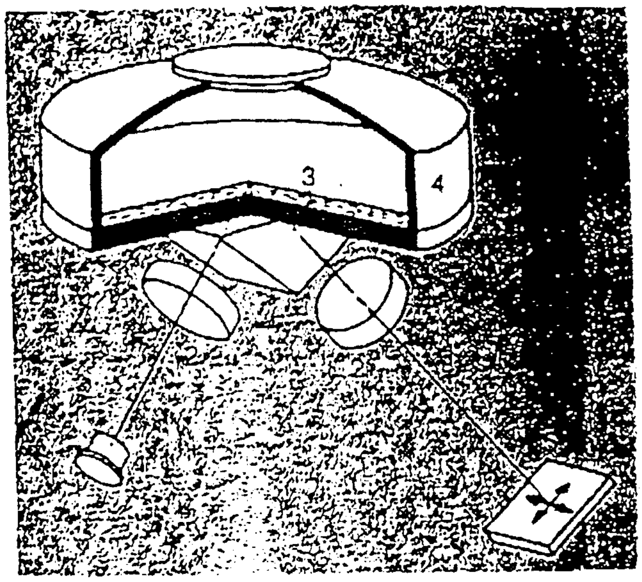

Fig. 1

Functional Principle of the NIVEL 20 Inclination Sensor

2.2 Scope of Application and Specifications

Thanks to its wear-free, sturdy and thermally stable construction, the NIVEL 20 is suitable for use even under extreme conditions in industry, research and construction trades. With available accessories it is possible to put together complete measuring systems suitable for many applications such as the setting up and aligning of machines and systems, flatness measurements on tables, monitoring of systems and structures, and many others.

Sensor Specifications (Valid For Both Measuring Axes):

Measuring range (deflection of the vertical	±1.5	mrad or mm/m
	±5.2	arc min
Linearity error	±(0.005 + 0.5% d.M.W.)[1]	mrad or mm/m
	±(1 + 0.5% d.M.W.)	arc sec
Resolution	0.001	mrad or mm/m
	0.2	arc sec
Zero-point stability	<0.005	mrad/K
	<1	arc sec/K
Operating-temp. range	-20 to +50	°C
Storage-temp. range	-30 to +60	°C
Relative humidity	10 to 95	%
Dimensions (LxWxH)	ca. 90x90x63	mm
Weight	ca. 850	g
Supply voltage	9-15	V DC

Interfaces:

Analog version	Sensitivity	1000	mV/mrad
Digital version	Serial interface	RS-232 or RS-485	
	Baud rate	2400; 9400; 19200	baud

2.3 Measurement results

The graphs of two linearity error measurements shall be used for illustration. The measurements were performed at room temperature on a prototype sensor, once for inclinations in the X direction (Fig. 2) and once for inclinations in the Y* direction (Fig. 3). The tiltings were done without lateral inclinations.

The linearity error and the absolute inclination are indicated in mrad on the vertical and horizontal axes, respectively.

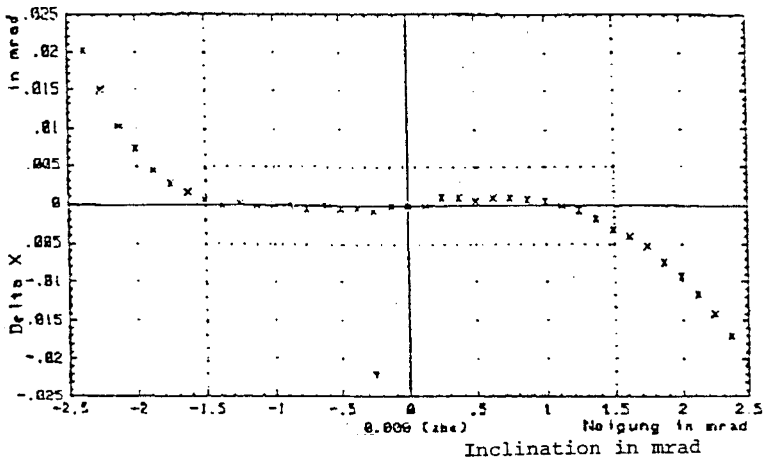

Inclination in X Direction

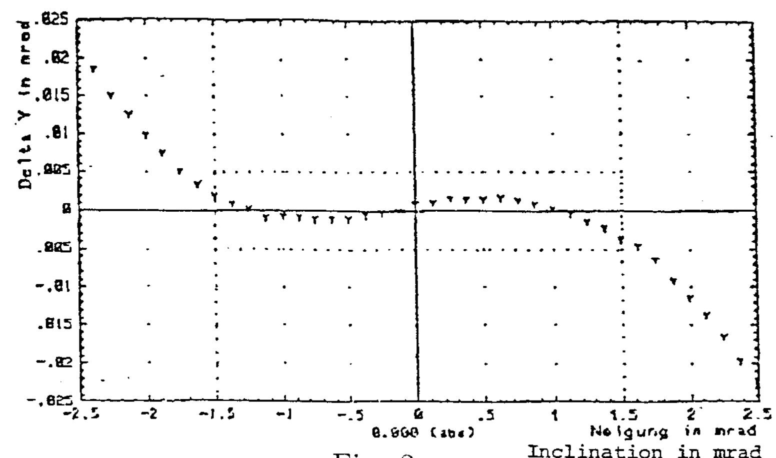

Fig. 2

Inclination in Y Direction

⋆ 1 Tr. note: Probably stands for "des Mittelwert" (of the mean value) or "des Maximalwert" (of the maximum value).

3. Tests With A Two-Color Distance Meter

3.1 General Discussion of Two-Color Distance Measurement

In the two-color method a distance is measured simultaneously with red and blue light /1/. The different propagation speeds of the light waves in the atmosphere result in two different distance values. The basic formulas (e.g., of Owens /2/) for calculating the propagation speed of light in the atmosphere as a function of wavelength, temperature, pressure and humidity are known for distance measurement with one color. The same formulas are used as the basis for calculating the distance in the two-color method. The reduction of a two-color measurement is very simple if a common propagation path is assumed.

We have:

$$D = L_{red} - A \cdot (L_{blue} - L_{red})$$

with

$$\frac{A = N_{red}}{(N_{blue} - N_{red})}$$

D = reduced distance

L_{red}, L_{blue} =	are distances measured with red and blue light and calculated with the speed in vacuum
N_{red}, N_{blue} =	are the indices of refraction refraction reduced by 1, calculated by the formula of Owens (n - 1)

Since the refractive index for both colors depends linearly on the air density, i.e., on the temperature and air pressure, the coefficient A is independent of pressure and temperature in first approximation. However, the water vapor causes another wavelength dependence, and the influence on the factor A is determined primarily by the variation of the mixture ratio of the atmosphere. Differences of 1°C or 1 hPa cause a distance change of about 0.001 ppm, while a change of the water-vapor partial pressure by 1 hPa results in a distance change of about 0.1 ppm.

Due to the refraction gradients in the zenith direction, the blue light beam deviates upward by about 10 cm at a distance of 30 km. This effect must be taken into consideration in an exact two-color distance formula /3/. The neglect of this effect results in an error of <1 mm ($3 \cdot 10^{-8}$) for a distance of 30 km.

As is evident from formula (1), the atmospheric correction results from the difference between "red" and "blue" measurements and from the factor A. Since the factor A in our setup (HeNe and argon lasers) is about 34, the error in the difference measurement due to the distance reduction of 0.1 mm is increased to 3.4 mm.

The first setup of a two-color distance meter was intended to allow basic tests of such a measuring system, to discover critical points and to create the foundations for estimating the attainable accuracies.

3.2 Description of the Two-Color Distance Meter

In principle, distance meters based on the FIZEAU principle offer high resolution and accuracy. The objective was to develop a measuring system that can measure the red-blue difference to an accuracy of about 0.05 mm at 15 km. This value corresponds to a distance uncertainty of 1.5 mm ($1 \cdot 10^{-7}$).

FIZEAU System

In the FIZEAU system (see Fig. 4) a light wave is modulated twice, once at transmission and the second time at reception.

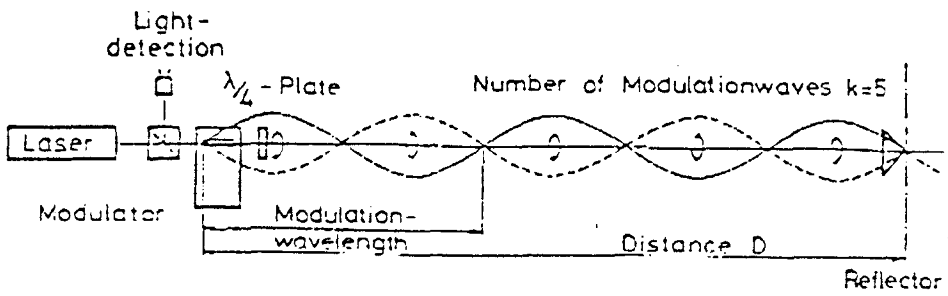

Fig. 4.
Fizeau System in the Tuned State

As with the Mekometer ME 5000, this system works with a variable-frequency polarization modulation of the light in the 500 MHz range. The frequency is shifted until the light detection is minimal (minimal point or 0 phase). This means that at this frequency there is a whole number of modulation wavelengths in the measurement path between the modulation crystal - reflector - modulation crystal.

We have:

$$2 \cdot D = k \cdot \text{modulation wavelength}$$

with

modulation wavelength = c/f

K = number of mod.wavelengths in 2 ·D = f/df

f = modulation frequency

df = frequency difference between 2 minima

The variation of the modulation frequency and thus of the modulation wavelength can occur only within the limits of the modulation bandwidth.

Determination of the Distance

To determine a distance it suffices to measure the frequency of a minimal point (fine measurement) and to measure the frequency difference between two minimal points (coarse measurement). At large distances especially (>10 km), a somewhat greater effort in the measurement of this frequency difference is necessary to avoid coarse measurement errors.

In our case, the determination was made via "quasi"- simultaneously measured pairs of minima at a maximally large frequency spacing. "Quasi"-simultaneous means alternating measurements at the lower and upper modulator band limits. After the measurement of 5 adjacent minima at the lower and upper band limits, the "spacing" of these groups is performed by seeking out and measuring other minima at doubled frequency spacings until the middle of the band is reached. Thus, for a distance of 5 km another 12 measuring points are obtained until the overlap in the middle is reached. Thus, a distance measurement of 5 km consists of 22 "red" and 22 "blue" frequency measurements distributed over the entire modulator range. The individual frequency measurement consists of an averaging of 4 frequency values weighted with the corresponding O-phase deviation. All measurements and the complete measurement sequence of the two-color distance meter are controlled by a laptop computer. A complete measurement takes about 10 minutes.

System Design

In a first test the setup shown in Fig. 5 was tested. It involves two complete FIZEAU systems which have common optics and two lasers as light sources (HeNe 7 mW, argon 5 mW). The advantage of two complete systems lies in the continuous and simultaneous measurement of the distance with two colors. The disadvantage lies in the possibly less stable difference of the mechanical-geometrical addition constants.

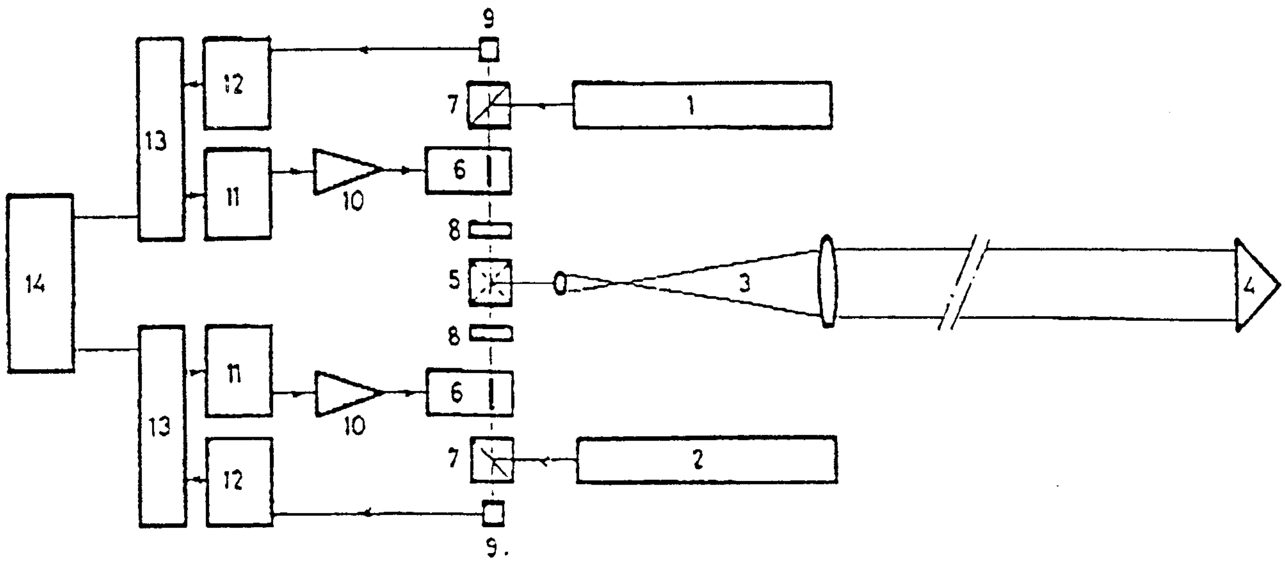

Fig. 5

Block Diagram of the Distance Meter with Two Modulators

(1) Red laser (He-Ne)
(2) Blue laser (argon)
(3) Transmit/receive optics
(4) Reflector
(5) Red-blue splitter
(6) Modulator
(7) Pol. beam splitter
(8) $\lambda/4$ plate
(9) Light detector
(10) Power amplifier
(11) Synthesizer
(12) Lock-in detector
(13) Controller
(14) Laptop computer

3.3 Results and Knowledge Gained

With this two-color distance meter built from two Mekometer ME 5000 electronic assemblies, a series of test measurements was performed at distances between 200 m and 10 km on different days. Some considerable inaccuracies were found, and the average errors reached values on the order of 3-4 mm. These results were basically within the expected range, and the actual primary goal of investigating the overall system and discovering the critical points was largely reached. A detailed working paper was produced with a number of points to be noted in developing such an instrument. In the following we report only on the crucial information for the user.

To estimate the maximum attainable accuracy, the master oscillator (10 MHz quartz crystal) was replaced by a Hewlett-Packard synthesizer, thus making it possible to perform the phase-O tuning in extremely small frequency steps.

The maximum measured distance resolution was about 0.02 ppm at 5 km, i.e., 0.1 mm. When a "red" and a "blue" minimum were measured simultaneously, atmospherically determined short-term drifts of equal order of magnitude could be found with an uncertainty of about 0.1 mm. By integrating over a measurement time of 5-10 minutes, a maximum resolution in the red-blue difference of 0.05 mm can be envisaged. This means that the basic accuracy of a two-color distance meter is about 1 mm, if an extrapolation factor of A = 22 can be assumed (see Equation (1)). However, especially in the measurement of large distances, calm atmospheric conditions are necessary to achieve this order of magnitude. Thus, the two-color instrument unfortunately is also again dependent on the atmospheric parameters.

For distances over 10 km, the signal quality necessary for optimal accuracy can be obtained only with correspondingly large reflectors. An array of 3 x 3 reflectors with a diameter of 60 mm each seems about right from the size standpoint. However, if the alignment is not sufficiently good, problems may arise for the red-blue difference because of the previously discussed divergence between the red and blue light beams.

A better solution is the Cassegrain configuration known from the Terrameter /4/. Besides treating the red and blue light waves identically, it also yields no additional polarization components.

4. Precision Distance Meter for Short Distances

The Mekometer ME 5000 was originally designed and developed as an exact distance meter for the measurement range of from 20 m to 8000 m. The first experiences with the ME 5000 already showed that the potential hidden in this instrument far exceeds what is guaranteed by its specifications. By using a computer to control the ME 5000's measurement sequence, a certain expansion of its measuring range and possible applications could be achieved. In the meantime, the Development Department of KERN had begun to build a functional sample to be used to estimate the possibilities of this measuring principle. For this reason, the results of a series of test measurements are available which serve as the basis for the development of a precision distance meter for short ranges.

4.1 Possible Specifications as Basis For Development

The objectives in building the mentioned functional sample were oriented primarily toward the characteristics of an instrument for the general geodesy market. Only after the merger of WILD LEITZ with KERN did the aspect of maximum attainable accuracy become more important again. For this reason, with respect to instrument size and measuring time and also with respect to accuracy and shortest measurement distance, realistic requirements that far exceed the usual improvements made in a developmental step can be imposed as a basis for development. The most important specification features as well as a few key words indicating how the technical solution is possible are listed below.

The FIZEAU principle already described in Section 3.2 and the distance-determination solution applied in the Mekometer ME 5000 serve as the basis.

Shortest Measurement Distance $\leq$ 2 m:

The raising of the modulation frequency from ca. 500 MHz to 1.3 GHz the modified construction of the modulator and the special programmability of the frequency drift for the zero-point detection permit unambiguous measurement of distances < 2 m.

Measuring Time < 5 Seconds:

The time needed for the measurement of a distance depends on the speed of the synthesizer, the time for the signal integration, the measurement algorithm and the computation speed of the CPU. A completely new synthesizer circuit design with transient buildup times in the range of 1 millisecond and the test results with correspondingly short integration times make the requirement for a measuring time of < 5 seconds seem realistic.

0.001 mm Resolution Time of the Measuring System:

The special coupling of the synthesizer circuit makes possible not only the relatively large frequency steps that are necessary for high speed, but also an extremely small step on the order of 0.1 ppm, which corresponds to a distance resolution of ca. 0.001 mm at 5 m. Under the assumption of an averaging of several measurements and taking into consideration the influence of temperature (0.2° C corresponds to 0.001 mm at 5 m), this value is surely sufficient.

Measuring Accuracy <0.01 mm + 0.1 ppm:

The tests showed that the temperature compensation by means of a $\lambda/4$ plate with a semiconductor laser works better. Ideas also exist concerning a better optical isolation of the sensor beam from the reflected light.

The <u>coupling with an exact angle-measuring system,</u>

the <u>use of small reflectors</u>

and the <u>instrument size of 120 × 120 × 70 mm</u> are other specification features.

4.2 Results of Test Measurements

A series of test measurements was performed with the available functional sample. Although the controller software of this instrument setup met only the simplest requirements, informative results were obtained.

At ranges between 2 m and 200 m a large number of measurements was performed in which individual instrument parameters were tested at a wide variety of settings. Figures 6 and 7 show two representative results.

5. Summary

The new NIVEL 20 and Laser Tracking System instruments document that in the field of instrument development technological progress necessarily leads to a continuous improvement of instruments and measuring methods.

The descriptions of the possibilities for further development of the Mekometer principle provide evidence that much more could be realized technically. Another prerequisite for the beginning of a new instrument development is that corresponding results can be expected on the economic balance sheet. Unfortunately, at this time there is no funding plan for the two possibilities presented here for the development of distance meters, and so for the time being there are no plans to implement these projects.

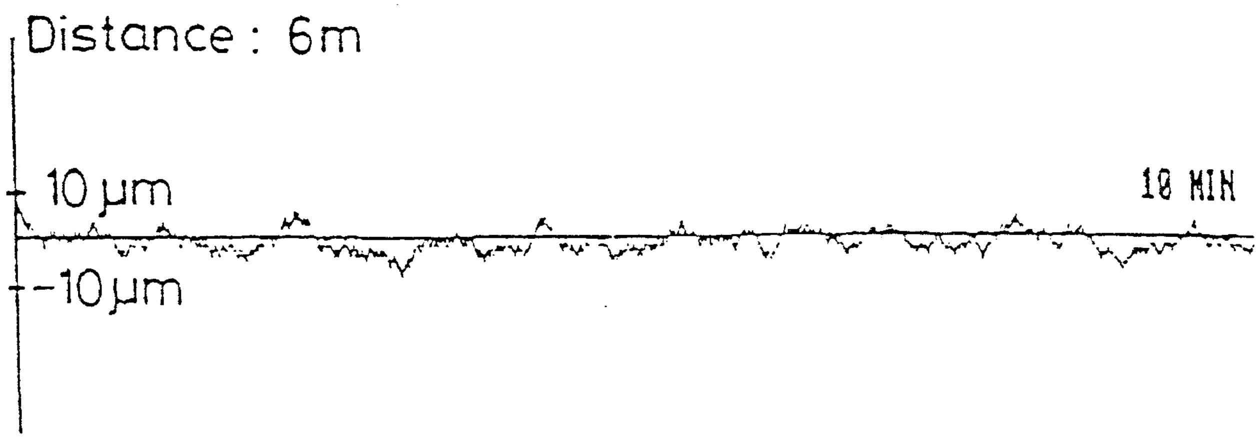

Fig. 6

Continuous Measurement For 10 Minutes

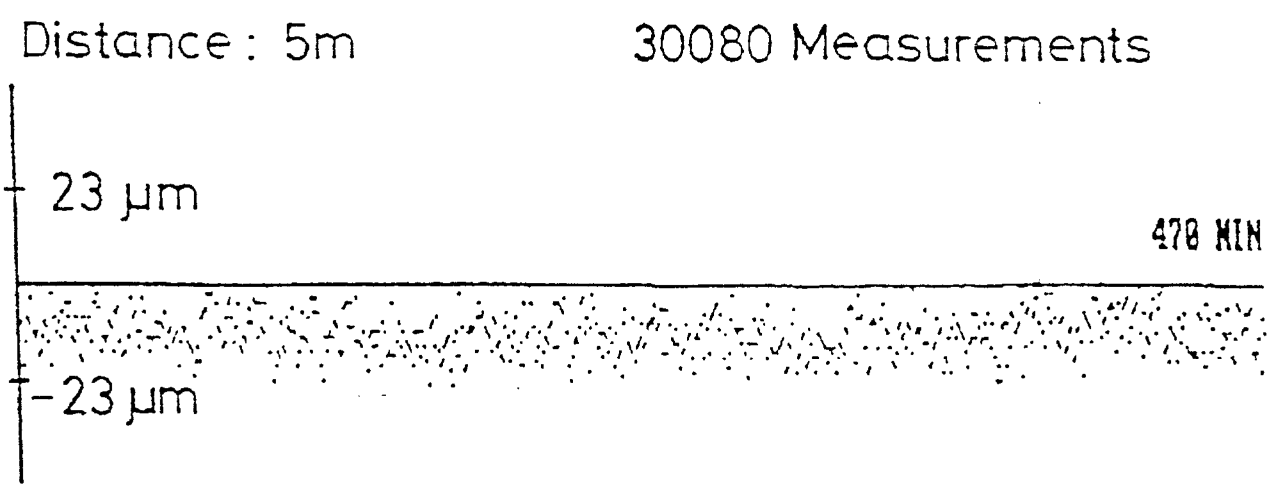

Fig. 7

Continuous Measurement For 8 Hours

Selected literature:

1. Owens, J.C.: Laser Applications in Metrology and Geodesy. Published by Ross M. Academic Press, NY/London (1971)

2. Owens, J.C. : Optical refractive index of air. Applied Optics, vol. 6, No. 1, pp. 51-59 (1967)

3. Hübner, W. : On the use of dispersion for electromagnetic measurement. DGK, Series C, No. 310, Munich (1985)

4. Huggett, G.R. and Slater, L.E.: Recent advances in multiwavelength distance measurement. Proc. Int. Symp. on EDM and the Influence of Atmosph. Refr., Netherlands Geod. Comm. Published by Richardus P, Wageningen, pp. 141-152 (1977)

5. Meier, D. and Loser, R. : The Mekometer ME 5000 - A new precision distance meter. AVN, no. 5, May 1986

6. Meier, D. and Loser, R. : Experiments with a two-color distance meter. Ingenieurvermessung 88, published by Schnädelbach/Ebner, Vol. 1, Dümmler Verlag, Bonn Authors: R. Loser, D. D. Meier, Th. Scholian KERN & Co. AG Schachenallee CH-5OOl AARAU

THE MAGNET FIDUCIALIZATION PROBLEM

ALEX HARVEY

Stanford Linear Accelerator Center
Stanford, CA

Magnets in accelerator beamlines have, for the most part, been made with ferromagnetic poles and traditionally these pole surfaces have been used as the references for external alignment aids, tooling balls, CERN sockets and so on.

This practice assumes that the magnetic field is well-defined by the poles (which fails in the presence of saturation). It also fails in the case of superconducting magnets, which have no tangible poles.

Other difficulties are well-known to those working in the field: the poles of an iron dipole magnet are never perfectly flat, or perfectly parallel. Where, then, is the magnetic mid-plane? The corresponding problem for iron quadrupoles, sextupoles etc, is that there is no unique inscribed circle that is tangent to more than three of these poles. The magnetic axis is then difficult to define. The greater the precision that is sought in the alignment, the more apparent these problems become.

The answer, I believe, is to use magnetic field measurements to establish the references. Most magnets undergo some magnetic measurement before use - they certainly should - and so the opportunity is there to combine fiducialization with magnetic field definition. A substantial part of the Final Focus Test Beam program at SLAC will address this problem.

Meanwhile I would like to use the work of some other SLAC colleagues to illustrate one approach. As part of the installation of the new SLD detector at the Linear Collider, a pair of superconducting triplet quadrupoles will be added as the final focusing elements before the detector. Fiducials (tooling balls) on the outside of the cryostats are referenced to the magnetic axis of the quads in a set-up as shown in Fig. 1. The probe P is a small rotating coil in a warm-bore insert in the quadrupole. Its center of rotation, X_p, Y_p, can be found by a transit focused on an illuminated target attached to the coil, (see Fig. 2). Analysis of the dipole component of the coil output in a local PC gives the coordinates, X_{pf} and Y_{pf}, of the magnetic axis, see Fig. 3 for the schematic. These coordinates are then referenced to sets of tooling balls, B1, B2, B3 and B4, on the outside of the cryostat.

Since the coil has an angular shaft encoder, the azimuthal orientation of the quadrupole field can also be established, and the plot in Fig. 4 shows that this magnet lies within ± 2 mrad except at the ends.

Other magnetic measurement techniques and alignment methods can clearly be used, but the relationship between surveyors and the field measurers must grow closer.

To close, I must acknowledge that the work I have reported is that of Jim Ferrie, Joe Cobb, Dave Jensen, Bill Burgess and others at SLAC. I am grateful for their friendly co-operation.

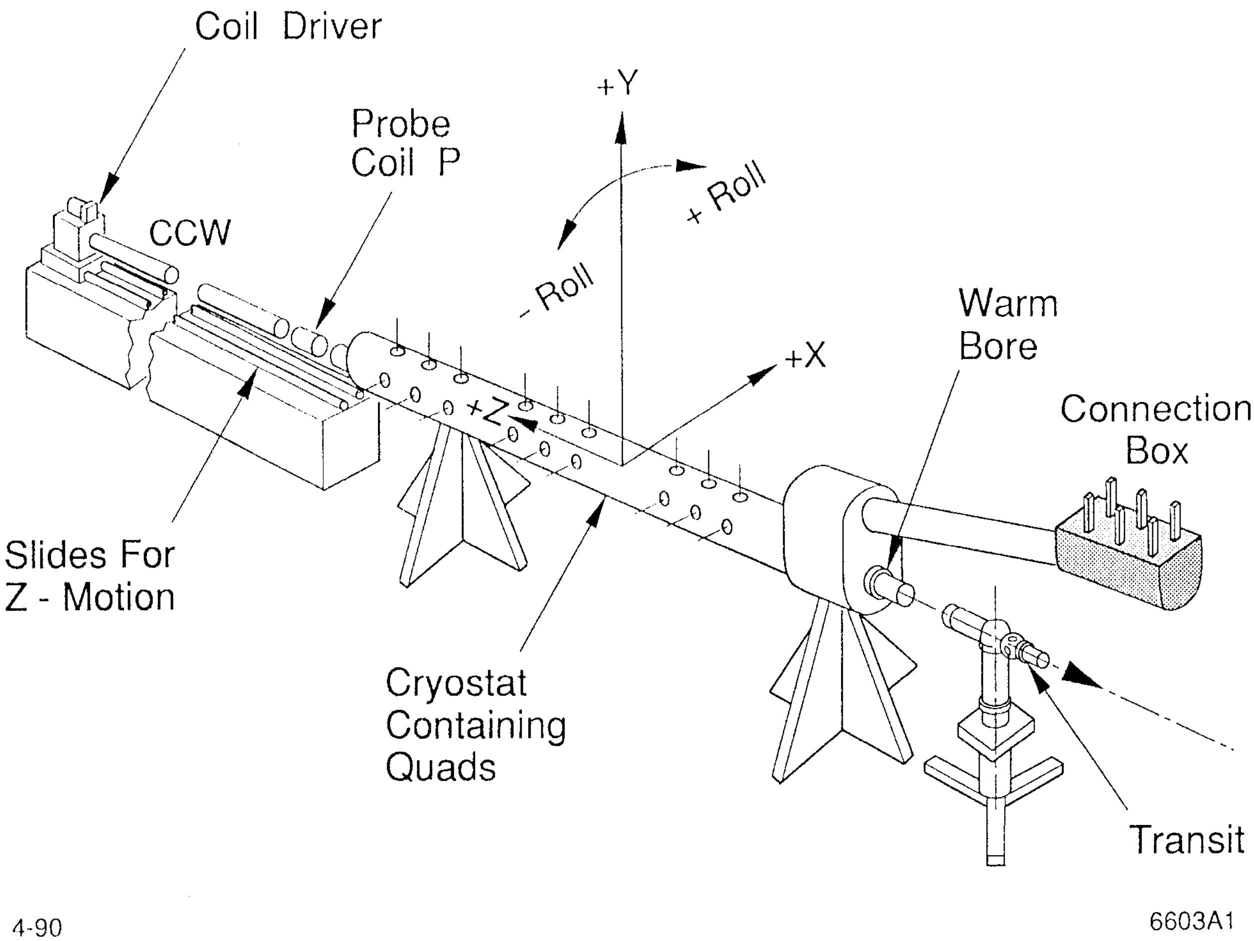
Coil Driver
+Y
Probe
Coil P
CCW
+ Roll
- Roll
Warm
Bore
+X
+Z
Connection
Box
Slides For
Z - Motion
Cryostat
Containing
Quads
Transit
4-90
6603A1

Figure 1.

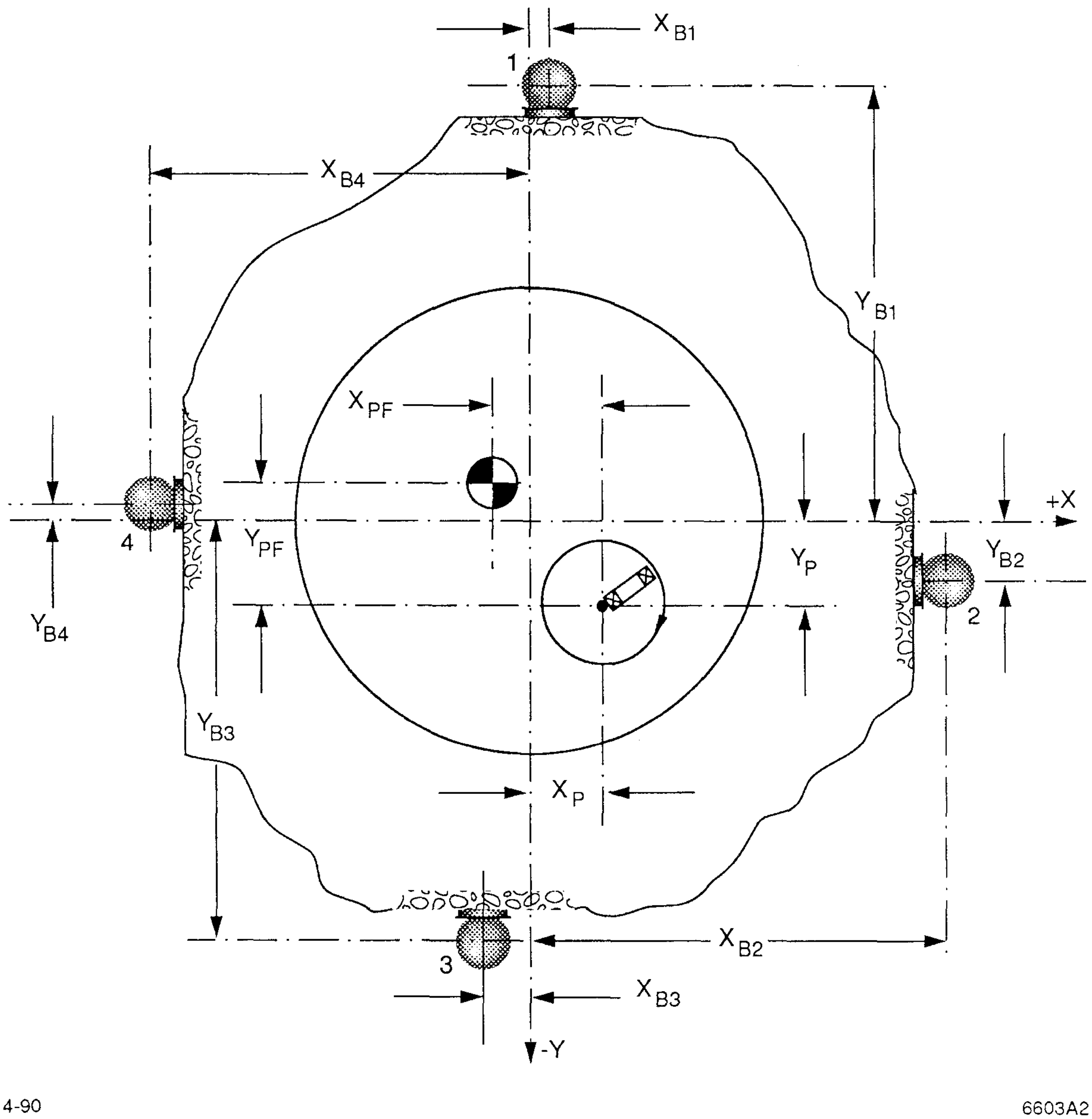

Figure 2.

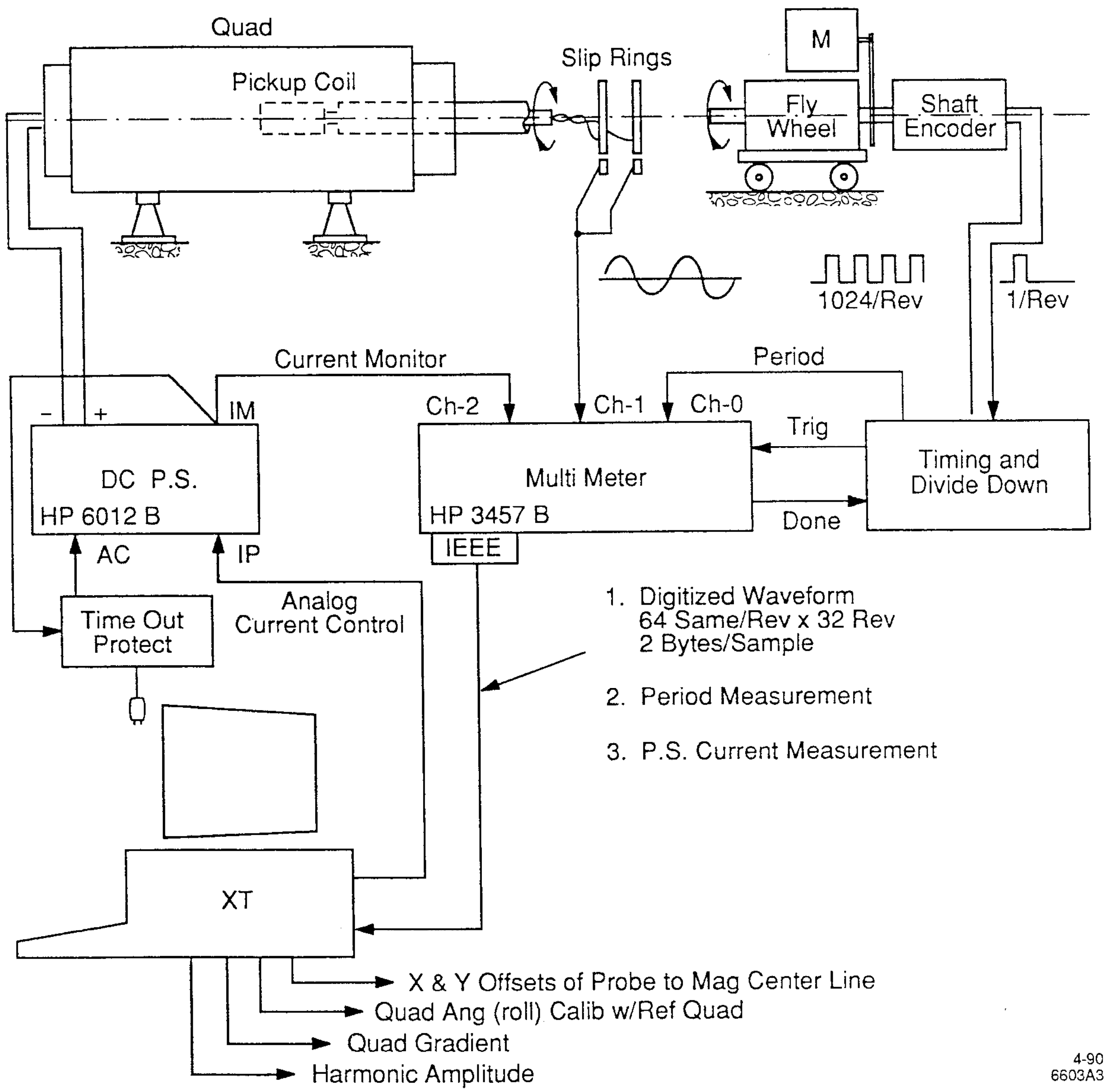
Quad
Pickup Coil
Slip Rings
M
Fly Wheel
Shaft Encoder
1024/Rev
1/Rev
Current Monitor
Period
Ch-2
Ch-1
Ch-0
Trig
IM
DC P.S.
HP 6012 B
Multi Meter
HP 3457 B
IEEE
Timing and Divide Down
Done
AC
IP
Time Out Protect
Analog Current Control
1. Digitized Waveform
64 Same/Rev x 32 Rev
2 Bytes/Sample
2. Period Measurement
3. P.S. Current Measurement
XT
X & Y Offsets of Probe to Mag Center Line
Quad Ang (roll) Calib w/Ref Quad
Quad Gradient
Harmonic Amplitude
4-90
6603A3

Figure 3.

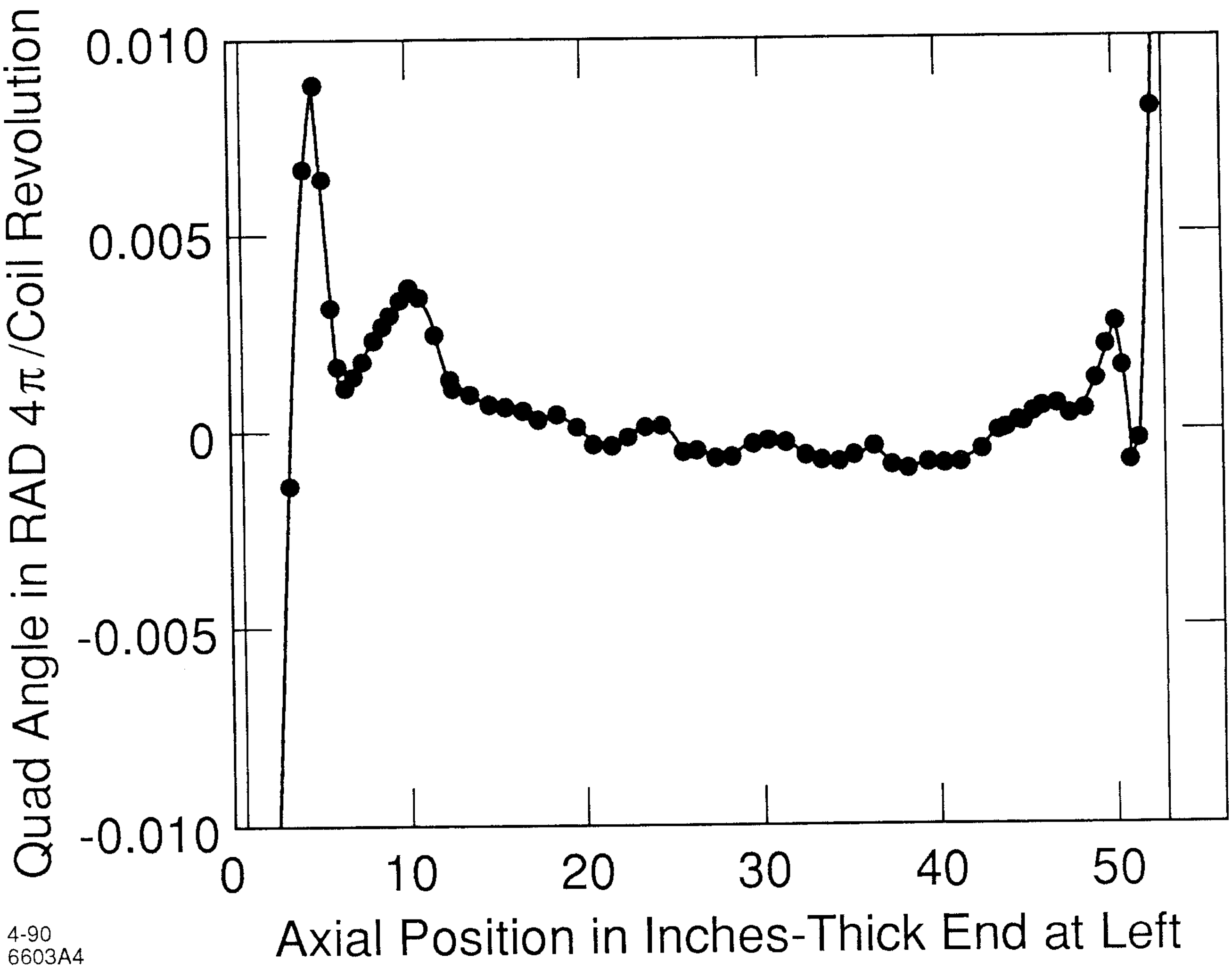

Quad Angle in RAD 4π /Coil Revolution
0.010
0.005
0
-0.005
-0.010
0
10
20
30
40
50
Axial Position in Inches-Thick End at Left
4-90
6603A4

Figure 4.

MAGNET FIDUCIALIZATION WITH COORDINATE MEASURING MACHINES

H. Friedsam, W. Oren, M. Pietryka

Stanford Linear Accelerator Center

Stanford University, Stanford, CA.

Introduction

One of the fundamental alignment problems encountered when building a particle accelerator is the transfer of a component's magnetic centerline position to external fiducials. This operation, dubbed fiducialization, is critical because it can contribute significantly to the alignment error budget. The fiducialization process requires two measurements:

1. from magnetic centerline to mechanical centerline, and
2. from mechanical centerline to external fiducials.

This paper will focus on methods for observing the second measurement. Two Stanford Linear Collider (SLC) examples are presented.

Goals

The object of magnet fiducialization is to relate the magnet-defined beamline position to exterior reference surfaces. To be useful for later component alignment, this relationship must be established in a manner consistent with overall positioning tolerances. The error budget for the SLC's $\pm 100\mu m$ component to component alignment tolerance is as follows:

magnetic centerline to mechanical centerline	$\sigma = \pm 30\mu m$
mechanical centerline to fiducial marks	$\sigma = \pm 50\mu m$
fiducial marks to adjacent components	$\sigma = \pm 80\mu m$
TOTAL	$\sigma = \pm 100\mu m$

The offset between the mechanical and magnetic centerlines of well-known magnets is generally smaller than the $\pm 30\mu m$ measurement tolerance. It is commonly assumed to be zero without measurement. When this tiny value must be measured, extreme care is necessary to avoid obscuring the offset with measurement tool registration errors. In contrast, the mechanical centerline to fiducial measurement must be performed on every magnet. The $50\mu m$ tolerance for this operation is only slightly larger and pushes conventional surveying technology to its limit.

This has forced the search for other means of measuring these quantities reliably and accurately.

Methodology

To complete the transfer for mechanical centerline to the fiducials, a magnet coordinate system must be defined. This includes establishing its origin and the three orientation angles of the rigid body. Often the X and Y origins are determined by the centerline of the pole tips while the zero coordinate for Z is the longitudinal center of the magnet. Roll is set by the midplane of symmetry and yaw and pitch are defined by locating the center of the pole tips at both ends of the magnet.

All measurement systems used to make this transfer establish this coordinate system. Then all fiducial coordinates are defined within this coordinate system.

Tools

The measurement tools for transferring the pole-defined centerline to outside reference marks must have some basic capabilities. They must be able to measure the size and shape of the poles as well as the midplane of symmetry. The length of the magnet and the fiducials must also be inspected by the same tool. The method should be quick and reliable providing accuracy better than $\pm 50\mu m$. The inspection services should be nearby to provide for a timely delivery of results. Three methods which utilize existing hardware and software systems are available. Each has its limitations as well as its strengths.

Optical tooling provides a tried and proven fiducialization technology. It is simple and well understood. The equipment is readily available and reasonably priced. However, the reliability of optical tooling is questionable. This stems from the lack of redundant, independent observations inherent to the process. Therefore, no statistical calculations or blunder checks are possible. Also, magnet features must be targeted, thus mechanically approximating the actual surface or center. Given a case with no blunders, the limitations of human observers, instruments, and targeting hold the system's intrinsic accuracy to ± 50 to $75\mu m$.

Theodolite-based industrial measurement systems (IMS) provide an optical alternative to optical tooling. This system is highly accurate (25 - $50\mu m$) with reliability provided by redundant observations and least squares data processing. The hardware and software if available to industry. However, magnet features must still be targeted, which limits the measurement accuracy. Intimate knowledge of a complex software is also required.

Coordinate measuring machines (CMM) (Figure 1) provide a third alternative. These highly accurate machines ($\pm 3\mu m$ to $\pm 5\mu m$) can measure magnet features directly using a touch probe system. They are fast and reliable if used correctly.

Form fit quality checks are available, but the user is required to provide a global "common sense" check.

On the other hand, CMMs are powerful, complex systems whose operators require extensive training. They are also quite costly. Hourly rates at local inspection shops can be quite reasonable, however.

All three of these methods are used at SLAC. Optical tooling continues to take most of the load with CMM measurements used only for special components. The IMS systems are used for components which are too large for a CMM but require the redundancy checks not provided by optical tooling. Two SLAC CMM experiences are outlined below.

Experience With CMM Measurements

The Final Focus CQ-SQ Quad Pair

This magnet pair consisted of two 200lb solid steel cored magnets 5 inches long with a width of 10 inches and a height of 12 inches. The bore diameter was $\frac{3}{4}$-inch and four tooling balls at the top corners served as external fiducials (Figure 2). The purpose of the CMM inspection was to check the optical tooling measurements taken before installation. Beam steering studies indicated possible errors in the original fiducials.

The inspected procedure consisted of scanning a sample of 180 points per pole tip to determine the best fit circle for each pole tip surface. Another circle was fitted to the centers of the four pole circles to find a best fit geometric center. (Figure 2). This was repeated at both ends to set the X, Y and Z origins as well as the yaw and pitch angles. Roll was to be defined by the split plane.

The quality of the results were greatly diminished by the configuration of the magnet. Roll could not be accurately set because the split plane was not accessible. Attempts to use the centers of the pole tips to set the orientation proved unsuccessful due to the extremely short lever arm (1.5 inch). Also, tooling the CMM probe could not fully access all balls. The results which could be compared to previous measurements showed discrepancies of up to 400μms. Since the CMM measurements did not repeat well and the geometry was poor, the results were discarded. Repeated optical tooling inspection showed changes in fiducial coordinates of up to 150μm. This illustrates that for this case neither method satisfied the 50μm inspection tolerance.

The conclusion is that magnets should be designed with CMM measurable features. "After the fact" fiducialization may be difficult if not impossible for magnets without them. However, new video systems technology may improve this situation.

The Final Focus Sextupoles

The relative alignment of these 800lb steel cored magnets to their adjacent beam position monitor was extremely critical for producing small spots at the SLC interaction point. The magnets are 12 inches in diameter, 30 inches long, with a bore diameter of 2 inches. 16 tooling balls, 8 at each end of the magnet were pressed into the magnet body to serve as alignment fiducials.

The CMM measurement routine was almost identical to the one used for the CQ-SQ quadrupole pair. The pole tips were probed at each end and circles were fit to determine the mechanical centerline (Figure 3). The roll of the magnet was defined by a tooling ball placed at the "top center" of the magnet. Precise roll orientation was not critical to the measurements, however, a second measurement was made to check the assumption that the mechanical and magnetic centerlines were coincident. Optical tooling target registration pins were measured during the CMM inspection. This provided a method to tie the mechanical centerline to the magnetic probe location mechanical probe location (Figure 4). Wire targets were mounted on the target registration pins. An alignment scope was bucked in on the line between the targets. The magnetic probe was then inserted and electronically loaded on the magnetic centerline. The distance from the remaining target to the probe was observed. This measurement combined with the target pin locations provided the magnetic centerline offset.

The results indicated that the mechanical and magnetic axes, coincided within the total measurement accuracy of 50 microns. This shows that high precision connections between fiducial marks and magnetic axes can be achieved. However, optical tooling observations remain the largest error source in the procedure and must be eliminated to reduce the measurement uncertainty.

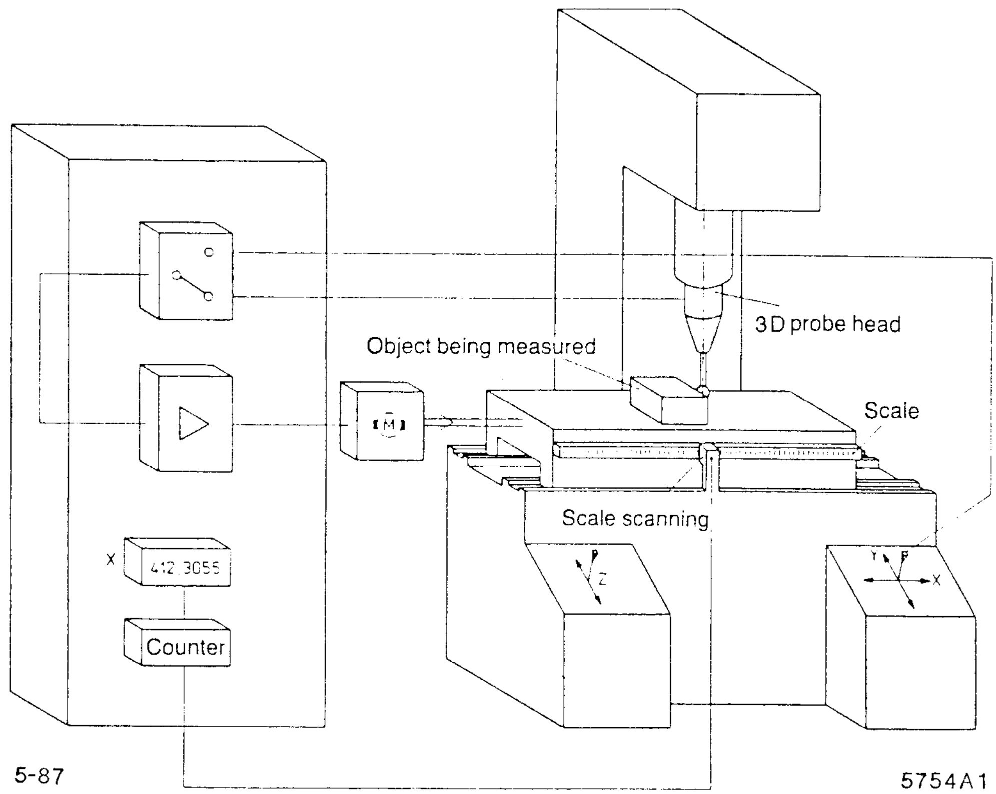

Basic Components of a Coordinate Measuring Machine

Figure 1.

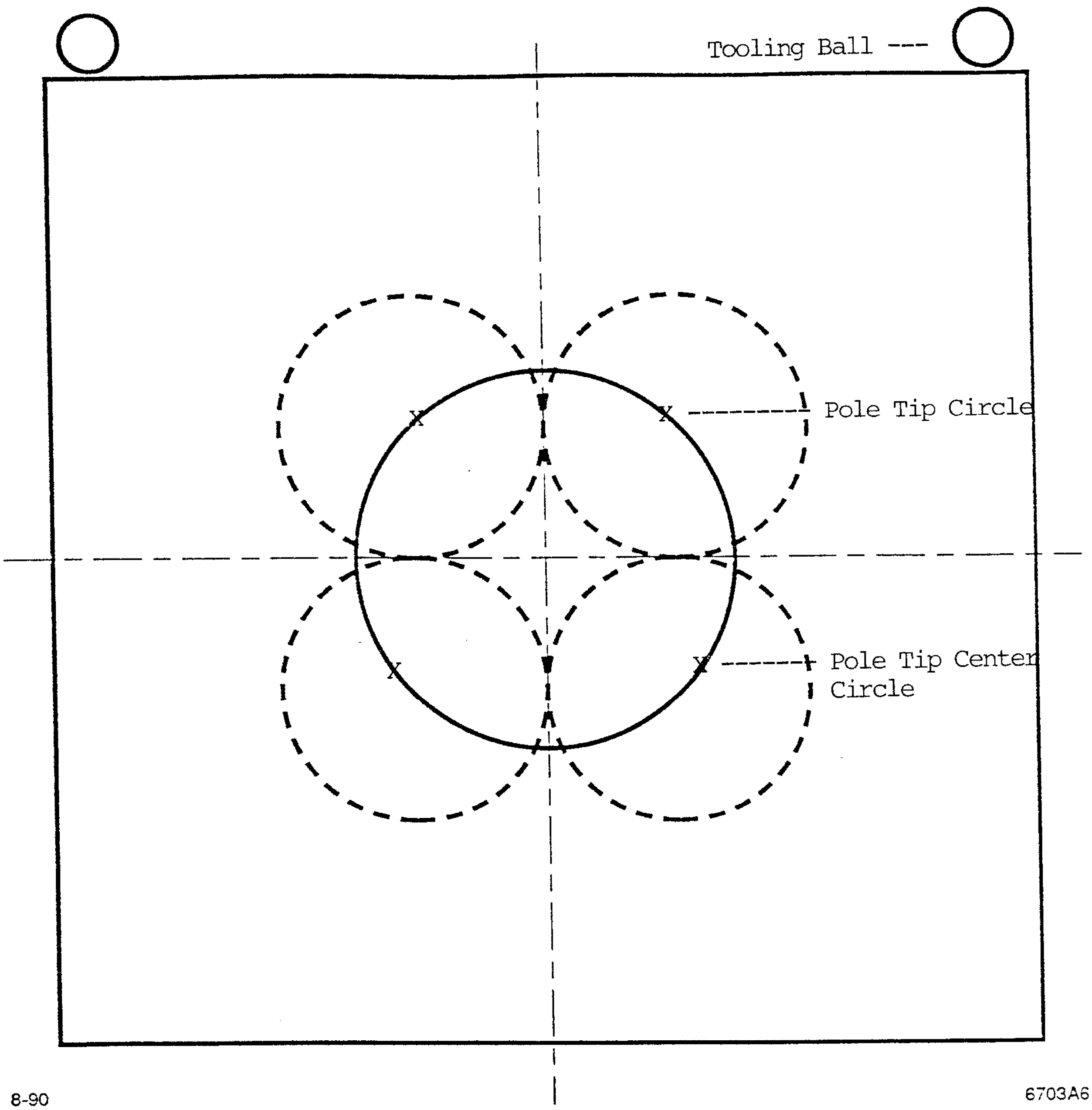

Sketch of a Final Focus CQ-SQ Quadrupole

Figure 2.

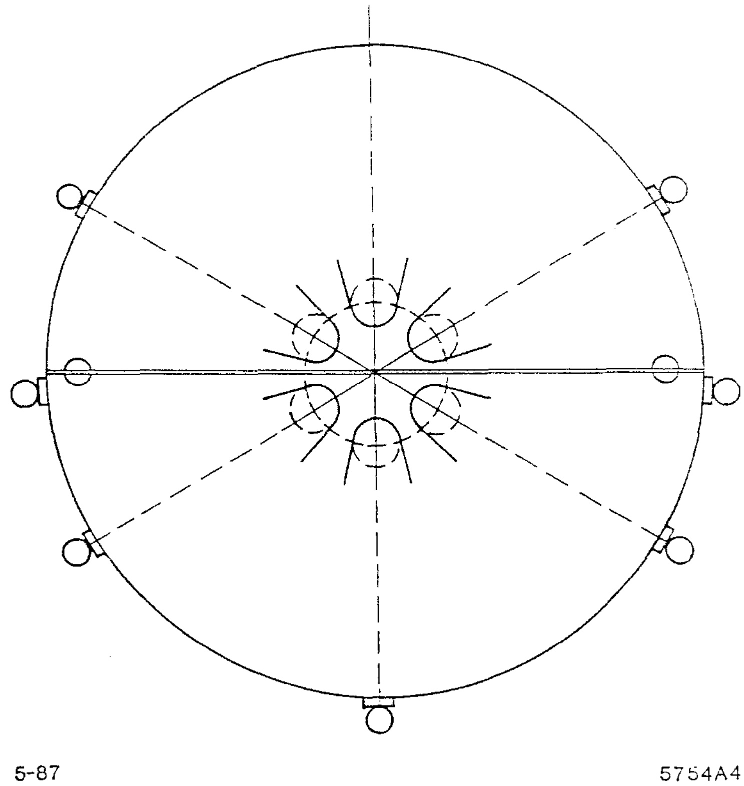

Sketch of a Sextupole
Figure 3.

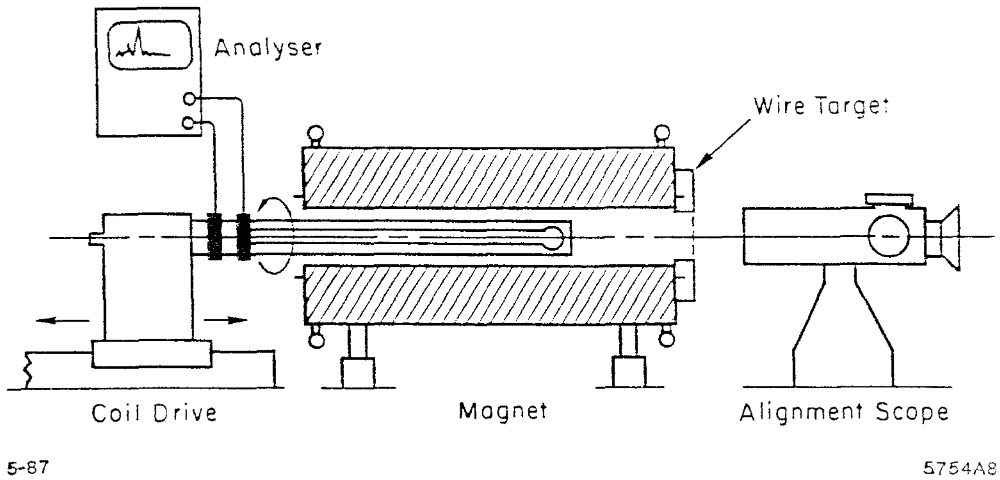

Setup for the Determination of the Magnetic Centerline
Figure 4.

FINDING THE MAGNETIC CENTER OF A QUADRUPOLE TO HIGH RESOLUTION

G. E. FISCHER, J. K. COBB, D. R. JENSEN

Stanford Linear Accelerator Center

Stanford, CA.

1. Introduction

In a companion proposal[1] it is proposed to align quadrupoles of a transport line to within transverse tolerances of 5 to 10 micrometers. Such a proposal is meaningful only if the effective magnetic center of such lenses can in fact be repeatably located with respect to some external mechanical tooling to comparable accuracy. It is the purpose of this note to describe some new methods and procedures that will accomplish this aim. It will be shown that these methods are capable of yielding greater sensitivity than the more traditional methods used in the past.[2][3] The notion of the "nodal" point is exploited.

2. Concept

Consider the arrangement depicted in Figure 1. A fine wire is suspended through a quadrupolar field, fixed at each end at coordinates x_1, y_1, z_1 and x_2, y_2, z_2. The tension in the wire is effected by the hanging weight $W = mg$. An infinitesimal disturbance δx is introduced at coordinate 1. The wire will execute resonant oscillations at modal frequencies n given by:

$$f_n = \frac{n}{2D}\sqrt{T/\mu}$$

in which D is the length of the suspension and μ is the mass per unit length.

⋆ Work supported by the Department of Energy, contract DE-AC03-76SF00515.

If the two ends of the wire are connected to form a loop (the return wire being stationary with respect to the magnetic field) a voltage will be developed across the terminals that is characteristic only of the induction that the wire is cutting. For the purposes of a simple calculation, let $x_1 = x_2 = x$ and $y_1 = y_2 \approx 0$. For $D \gg L$ we can write:

$$x = x_o + a \sin(2\pi f t) \tag{2.1}$$

in which x_o is a constant offset from the axis and a is the amplitude of oscillation. The voltage then developed will be:

$$E = -\, d\Phi/dt = -\, dBA/dt = -\, d(kx)(Lx)/dt \tag{2.2}$$

in which k is the gradient of the magnet such that $B = kx$ and L is its effective magnetic length. Substituting for x and differentiating we obtain two terms for the voltage:

$$E = 2kLa\omega[x_o \cos\omega t + a \sin 2\omega t] \tag{2.3}$$

the first at the first harmonic of the driving frequency proportional to the offset, the second a term independent of the offset at the second harmonic. As expected, this equation demonstrates the benefit on signal strength of being able to use relatively high oscillating frequencies.

3. Some experimentally relevant numerical parameters

3.1. THE WIRE

For a simple test we have chosen the length of the wire to be 100 cm. Using a 1.5 mil (38 μ) gold plated tungsten wire, density say 19 gr/cc , the calculated frequency of the fundamental, with a mass m = 25 gr providing the tension is 47 Hz. The observed frequency was 49 Hz.

3.2. Signal Strength

The magnet was 20 cm long, had a bore diameter of 1cm and a pole tip field of 1.2 Tesla. Hence the integrated gradient strength kL was 48 Tesla. It is not possible to measure the amplitude "a" but we can judge the sensitivity to offset as follows. If the second harmonic term is equal to the first in peak voltage then $a = x_o$. Let "a" be 30 microns, then we may expect to see rms voltages of about 19 microvolts. Put slightly differently the sensitivity would be 0.63 $\mu V/micron$.

4. Some experimental results

A photograph of the apparatus is shown in Figure 2. The pulley transferring the weight W into tension was at first a balanced razor blade. It was necessary to take great care that the mechanical shaker did not introduce unwanted mechanical motions or generate a common mode field that could be picked up by the flux loop. It was found that a 4 inch loud speaker pushing on a fiber rod, pushing on the wire mount, (or better yet on the wire directly) produced stable, non-interfering oscillations of the wire.

The very first plot of signal versus off-set (one end only) yielded a resolution of detecting the null point and repeatability of the micrometer setting of 0.0001 inches.

Improved wire shaking techniques led to the data taken one week later which is shown in Figure 3a. The ability to find the intercept can be inferred from Figure 3b. It is about 1 micron. This translates to 0.5 micron at the quadrupole.

In order to achieve a good null it was useful to adjust the orthogonal coordinate by iterating. The sensitivity to the coordinate at right angles to the motion is not severe. This is apparent when one examines the flux lines of a quadrupole. The flux lines are parallel to the motion are not cut.

The signal was also processed by a lock-in amplifier[4] with which the phase of the signal could be unambiguously seen with respect to the driving signal. This detector has several more decades of gain. Attempts to suppress common mode noise continue. We believe the method holds promise of even higher resolution. Best results are obtained after 4 pm and the building environment to mechanical disturbances improves. Footsteps and loud speech currently limit improvements!

5. The "Nodal" point concept.

In the foregoing simple sample calculation we have set $x_1 = x_2$. In the experimental world we have no a-priori knowledge that the wire is parallel to the real magnetic axis (whatever this means). What the wire coordinates measure is a family of lines all of whom satisfy the condition that the net flux cut is zero. This is precisely the condition we wish to achieve for the trajectories of the beam particles. To first order then, we have accomplished the task. Setting $x_1 = x_2$ is not critical therefore and can be accomplished by more traditional means (jig-transit) if one chooses.

The aforementioned family of lines should all intersect at a common point. We call this position z_o the "nodal" point. Around this point we can rotate the magnet (in yaw and pitch) without deflecting the beam. In practice this point may not lie in the exact axial center of the steel because, as we have observed in earlier studies, coil configurations on the lead and non-lead ends of the magnet are not identical.

To verify this belief, studies were carried out in the following way: coordinates for a null condition were found, then the wire at one end of the magnet was moved a given distance (say 60 microns) and the motion required at the other end to restore the null condition recorded. The results were, as expected, that the motion at other end was equal and opposite within the resolution of the set up.

6. Field Use of Centering Data

It is not sufficient to find the "center" of a lens in the laboratory. One must be able to reproduce the coordinates in the field. Experience with magnets in the past has shown that they cannot be taken apart and reassembled if one wishes to achieve micron reproducibility. This fact leads to the notion that they must be measured with vacuum chamber in place. This immediately leads to the notion that the same tooling used to position and reference the wire remains permanently attached to the magnet. In fact it becomes the same tooling to which the beam position monitor must be referenced. (This notion of carrying part of the calibrating apparatus into the field is not at all unusual in magnetic measurement technique. For example, if one truly wants to reproduce the strength versus current relationship in the field, one often uses the very same current measuring device in the field as that which was used in the lab).

One conceivable (and very simple) readout is shown in Figure 4. Very accurately machined flanges are permanently fixed to the quad bore by clamping the bore tube to the pole pieces. A ring guage with three bearing pads can be rotated in the plane perpendicular to the quad axis. One of the three pads is spring loaded so that the gauge can be mounted on the flange. The micrometer post is run in so that the wire barely touches it. This condition is observed when the oscillating wire shorts to ground periodically. The micrometer reading is recorded. The ring gauge is now rotated by 180 degrees and the process is repeated. The wire must have been half-way between the readings with respect to the edges of the flange. The process is repeated with the wire oscillating in the other plane. The flange, and its mate at the other end of the quadrupole, are the tooling to which the field survey is referenced. Experimental tests of wire touching resolution show repeatability at the 0.2 micron level.

7. Proposal

We intend to develop the method outlined above (we have only scratched the surface of many possibilities that come to mind) and propose that the resulting apparatus and tooling be used in connection with the construction of the Final Focus Test Beam in the coming year.

8. Acknowledgements

We gratefully acknowledge Ed Garwin for lending us the lock-in detector and Dan Jones for setting up the driver electronics.

9. References

1. Final Focus Test Beam Alignment, R.E.Ruland and H.E.Fischer, February 1989 SLAC-TN-89-02 2nd this workshop.
2. Magnetic center location in Multipolar Fields, J.K.Cobb and J.J Murray, Nuc.Instr.Methods Vol.45, p1 (1967)
3. The most common method used in the past is to identify the magnetic center of a lens with its mechanical center of construction; often "defined" to be centered with respect to its iron pole surfaces, or better, its mechanical split planes.
4. Model HR-8 Princeton Applied Research

QUADRUPOLE ALIGNMENT METHOD

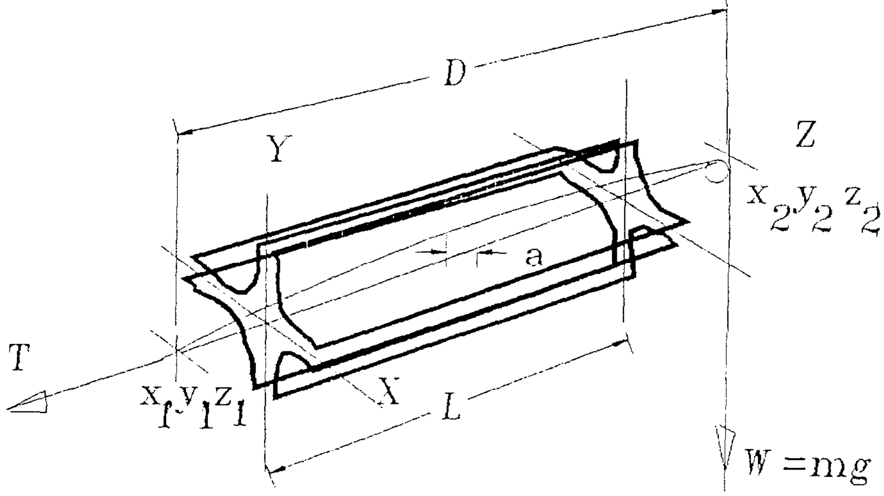

SIGNAL GENERATION AND ANALYSIS

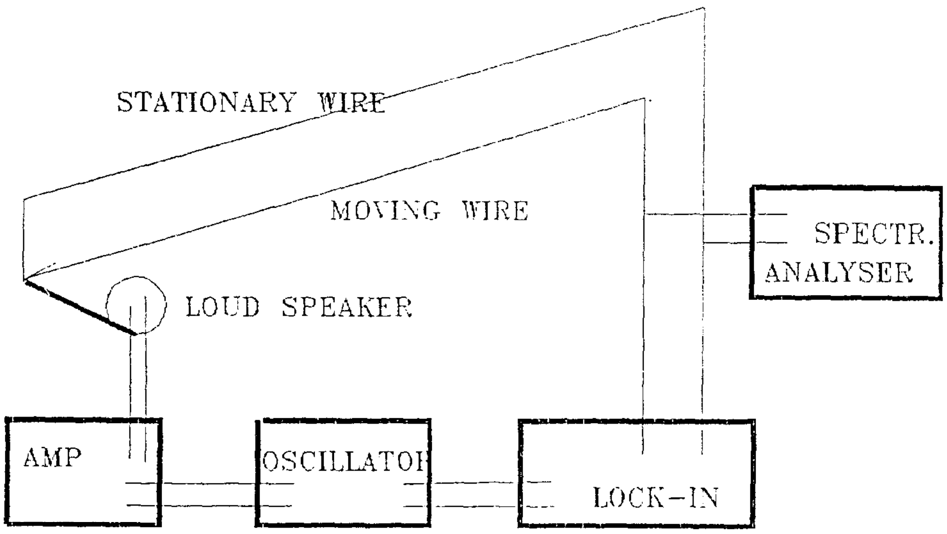

Figure 1.

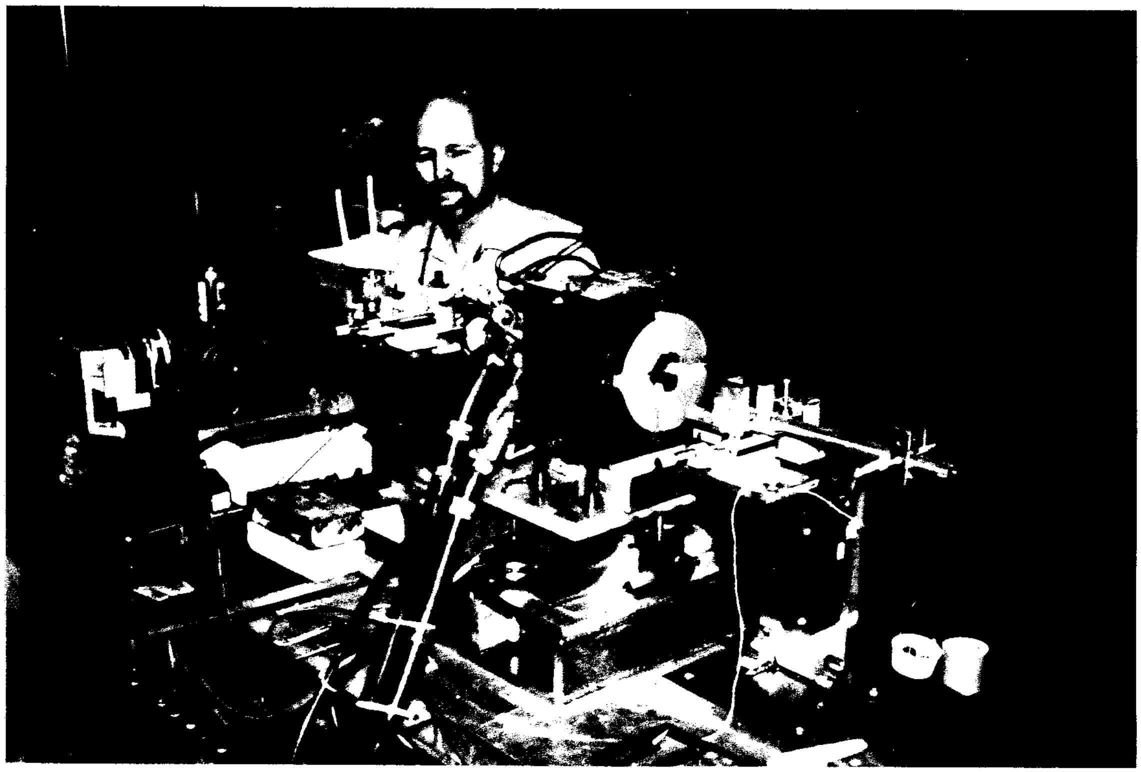

Figure 2.

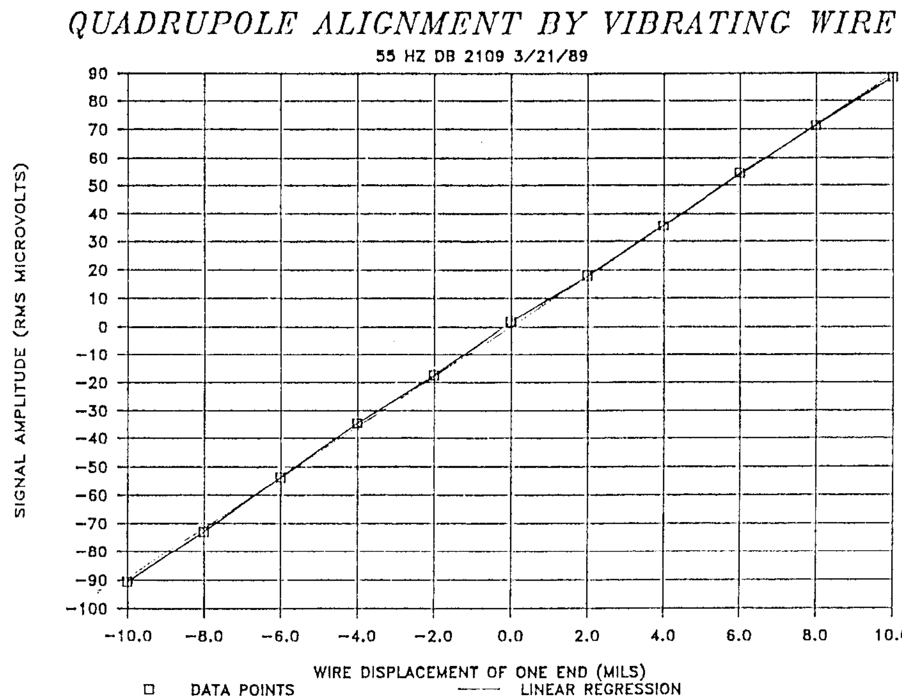

Figure 3a.

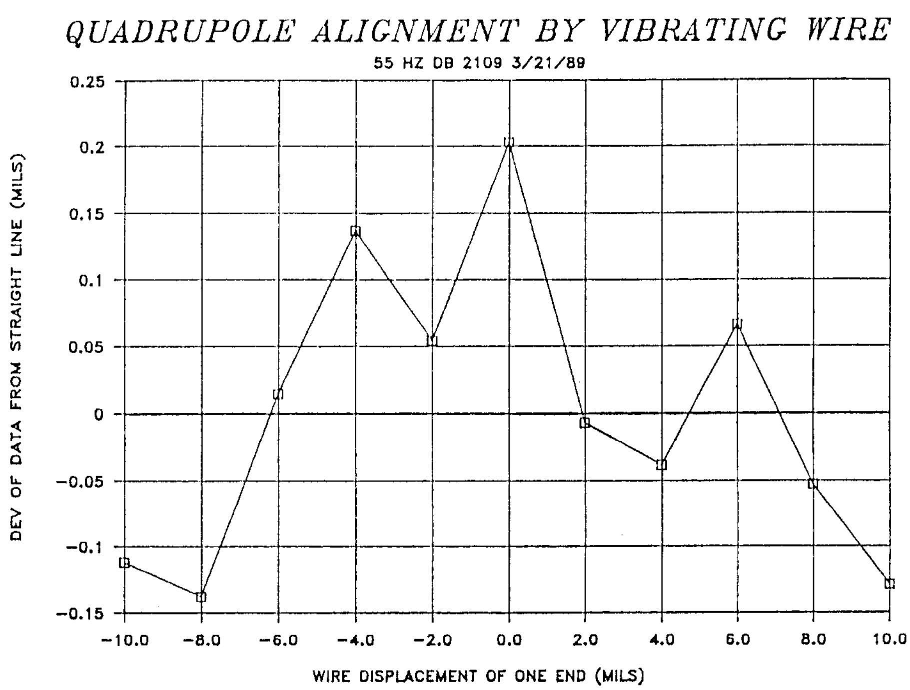

Figure 3b.

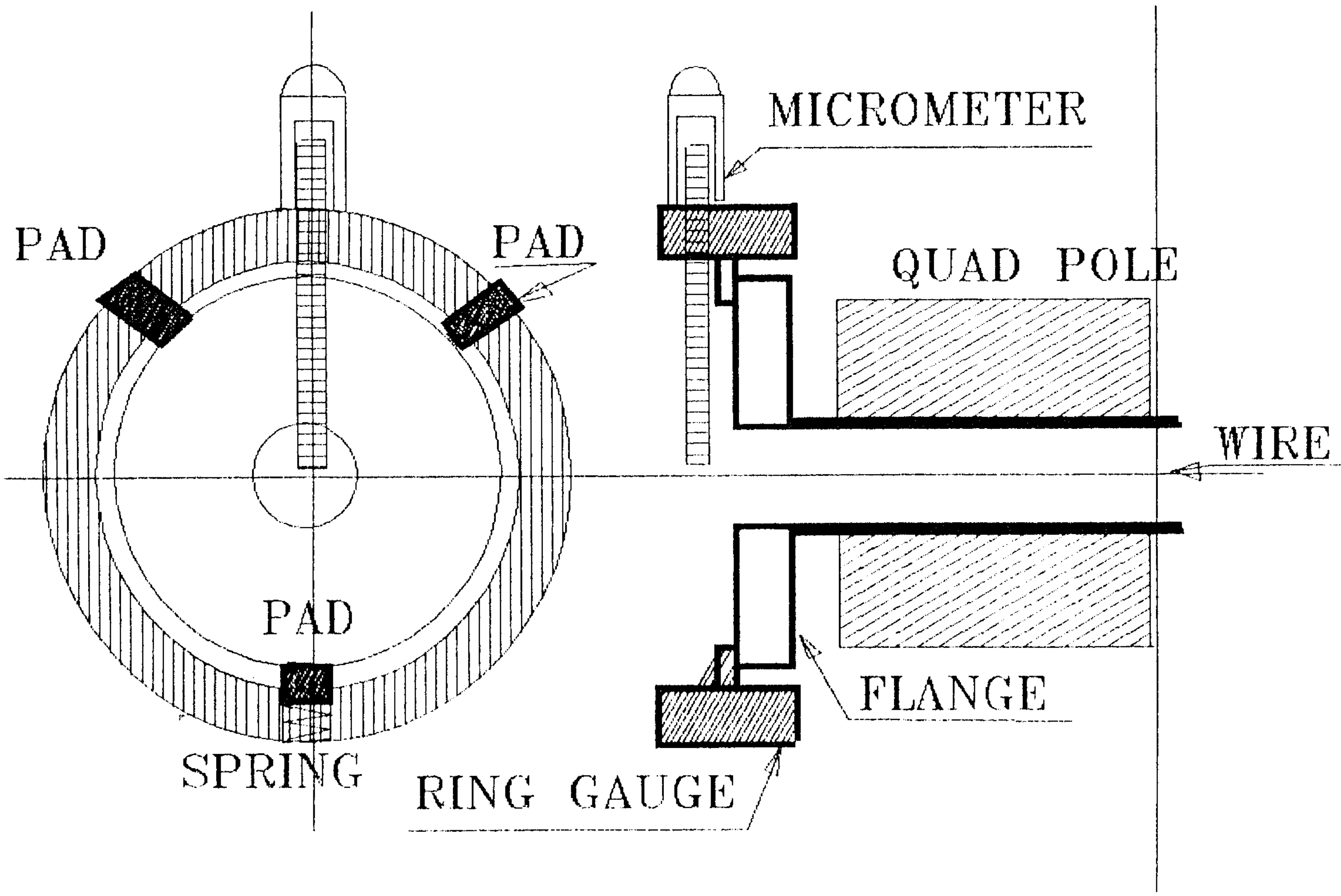

PAD
PAD
PAD
SPRING
MICROMETER
QUAD POLE
WIRE
FLANGE
RING GAUGE

Figure 4.

LOCATING THE MAGNETIC CENTERLINE WITH A LOW ENERGY ELECTRON PROBE

Flux Line Mapping in a Linear Induction Accelerator

LEE V. GRIFFITH

Lawrence Livermore National Laboratory

Livermore, CA.

Summary

The following is a narrative of the oral report on "Locating the Magnetic Centerline with a Low Energy Electron Probe" presented at the First International Workshop of Accelerator Alignment. The low energy electron probe (LEEP) was originally developed at LLNL by Gene Lauer and has seen many modifications to improve accuracy and resolution. The technique is specifically designed to map the transverse position of a field line vs. its axial position in a solenoidal coil. The diagnostic uses a low energy (≈4keV) electron beam, which is propagated from within the focusing field of the first accelerator cell. Due to the low energy of the electron beam, it will remain on the same flux potential that it is launched on, ie. it will follow a flux line (this statement can be in error if the electron beam is launched several mm from the solenoid axis, but for paraxial measurements the errors remain below the resolution of our detectors, < 10 μm). A phosphor screen has been used, in the past, to intercept the electron beam and convert it to a light spot which can be located in X and Y. The axial position of the phosphor screen is recorded with the X-Y location to produce a flux line map (for a single flux line) through the entire accelerator.

The linear induction accelerators at LLNL employ solenoidal coils to maintain electron beam focus throughout the accelerator. The coils are surrounded with ferrite toroids which increase the inductance in the high voltage accelerating gaps. Sin/Cos coils also surround the focusing magnets to "trim" the magnetic field. The Sin/Cos coils produce less than 1% of the field strength of the focusing coils but are nevertheless essential for producing a straight paraxial field line.

ETA II cell

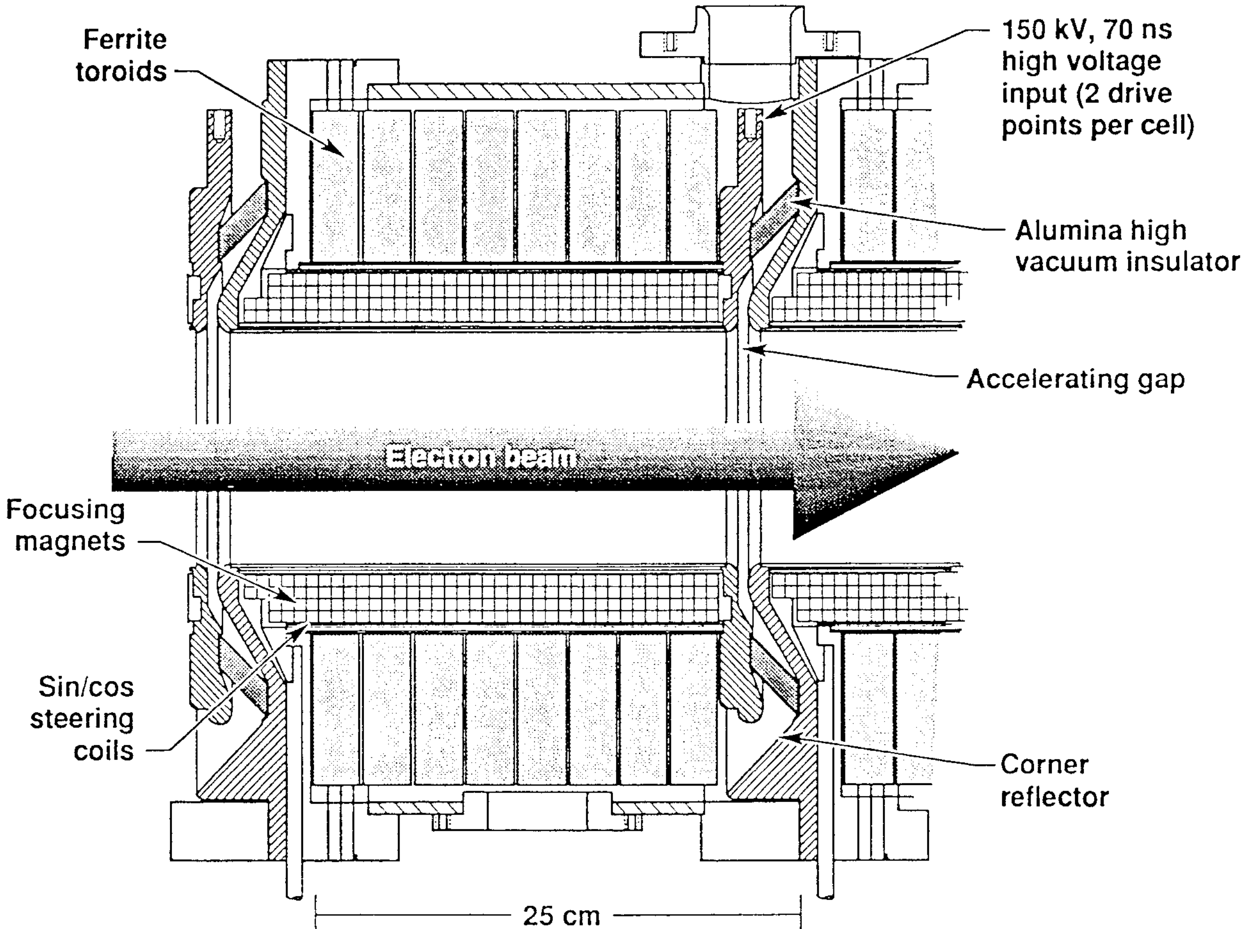

40-D-0289-0008
DM

The solenoidal cells are linked together into 10-cell blocks. There is precise mechanical adjustment of each 10-cell block, via a five-axis geared lead screw system (commercially available jacks). The 10-cell blocks are installed to form an accelerator, for example the Advanced Test Accelerator has 20 10-cell blocks or 200 cells. By measuring the linearity of the field throughout the installed accelerator, a linear least squares fit can be generated to show how to adjust the mechanical position of each 10-cell block to minimize the field nonlinearity. Now, after mechanically aligning the accelerator, the LEEP diagnostic can be used to produce real time feedback on how to set the current of the Sin/Cos (trim) coils, and thus provide the final touch in straighting the magnetic field.

ETA II individual cell

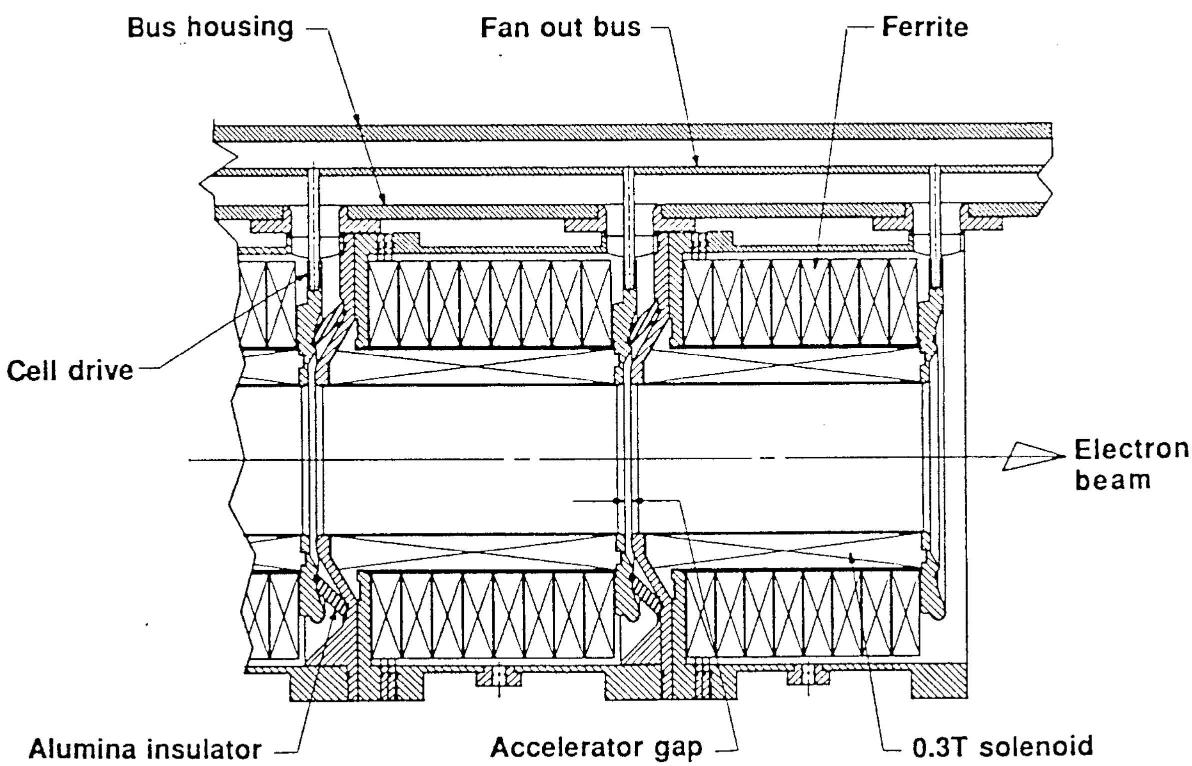

40-D-0988-0638D

Measuring the linearity of the magnetic field off-axis reveals the field line deviations that occur at each accelerating gap. The electron beam does not follow these large field deviations exactly. However, near the accelerator axis there is relatively little field deviation and the electron beam will follow a flux line with negligable error.

4.6 cm off axis, 90 deg. CC from leads

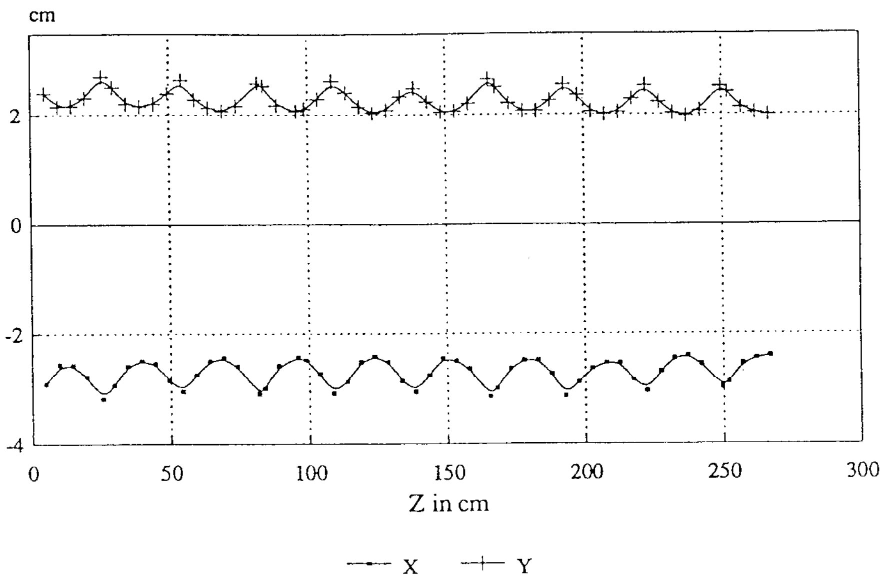

10-cell at 500 A, Aux. coil at 200 V
e-gun 3 kV, 2.3 V, 260 V screen

On axis

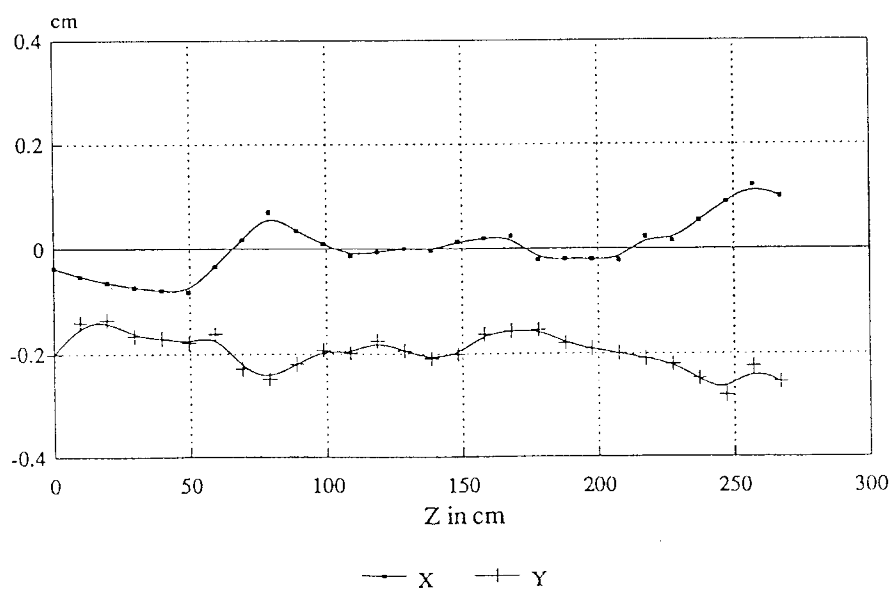

10-cell at 500 A, Aux. coil at 100 V
e-gun 2 kV, 2.4 V, 260 V screen, (rp3)

The electron beam does not have to be exactly on axis to be a useful diagnostic in determining the proper trim for the Sin/Cos (trim) coils.

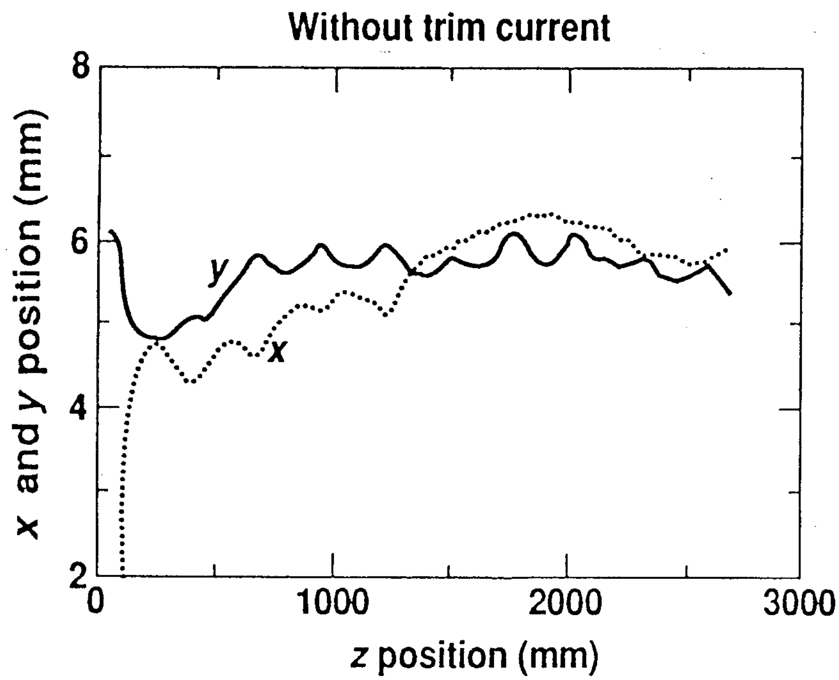

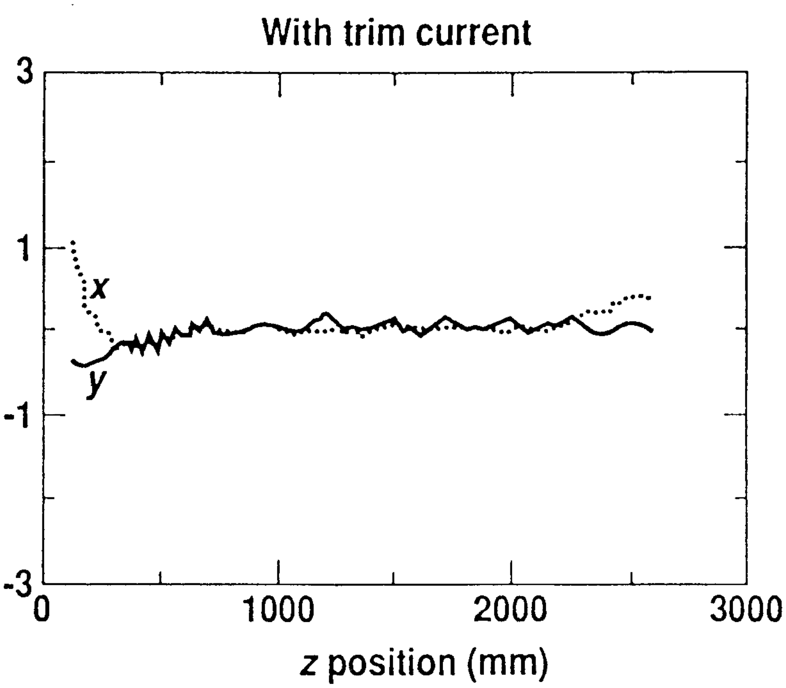

The latest version of the LEEP diagnostic is aimed at solving several systematic problems or uncertainties that have existed with previous versions. The transverse position of the electron beam has, in the past, been determined by first converting it to a light spot on a phosphor screen. The phosphor screen was moved through the accelerator on a carriage, that also carried a TV camera to observe the spot. To know the true position of the electron beam required tracking the carriage with a laser beam and another camera. The cameras produced several problems such as; slow operation due to image processing requirements, camera failure in high magnetic fields (> 500 kG), and finally the cameras effected the field. These problems were solved by replacing the cameras with lateral effect photodiodes, which provide a direct analog determination of the X-Y position of either the electron beam or the laser beam. The photodiodes were specially built to eliminate magnetic materials. Another advantage of using the lateral effect photodiodes was that the carriage could be completely exposed to vacuum, so the laser beam could propagate past the carriage. By splitting the reference laser beam and propagating one half of the beam past the carriage, to a detector at the far end of the accelerator, the pointing direction of the laser could be stabilized to a couple of microns over the roughly 4 hour scan time.

LEEP II provides several essential advances in accelerator alignment

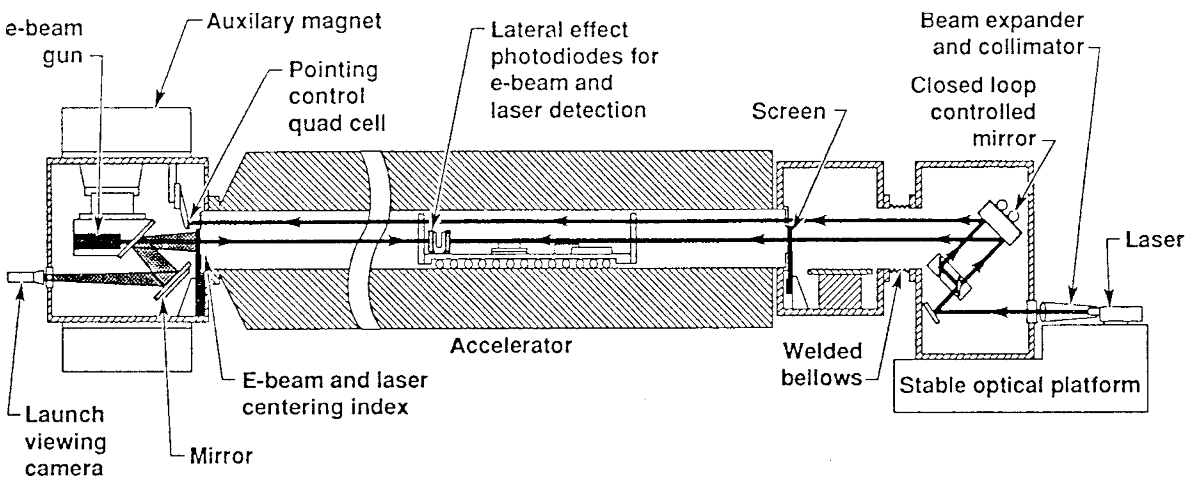

- Two point stabilized laser tracking
- Higher resolution and higher accuracy
- Correlation of magnetic axis to mechanical axis
- Elimination of magnetic effects on sensors and vice versa
- Higher speed of operation
- Capability to scan up to 80 meters
- Reduced risk to intrabeam-tube diagnostics

The reference laser beam is split with two cemented cube beam splitters. It is not necessary that the beams emerge from the beam splitter exactly parallel (10^{-4} radians is adequate). However, it is essential that the movement of one beam is matched by the movement of the other beam. One of the two emerging beams is intercepted by the carriage to determine the transverse position of the carriage. The other beam propagates past the carriage to a quad-cell detector at the far end of the accelerator. The quad-cell produces an error signal that is used to control a pointing mirror, and thus assure that the laser beam is held in a constant position.

The feedback control loop has sufficient bandwidth to actively damp out laser jitter due to normal environmental vibrations

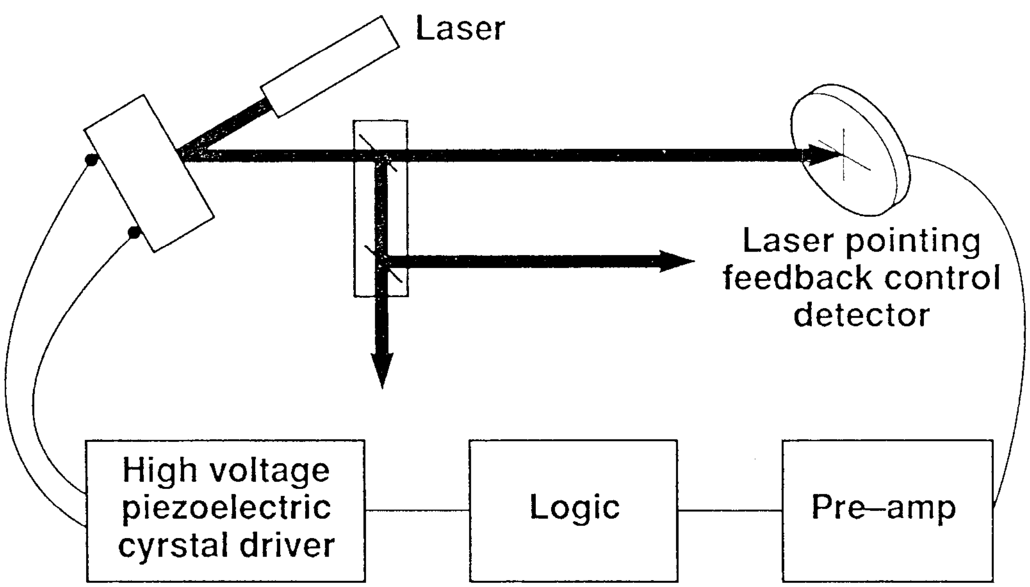

Although the lateral effect photodiodes will provide high resolution over their entire surface, their accuracy may be inadequate for our purposes. Each photodiode will be calibrated to produce a response for its entire surface, to address this issue. The correction surface below is for illustration only.

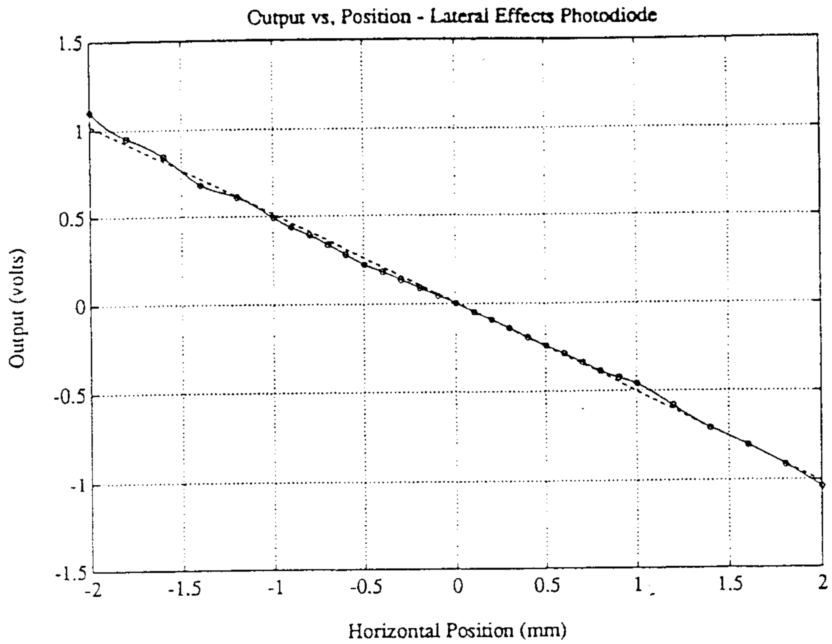

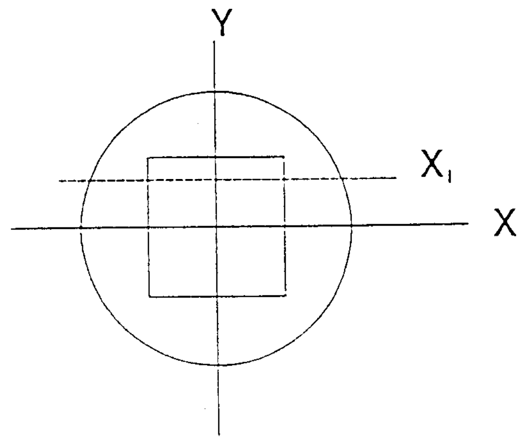

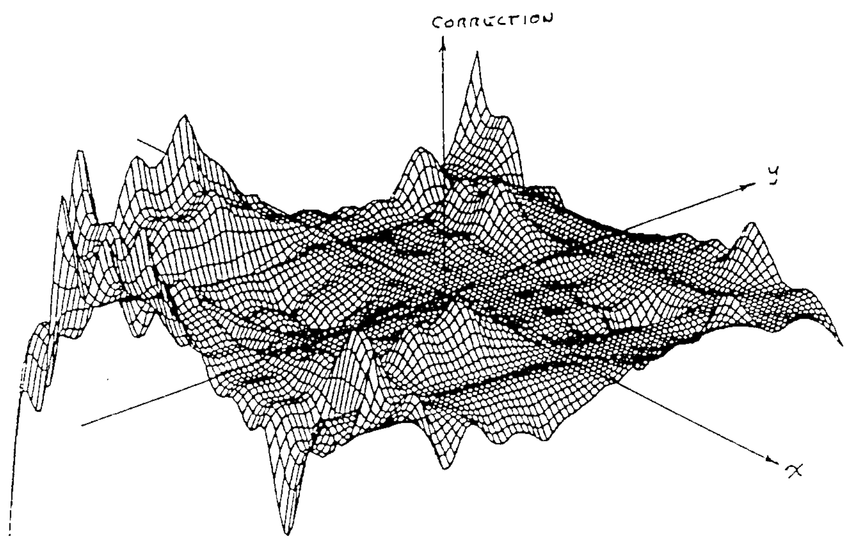

The Low Energy Electron Probe (LEEP) Diagnostic

A diagnostic for mapping flux lines through an accelerator

Review

The LEEP diagnostic provides a precise measurement of the linearity of the magnetic field through a solenoidal magnet or more cogently through a series of such magnets in an accelerator. The LEEP diagnostic provides information necessary for both mechanical alignment and for fine tuning the trim current of the Sin/Cos coils, which are the final adjustment of the field linearity. The essence of the system is as follows:

- The first and last cells of the accelerator are positioned using conventional computer aided theodolite techniques.
- Lateral effect photodiodes are indexed to the first and last cells to serve as an alignment target for a reference laser.
- The reference laser is split into two beams, one of which is used to stabilize the laser pointing and the other is used to track the position of the flux line diagnostics carriage.
- A low energy electron beam is launched along a flux line near the beam tube center at one end of the accelerator.
- The transverse position of the electron beam (and thus the flux line) is determined with a lateral effect photodiode on the diagnostics carriage.
- The diagnostics carriage is moved from one end of the accelerator to the other. As it moves, the transverse position of the electron beam is recorded as a function of carriage position, thus producing a flux line map.

REFERENCING THE MAGNETIC AXIS FOR HERA'S SUPERCONDUCTING MAGNETS

F. LÖFFLER

Deutsches Elektronen Synchrotron
Hamburg, Germany

Abstract

For the alignment of the superconducting magnets of HERA the survey datums have to be referenced to the magnetic axis and the direction of the magnetic field. The necessary measurements are described in the following.

1 Definition of the survey datums

For the alignment of the superconducting magnets of HERA /1/ each magnet can be equipped with two survey platforms. They are attached to the side of the magnets (Fig. 1). Reference points for these platforms are screws, which are prealigned by the manufacturer (Fig. 2). Three radial screws define a plane, which gives the position of the surveypoint with respect to the geometrical axis and the roll and yaw of the survey platform. Two vertical screws, on which the platform rests upon, provide the fixed-points for the height and the pitch of the survey platform. The azimuthal orientation is achieved by two horizontal screws, which locate a finger of the platform.

2 Optical control measurements

The position and the inclination of the survey platforms with respect to the geometrical axis and the reference planes of the magnet have to be controlled after delivery to DESY. This is performed on "Optical Control Stands", which consist of two steel supports with horizontal machined surfaces at both ends of a magnet. Each of them carries two conical baseplates, on top of which Taylor–Hobson alignment telescopes or spherical targets can be mounted. The four baseplates of a control stand form a rectangle. The distances of the two plates of each support are set to the nominal value of the distance between the geometrical axis of the superconducting magnet and a spherical Taylor–Hobson target on top of its survey platforms. The connecting lines between corresponding base plates at each end of the magnet are therefore parallel and within the same horizontal plane. These reference lines are represented by the centers of the mounting sphere of an aligment telescope at one end and respectively a spherical target at the other. Fig. 3 shows the centering fixtures for the telescopes at one end of a magnet, Fig. 4 the corresponding base plates at the other end of the magnet with a spherical target.

The magnet between the two supports has to be aligned with respect to the first reference line. First the roll of the magnet is eliminated by reading coincidence levels on top of the two survey platforms while using jacks for the correction. If the readings of the levels show differences within some tenths of a millirad the average value is chosen. Then the magnet is moved by jacks and guide rods in vertical and radial position until the spherical targets on top of the two survey platforms are on the line of sight of the telescope. Remaining offsets are measured with the optical micrometers of the alignment telescope.

After this alignment the second reference line can be used for controlling the geometrical axis of the magnet. For the superconducting quadrupoles (Fig. 5) it has the nominal distance of 635.00 mm from the first reference axis and the survey platforms respectively. By inserting a special self centering target in the beampipe of the magnet its vertical and radial deviations with respect to the reference axis can be measured with the micrometer of the alignment telescope. With the offsets Δr_2 and Δh_2 for the beampipe and respectively Δr_1 and Δh_1 for the targets on the survey platforms their distance and height with respect to the beampipe axis can be calculated

$$\begin{aligned} dr &= 635.00 + \Delta r_2 - \Delta r_1 \\ dh &= \Delta h_1 - \Delta h_2 \end{aligned}$$

In addition to the control measurements for the position of the spherical targets on top of the survey platforms the roll of the magnet with respect to the reference bars of the survey platforms has to be determined. The reference plane of the quadrupole is marked by the manufacturer by scribed lines on the endflanges. They should be horizontal after the described alignment of the magnet. Deviations can be easily measured with a precision leveling instrument.

For the superconducting dipoles the second reference line can be set at two additional distances from the first reference axis and the survey platforms respectively. The first position has the nominal distance of 630.83 mm, the second is 640.35 mm (Fig. 6). The second value defines the vertex "b" of the magnet axis, the first a point "a", which lies 3343 mm left of the vertex. A third point a' lies symmetrically 3343 mm right of the vertex. Its distance from the first reference axis is 630.74 mm. The difference between the two values for "a" and a' is caused by the asymmetric position of the survey platforms: One is fixed 2507.5 mm left of the vertex, the other 2492.5 mm right of the vertex, while their nominal distance from the magnet is still 635.00 mm. The points a, a' and b once more are represented by self centering targets, which are inserted in the beampipe of the magnet. Their radial and vertical deviations are measured with the micrometer of the alignment telescope: for a and a' from the first position of the reference axis, for b from the second position. With this data and the measured offsets of the targets on the survey platforms their actual distance from the magnet axis can be calculated as well as their height.

The roll of the magnet with respect to the survey platforms in this case is measured by a frame level, referenced to two pins at the magnet end. Like the scribed lines of the quadrupole these pins define the average reference plane of the magnet.

If the deviations from the nominal radial, vertical and inclination values are within some tenths of a millimeter and respectively of a millirad and if other control data, such as flange positions and so on, are within the demanded tolerances the magnet is accepted for further use at DESY. If they are too large, the magnet is send back to the factory for improvement. If possible the necessary corrections are done by DESY itself, while the magnet is still on the "Optical Control Stand".

3 Magnetic measurements[1]

After the optical measurements the magnets are mounted on "Magnetic Measuring Stands". These stands are very similar to the "Optical Stands". On each end of the magnet a steel support with a horizontal machined surface is mounted. In this case they are equipped with only one Taylor–Hobson baseplate (Fig. 7). The baseplates on the two supports define the reference axis for the alignment of the magnet: one carries the alignment telescope, the other the spherical target. The aligning procedure for the

[1]The devices described in this paragraph have been developed by the group PMES at DESY which is in charge of all cold magnet tests

quadrupoles and the dipoles is the same as described for the "Optical Control Stands". Remaining offsets of the reference spheres on top of the survey platforms of the magnets are measured with the micrometer of the aligment telescope. Additionally the actual inclinations β of the two reference bars on top of the survey platforms are measured.

After the alignment the magnet is connected to the He–system and cooled down. Then the magnetic field measurements can be performed. For the quadrupoles the magnetic axis and the direction of the magnetic field have to be determined.

Therefore a Stretched Wire System is used. A single wire is supported by precise quartz cylinders at both ends of the magnet. They are attached to high precision carriages, which are mounted on top of the two steel supports and allow a movement in radial and vertical direction with a reading of better than 0.01 mm. The radial direction is perpendicular to the reference axis, the horizontal and vertical movement guaranteed by a precise adjustment of the carriages.

Fig. 8 shows the principle of the Stretched Wire System. The position of the wire is defined by a groove on the quartz cylinder. By changing the position of the quartz cylinders on both sides simultaneously one can shift the wire parallel from A to B. By this movement voltage is induced in the wire by the magnetic field. Since the wire forms a closed circuit the

$$\int_A^B U_{ind}\,dt = \Delta\,\Phi$$

can be measured via an amplifier ($\Delta\,\Phi$ = change of the magnetic flux).

By moving the wire up and down one can find voltages U_1 and U_2, where $U_1 = -U_2$. The vertical position of the magnetic axis then is exactly in the middle between the two corresponding height readings. The radial position can be determined similarly by horizontal movements of the wire. Here the two positions have to be found, where $U_3 = -U_4$.

The vertical measurements are made in several positions of the horizontal carriage and vice versa for the horizontal measurements. Thus the magnetic axis and the inclination α of the magnetic field are defined with respect to the carriage readings.

The connection between the carriage–readings and the reference axis is achieved by optical measurements. The distance between the wire and the reference axis can be directly measured with a precision rule, which is held against the end of the quartz cylinder. It can be read from the alignment telescope at the other end of the magnet (Fig. 7). Since the distance of the wire from the end of the cylinder is well known from manufacturing, the distance from the reference axis then is determined also.

The height of the stretched wire can be measured on both sides with a precise leveling instrument with respect to the adjacent reference sphere.

Both measurements are made in a position of the wire near the nominal magnet axis. The corresponding readings of the carriages give the reference for any position of the wire.

These reference measurements are made regularly. The results can be reproduced within 0.03 mm.

The overall accuracy of the determination of the magnetic axis with respect to the reference axis is about 0.1 mm, that of the field direction 0.2 mrad. To refer this data to the survey platforms of the magnet it is very important, that the remaining offsets of their spheres are measured carefully. Then the radial distance and the height of the magnetic axis with respect to the magnet spheres can be determined. The obtained values have to be transformed into the coordinate system of the magnet. The origin of this system is given by the magnetic axis, one coordinate axis by the direction of the magnetic field.

This data has to be used for the alignment of the magnet in the tunnel. Additionally the measured field direction α and the actual inclinations β of the survey platforms during the field measurements have to be taken into account (Fig. 7).

Fig. 9 shows the precision carriages for the Stretched Wire System and the Taylor–Hobson target at one end of the magnet.

The magnetic measurements for the dipoles have to check mainly the field integral and the field direction. The first point is solved by a NMR–probe (Nuclear Magnetic Resonance). The field direction, which is much more important for us, can be measured by a combination of two hallprobes with a tilt sensor. The hallprobes are mounted perpendicular to each other and rigidly fixed to the tilt sensor. The whole assembly is supported like a pendulum, so that one hallprobe is almost vertical, the other almost horizontal. The signal of the vertical hallprobe is zero as long as the field is parallel to it. The other then gives maximum signal. If the field has an angle γ with respect to the hallprobe the induced voltage

$$U_H \sim B \sin\gamma$$

is used to derive the value of γ. With the additional reading from the tilt sensor the field direction can be referenced to gravity.

Fig. 10 shows the measuring device, which has been developed by the DESY–magnet–devision. It is mounted in a cylindrical carriage, which centers itself by special wheels in the vacuumpipe of the magnet. It is moved from one end of the magnet to the other by a synchronous toothed belt. Measurements are made in well defined positions along the magnet axis, which are established by a step up motor and angle decoders at each end of the magnet (Fig. 11).

The results of the inclination measurements for one magnet are shown in Fig. 12. Looking from left to right the field is inclined clockwise. Obviously there is a twist to the other side in the last part of the magnet.

The magnetic measurements were repeated several times. The reproducibility was within some hundreds of a mrad. The average value for the inclination of the whole magnet was $<\varphi> = -0.64$ mrad. The mechanical adjustment of the magnet by reading the level on top of the survey platforms was set to -1.5 mrad. So the difference between mechanical and magnetic measurement was -0.86 mrad.

As a control for the accuracy of the measurements the magnet was rotated by $+3.04$ mrad. The magnetic measurements then gave the same magnet twist and an average value for the inclination of $<\varphi> = +2.43$ mrad. That means that $\Delta\varphi_{measured} = +3.07$ mrad. The mechanical rotation of the magnet could be reproduced exactly by the magnetic measurements. That confirms, that the actual inclinations β of the reference bars on top of the survey platforms have to be measured in conjunction with the magnetic measurements. For the alignment in the tunnel the differences $\Delta = \beta - \gamma$ then have to be considered.

For the radial and vertical positioning of a dipole in the tunnel the results of the optical measurements have to be used. Nevertheless these values first have to be transformed to the measured field direction.

Overall 246 quadrupoles and 453 dipoles have to be measured on both the optical and magnetic control stands. Therefore a special hall was constructed, where several Magnetic Measuring Stands were installed. Fig. 13 shows this part of the hall with four stands for quadrupoles and four for dipoles.

After the magnetic measurements each magnet is controlled once more on the optical stand. Only when the values from the first measurement can be reproduced the magnet will be taken to the tunnel.

4 References

/1/ **Löffler, F.:** The Geodetic Approach for HERA. First International Workshop on Accelerator Alignment, S1-2 / S2-4, July / Aug. 1989

5 Figure captions

Fig.	1:	Proton magnets in the HERA–tunnel with survey platforms
Fig.	2:	Reference screws of the superconducting magnet
Fig.	3:	Control Stand with the centering fixtures for the alignment telescope
Fig.	4:	Reference bases for spherical targets
Fig.	5:	Scheme of the optical control measurements for the superconducting quadrupole
Fig.	6:	Optical control measurements for the dipole
Fig.	7:	Scheme of the Magnetic Measuring Stand for the superconducting quadrupole
Fig.	8:	Principle of the Stretched Wire System
Fig.	9:	Carriages for the Stretched Wire System and Taylor–Hobson target
Fig.	10:	Device for the field–measurements for the dipole
Fig.	11:	Principle of the Magnetic Measuring Stand for dipoles
Fig.	12:	Results of the field–measurements for a dipole
Fig.	13:	Magnet measurement–hall

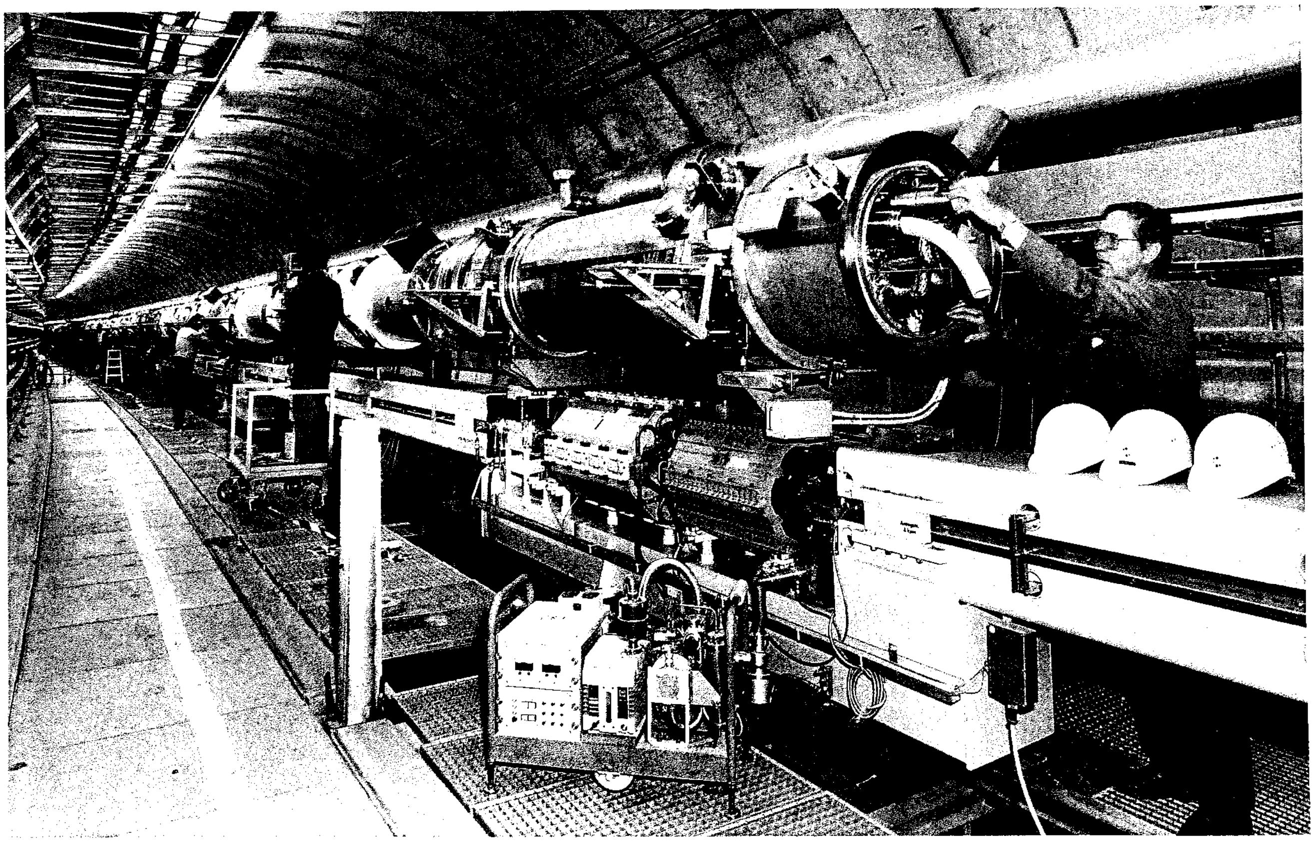

Fig. 1

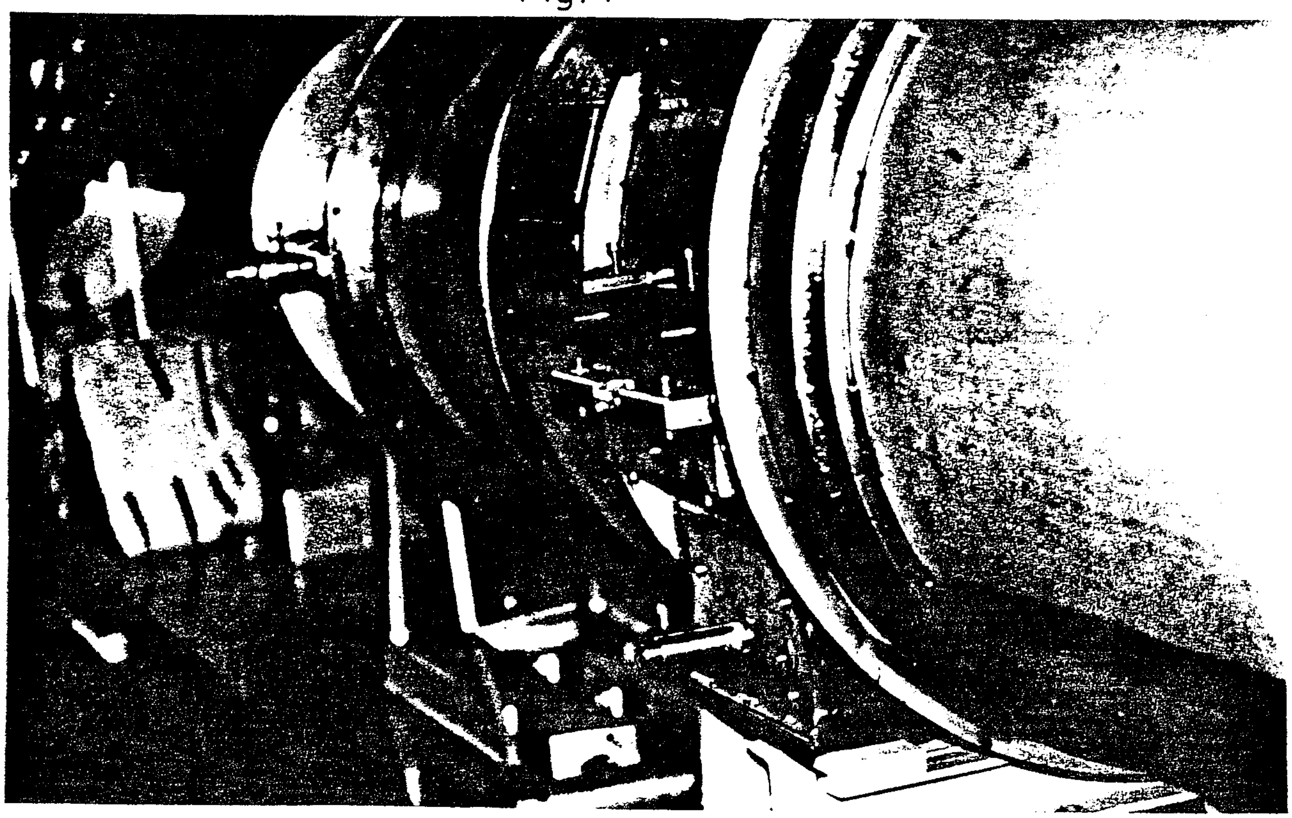

Fig. 2

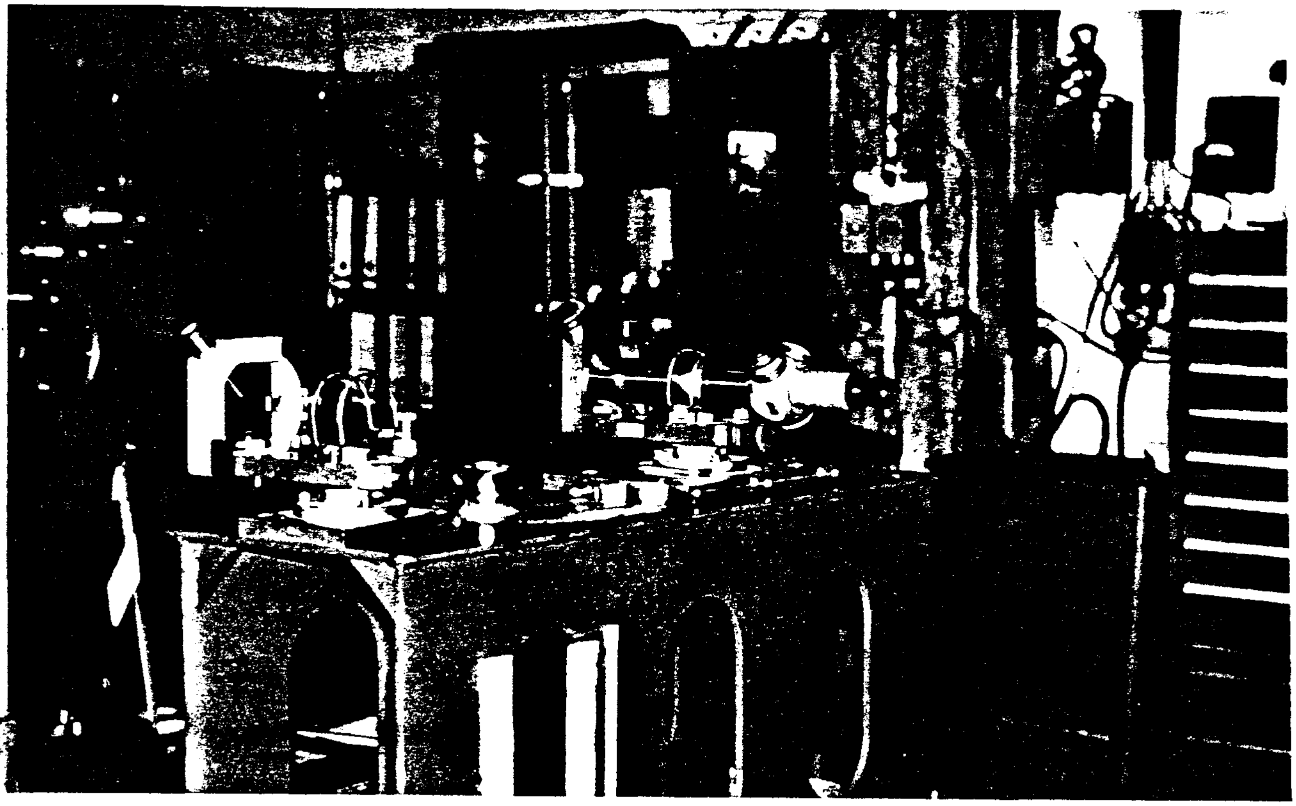

Fig. 3

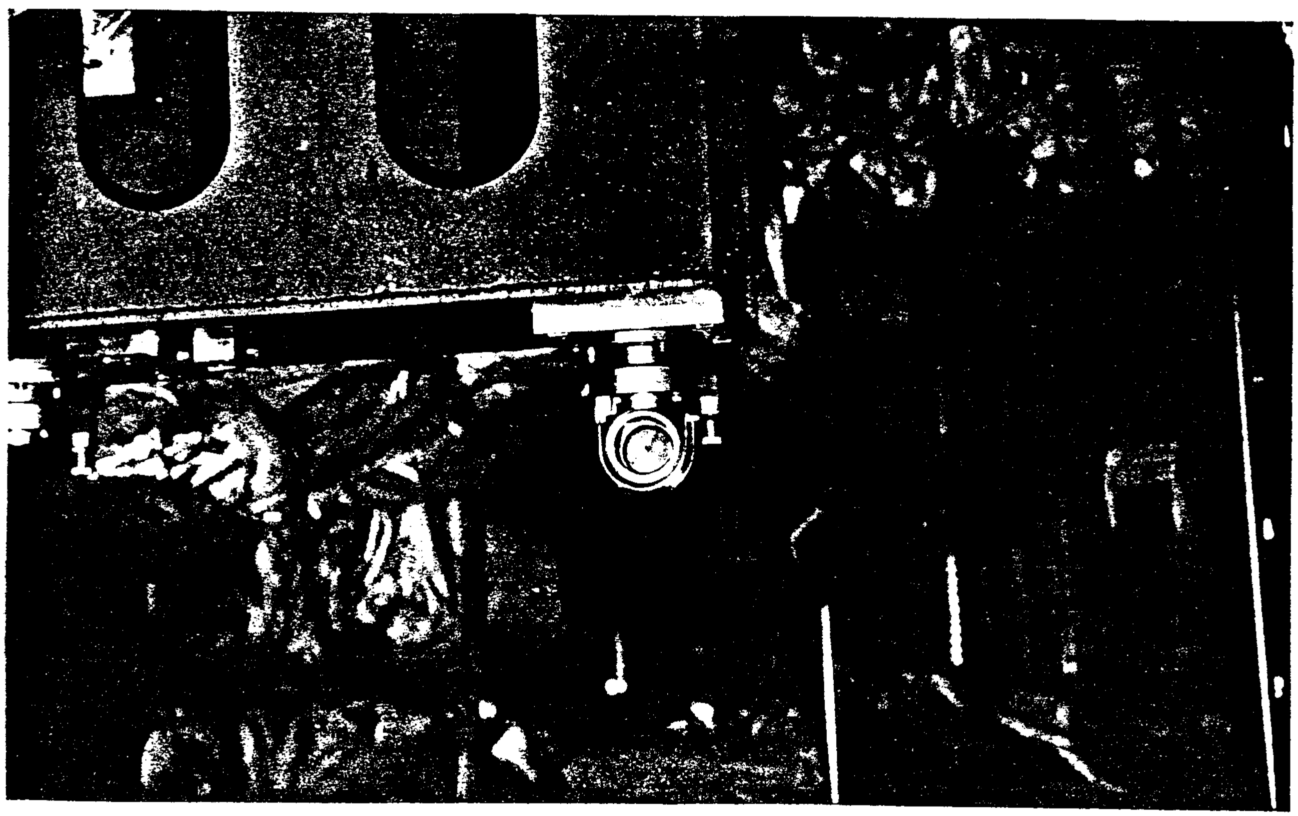

Fig. 4 Fig. 4

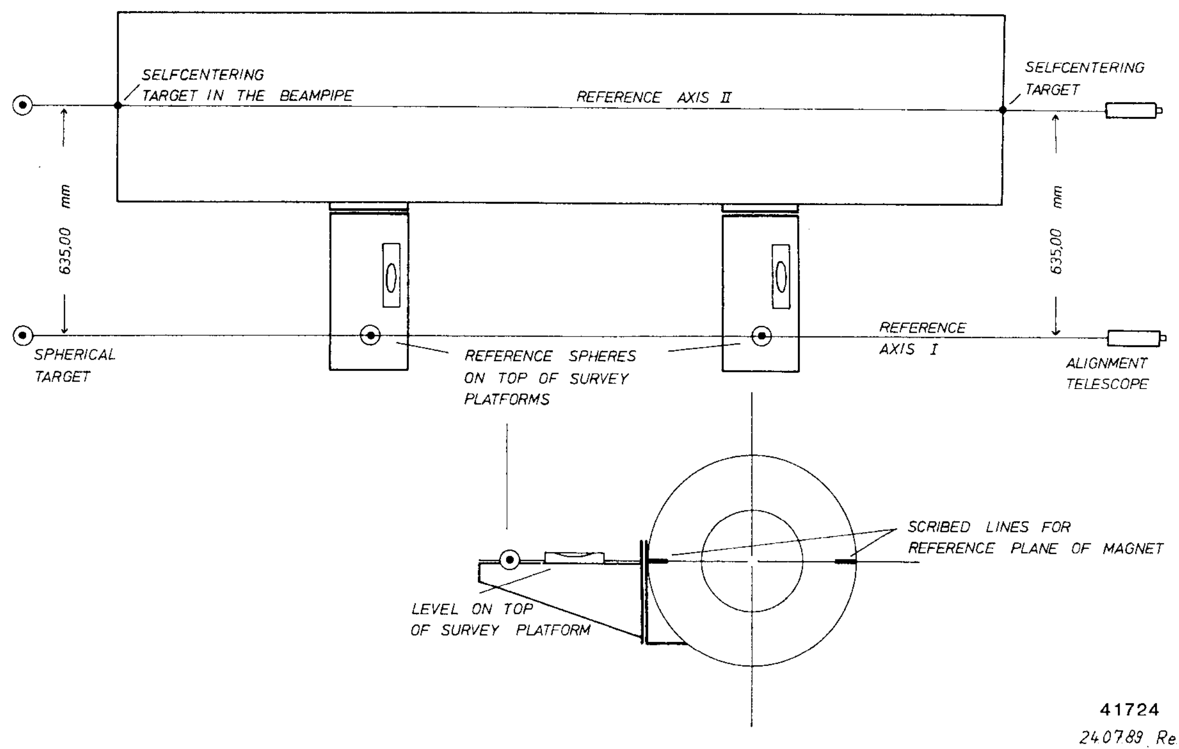
SELFCENTERING
TARGET IN THE BEAMPIPE
REFERENCE AXIS II
SELFCENTERING
TARGET
635,00 mm
635,00 mm
SPHERICAL
TARGET
REFERENCE SPHERES
ON TOP OF SURVEY
PLATFORMS
REFERENCE
AXIS I
ALIGNMENT
TELESCOPE
SCRIBED LINES FOR
REFERENCE PLANE OF MAGNET
LEVEL ON TOP
OF SURVEY PLATFORM
41724
24.07.89 Re

Fig. 5

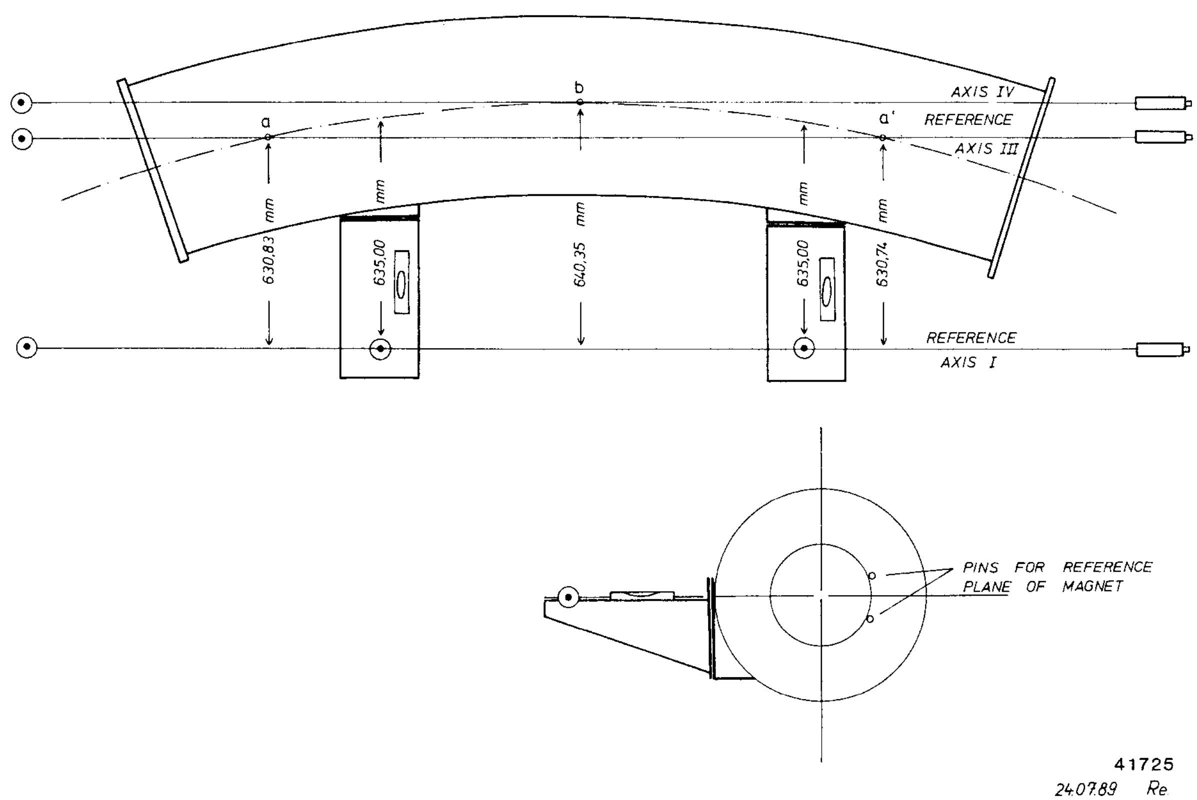
b
a
a'
AXIS IV
REFERENCE
AXIS III
630,83 mm
635,00 mm
640,35 mm
635,00 mm
630,74 mm
REFERENCE
AXIS I
PINS FOR REFERENCE
PLANE OF MAGNET
41725
24.07.89 Re

Fig. 6

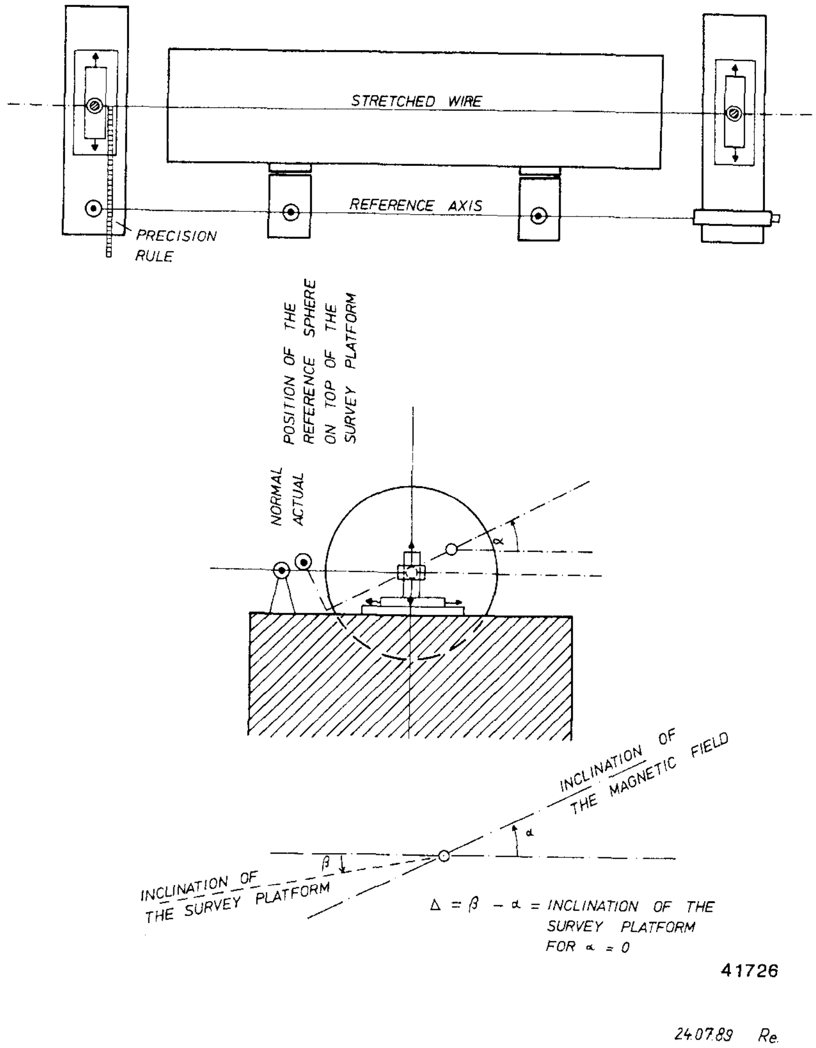
STRETCHED WIRE
REFERENCE AXIS
PRECISION RULE
POSITION OF THE REFERENCE SPHERE ON TOP OF THE SURVEY PLATFORM
NORMAL
ACTUAL
INCLINATION OF THE MAGNETIC FIELD
INCLINATION OF THE SURVEY PLATFORM
Δ = β − α = INCLINATION OF THE SURVEY PLATFORM FOR α = 0
41726
24.07.89 Re.

Fig. 7

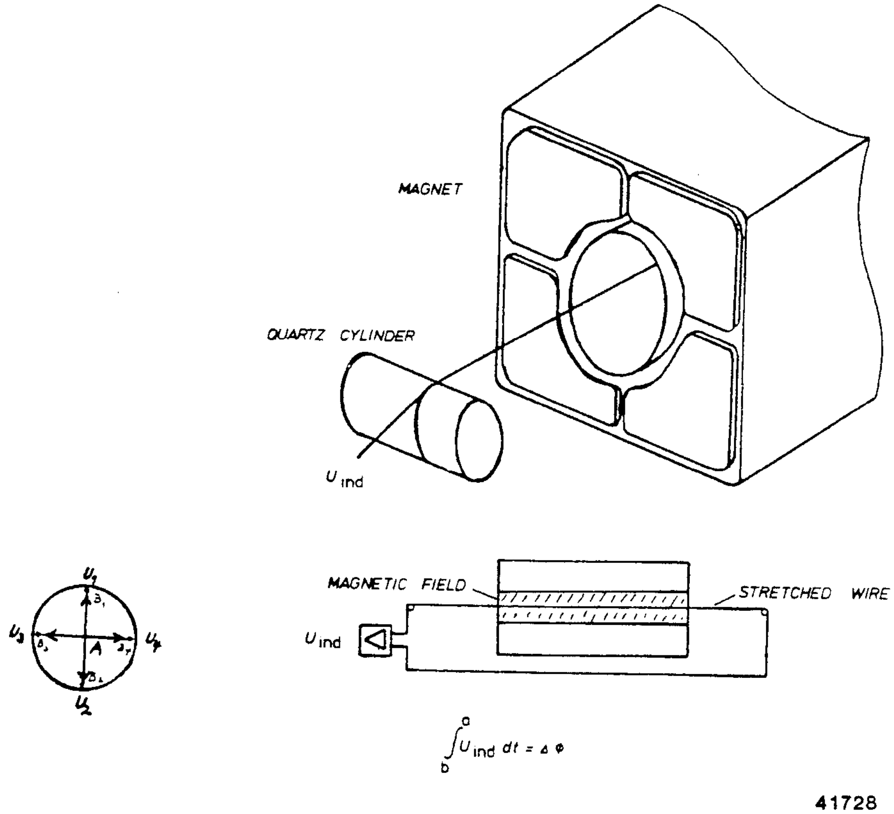
MAGNET
QUARTZ CYLINDER
U ind
MAGNETIC FIELD
STRETCHED WIRE
U ind
41728

Fig. 8

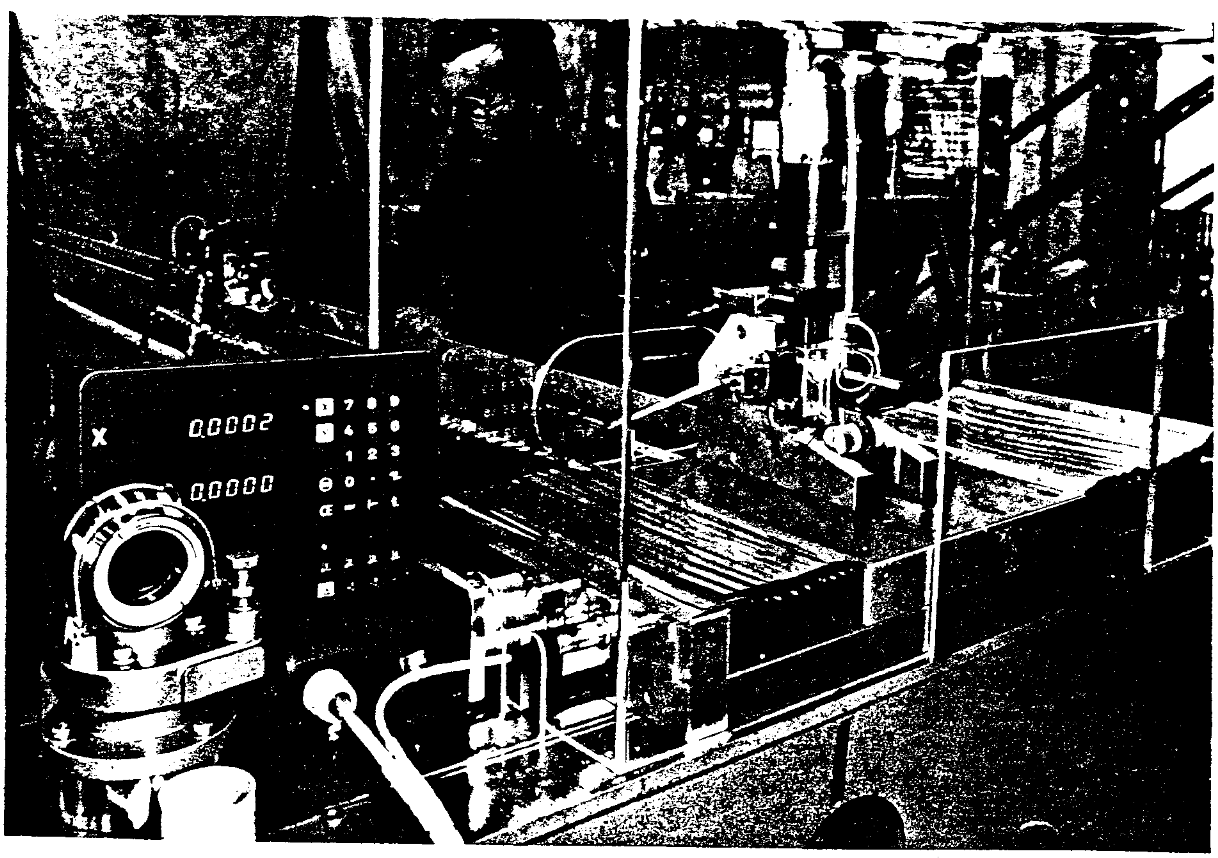
X
0.0002
0.0000

Fig. 9

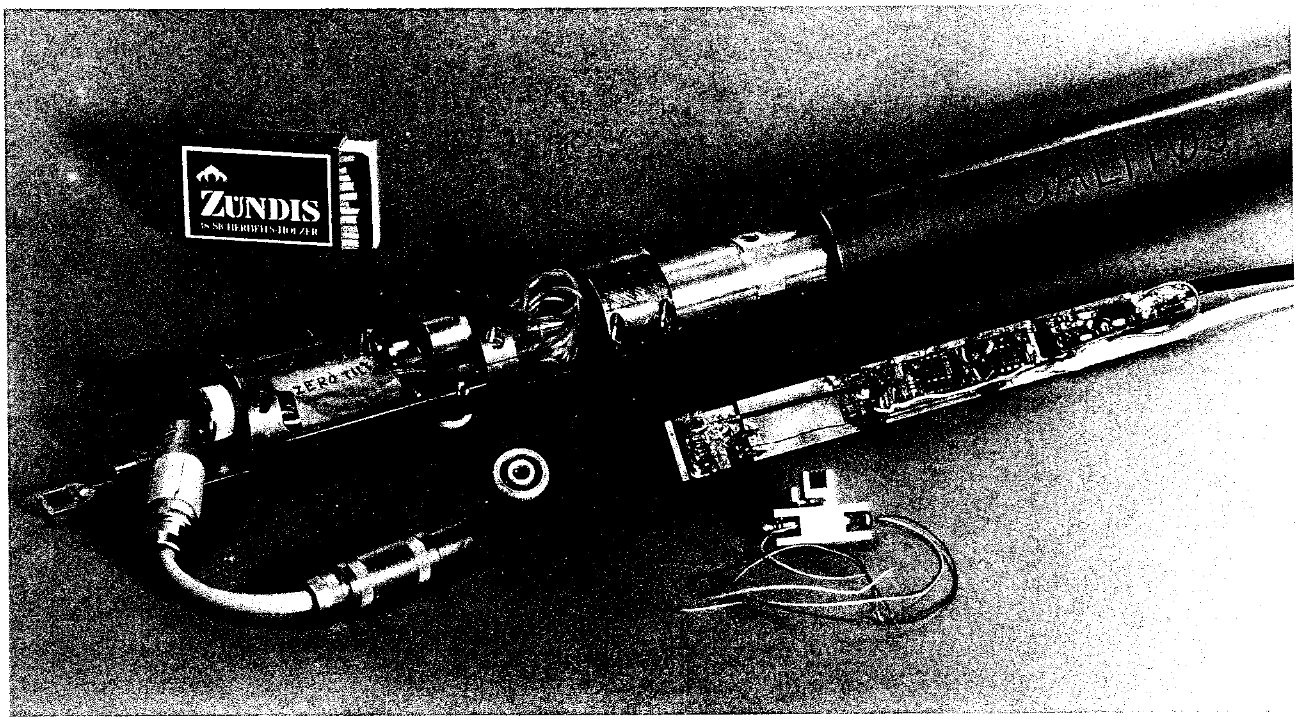
ZÜNDIS
ZERO

Fig. 10

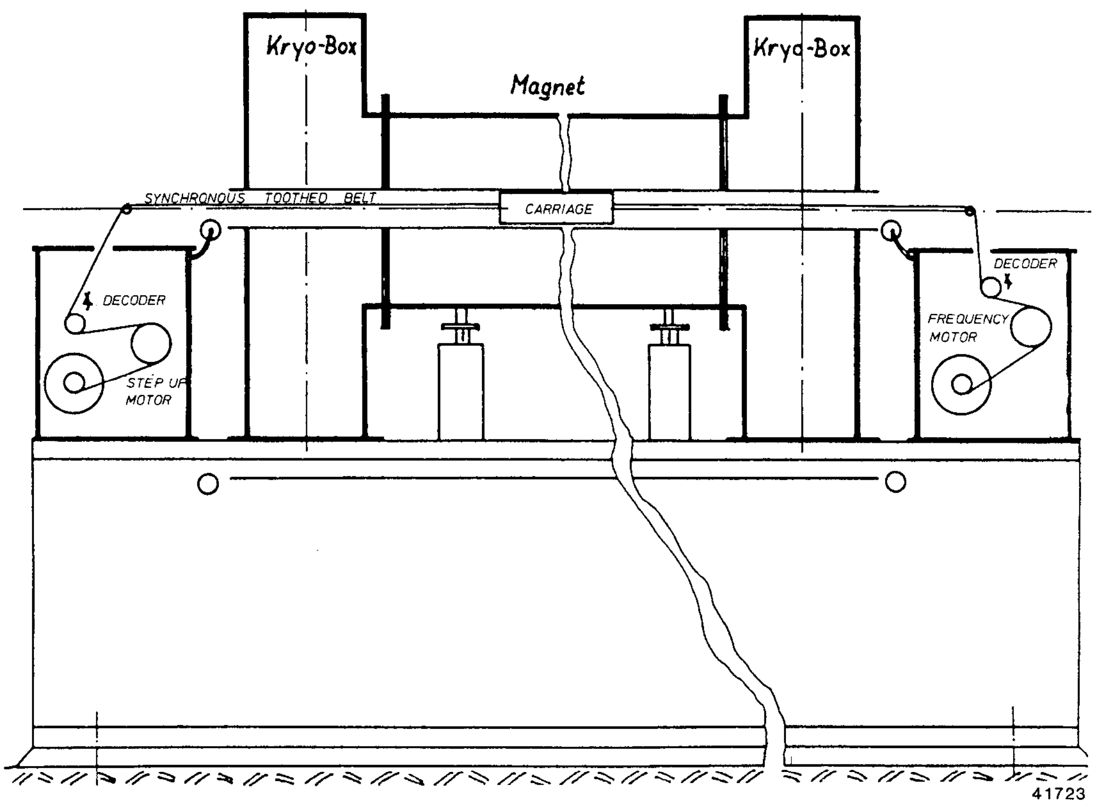
Kryo-Box
Kryo-Box
Magnet
SYNCHRONOUS TOOTHED BELT
CARRIAGE
DECODER
STEP UP
MOTOR
DECODER
FREQUENCY
MOTOR
41723

Fig. 11

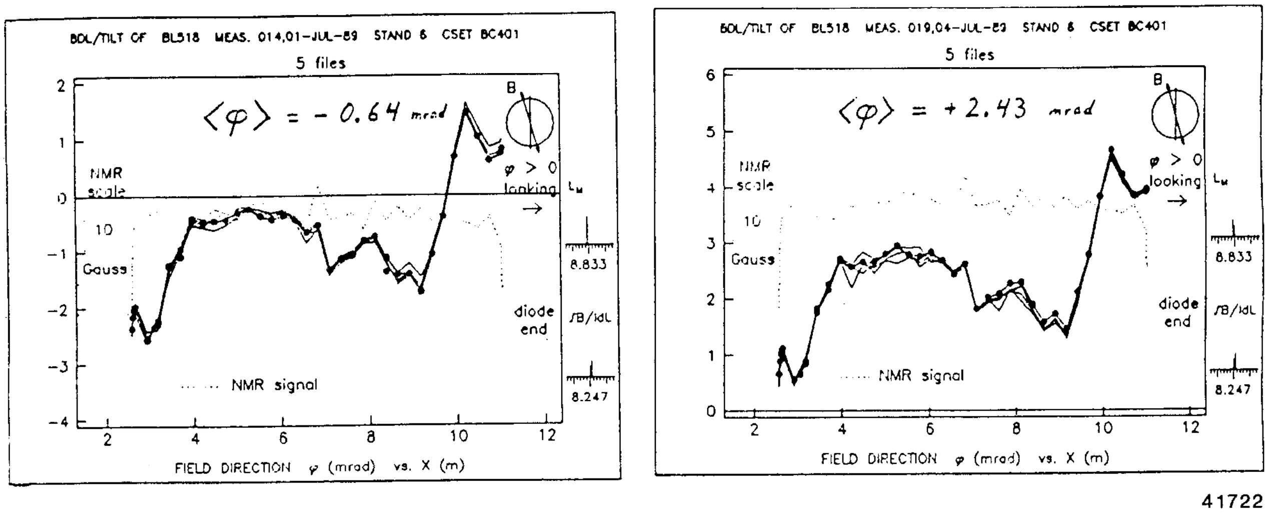

Magnet mechanically positioned to ~ −1.5 mrad

Magnet mechanically rotated by +3.04 mrad
$\Delta\varphi_{measured}$ = + 3.07 mrad

Dipole magnets
Test for measurement of field direction

Fig. 12

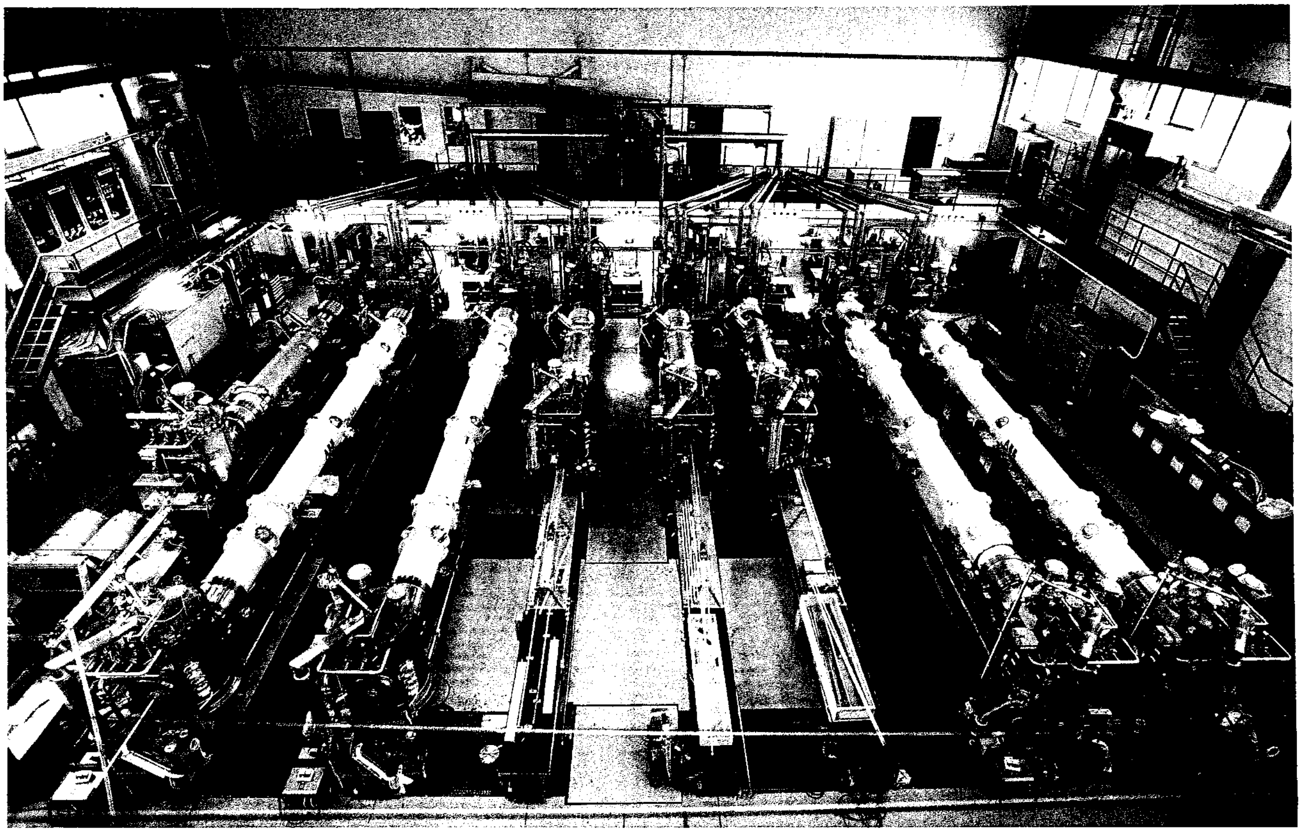

Fig. 13

SSC LONG DIPOLE INTERNAL ALIGNMENT FROM BEAM TO FIDUCIALS

PIERRE F. PELLISSIER

P & S Enterprises, LTD.

Denver, CO.

The SSC long dipole cold mass is 56 feet long, 11 inches in diameter, weighs 16,000 lb. The center of the magnetic field can be assumed to be located at the center of the iron yoke. The $1\frac{1}{8}$ inch diameter beam tube is not accurately located at the center of the cold mass, but it can be assumed to remain in its installed location.

The cold mass is supported by 5 short stiff posts spaced 135 inches apart.

Prior to insertion into the vacuum vessel, the center post is welded to the cold mass, constraining it axially and rotationally. The other posts are fitted with saddles which permit rotation and which permit axial sliding to accommodate cooldown contraction of about $1\frac{1}{2}$ inches.

The vacuum vessel is a 55 foot long, 24 inch diameter, $\frac{1}{4}$ inch wall steel pipe, with 5 stiffening rings. It is made up of short pieces which are welded on a special fixture which accounts for the $\frac{3}{8}$ inch vertical deflection when the cold mass is installed. This welded structure, so far not annealed, has changed its shape in transportation tests. Further work to produce a stable structure is in process.

The cold mass/post assembly is pulled into the vacuum vessel. The 5 cold mass support posts are bolted to flat surfaces on the inside of each of the vacuum vessel stiffening rings.

Provision is made at the base of each post for vertical shimming and for lateral adjustment via oversized holes. Uniform thickness shims are planned.

The vacuum vessel is provided with 4 support feet. The rather low torsional rigidity of the vacuum vessel requires that, during the alignment and measurement process and when installed in the tunnel, one pair of feet be supported to allow axial and rotational freedom in a reasonably semi-kinematic fashion.

The alignment task consists of assuring that, with respect to accessible external fiducials, the center of the magnetic field is everywhere in its correct position within $\pm$ 0.020 inches including a 3.2 mm sagitta and that the average V-plane is correct to within ± 1 milliradian.

The essential larger issue is that, once aligned, the dipole must stay in alignment throughout its 20 year life. This life includes cooldowns, handling, transportation, installation, and normal operation. After installation in the ring, no verification of correct internal alignment is possible.

Status of Dipole Alignment Activity at SSC/Fermilab

1. SSC dipoles for use in the accelerator must be aligned to be within $\pm$ 0.020 inches of the shape of a "perfect" magnet. Eighteen development magnets have been built to date.
2. The assembly and alignment methods in use have produced magnets which are within about $\pm$ 0.040 inches of expected alignment.
3. These methods are capable of improvement to meet alignment requirements and have been more than adequate for the development program.
4. Alignment verification has been done using optical tooling which has an accuracy of about $\pm$ 0.005 inches. It takes two men about $1\frac{1}{2}$ shifts to measure a magnet.
5. An alignment bench using stretched wires is being built which will increase the attainable accuracy, reduce the measurement time, and provide for future automated data collection and analysis.
6. This bench will be used on DD0019 to shim and to adjust the support posts prior to final tightening.
7. DD0019 will be aligned on this bench with the correct sagitta, to be within about $\pm$ 010 inches of the "perfect" shape.
8. The bench will also support vacuum vessel stability studies and is being planned so that measurements can be made during cooldown to liquid nitrogen temperature.

Appendix

Alignment Criteria From SSC Magnet Industrialization Program Technical Orientation – Roger Coombes; 4\89.

1. Alignment

   (Preliminary, for reference only)

   a. Alignment References

   i. External Fiducials

   During installation in the tunnel, the magnet will be accessible to survey equipment from one side only.

   The fiducials will therefore be mounted on one side of the magnet at the location of the exterior feet.

   At each location two survey references will be required.

   ii. Magnet Axis

   The physical center of the yoke can be taken to represent the magnetic axis.

   The vertical field direction will be confirmed during warm testing.

   b. The *overall* requirement for magnet field positioning accuracy for a series of magnets in the ring is stated in terms of the RMS deviation of the magnet axis with respect to the ideal orbit of the beam.

   We assume that systematic errors are eliminated, and that we are dealing only with random errors.

   To first order equal errors in opposite directions tend to cancel each other.

   The assembled collider ring will conform to requirements when the magnetic fields provided by the dipole magnets are positioned within the following tolerances:

   Collider Ring Accuracy

X rms	1 mm (horizontal)
Y rms	1 mm (vertical)
0 rms	0.6 mrad (roll about magnetic axis)

   c. As the beam passes through a dipole magnet, the horizontal curvature of its path is significant and will require the dipole to be "curved" accordingly.

The sagitta is given by:

$$S = \frac{1^2}{8r} = 3.4\ mm$$

$$1 = 16.54\ m$$

$$r = 10.108\ km$$

[Ref. Prime Item Requirements Document (PIRD) sec. 3.2.2.7.2.]

The ends of some dipole magnets will interface with spool-pieces, quadrupoles, or other magnets, and this will require the ends of the magnet to be centered in the cryostat.

d. The overall requirement for the field positioning accuracy can be broken down into two main components which interface at the fiducial marks on the outside of the magnet cryostat.

i. Exterior survey and positioning system (SSC).

ii. Magnet accuracy (Vendor).

Our current belief is that the total tolerance can be divided equally between these two components.

The tolerance assigned to the component relating to magnet accuracy then becomes:

Magnet Overall Accuracy
[Ref. PIRD sec. 3.2.2.8.2.]

X rms	0.7 mm
Y rms	0.7 mm
0 rms	0.6 mrad

e. Magnet overall accuracy

The magnet accuracy specified above is the required accuracy of the relationship of the exterior fiducials to the true axis of a magnet.

This relationship is again made up of two components:

i. Manufacturing precision

ii. Transfer of axis to fiducials

Again, we believe that the error budget can be divided equally between these two components and the error budget assigned to the manufacture and assembly of the magnet becomes:

Magnet Manufacturing Accuracy

X rms	0.5 mm
Y rms	0.5 mm
0 rms	0.4 mrad

An identical error budget is assigned to the transfer of the axis to the fiducials, including measurement errors.

f. Other requirements:

In addition to the average values that must be achieved over a series of magnets, we can also define acceptance limits for an individual magnet.

The manufacturing precision of an individual magnet must meet the following requirements:

i. Departure of the centerline of the cold-mass from the ideal curve shall be within ±1mm horizontally and vertically (with an RMS requirement to be added later).

ii. When the average field angle is vertical, the deviation of a subsection of the field angle from vertical shall not exceed 10 mrad m.

iii. The overall accuracy of the magnet must enable the average roll axis to be located to ±1 mrad.

g. Cooldown

It is predicted that the change in position of the cold mass relative to yoke during cooldown will be uniform for all magnets. This change will be measured during the R&D program at the labs.

C-LINE # 61003

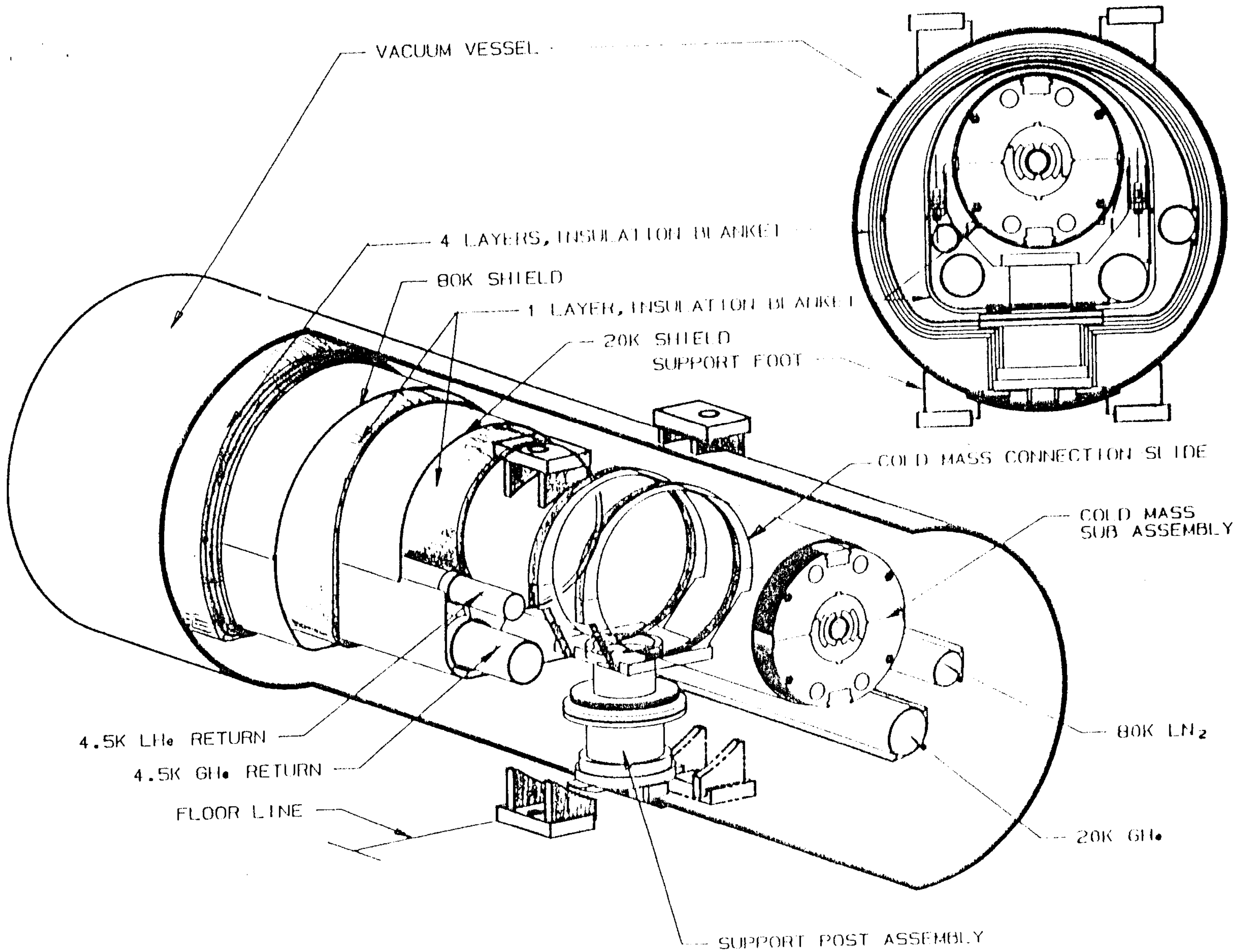
VACUUM VESSEL
4 LAYERS, INSULATION BLANKET
80K SHIELD
1 LAYER, INSULATION BLANKET
20K SHIELD
SUPPORT FOOT
COLD MASS CONNECTION SLIDE
COLD MASS
SUB ASSEMBLY
80K LN2
20K GHe
4.5K LHe RETURN
4.5K GHe RETURN
FLOOR LINE
SUPPORT POST ASSEMBLY

SSC Accelerator Rings
Superconducting Components

Element	Function	Length	Quantity
• Dipole magnet	• Beam steering	17.5m	7,680
• Quadrupole magnet	• Beam focusing	4.5m	1,356
• Spool piece	• Magnet power • Magnet instrumentation • Magnetic corrections • Cryogen supply/return • Vacuum (beam and insulating) • Safety	3.5 - 5.0m	1,656
			10,692

THE NEED FOR THE NEXT LINEAR COLLIDER*

FREDERICK J. GILMAN

Stanford Linear Accelerator Center
Stanford University, Stanford, California 94309

ABSTRACT

The need for the next generation electron–positron collider is discussed within the context of the Standard Model and the physics that must lie beyond it.

INTRODUCTION

High energy physics is beset by the problem of too much success. The Standard Model of strong and electroweak interactions between quark and lepton constituents of matter is in excellent agreement with experiment up to the highest explored energies and at the highest precision.

Along with the Standard Model comes 18 or so parameters (masses, couplings, mixing angles) which are not fixed *a priori* by present theory. The known quarks and leptons seem to know about each other, as they can be neatly grouped into three generations or families. Why are there generations? Why are there three of them? How are the 18 parameters fixed or at least related to each other? Are the quarks and leptons composed of common constituents? Are they grouped together by some larger symmetry? To these and many other questions we can only answer: We don't know. It is paradoxical that with all the success of the Standard Model comes its main problem: It can't be the whole story, but its very success means that we have precious little evidence on what larger theory encompasses it.

THE FRONTIER

With this background, where do we go? What is the frontier?

- We need to pin down the parameters of the Standard Model. This is not necessarily just a process of making things neat and tidy, for we might find with all the parameters known precisely that even some presently known phenomenon, like CP violation, would not agree with Standard Model expectations. The exquisite experiments in progress or planned on rare and/or CP-violating K and B decays are prime examples of this work.

⋆ Work supported by Department of Energy contract DE–AC03–76SF00515.

- We need to check the Standard Model up to quantum corrections. With the mass of the Z known with high precision, the parameters associated with the electroweak gauge boson part of the Standard Model are fixed to a sufficient degree that one can now compare with M_W or with coupling strengths, e.g., using the polarization asymmetry at the SLC, and check the quantum corrections that enter in graphical terms at one-loop order. Depending on how one views it, this is either a check on the consistency and correctness of the theory or a telescope to get a first glimpse of particles at still higher mass which affect the results through their presence as virtual states at one-loop.
- We need to find the top quark. It already appears that its mass is greater than about M_W. It could well be out of the range of LEP II. Then, of present or near-term accelerators, only the Tevatron collider has a chance of finding it. Here is a place where the next linear collider could play a key role. While top might be discovered at the Tevatron and produced in abundance (or even discovered?) at the SSC, detailed studies of the properties and decays of a very heavy top quark are likely the province of an electron–positron machine. One is in a regime of masses where Quantum Chromodynamics (QCD) is truly capable of perturbative application, and incisive tests of the theory of strong interactions become possible as well in the top–antitop system produced (near threshold and in a well-defined state) in e^+e^- annihilation.
- We need to search for extensions and additions to the Standard Model in the "modest" form, for example, of new quarks and new leptons, but also in the dramatic form of whole new classes of particles such as occur in theories with supersymmetry. Such searches have turned up nothing up to now; the torch will be passed to the next generation of electron–positron and hadron colliders.
- We need to check on the gauge structure of the electroweak theory. This entails especially checking the correctness of the $W^+W^-Z^0$ triple gauge boson vertex. This can be done especially cleanly at an e^+e^- collider, and will be a prime focus of LEP II. Further, more sensitive probes of the $W^+W^-Z^0$ and $W^+W^-\gamma$ vertices await the still higher energies available at the next linear collider.

However, barring total surprises, the prime task facing high energy physicists over the next decade or so is that of uncovering the nature of electroweak symmetry breaking, the mechanism by which mass is given to the W and Z, as well as quarks and leptons.

The massless gauge theory is beautiful and well behaved. At first glance, it appears that masses can be inserted in the crudest way by simply writing mass terms into the Lagrangian. However, with such a "hard" mass term the theory becomes sick—infinities arise and cross sections become divergent at high energy. A particularly salient example is provided by considering the scattering of two W bosons with longitudinal polarization, i.e., $W_L W_L \to W_L W_L$. This sounds like a theorist's gedanken experiment at best; it is not. In electron–positron or hadron–hadron collisions the leptons or quarks (in the hadrons) can emit (virtual) W's, which then collide with each other. Such would be the case at a linear collider operating in the TeV range. Calculations of this process with just gauge bosons alone gives answers that blow up as $E \to \infty$.

The Standard Model solves this by a "soft" mechanism for giving masses to particles. In picturesque terms, the originally massless W and Z bosons of the weak interactions "eat" spinless bosons put in the theory to be available for just this purpose, and acquire mass. In addition to the three (2 charged and 1 neutral) spinless bosons which disappear into the stomachs of the $W^{\pm}$ and Z, a fourth, neutral, spinless boson is left behind as a physical particle and witness to what has happened; this is the Higgs boson. With this particle present cross sections no longer blow up, the worst infinities disappear, and the theory is altogether much better behaved.

There are many variants on the same basic theme of breaking electroweak symmetry — "soft" ways of introducing mass into the theory so as to keep it well behaved. There could be many Higgs particles, composite Higgs bosons, technicolor theories, or even no extra particle(s) at all, and the nature of the symmetry breaking found in W's and Z's undergoing strong interactions at high energies, with a rich dynamics at energies in the TeV region.

Where is the Higgs, or more generally at what mass scale does the electroweak symmetry breaking mechanism become manifest physically? The Higgs boson could in principle be found at masses anywhere from a few GeV up to of order a few TeV. We cannot presently pinpoint the scale of symmetry breaking better than to say that very, very roughly, one expects it to be of the order of the W and Z boson masses or a few times that, i.e., several hundred GeV.

This can be studied in electron–positron collisions in a number of ways. Most important, there is the process already noted above:

$$e^+e^- \to \bar{\nu}\nu\ W^+W^- ,$$

with the W^+ and W^- scattering off each other. The prime issue is the nature of the interaction of the longitudinal bosons. In the simplest case, if a resonance (Higgs or other) is present, it will form a bump in the WW cross section. More generally, one wants to study this scattering process up to energies of a few TeV, if necessary, to be sure of being able to understand the nature of electroweak symmetry breaking. To do this will require pushing the frontier of accelerator physics and detector capabilities at both hadron–hadron colliders such as the SSC and at the next electron–positron linear collider

LINEAR COLLIDER ACCELERATOR PHYSICS ISSUES REGARDING ALIGNMENT

JOHN T. SEEMAN

Stanford Linear Accelerator Center
Stanford University, Stanford, CA

Abstract:

The next generation of linear colliders will require more stringent alignment tolerances than those for the SLC with regard to the accelerating structures, quadrupoles, and beam position monitors. New techniques must be developed to achieve these tolerances. A combination of mechanical-electrical and beam-based methods will likely be needed.

Design of a Future Linear Colliders:

The next linear colliders require damping rings, linacs, and final focus systems which produce and deliver beams with emittances one to two orders of magnitude smaller than the SLC. The necessary placement tolerance of the components in these systems varies from system to system but range from 5 to 25 microns in the damping ring, linac, and upstream part of the final focus to well below a micron for components in the final focus near the collision point. Different alignment methods must be used in these varied geometries, adding to the complexity of the placement problem. Furthermore, the transitions between the major systems, for example the injection point of the damping ring beam into the linac, tend to have difficult beam dynamics match conditions as well as complicated alignment geometries. Special attention must be given to these transitions.

Damping Ring:

The issues for the damping ring are to provide an adequately corrected beam orbit and to control the vacuum chamber impedance. The beam trajectory needs proper correction so that radiation damping produces the desired low beam emittance. The rolls of components must be carefully measured to minimize any residual horizontal-vertical coupling so that the required 100 to 1 emittance ratio can be achieved. The vacuum components must be carefully placed so that spurious wakefield effects do not reduce the intensity threshold of longitudinal and transverse instabilities.

Linear Accelerator:

The alignment tolerances in the linac are set to minimize the emittance enlargement of the beams during acceleration. Placement errors of the quadrupoles and position monitors introduce off-axis absolute trajectories even after correction which lead to chromatic phase space mixing. In addition, off-axis accelerating structures generate transverse wakefields which also enlarge the emittance.

Several examples of wakefield emittance enlargement are shown in Figs. 1, 2, and 3. The effects of an oscillating beam in an accelerating structure are shown in Fig. 1. The head of the bunch interacts with the accelerator irises and produces a transverse force on the bunch core and tail. As the beam advances along the trajectory the effects of the wakefields become evident as an off-axis beam tail grows. The resulting increase in beam size can be quite large if not corrected. The same enlargement effects can be produced by displacements of the accelerating structure even though the beam passes through on-axis, hence the tolerances on alignment. In Fig. 2 is shown an induced beam oscillation measured in the SLC linac using the beam position monitor system. About 275 positions are measured and displayed. The amplitude of oscillation can be varied using a dipole magnet to produce (or correct) off-axis beam tails at the end of the linac. Several photographs of beam profiles with and without induced wakefield tails are shown in Fig. 3. The shapes and dimensions of these nongaussian beam profiles attest to the need for precision alignment.

The use of measured trajectories combined with knowledge of the quadrupole and correction dipole settings have been shown to provide precise alignment predictions for quadrupole and position monitor errors. This technique has been used successfully on the

SLC (see C. Adolphsen et.al., SLAC PUB 4902). This and other beam-based alignment methods will be applied to the next collider.

Final Focus:

The alignment tolerances for final focus components are tighter than for other upstream components. Since there are finite bend angles in the final focus the alignment methods are more complex. Also, the physics detector must be shielded from backgrounds requiring careful placement of the beam collimators, synchrotron radiation masking, and particle detectors near the beam. These considerations set the final focus apart from the rest of the collider. Much work needs to be done here.

Other considerations:

There are special circumstances in the next linear collider which make its alignment different than the SLC and other conventional colliders. (1) The beam shape will be vertically flat with about a ten to one aspect ratio. In the linac the sizes will be about one to ten microns. This ratio forces tighter roll tolerances and measurement requirements. (2) The beam oscillation frequency produced by the quadrupole lattice introduces spatial frequencies at which the beam is very sensitive. Special care must be taken, for example in the linac, that offset errors with wavelengths of 20 to 100 meters be controlled. (3) A remote alignment system is desired. The tight tolerances, the large number of effects which can misalign the accelerator (temperature, tides, ground motion, ...), and the nearly continuous operation of the collider strongly indicate that the collider be remotely alignable. (4) Finally, the connections of the accelerator to the outside world (e.g. power and control cables, cooling pipes, RF waveguides, remote alignment fixtures) must be designed so that they have minimal impact on alignment and stability.

Figure Captions:

Fig. 1 The head of an oscillating bunch in a linac produces transverse wakefields which drive the core and tail particles to ever increasing amplitudes and increase the beam emittance. Misaligned accelerating structures also produce this effect.

Fig. 2 A measured beam trajectory in the SLC linac showing an induced oscillation.

Fig. 3 Images of an electron beam on a profile monitor showing wakefield growth with increasing oscillation amplitude. The left image is for a well-steered beam and the right one for an oscillation amplitude of 1 mm. The beam intensity is 2 X 10 **10 electrons. The core sizes are about 120 microns.

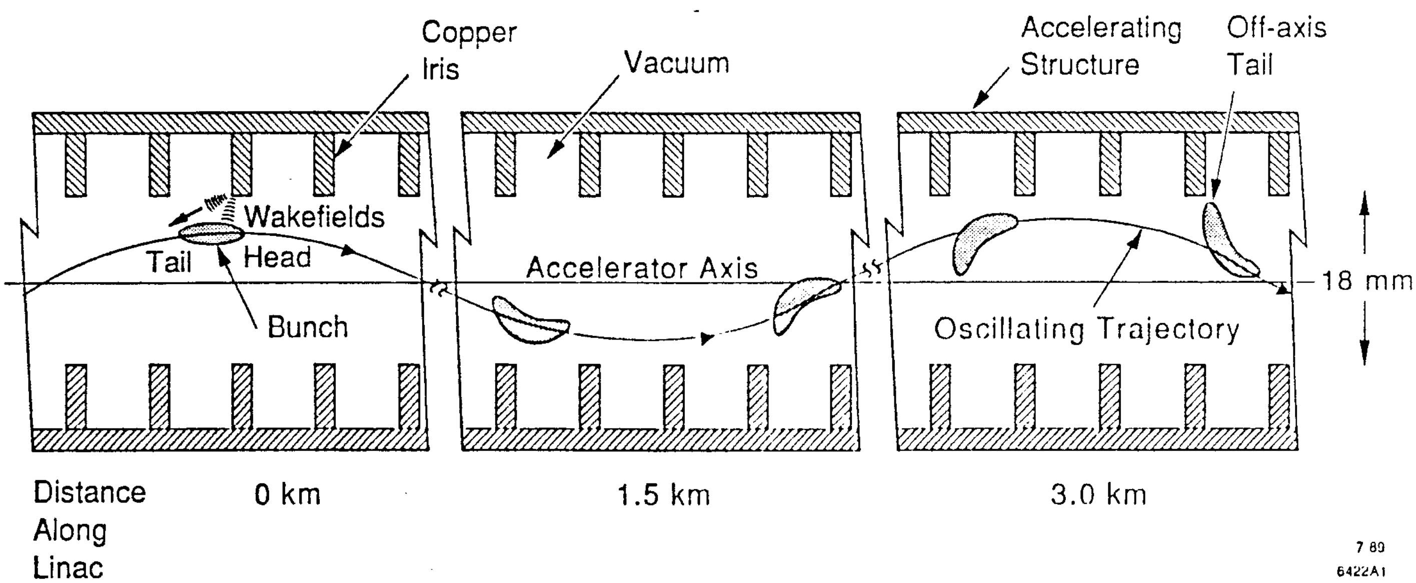

Figure 1. The head of an oscillating bunch in a linac produces transverse wakefields which drive the core and tail particles to ever increasing amplitudes and increase the beam emittance. Misaligned accelerating structures also produce this effect.

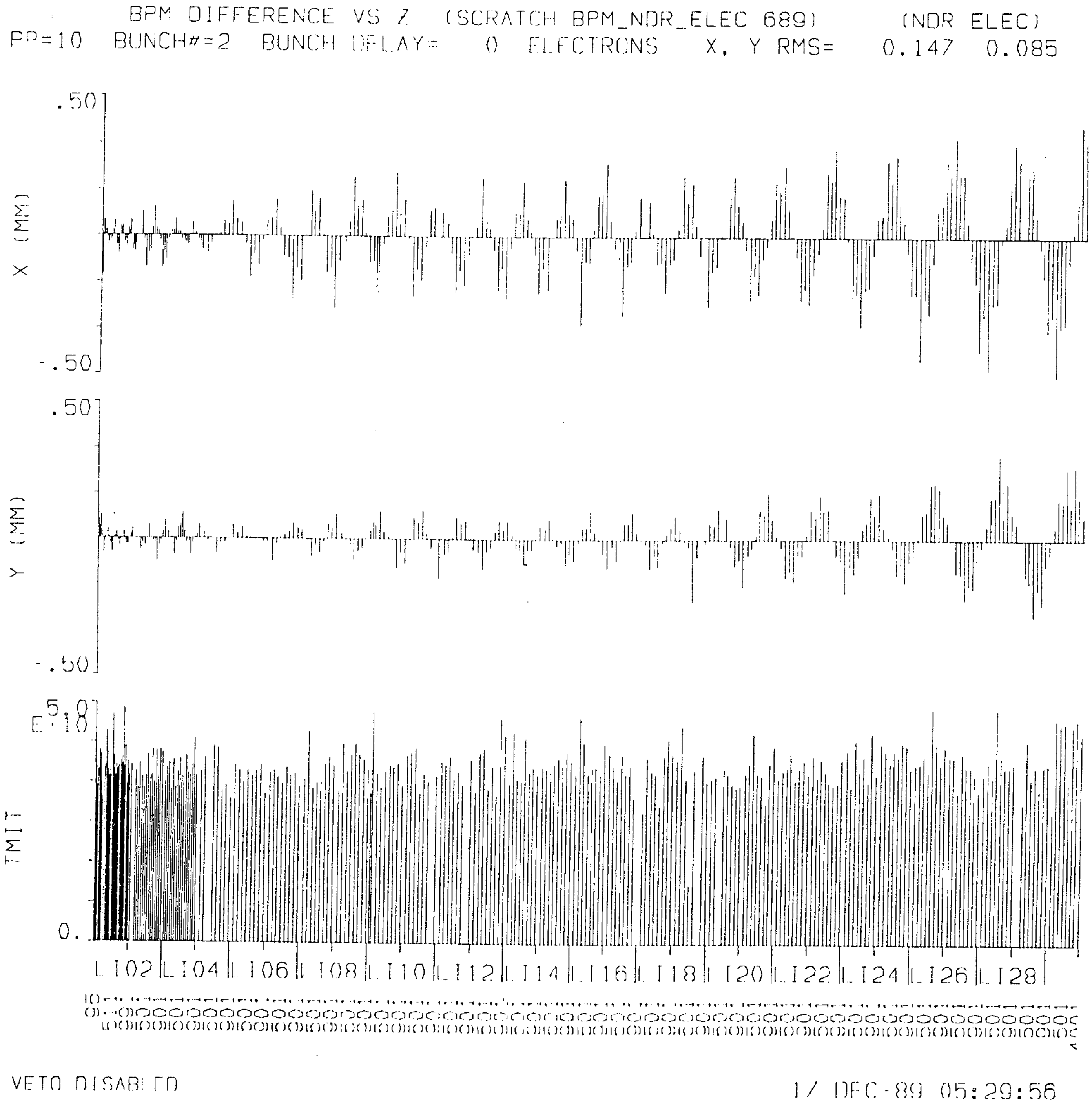

Figure 2. A measured beam trajectory in the SLC linac showing an induced oscillation.

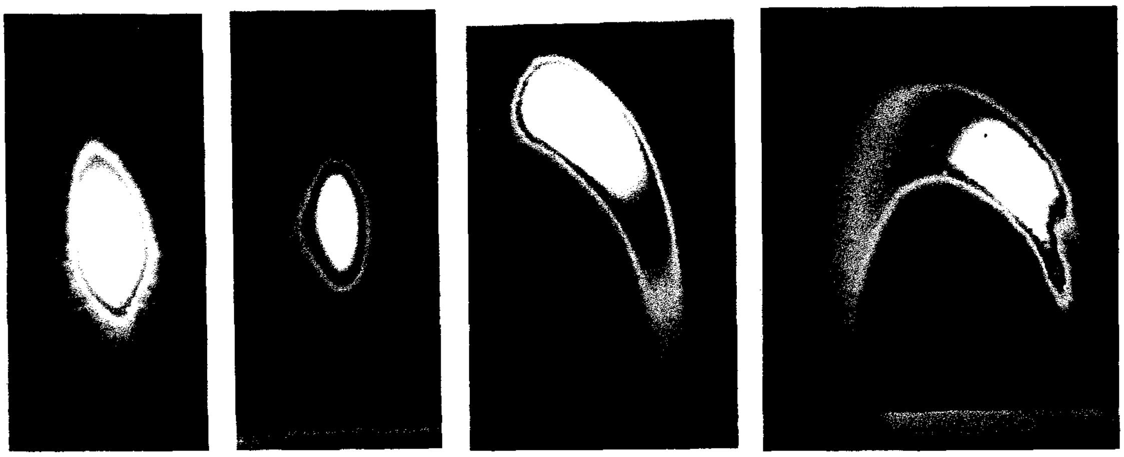

9-89 6438A6

Figure 3. Images of an electron beam on a profile monitor showing wakefield growth with increasing oscillation amplitude. The left image is for a well-steered beam and the right one for an oscillation amplitude of 1 mm. The beam intensity is $2 \times 10^{**}10$ electrons. The core sizes are about 120 microns.

THE POISSON LINE AS A STRAIGHT LINE REFERENCE

LEE V. GRIFFITH

Lawrence Livermore National Laboratory

Livermore, CA.

Summary

The Poisson Alignment Reference (PAR) system was developed in response to the need for a highly accurate linear reference that could operate as an element in a "real time" alignment feedback loop. The system will (or at least is expected to) provide transverse positional data on approximately 60 targets distributed over 300 m, with an accuracy of better than 25 µm. The PAR system employs a large diameter (46-cm-diam for 60 targets) collimated laser beam. The beam must be propagated in a vacuum, to avoid refractive bending. The stability of the beam is guaranteed via a high bandwidth feedback loop, that maintains beam pointing within 5 µm over 300 m. Resolution of target position within the large laser beam is achieved by employing the Poisson spot formed in the shadow of spheres (the targets) in the beam. The Poisson spot from a 2.5-cm-diameter sphere in a HeNe beam is approximately 8-mm in diameter at 300 m, and its center can be resolved to about 2-3 µm using a photo-electric quadrant detector. Much of the advantage of this system resides in the fact that the targets can remain in place at all times, there are no radiation sensitive detectors employed along the alignment axis, and the targets are extremely simple. This paper describes, in some detail, the mathematical modeling of the refractive effects common to all optical alignment systems. The paper continues to describes the Poisson spot and the conceptual design for employing the PAR system in accelerator and free electron laser (wiggler) alignment.

Propagating a Laser Beam

Refractive Effects

The principal feature of an alignment system is a straight line reference, or SLR. It would be inconceivable to make a mechanical SLR to the tolerances needed for an FEL. Lasers form what is generally considered a straight line, but as is shown in Eq. (6), this is not true in air. The beam will bend in the atmosphere from changes in the refractive index. The refractive index is sensitive to both temperature and pressure variations. Some perspective on the atmospheric bending effect on light is provided in Ref. 5. If one were to use the SLAC approach, a deviation from a straight line path can be calculated from the following considerations: if only deviations in the vertical direction are considered, the refractive index can be written as

$$n(y) = n_o(1 - \varepsilon y) \ , \tag{3}$$

where $n(y)$ is the index of refraction as a function of the vertical position y and $n_o\varepsilon$ is the gradient in the vertical direction. The vector form of the differential equation of a light ray is

$$d/ds\,(n\,d\mathbf{r}/ds) = \text{grad}\ n \ , \tag{4}$$

where $\mathbf{r} = \mathbf{j}y + \mathbf{k}z$; $\mathbf{j}$ and $\mathbf{k}$ are the unit vectors in the y and z directions, respectively; and s is the distance along the ray. To a very good approximation, $s = z$; thus Eq. (4) can be reduced to

$$d/dz\,(n\,dy/dz) = -n_o\varepsilon \ . \tag{5}$$

For a paraxial ray starting on the axis, where $n = n_o$, the solution to Eq. (5) is

$$y = -\varepsilon z^2/2 \ . \tag{6}$$

The problem is to find ε, which can be derived by starting with the Lorentz-Lorentz formula[5,15]:

$$A = (RT/p)\,(n^2 - 1)/3 \ , \tag{7}$$

where A is the molar refractivity, R is the gas constant, T is the temperature, and p is the pressure. Equation (7) can be rearranged as

$$n - 1 = \frac{3A\,p}{[RT(n+1)]} \ , \tag{8}$$

and noting that $n + 1 \cong 2$:

$$n - 1 \cong \frac{3A(p/T)}{2R} \ . \tag{9}$$

At standard temperature and pressure (298 K and 760 Torr), $n - 1 = 3 \times 10^{-4}$; thus $3A/(2R)$ is equal to 1.2×10^{-4} K/Torr. Pressure and temperature can be expressed as a function of y, to the first order, as

$$p(y) = p_o + (dp/dy)y = p_o + p'\,y \ , \tag{10}$$

and

$$T(y) = T_o + (dT/dy)y = T_o + T'\,y \ . \tag{11}$$

If the ratio $p(y)/T(y)$ is expanded in a Taylor series about $y_o = 0$, then

$$p(y)/T(y) = p_o/T_o + p'y/T_o - p_oT'y/T_o^2 + \text{(higher order terms)} \ , \tag{12}$$

where p_o and T_o are the nominal pressure and temperature in the line of sight at y_o. Now substituting for n,

$$n(y) = n_o - \varepsilon y \tag{13}$$

yields

$$n_o - n_o\,\varepsilon\,y - 1 = \frac{3A}{2R}\left(\frac{p_o}{T_o} + \frac{p'y}{T_o} - \frac{p_oT'y}{T_0^2}\right) , \tag{14}$$

At $y = 0$,

$$n_o - 1 = \frac{3A(p_o/T_o)}{2R} = 1.2 \times 10^{-4}\,p_o/T_o \ ; \tag{15}$$

thus

$$n_o\,\varepsilon = 1.2 \times 10^{-4}\ \text{K/Torr}\left(\frac{p_o\,T'}{T_o^2} - \frac{p'}{T_o}\right) . \tag{16}$$

The value of n_o is 1.0003 and the pressure and temperature (p_o and T_o) are in Torr and Kelvin. The pressure gradient, p', is $-1.15 \times 10^{-4}\,p_o/m$ (for air) and is generally a minor contributor to refractive bending. However, a temperature gradient as small as 1 K/m would bend the beam 4.5 mm over a 300-m path. To keep the refractive bending from the temperature gradient (T') at tolerable levels, the pressure (p_o) should be below 10^{-3} Torr. The maximum allowable pressure in the propagation path depends on the allowable uncertainty in the straightness of the laser beam, the length of the path, and how well temperature gradients can be controlled.

Divergence

If a Gaussian laser beam is used as an alignment reference, the ability to resolve the location of the beam is proportional to the beam radius. However, due to divergence, the beam radius increases with propagation distance. To keep the beam radius minimized over the entire propagation path, it is necessary to focus the beam to a waist at the midpoint. The equation for the beam waist, w_o, for a given beam radius, $w(z)$, is[16]

$$w_o^2 = \frac{w^2 \pm \left[w^4 - \left(\frac{2\lambda z}{\pi} \right)^2 \right]^{0.5}}{2} , \tag{17}$$

where z is the distance between the waist and the observation plane. If a 5-mm radius beam is required at a distance of 150 m (one half the total propagation distance), then there is no real solution for w_o (assuming $\lambda = 488$ or 632 nm). Therefore, a Gaussian beam is less suitable for the SLR than the Poisson line.

The Poisson Line

The key element of any alignment scheme is the SLR.[5,10,13,14] The Poisson line is one method of generating this line by diffraction. When an opaque sphere is illuminated by a plane wave, as shown in Fig. 2, a diffraction pattern that has the following characteristics is formed behind the sphere:

- There is a line of light, the Poisson line, generated behind the sphere. This line is perpendicular to the incident plane wave and, if extended backwards, passes through the center of the sphere.

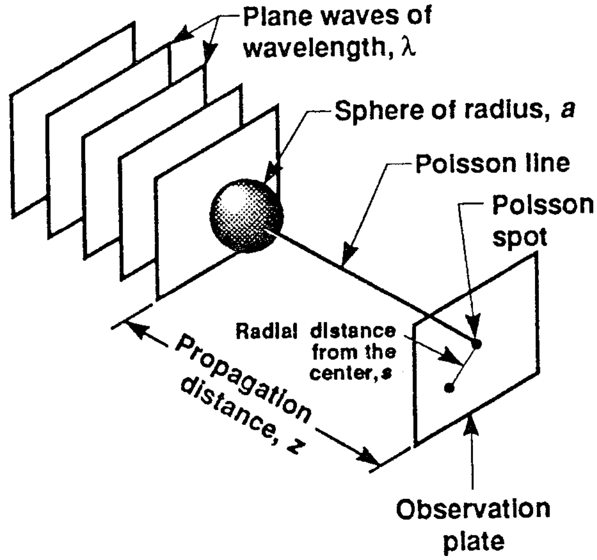

Figure 2. A sphere illuminated by a laser will produce a line of light (the Poisson line) in the shadow of the sphere. The intersection of the Poisson line with an observation plane identifies the sphere location relative to the laser beam or other spheres in the beam.

- The intensity of the line increases asymptotically to the incident intensity as distance from the sphere increases.
- The diameter of the line decreases as the diameter of the sphere increases.
- The diameter of the line increases for increasing distances from the sphere; however, the diameter of the line over any distance behind the sphere can always be kept smaller than a Gaussian beam propagating over the same distance.

The diffraction pattern can be observed by placing an observation screen or camera perpendicular to the Poisson line at any plane behind the sphere. Typical diffraction patterns are shown in Figs. 3(a) and (b). These photographs were taken with a Graflex camera that allows the light to be directly imposed on the film. The diffraction pattern was formed by a 12.7-mm-radius sphere, which was 50 m from the observation plane in Fig. 3(a) and 100 m from the observation plane in Fig. 3(b). The bright area around the shadow of the sphere is part of the 150-mm-diam incident laser beam. The central bright area in the shadow is the Poisson spot, which is the intersection of the Poisson line and

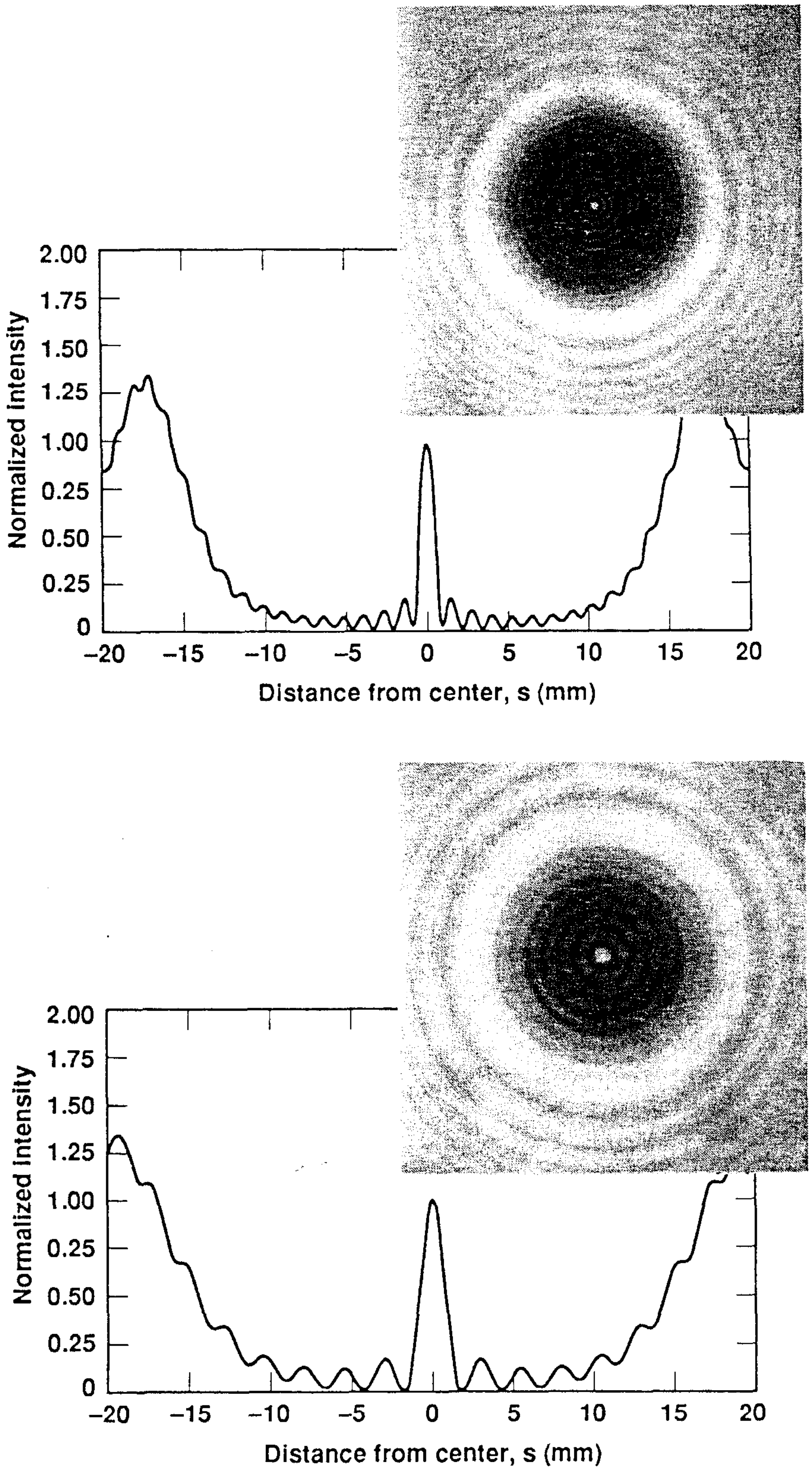

Figure 3. These photos show the Poisson spot from a 25-mm-diam sphere in an observation plane at (a) 50 m and (b) 100 m. The associated plots are the calculated intensity profiles out to the edge of the shadow.

the observation plane. The intensity, I, of the diffraction pattern is given by[17]

$$I(s) = 1 - 4(\pi u)^{0.5} (S_1 \sin \alpha + S_2 \cos \alpha) + 4\pi u(S_1^2 + S_2^2) \;, \tag{18}$$

where s is the radial distance from the center of the Poisson spot, S_1 and S_2 are summations of Bessel functions given by

$$S_1 = \sum_{n=0}^{\infty} (4n + 1) (-1)^n J_{2n+1/2} (u/2) J_{4n+1}(v)/v \,, \tag{19}$$

and

$$S_2 = \sum_{n=0}^{\infty} (4n + 3) (-1)^{n+1} J_{2n+3/2} (u/2) J_{4n+3}(v)/v \;, \tag{20}$$

where

$$u = ka^2/2z \;, \tag{21}$$
$$v = ksa/z \;, \tag{22}$$
$$\alpha = ks^2/2z + u/2 \;. \tag{23}$$

In Eqs. (18)–(23) a is the radius of the sphere, λ is the laser wavelength, and k is the propagation number $2\pi/\lambda$. Figures 4(a) and (b) show the calculated intensity, $I(s)$, for the Poisson spot of a 6.35-mm-diam sphere 26.5 m from the observation plane and of a 25.4-mm-diam sphere 300 m from the observation plane, respectively.

The Poisson line generated as described above only passes through one fixed point, the center of the sphere. To serve as a reference line, the Poisson line must be constrained to pass through a second fixed point. The center of a quad-cell (quadrant detector) serves as the second fixed point. By centering the Poisson spot on the quad-cell, using a feedback circuit between the quad-cell and a mirror that actively steers the incident plane wave, one forms the Poisson reference line, which is ostensibly as stable as the two fixed points.

Since there is a significant amount of energy in the rings around the bright central spot, an aperture over the quad-cell should be sized to match the first dark ring. The quad-cell determines the location of the mean of the energy in the Poisson spot relative to the center. Let A, B, C, and D represent the sum of the energy in each quadrant; then the offset from center can be expressed as

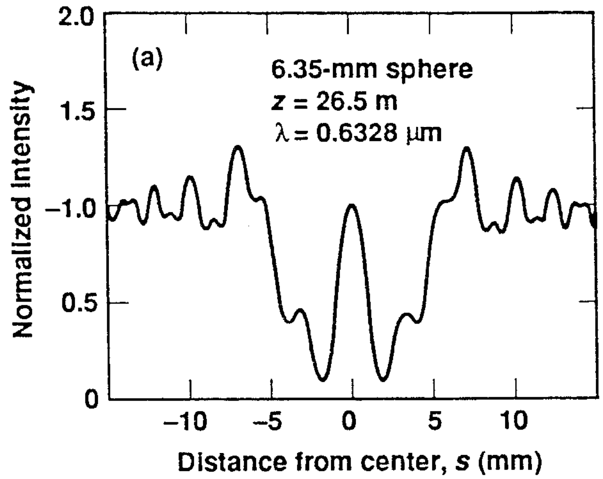

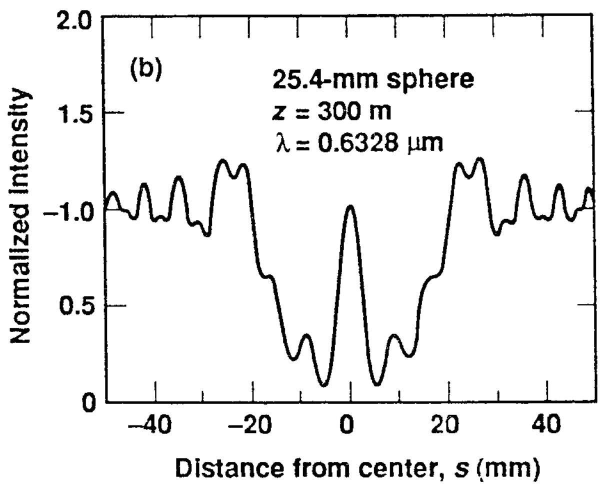

Figure 4. A 6.35-mm sphere (a) was used in a 26.5-m test to simulate the effects of a 25.4-mm sphere (b) 300 m from the observation plane.

$$\delta x = K[(A + D) - (B + C)] \tag{24}$$

and

$$\delta y = K[(A + B) - (C + D)] \;. \tag{25}$$

where A, B, C, and D are the currents from each quadrant, as illustrated:

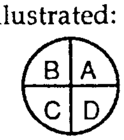

K is a proportionality constant to convert the quad-cell current output to a linear dimension. Figure 5 is a calibration curve that shows that K is quite linear through a region near the center. Although quad-cells can be used for measuring offsets, they are generally better as nulling or centering devices. The curve eventually changes direction because the quad-cell has been moved more than the width of the first dark ring. This causes part of the central bright spot to be masked by the aperture, while on the opposite side of the quad-cell, energy is starting to be added by the first bright ring. It is also important to note that quad-cell output indicates location of the mean of the energy. From a computational standpoint, it is important to distinguish the location of the mean of the energy from the centroid of the energy.

There are major advantages to placing several spheres in a very large diameter beam simultaneously, as discussed in the next section. When there are two (or more) spheres in the collimated laser beam, there is some degree of mutual influence of one sphere on the diffraction pattern of an adjacent sphere. The symmetry of the diffraction pattern is altered, causing a shift of the center of energy of the Poisson spot. Figure 6 illustrates the pertinent dimensions in calculating the offset of a Poisson spot as a result of diffraction from an adjacent sphere. The intensity at a point P is[17]

$$\begin{aligned} I(s_1,\theta) &= 1 - 4(\pi u_1)^{0.5}\,(S_{11}\sin\alpha_1 + S_{21}\cos\alpha_1) \\ &\quad - 4(\pi u_2)^{0.5}\,(S_{12}\sin\alpha_2 + S_{22}\cos\alpha_2) \\ &\quad + 4\pi u_1(S_{11}^2 + S_{21}^2) + 4\pi u_2(S_{12}^2 \\ &\quad + S_{22}^2) + 8\pi(u_1u_2)^{0.5} \\ &\quad \times \{\cos(\alpha_2-\alpha_1)[S_{11}S_{12} + S_{21}S_{22}] \\ &\quad + \sin(\alpha_2-\alpha_1)\,[S_{12}S_{21} - S_{11}S_{22}]\}\ . \end{aligned} \tag{26}$$

The arguments of this function are defined in Eqs. (27)–(32), where $i = 1,2$ identifies the sphere.

$$\alpha_i = ks_i^2/2z + u_i/2\ , \tag{27}$$

$$\begin{aligned} S_{1i} &= \sum_{n=0}^{\infty}(4n+1)(-1)^n J_{2n+1/2}(u_i/2) \\ &\quad \times J_{4n+1}(v_i)/v_i\ , \end{aligned} \tag{28}$$

$$\begin{aligned} S_{2i} &= \sum_{n=0} (4n+3)(-1)^{n+1} J_{2n+3/2}(u_i/2) \\ &\quad \times J_{4n+3}(v_i)/v_i\ , \end{aligned} \tag{29}$$

$$u_i = k\,a_i^2/2z\ , \tag{30}$$

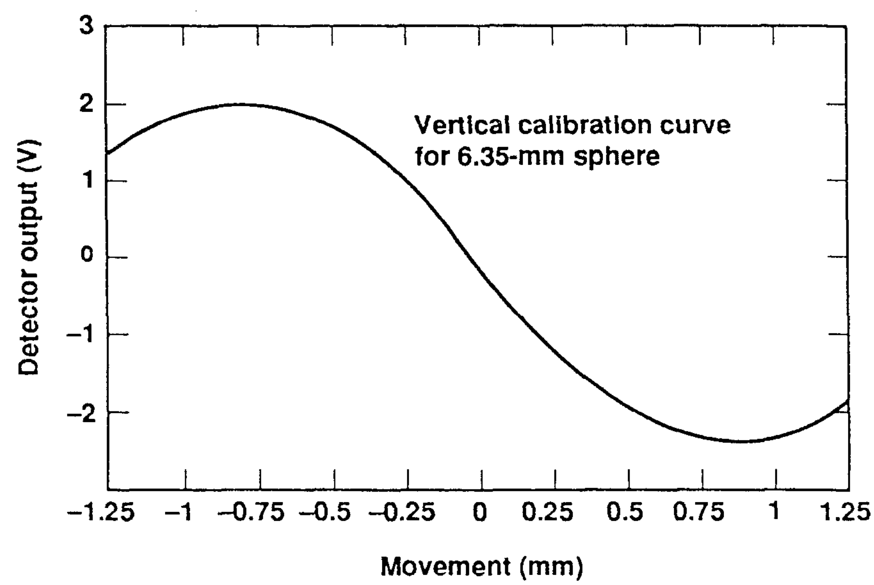

Figure 5. Quad-cell calibration curves are influenced by beam intensity and might be distorted by stray light.

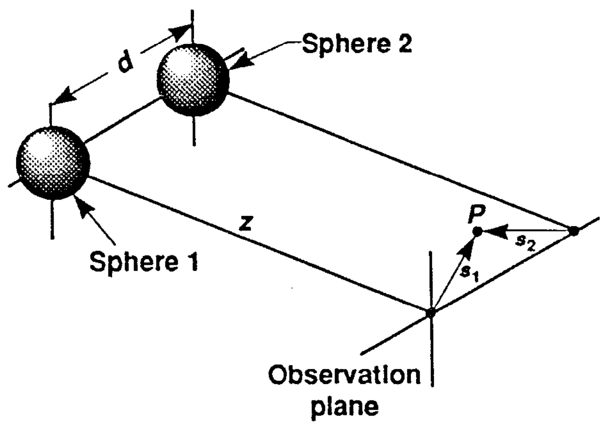

z ≡ Distances from spheres to observation plane

P ≡ Point in the observation plane

s_1, s_2 ≡ Radial distance from the center of the Poisson spots to the point p

Figure 6. Diffraction from two adjacent spheres will interact. The separation of the spheres (d) must be about 25 mm edge-to-edge to assure an acceptably small shift in Poisson spot in the observation plane. Z is the distance from the spheres to the observation plane; P is a point in the observation plane; and s_1 and s_2 are radial distances from the center of the Poisson spots to the point P.

$$v_i = ks_ia_i/z \ , \tag{31}$$

and, as before,

$$k = 2\pi/\lambda \ . \tag{32}$$

In Eqs. (26)–(32), a_i is the radius of the sphere i, z is the propagation length between the spheres and the observation plane, and λ is the laser wavelength. Techniques for solving the fractional-order Bessel functions can be found in *Handbook of Mathematical Functions*.[18] The value of s_2 is easily found from the cosine law

$$s_2 = (s_1^2 + d^2 - 2d\, s_1 \cos\theta)^{0.5} \ , \tag{33}$$

where s_1 and θ are the coordinates of the point P. Point P is the spot in the observation plane where the intensity is being calculated. Distance d is the center-to-center separation between the spheres.

Figure 7 shows the experimentally determined shift of a Poisson spot, from a stationary 6.35-mm-diam sphere, as a matching sphere moves toward it. The abscissa shows the center-to-center displacement of the spheres, and the ordinate shows the displacement of the mid-point of the energy distribution of the Poisson spot from the stationary sphere. The moving sphere is aligned such that its axis of motion will cause it to overlap the stationary sphere. The quad-cell that is monitoring the Poisson spot

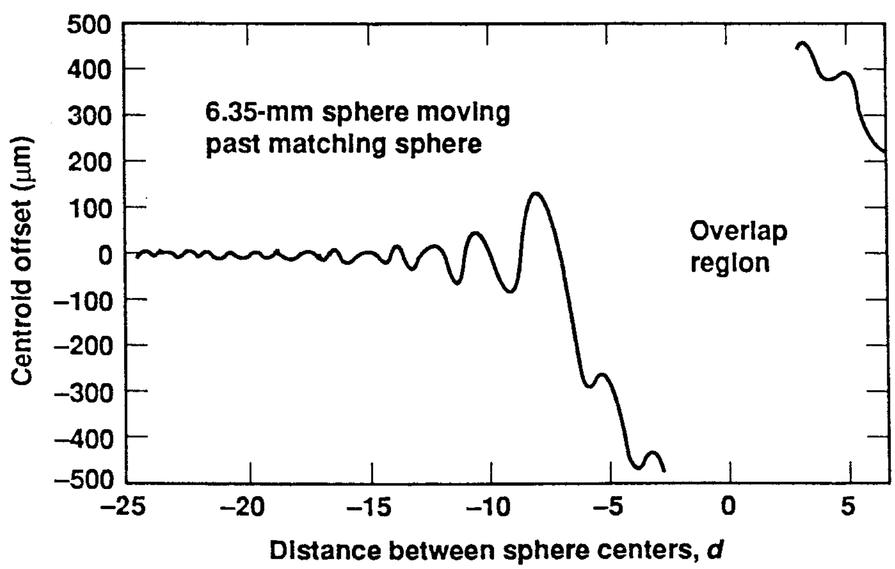

Figure 7. The center of a Poisson spot will move in an oscillatory manner as another sphere is moved toward the sphere creating the Poisson spot.

of the stationary sphere is on a calibrated stage that moves parallel to the moving sphere.

Two spheres were placed on the inlet window of the vacuum pipe as shown in the experimental setup (Fig. 8). A third sphere was attached to a ring on a calibrated stage. This third sphere, or probe sphere, could be moved vertically past a stationary sphere on the inlet window. The Poisson spot of the stationary sphere was centered on a quad-cell at the far end of the vacuum pipe, 26.5 m away. As the moving sphere was moved toward, over, and beyond the stationary sphere, the quad-cell was moved to keep the Poisson spot centered. Figure 7 shows the necessary displacement of the quad-cell as a function of sphere separation. The diffraction rings from the moving sphere have little effect on the stationary (measurement) sphere when the center-to-center separation is greater than about 20 mm.

The control sphere on the inlet window created a Poisson spot on a quad-cell in the closed-loop control system. This sphere was placed far enough away from the probe sphere that the two Poisson spots would not significantly interact.

The FEL might require a 300-m SLR. Calculations based on the equations above show that, at 300 m, 25-mm-diam spheres separated by 50 mm would produce no more than 10 μm of disturbance (error) in the Poisson spot of an adjacent sphere.

In the experimental setup to verify Eq. (26), it would have been possible to support the spheres on a glass plate perpendicular to the laser beam. However, in an FEL, there might be sufficiently high radiation levels to darken the glass; therefore, the spheres were supported on thin (25 or 50 μm), taut wires. Figures 9(a) and (b) show the effects of moving a 25-μm and a 50-μm wire past a 6.35-mm sphere. Note that if the wire is more than about 10 mm from the edge of the sphere, the wire's movement has a reasonably small influence on the apparent position of the sphere's Poisson spot. More important, once the wire moved between the edges of the sphere, the wire effects were less than 5 μm for any of the wires we tested.

There are a number of ways to attach the spheres to the wire. Holes of 250 μm have been electron-discharge machined into the spheres, and the wires have been laser welded into the holes. This technique has the advantage that there is no cantilevered load on the wire, but the machining and laser welding are expensive. Another method that has worked well is to machine-off two parallel flat surfaces (as in Fig. 21). Now, the wires can be contact welded

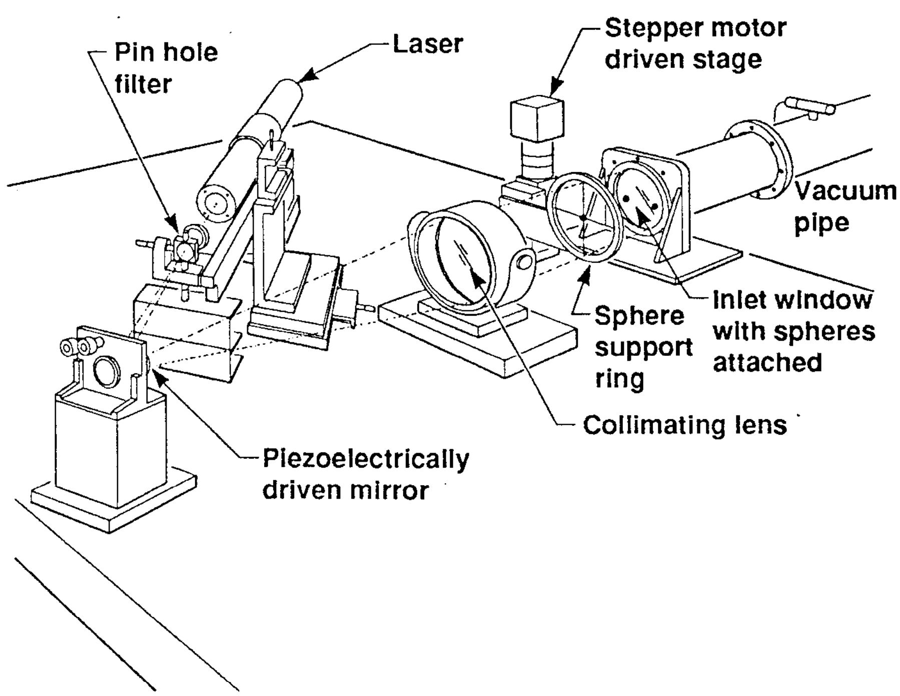

Figure 8. Experimental setup to measure diffraction interference effects.

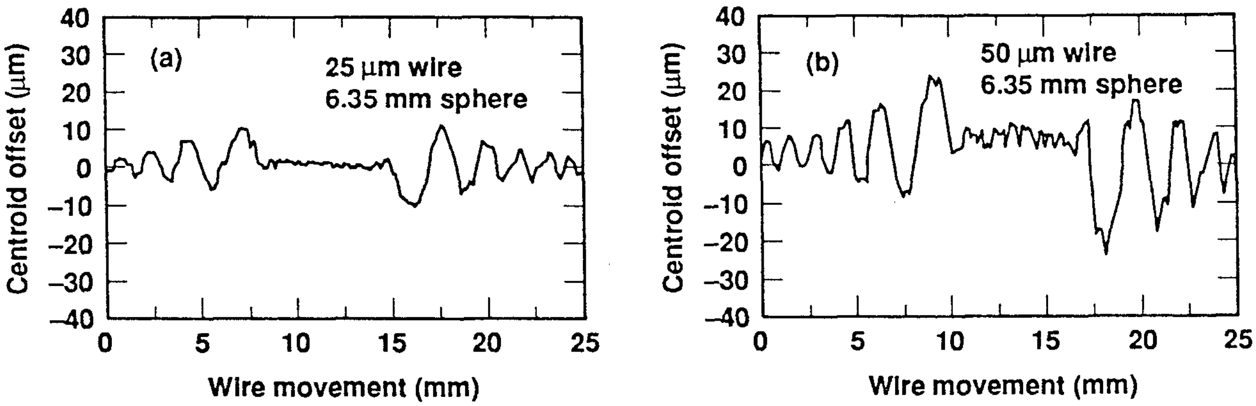

Figure 9. The alignment fiducials (spheres) can be supported on wires. Diffraction from wires of adjacent spheres will cause the Poisson spot of a given sphere to move in an oscillatory manner, as indicated by moving a wire past a 6.35-mm sphere and observing the movement of the Poisson spot at 26.5 m; (a) 25-μm wire and (b) 50-μm wire.

into place on one of the flat surfaces. Although there is clearly some movement on the wires, it has not resulted in vibrations that could be sensed on the quad-cells. Using a section of a sphere rather than a disk eliminates the need for tight tolerances on the pitch and yaw of the target support.

The Alignment Concept

To develop an understanding of how the Poisson spots can be used to align something, consider the following simplified case. Imagine that we want to align five magnets. For the moment, assume that we know exactly where the magnets are relative to a sphere that is attached to a perfectly transparent support. The laser beam and Poisson line in Fig. 10(a) will be the reference axis for the five magnets. The reference sphere and the center of the detector are the two fixed points necessary to define a straight line. Note that the laser beam can be translated in x and y, but not tilted, without changing the location of the Poisson spot on the detector. The fact that the laser beam can be translated emphasizes that the reference sphere and the quad-cell position detector are defining the line. By removing the reference sphere, we begin the alignment process by placing the sphere associated with the first magnet in the beam. As this sphere is moved up, down, and sideways in the beam, the Poisson spot it produces in the observation plane can be centered on the detector. The attachment of the sphere to the magnet must assure that the two move in unison and that there is no pitch or roll. Now, by holding the first magnet in place and removing the sphere, the next magnet [Fig. 10(b)] can be aligned by placing its sphere in the beam and moving it until the Poisson spot it produces is centered on the detector. This process can be repeated until all five magnets are aligned.

What would happen, in the example above, if the laser beam started to drift, i.e., tilt, during the alignment process? Typical alignment lasers have stability specifications of 10^{-5} to 10^{-4} rad/hr. The reference sphere would have to be reinserted to detect the problem. The alignment of some of the magnets would have to be rechecked to assure that they were not aligned while the beam was tilted, or alternatively the reference sphere could be inserted before and after each magnet was aligned. Only a small part (say 10 μm) of the total alignment budget can be allocated to beam pointing in an FEL alignment system. A 10-μm laser pointing error would occur every 12 s (at 300 m) if the beam drifted at a linear rate of 10^{-5} rad/hr. However, laser drift can

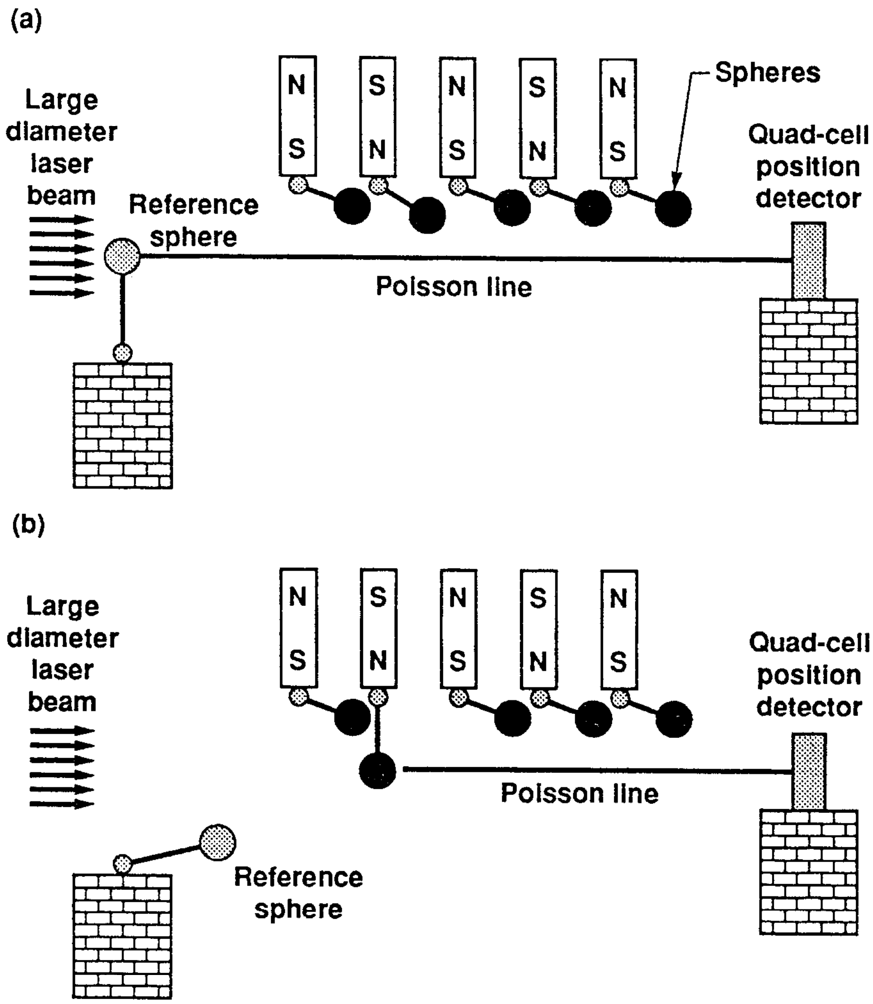

Figure 10. Magnets can be aligned by aligning the spherical fiducials, which are much more readily identified than magnetic centerlines; (a) establish a reference line and (b) move magnets so their fiducials fall on the reference line.

be more than adequately controlled with a closed loop feedback system if the reference sphere can be left in place.

Simultaneous alignment of many points in the FEL and continuous monitoring of beam pointing are essential because of ground motions and vibrations. Ground motion can be expected in response to a changing water table, post construction settling, nearby construction, and ground faults. Vibrations cover a frequency spectrum from thousandths of Hertz to thousands of Hertz. Earth tides, with a period of 94 min, are as much as 300 mm in amplitude,[19] but the long wavelength results in negligible bending over the length of an FEL. Settling of the building and seismic activity are of much greater concern. The SLAC has been observed to move several millimeters each year, and typical construction practices indicate an expected settling of as much as 50 mm/yr. Even if this settling occurred linearly in time, the FEL would need to be realigned every 2–4 hrs. However, the difficulties that ground motion introduces for alignment are overwhelmed by the transient effects of internal heating during operation of the FEL. Internal heating is expected to necessitate realignment of the entire FEL every 10 seconds.

The alignment laser is particularly sensitive to vibrations since its pointing needs to be controlled to about 20 nrad. The laser and collimator should be mounted on a table with a high level of internal damping. The collimator pointing system will actively damp vibrations below about 300 Hz (bandwidths over 1000 Hz should be possible). The high bandwidth of the active control loop is largely due to the low moment of inertia of the beam-directing mirror, schematically illustrated in Fig. 11. Fractional gain in the pointing resolution of the piezoelectrically driven mirror mount is achieved by adjusting the separation between the mirror and the pin hole. If the resolution of the mirror mount is θ_m, then the beam pointing resolution for small angles is[20]

$$\theta_p = 2L\theta_m/f , \quad (34)$$

where L is the distance from the pin hole to the mirror and f is the focal length of the collimating lens.

The reference sphere is to be kept in place at all times with a large-diameter laser beam. With some ingenuity, the spheres associated with all the magnets could also be in the beam simultaneously. Leaving the spheres in place would eliminate several problems including, but not limited to, the repositioning error for the target inserter, high cost and poor reliability of the sphere insertion and retraction mechanism, and the low speed with which the magnets could be aligned or checked for alignment.

The reference sphere and all the other spheres can be in a single, large-diameter laser beam if an array of detectors is used as the second fixed point in defining a straight line. Each detector in the array would be given a specific x–y coordinate, and the sphere associated with each magnet would be offset to correspond with a particular detector, as shown in Fig. 12. Errors due to divergence of a large-diameter beam can be shown to be negligible. The radius of a beam is[16]

$$w(z) = w_o\,[1 + (z/z_R)^2]^{0.5} , \quad (35)$$

where w_o is the waist radius at $z = 0$ and z_R is the Rayleigh range

$$z_R = \pi w_o^2/\lambda . \quad (36)$$

In a large diameter diverging laser beam, a point that is a_o off axis at $z = 0$ will move further off axis. At some distance z, this would produce an error

$$a(z) - a_o = a_o\,\{[1 + (z/z_R)^2]^{0.5} - 1\} . \quad (37)$$

The Rayleigh range, z_R, of a 0.4-m-diam helium-neon laser beam is 198 km; thus the term $\{[1 + (z/z_R)^2]^{0.5} - 1\}$ is 1.1×10^{-6} at $z = 300$ m. Since the maximum a_o in this beam is 0.2 m, the error due to divergence is less than 2.3×10^{-7} m for any sphere in the beam.

Several detector arrays can be made identically by calibrating each against a quasi-Hartmann plate. This Hartmann plate will be made from a glass plate with an array of spheres attached to one surface. The centers of the spheres will be arranged to match the desired array spacing. The size of the sphere will vary so that when the array is placed perpendicular to a laser beam, the resulting Poisson spots will match the Poisson spots of spheres distributed along a 300-m SLR.

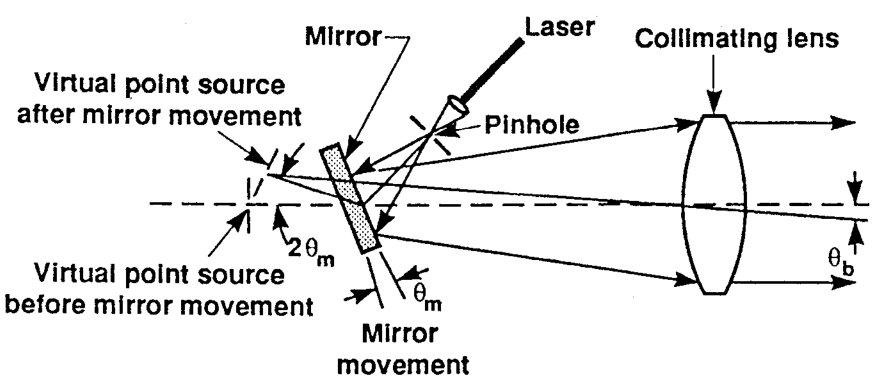

Figure 11. The folded collimator provides fractional gain in the beam-pointing resolution of the mirror mount.

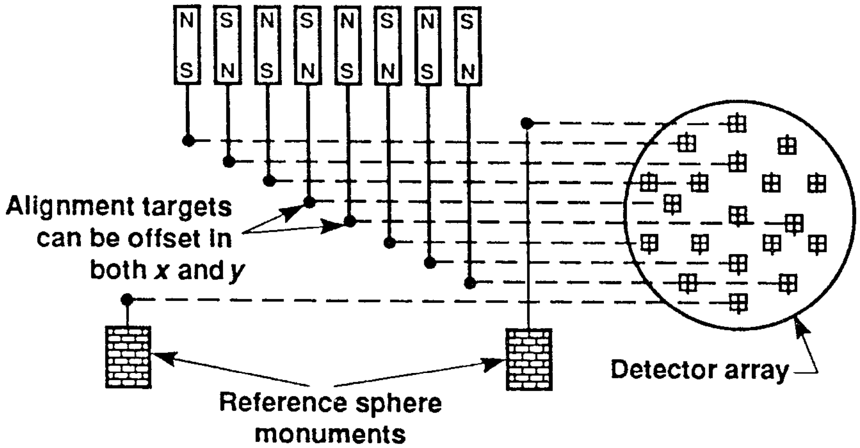

Figure 12. Many points along a magnetic axis can be monitored for alignment simultaneously by offsetting the targets in a large-diameter laser beam.

ALIGNMENT AND VIBRATION ISSUES IN TeV LINEAR COLLIDER DESIGN

G. E. FISCHER

Stanford Linear Accelerator Center
Stanford University, Stanford, CA

Abstract The next generation of linear colliders will require alignment accuracies and stabilities of component placement at least one, perhaps two, orders of magnitude better than can be achieved by the conventional methods and procedures in practice today. The magnitudes of these component-placement tolerances for current designs of various linear collider subsystems are tabulated. In the micron range, long-term ground motion is sufficiently rapid that on-line reference and mechanical correction systems are called for. Some recent experiences with the upgraded SLAC laser alignment systems and examples of some conceivable solutions for the future are described. The so called "girder" problem is discussed in the light of ambient and vibratory disturbances. The importance of the quality of the underlying geology is stressed. The necessity and limitations of particle-beam-derived placement information are mentioned.

INTRODUCTION

The surface of Mother Earth, on which we wish to build well aligned accelerators, is not *Terra Firma* but is constantly in motion. The purpose of this talk is to review some facets of this motion, to examine whether they present fundamental limitations and to estimate whether the problems encountered can be solved by sound engineering in the foreseeable future. I submit that, in the case of the next linear collider, the answer to this question is "Yes," but it will take a good deal of effort and money.

The earth is a glob of material held together by its own gravitation and subject to a variety of internal and external forces. Portions of its interior are thought to be liquid (will not support shear waves), and its relatively thin, elastic, wrinkled and, in places, broken crust swims around on an outer mantle that can hardly be called an engineering material. Peoples who live along the Pacific rim have become quite used to this concept, but I nevertheless thought you might be interested to know that Japan and California, separated by almost one billion centimeters, are approaching each other at the rate of between 2 and 5 cm/year depending on where and how this measurement is made[1]. I might add that California is drifting away from Europe at a similar rate.

⋆ Work supported by Department of Energy contract DE–AC03–76SF00515

About ten years ago, when we first began to think about the bizarre world of ground motion in relation to the construction of linear colliders, we became alarmed about motion in the frequency band ≈ 0.1 to 50 Hz. The reasons for concern in specifically this domain were (a) that high frequency jitter appeared to present difficult engineering problems and (b) that disturbances at slower rates, that is with wavelengths greater than site dimensions, would move the machine monolithically causing no relative motions between focussing elements and hence produce no deleterious orbit distortions. In the intervening years we have learned to live with microseismic disturbances. For example: The magnitudes and signatures of natural and man-made sources were identified[2]. From such considerations project site tolerance recommendations could be made[3]. Common sense solutions to local groundnoise abatement followed. Great strides were made in the understanding of how circular machines react to random plane wave excitation through the extension of the pioneering work of Aniel and Laclare[4] and by Rossbach[5]. The importance of resonances in magnet supports was quantified by Chou[6] and more recently by Rossbach[7]. Vibration isolation of final focus elements by means similar to those used by workers in Gravitational Wave detection was discussed by Ash[8], and recently we have heard of the Active Alignment System at KEK[9] and of the commercial vibration isolation system "TACMI"[10]. For such reasons and the fact that the general level of consciousness regarding vibration problems has been raised, I wish to turn to another region of the motion spectrum: — namely *slow drift.* We will see that in the world of micron-level alignment, these problems can become pernicious.

COMPONENT PLACEMENT TOLERANCES

In this section we will attempt to define the general level of alignment tolerances likely to be found in various linear collider concepts, designs and subsystems. I say it this way because tolerance setting is an unpopular and odious task — very often an ongoing debate between the desired and the achievable that may still be carried on even after the collider is in operation when effects, not dreamed of at conception, rear their ugly heads. All values listed in the table below were kindly provided with this caveat in mind and are meant, at this time, to be only *guidelines* to workers developing alignment techniques.

I should now try to explain what I mean when one says "alignment tolerance". There has been some confusion about this term. I hope you will bear with me for the following, somewhat pedantic, definitions.

Quite often simple calculations or computer simulations are performed in which the effects of offsetting any single element from its correct "on-axis " position are measured in terms of, say, a 10% loss of luminosity. Since making luminosity is the purpose of a collider, this seems like a not unreasonable way to proceed and immediately gives the relative sensitivities of element placement. For reasons that will become clearer later, let me call such displacements *incoherent jitter tolerances.* There are, however, at least two serious conceptual flaws with this method. No account is taken of the facts that in a *real* machine (a) all elements (not just one at a time) are out of place simultaneously, and (b) elaborate orbit and tune correction systems are applied to recover the lost luminosity. Permissible alignment errors (either systematic or random) under these more realistic assumptions are much harder to estimate because they require an understanding of all conceivable interactive effects that go into a simulation and a detailed scenario of tuning and correcting. Let us define *survey and alignment tolerances* to be those values of placement error which, if exceeded, lead to a machine that is *uncorrectable* — with its unacceptable loss of luminosity. In recent years, experience with higher order optical systems has shown that alignment tolerances derived in this manner tend to be about an order of magnitude looser than those derived for one component at a time. The reason for choosing the name jitter is now more apparent. Jitter tolerances are the magnitudes of errors that are *NOT* amenable to compensation by either static or dynamic (including BNS) methods. To recapitulate: It is the loosest survey errors that we are now looking for, not those tolerances associated with keeping an already operating machine running at peak luminosity.

TABLE I. Estimated Transverse Component Survey and Alignment Tolerance (μm) ⋆

System\ Project	CLIC$^\diamond$(CERN)	VLEPP† (USSR)	JLC‡(KEK)	TLC$^\heartsuit$(SLAC)
Injector Accelerator:			200	standard
Damping Rings:				
Quads (Horiz.)			100	100
Quads (Vert.)			50	30
Compressor #1:			50	?
Intermediate Linac:				
R.F.Structure			50	
Magnetic Foc.(H)			50	
Magnetic Foc.(V)			50	
Compressor #2:			50	?
Main Linac:				
R.F.Structure	10	.3*	50	10 - 50
Magnetic Foc.(H)	1.7	.03*	10	100
Magnetic Foc.(V)	1.0	.03*	10	20
Final Focus Elements (V)			5	10
Final Focus Elements (H)			5	30
Final Lenses (V)			5	2nm*
Final Lenses (H)			5	200nm*
Beam Analysis before dump			5	?

$\star$ 1 σ value of the population unless otherwise indicated, jitter values are denoted with an * . $^{\diamond}$ Provided by H.Henke. † Provided by V.Balakin, for a bunch population of 2×10^{11}. ‡ Provided by K.Takata, Values are tentative and are meant to be maximum deviation from central orbit. $^{\heartsuit}$ Provided by R.Ruth.

In the above table, distinction is drawn between the linac's RF structure and its Magnetic lattice elements; both of which may focus and steer. Further, for those groups who engage in asymmetric beams, vertical and horizontal tolerances may be substantially different. This is of import for those wishing to align, since techniques in these planes may be quite different. Finally, there is clearly something very special about the final lenses.

REFERENCE SYSTEMS

An examination of periodic realignment records of several large accelerators [Linac, PEP (SLAC), PS, SPS (CERN) and others] shows that, on the average, tunnel floor motion is at least about 50μ per 6 month interval. Much higher rates are seen in certain well known locations which are associated with the trauma inflicted on the ground by construction activity resulting in rebound, recompaction etc.. Ground water levels, varying with rainfall, have been shown to cause both vertical and horizontal tunnel displacements[11,12]. We see therefore that in the micron world, the rate of drift, albeit slow compared to conventional vibratory motion, is faster than can be corrected by conventional survey and realignment. We need servo-realignment, and for this we need reference systems more or less independent of the earth! Four such systems are listed below.

The Large Rectangular Fresnel Lens System [13] The principle of this system is shown in Figure 1. Divergent laser light is made to impinge on lenses which are inserted into an optical path one by one, and the relative displacements of their images is measured at the far end. The resolution of such a system depends on three terms: (1) the size of the diffraction limited images, $w \approx \lambda s/D$, in which D is the effective width of a lens, (2) the ability of a scanner to locate the centroid of an image, and (3) the optical lever arm $(r + s)/r$. A 3 km long system of this kind has been used to keep the SLAC linac aligned for 20 years. With $\lambda = 628$ nm, $D \approx 30cm$ and centroid discrimination $w/100$, the resolution at midspan (the most difficult region) is about 25 microns. Systematic errors can creep into the results from (a) constructional asymmetries in lens etching, (b) nonuniform illumination or improper masking and (c) most seriously in the transfer of lens coordinates to those of the accelerating guide. Overdesigned for its originally intended use, it can nevertheless be improved in the future. Already the scanner has been replaced with a CCD-based camera whose output is digitized and can be processed with all the mathematical armament of image enhancement. One can imagine also shortening the wavelength and/or increasing the diameter of the lenses. The chief conceptual advantage is the following: A perfectly straight line (neglecting general relativity) is established by the classical method of path differences (interfering wavefronts in this case) without resorting to extreme laser pointing requirements. The chief disadvantage is having to insert targets mechanically, a process which is time consuming and prone to mechanical problems.

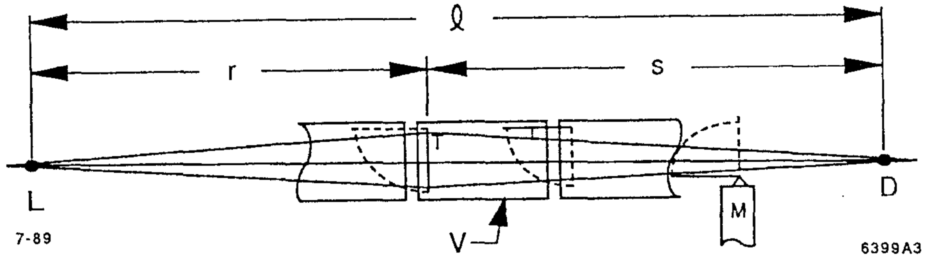

Fig. 1. Schematic illustration of the SLAC alignment system. T is one of 294 rectangular Fresnel lenses which focus laser light L to an image at the detector D. V is one of 60-cm diam. vacuum pipes, each 12 meters long which also serve to support the accelerator

We propose to exploit the optical lever arm of the SLAC Beam Switchyard laser alignment system[14] to align the Final Focus Test Beam[15],[16] with resolutions in the 1 to 10 micron range. One nice thing about linear colliders is that they are linear, or very nearly so.

The Poisson Alignment Reference System [17] This novel system, which was conceived to align a free electron laser, illuminates spheres with plane waves whose diffraction- limited shadows are cast onto the observation plane as shown in Figure 2. The location of the "Poisson spots" ie. the bright center of the diffraction patterns, is determined by four-sectored detectors. Since the incident beam of collimated light has a large diameter, many spheres can be illuminated and detected simultaneously, provided they are sufficiently far apart so that the resulting patterns are still interpretable. Based on results from a 26.5 meter long prototype exhibiting submicron resolution, simulations indicate that $\approx 2\mu$ should be possible at 300 meters. Its chief advantage is readout of many sheres at kHz rates. Its disadvantages are that only a limited number of spheres may be used in a given pipe diameter and that since pointing accuracies of order 20 nrad are required, it is sensitive to ground vibration. That such pointing accuracies have been achieved today attests to the skill of the proponents and miracles of modern piezoelectric technology and opens the way for other schemes that depend on highly accurate laser steering.

The Egyptian Method Drawing a straight line by means of a stretched string must predate Pythagoras, but I havn't been able to find the reference. This method has been used with success at CERN[18] and other laboratories[19] but was limited to about the 50 μ level due to air currents. Its length is ultimately limited by the strength of

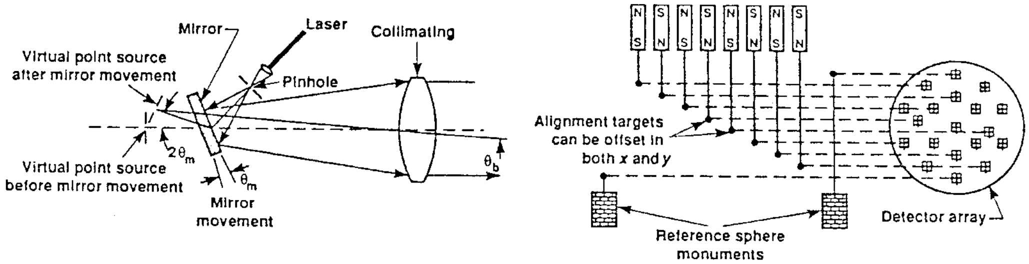

Fig. 2. Schematic of the Poisson Alignment Reference System

the string (kevlar), although proposals years ago[20] suggested this limitation could be overcome by intermediate supports floating on liquids. Updating this method with modern proximity sensors and with the wire inside a vacuum tube seems like an opportunity that should not go unexplored for intermediate length linac straightness testing.

The Archimedes Method (Hydrostatic Levels) The history of "height difference" measurement is also long and continues to be an exciting one in the fields of precision alignment and in crustal deformation[21,22]. Water levels have been used to align the PEP storage ring[23] (100 μ rms), and are proposed for use at the European Synchrotron Light Source with about one order of magnitude better performance [24]. At SLAC we are trying to develop a mercury liquid transfer level in connection with the Final Focus Test Beam that we hope will have micron accuracy over limited distances. Limited distances because, not only is the world not flat, its geoid (local equipotential surface) is not smooth; rather it is distorted by static gravity anomalies such as mountains and oil deposits. Worse yet, it is time dependent!

THE EFFECTS OF EARTH TIDES [25]

It was pointed out by Lord Kelvin in 1876 that the varying gravitational potential exerted by the moon and sun on the earth should cause radial excursions of a non-rigid earth. By comparing long-period ocean tides (monthly and semimonthly) with theory, G.H.Darwin concluded in 1883 that the earth's crust is rising and falling with amplitudes approximately 1/3 that of the oceans that cover it. One can see that semidiurnal and diurnal effects can occur because the declinational plane of the moon is not earth equatorial. Nor are orbits circular. A hundred years of observation by scientists in every country have yielded a very rich spectroscopy of planetary motions (at least 10 dominant and 19 periods of lesser amplitude). Although 'table top' experiments exploiting this effect can yield interesting information regarding the constituency of our globe, what concerns us here is that all aspects of geodesy and precision alignment are affected.

Leveling The concept *"horizontal"* begins to loose its meaning. Theoretically the direction of gravity may swing up to 1/4 μradian and in practice many times this amount due to ocean or atmospheric loading (Fig.3)[26]. One need not add that one micron displacement at one meter — the kind of dimensions we are concerned about here — is one microradian. Moreover the NS and EW tilts are not likely to be the same in either magnitude or phase.

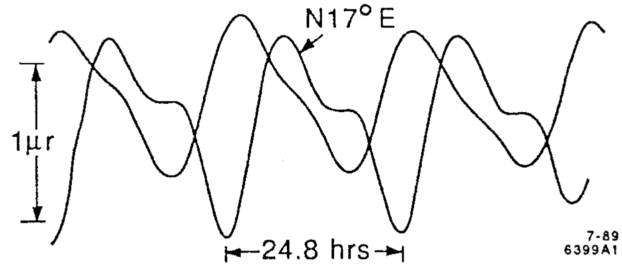

Fig. 3. A 100 hour record segment of two orthogonal tilt components showing their amplitude and phase. (Taken in a gun gallery at the San Francisco Presidio in 1969, Ref.25)

Strain[27] It is not hard to imagine that if the earth undergoes radial strain, the other five components of the strain *tensor* will manifest themselves as well. Typical values are $\Delta L/L \approx 10^{-8}$. Such variations, usually measured interferometrically or by means of stretched wire extensometers, are somewhat beyond our current interest. But one day, data from the 55 km baseline between Tsukuba and Kashima will have to be corrected for this effect!

Variations in the magnitude of "g" All devices that are affected by gravity will experience periodic change. On the rising and falling surface of the earth the fractional variations of "g" are of order 2.5×10^{-7}. Probably the most important effect is on the orbits of satellites with which precision laser ranging is carried out in establishing baselines. Very sophisticated programs are employed to take care of this effect but the concept of *mean height above sea level* might have to be replaced by *mean height above the center of mass of the earth* .

What does all this have to do with the practical aspects of aligning a large future accelerator? Quite simply, precision measurements require reference systems independent of mother earth. Further, since mother earth is used to support the accelerator, we should not be surprised that measurements and correction contain less noise if they are carried out by a data acquisition system on time scales small compared to the shortest period of the moon. Since planetary motion is after all a rather predictable sport, should not all this be calculable? Yes, if it were not for the weather. We note that another time scale, that of the rising of the sun, turns out to be just as, if not more, important. In California, the onset of light brings on rapid air temperature rises.

THE GIRDER PROBLEM

It is now time to get down to earth regarding accelerator supports. The issue that needs to be addressed is: "What style of fabrication and installation are the proponents of the next linear collider going to adopt?" I will assume that the issue of the need for a reference system and mechanical movers to bring the machine back into alignment will be further debated and then settled[28]. Investigations on kinematic mounts, computer controlled movers and readbacks having micron accuracies are currently underway at CERN[29]. The question can be rephrased: "What is the function of a linac support *girder* and what is its optimum length?" Let us examine two cases.

1. No girder at all: In this case all the accelerating waveguide sections and their associated fittings lie directly on a shelf which is part of the tunnel structure. The consequences of such a style are (a) each section must have its own expensive mover and connection to the reference, (b) since the whole machine is assembled in the field, testing it for mechanical and electrical integrity becomes more difficult and (c) testing it with beam becomes a logistical horror.

2. A very long, perfectly rigid and aligned support member: This object provides for assembly, alignment and pretesting (even with beam) of long accelerator modules in the controlled environment the factory-laboratory. Position correction movers are provided only at its ends because the object maintains its perfect shape even when transported to and installed in the tunnel. Somehow, it has no resonant vibratory modes. I believe the strength of materials prevents the existence of such a member.

Perhaps we should separate the alignment and transportation requirements by suggesting that a light flexible girder, whose sole purpose is to hold the ends of components relative to each other, be placed on beds that permit fast realignment. This light girder is transported with the aid of a removable strongback. Fast sectional realignment is carried out in the lab with very long precision coordinate measurement machines and in the tunnel with portable secondary reference gadgets such as automated strung wires and levels. But what should the mattress beds be made of? Steel rails are probably wrong because they are terribly prone to distortion through thermal gradients. Traditional optical benches are made of massive granite for thermal and mechanical stability, but their internal ability to absorb vibration is poor. More modern tables are made using a honeycomb structure[30]. The high precision machine tool industry has resorted to polymer composites[31] which have good strength, vibration absorption, thermal mass, dimensional stability and can be relatively inexpensively cast with high order flatness and surface finish. To stimulate innovative engineering solutions, let me make a somewhat outrageous suggestion. Amateur holographers, who cannot afford expensive apparatus, successfully mount the optical components of their artistic creations on stakes stuck in large boxes filled with sand which are in turn supported by under-inflated automobile tire inner tubes. Should science imitate art? Surely nature and man have provided enough of these materials to construct 20 km of collider.

THE IMPORTANCE OF THE UNDERLYING SITE GEOLOGY

It has been pointed out before that the geology of the chosen site will have great bearing on the cost of tunneling. Good ground properties[32] probably also result in more economic solutions than having to mitigate the drift and vibration effects of a bad site. The ideal site would be well removed from man-made disturbances, have a water table well below the tunnel, have a uniform, homogeneous, competent material that can nevertheless be easily mined with boring machinery. It is a pleasure to note that the Austin Chalk of Waxahachie, Texas appears to come close to fulfilling such a description. The unweathered material near the surface is said to have [33] compressional sound velocity of between 2.6 to 3 km/sec. The shear wave velocities range between 1.1 and 1.8 km/sec. Ng and Peterson[34] have calculated, among other things, the detailed response of the two colliding beams at the interaction point of the SSC due to noise sources on the surface. These calculations, when applied to estimating the effects of trains passing through the site, show that the results depend sensitively on the absorptive properties of the medium. While the chalk bedrock appears to have attenuation lengths, (in the sensitive betatron wavelength region), in the many tens of kilometers, train noise may be sufficiently absorbed in the unconsolidated overburden and reflected at the dirt/bedrock interface.

Deep (depth >15m) underground tunnels have some of the properties of a wine cellar, namely remarkable constancy of tunnel wall temperature. Surface-temperature-driven thermoelastic strains are therefore likely to remain small[35]. But since temperature changes, worse yet temperature gradients, are probably the single most important cause of misalignment[36], early consideration should be given to the thermal engineering of the tunnel and its contents if we do not wish to pollute the naturally occurring stable conditions. Two problems arise. Accelerating waveguide cooling water temperature stabilization systems generally run at temperatures higher than the highest cooling tower temperature which is likely much higher than that of the tunnel wall. Permitting warm moist summer air to enter a cool tunnel will cause not only misalignments, but fog and rain as well!

One object guaranteed to cause distortions of the final focus is a massive detector. Figure 4. depicts the time dependence of the motion of the final lenses of the SLC when the weight of the 1800 ton Mark II detector was rolled on line and the east shielding wall reconstructed[37]. The floor of the experimental hall pit (61 cm of heavily reinforced concrete) rests directly on the very stable grey, unweathered, well-cemented, tertiary miocene sandstone that permeates the SLAC site. The time constant of the total (plastic and elastic) rather small deformation (2mm) was of order 30 days.

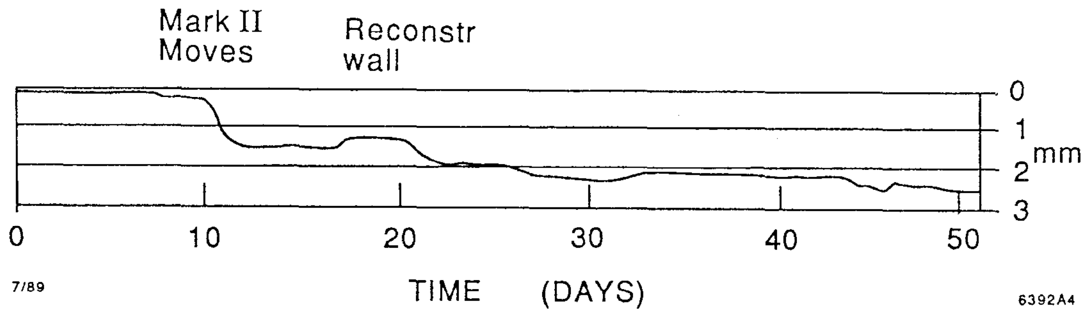

Fig. 4. Amplitude of Mark II detector settling on floor of SLC experimental pit. (Outboard levels are mounted in tunnels, inboard on piers in the pit supporting the final lenses.)

IMPORTANCE AND LIMITATIONS OF 'BEAM DERIVED' ALIGNMENT

At the very outset we have stipulated that we will allow relaxation of survey tolerances by about one order of magnitude over operational (ie. jitter) tolerances, provided that systems can be *tuned,* both on paper and in practice. This should help with the problem of systematic offsets in that, being under the influence of elements whose effective electric and magnetic centers do not *a priori* coincide with their surveyable mechanical centers, the final arbiter of where the beam wants to ride is, of course, the beam itself. In accelerating structures there have been the notorious effects of RF input couplers and the 'bookshelf' constructional errors; although for center finding of magnetic elements at the micron level there have fortunately been some recent advances using the singing wire technique[38]. In short we have always relied on the time honored fall back: – Feedback. Be it manual or automatic, fast or slow, we depend on the application of beam-derived intelligence to extricate us from the dilemma of not meeting tolerances.

But there are several traps we can fall into. The first of these is that the initial alignment must be good enough to get enough beam through to permit measurements to be made. Secondly, beam-position sensors too must have a certain modicum of electronic stability and immunity to beam spray to permit a meaningful analysis. (Under certain circumstances the absolute position of quads and BPM's is not required for a linac[39], provided the mathematical model of the machine[40] is adequate.) Thirdly, the proliferation of feedback systems will, if not held in check, lead to increasing inoperability since each system adds another layer of complexity. Sometimes, for example, downstream systems cannot begin to function if upstream systems are not tuned. To help in diagnosis, instrument and feedback stations should be located between sections of a collider that are functionally distinct. It is my unsubstantiated judgment that we should strive to do the very best we can, in both arenas, to make the future linear collider live up to its potential.

CONCLUSIONS

The Micron World, in which steel acts like butter and in which temperature excursions are like Gulliver's Travels, has been tamed and industrialized on the laboratory scale. I do not believe the problems that we are going to encounter in the design of future linear colliders on a kilometer scale will turn out to be *fundamental* . Rather, the challenge will be to be innovative enough to find sound engineering solutions that we can *afford* . Further, we should involve the alignment community in <u>all</u> aspects of the design decision making process at the earliest moment.

REFERENCES

1. For example, Kosuko Heki et al. at Kashima Space Research Center using data distributed by the NASA Crustal Dynamics Project, in IEEE Trans.Inst.Meas.Vol.38, No.2, April 1989
2. G.E.Fischer SLAC-PUB-3392 Rev.July 1985 and in A.I.P.Conf Series Report No 152 p.1260 1985
3. G.E.Fischer, P.L.Morton SLAC-PUB-3870 or SSC-55, Jan 1986
4. T.Aniel, I.Laclare, Saclay Report LNS/086 (1985)
5. J.Rossbach, DESY M-87-09 and Part.Acc.Vol.23, No 2 (1988)
6. W.Chou, Paper L-50 Part.Acc.Conf.Chicago March 1989
7. J.Rossbach, DESY 89-023 Feb 1989
8. W.Ash, SLAC-PUB-4782 and in DPF Summer Study Snowmass, June 1988
9. N.Ishihara et al. Presented at the First Int. Workshop on Acc.Align. SLAC July 31 1989
10. M.Naganoh et al. Takenaka Corporation, 5-14, 2-Chome, Minamisuna, Koto-Ku, Tokyo. Presented at the First Int. Workshop on Acc. Align. SLAC July 1989
11. J.Spranza, A.Nur, Jour. Soil Mechanics and Foundations Div. ASCE, Vol. 97, No.SM12, Dec.1971, p.1623-1634
12. G.A.Voss (DESY), 1mm vertical per 1meter of water table change - private communication.
13. W.B.Herrmannsfeldt et al., Applied Optics Vol.7, page 996, June 1968
14. W.B.Herrmannsfeldt et al., IEEE Trans. Nucl. Sci. NS-14.No.3 p.903-7,(1967)
15. K.Oide, SLAC-PUB 4953 and Presented at the Part.Acc.Conf. Chicago, March 1989
16. G.E.Fischer, R.Ruland SLAC-TN-89-02 and at the First Int. Workshop on Accelerator Alignment SLAC July 1989
17. L.V.Griffith et al. Lawrence Livermore Nat. Lab. Report UCID-21591 January 1989
18. W.Coosemans, CERN Accelerator School Proceedings, CERN 87-01 Feb 1987
19. W.Davies-White, SLAC-TN-65-070 and W.K.H. Panofsky, W.Marshall U.S.Patent No.3470460 Sept.1969
20. R.Sandkuhle, SLAC-TN-61-1 (1961) and private communication.
21. for an extensive review see K.Hurst, R.Bilham, Jour. of Geophysical Research Vol.91, No.B9 p.9202-9216 Aug. 1986
22. P.Baldi, M.Unguendoli, CERN Accelerator School, CERN 87-01 p.291 Feb 1987

23. T.Lauritzen and R.Sah, IEEE Trans.Nucl.Sci.Vol. NS-28 No.3, June 1981

24. D.Roux, ESRF Reports Alge 88.04, 88.06 Grenoble Nov.1988

25. For a comprehensive treatment of all aspects and containing over 2000 references see: "The Tides of the planet Earth" P.Melchior, 2nd Edition Pergammon Press Ltd. 1982

26. M.D.Wood, Doctoral Thesis, Dept.of Geophysics, Stanford University May 1969

27. See, for example, the work of I.Ozawa from Geoph.Inst.Kyoto Univ. No.13 p 87-92 1975

28. Conclusions reached at both the Capri and SLAC workshops, indicate that anomalous dispersion in the linac lattice is to be avoided. This is best done by correcting the very element that is causing damage, rather than relying on auxiliary dipole correctors exclusively.

29. I.Wilson et al. CERN-LEP-RF/89-30 and Part. Acc. Conf. Chicago March 1989 and W.Coosemans, private communication June 1989

30. Newport Corporation, 18235 Mt.Baldy Circle, Fountain Valley, CA 92728 (714) 963-9811

31. Anocast, a division of Anorad Corp., 110 Oser Ave. Hauppauge, NY 11788 (516) 231-1990

32. See for example the effect of the depth of Molasse in G.Fischer and M.Mayoud LEP-RF-SU-88-07 March 1988 p.13 and in Proceedings of Workshop on Linear Colliders Capri June 1988. This report also contains an appendix outlining alignment system design considerations that have been gained from past experience.

33. D.Goss, SSC Central Design Group, SSC-N-635 May 1989

34. K.Y.Ng, J.Peterson Central Design Group Report No. SSC-212 March 1989

35. J.Harrison, K.Herbst, Geophysical Research Letters Vol.4 No.11 November 1977

36. "Microns,microns everywhere and all of them out of line" W.Davison, R.Ulich SPIE Vol 608 Optical Alignment III (1986)

37. Data and analysis provided by J.Ferrie, private communication March 1989.

38. G.E.Fischer, J.Cobb, D.Jensen SLAC TN-89-01 March 15 1989

39. C.Adolphsen et al., SLAC PUB 4902 and in IEEE Trans. Nucl. Sci. of Part.Acc. Conf. Chicago, March 1989

40. K. Thompson et al., SLAC PUB 4847 and Part. Acc. Conf. Chicago, March 1989

ACTIVE CONTROL MICROTREMOR ISOLATION SYSTEMS

MASATAKE NAGANOH, NOBUYOSHI MURAI, YOSHINORI TAKAHASHI,
KAZUYOSHI KATAYAMA, TSUNEHIRO TAMAKI

Takenaka Corporation
Tokyo, Japan

Recently, problems caused by microvibrations are increasing in advanced science and high technology industries. Therefore, the alignment of high precision equipment and the isolation of microvibrations are becoming important subjects in various areas.

To meet these demands, we at Takenaka Corporation have developed an epoch-making vibration system called TACMI (Takenaka Active Control Microtremor Isolation system), which is entirely different from conventional vibration isolation systems. TACMI is an ACTIVE vibration control system which can eliminate microtremors in a wide frequency range. Photos 1 and 2 are of the layout of the TACMI System.

Outline of the TACMI System:

The TACMI System consists of:

1. A highly efficient passive vibration isolation table supported by soft air springs,
2. highly sensitive vibration sensors which sense microvibrations of the table,
3. a digital servo-module which computes the optimal control force, and
4. actuators which effectively transmit the computed control force to the table.

The passive vibration isolation table of TACMI itself can compete with conventional vibration isolation tables on the market since its natural frequency is as low as 1 - 3 Hz. We further added to the table active vibration control equipment to bring about a highly efficient vibration isolation effect from low vibrations in the area of a few seconds to some tens of Hz.

The highly sensitive and wide dynamic range vibration sensor and the digital servo-module compute the optimal control force in a mili.sec. and operate the actuator immediately.

We have developed two types of systems using different actuators in consideration of the environment where the actuators could be installed, and each has the following features:

1. TACMI-1 uses linear motors and is designed to control a high frequency area.
2. TACMI-2 uses air actuators which have high driving power and is designed to have a large loading capacity, i.e. large and heavy machinery and tools.

TACMI System has a vibration control ability of six degrees of freedom (the x, y, z axes and their rotations as shown in Figure 2) and it can create a static position as if the table were floating.

With conventional passive vibration isolation systems, which use vibration transfer characteristics, you cannot expect the vibration isolation effect except for the area where the vibration range is higher than the natural frequency. (See Figure 3).

To enlarge the vibration isolation range, it is necessary to lower the natural frequency. However, there is a limit to this, because by lowering the natural frequency, the vibration isolation system itself may become unstable.

The passive vibration isolation system is effective in eliminating disturbances from the floor, but when a force works on the table directly, the force will cause a large vibration. For example, when you touch the table carelessly and add an impulsive force to the table, it will create free vibrations and the table will vibrate for a long period of time and it will lead to trouble.

TACMI, however, exerts control force against direct disturbances and makes the table return to the static state in a very short period of time (within 0.1 sec.). (Figure 4).

When disturbances are random vibrations in a wide frequency range, TACMI works to eliminate the vibrational amplification and it can lessen the microtremor to a further extent (from a few seconds to several tens of Hz.), while conventional passive vibration systems cannot avoid the vibrational amplification in the area of the natural frequency.

Ultimately, TACMI can lower the microtremor (about 1 gal., 1 μm) in a relatively good vibrational environment to lower than 1/10. (Figure 5).

Figure 6 shows an example of the transfer function on the table affected by floor vibration. You can see how free of vibration the table is.

Moreover, since TACMI is structured so as to not have a friction portion in the system, it can also meet the demands of the "clean environment" standard.

Either TACMI-1 or TACMI-2 can take about 1 ton of loading and therefore either system is good for practical use.

With regards to shape and loading capacity, we can satisfy various demands.

We have developed this system bearing in mind its application to future semiconductor industries, but we believe that it can be applied to accelerator alignment and other scientific areas also.

We are going to apply this system to the linear accelerator at KEK.

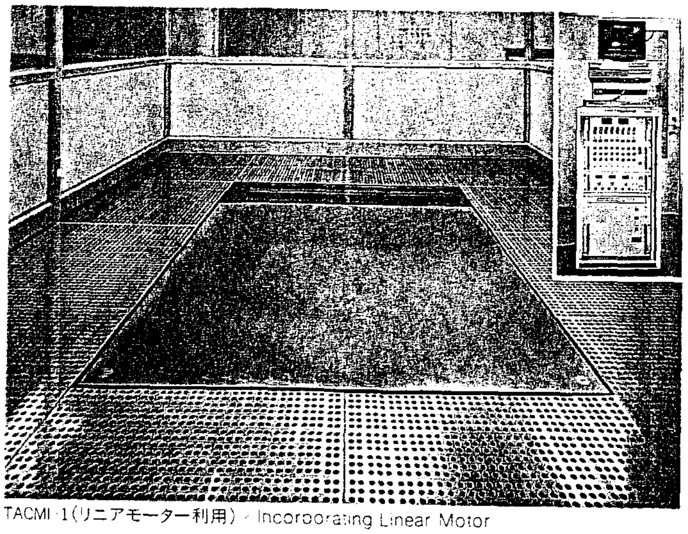

TACMI-1(リニアモーター利用) · Incorporating Linear Motor

PHOTO-1 TACMI-1:LINEAR MOTOR ACTUATOR TYPE

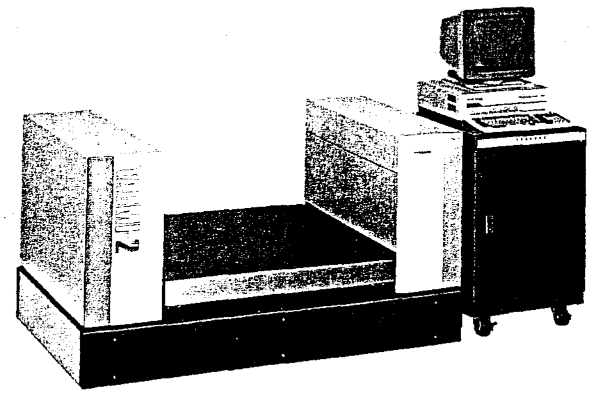

TACMI-2 (エアアクチュエータ利用) Incorporating Air Actuator

PHOTO-2 TACMI-2:AIR ACTUATOR TYPE

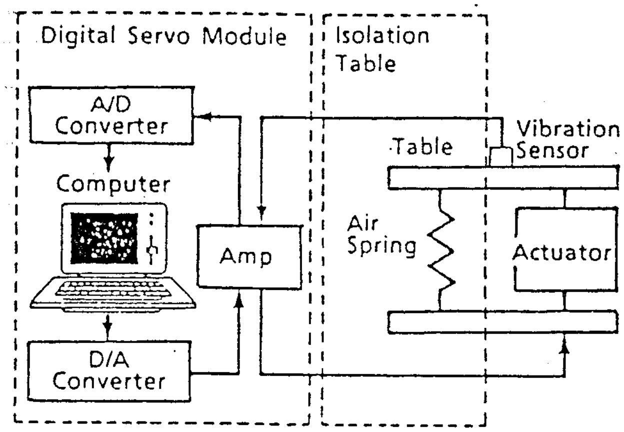

FIGURE-1 COMPOSITION of TACMI SYSTEM

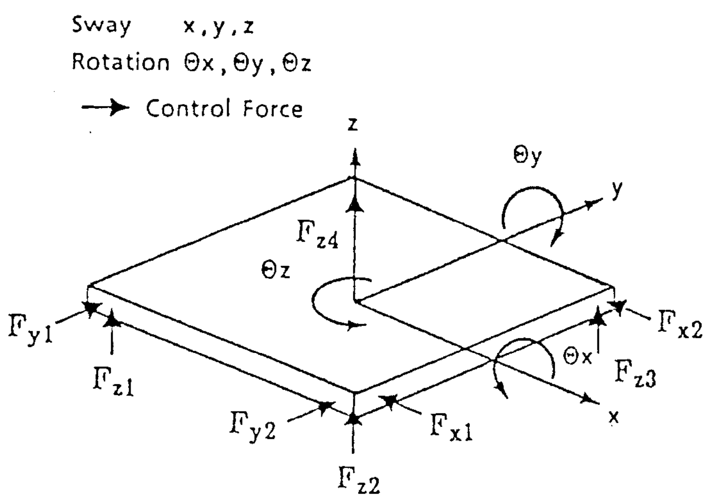

FIGURE-2 CO-ORDINATES of CONTROL FORCE

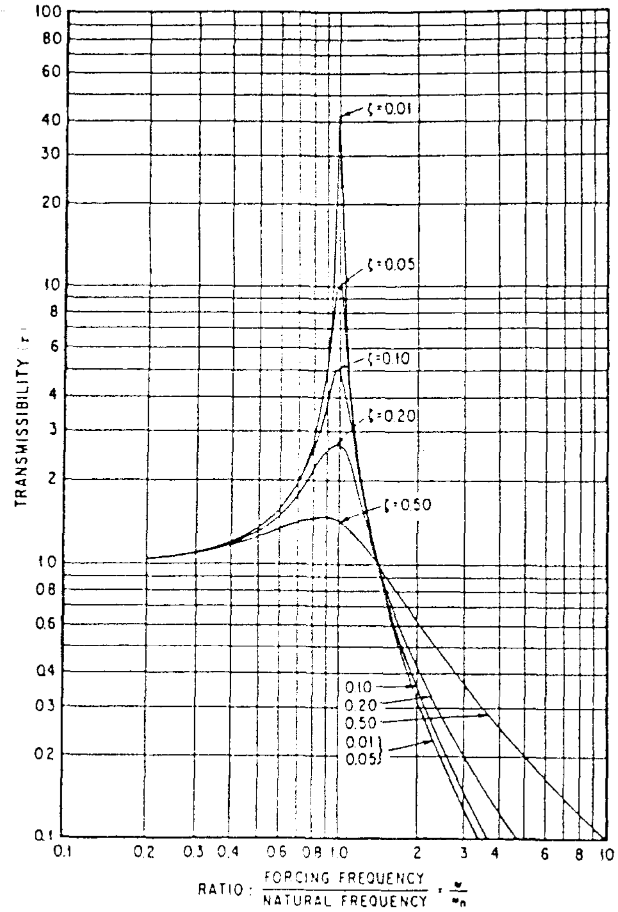

ζをパラメータとする伝達率曲線

FIGURE-3 TRANSFER FUNCTIONS of ONE MASS VIBRATION SYSTEM

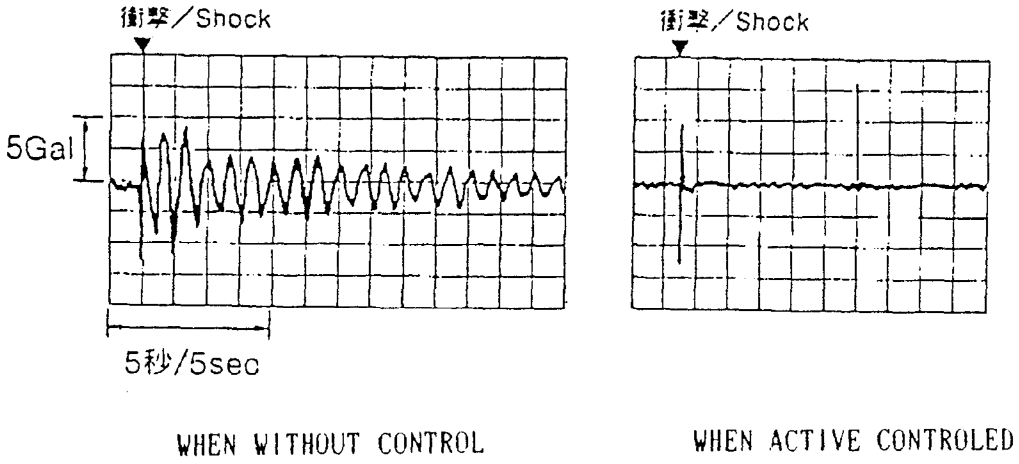

FIGURE-4 RESPONSE WAVEFORM of THE TABLE WHEN IMPULSIVE FORCE ADDED

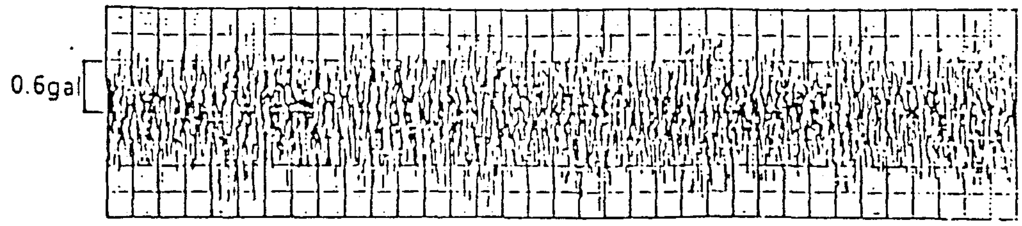

(a) ON THE FLOOR

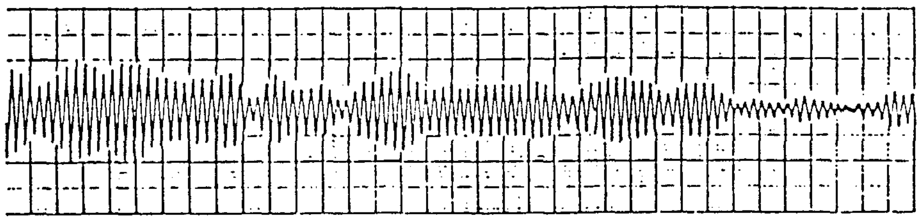

(b)CENTER of THE TABLE WHEN WITHOUT ACTIVE CONTROL

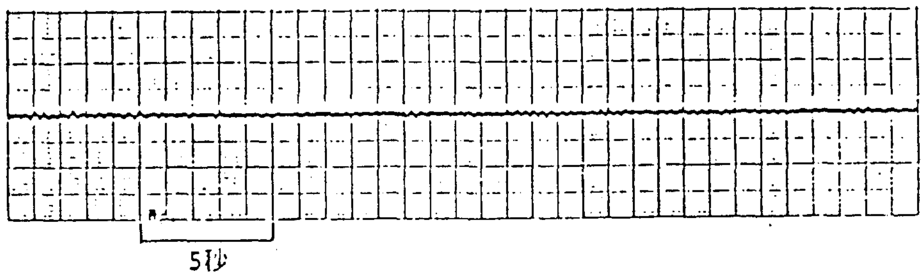

(c)CENTER of THE TABLE WHEN ACTIVE CONTROLED

FIGURE-5 COMPARISON WAVEFORM

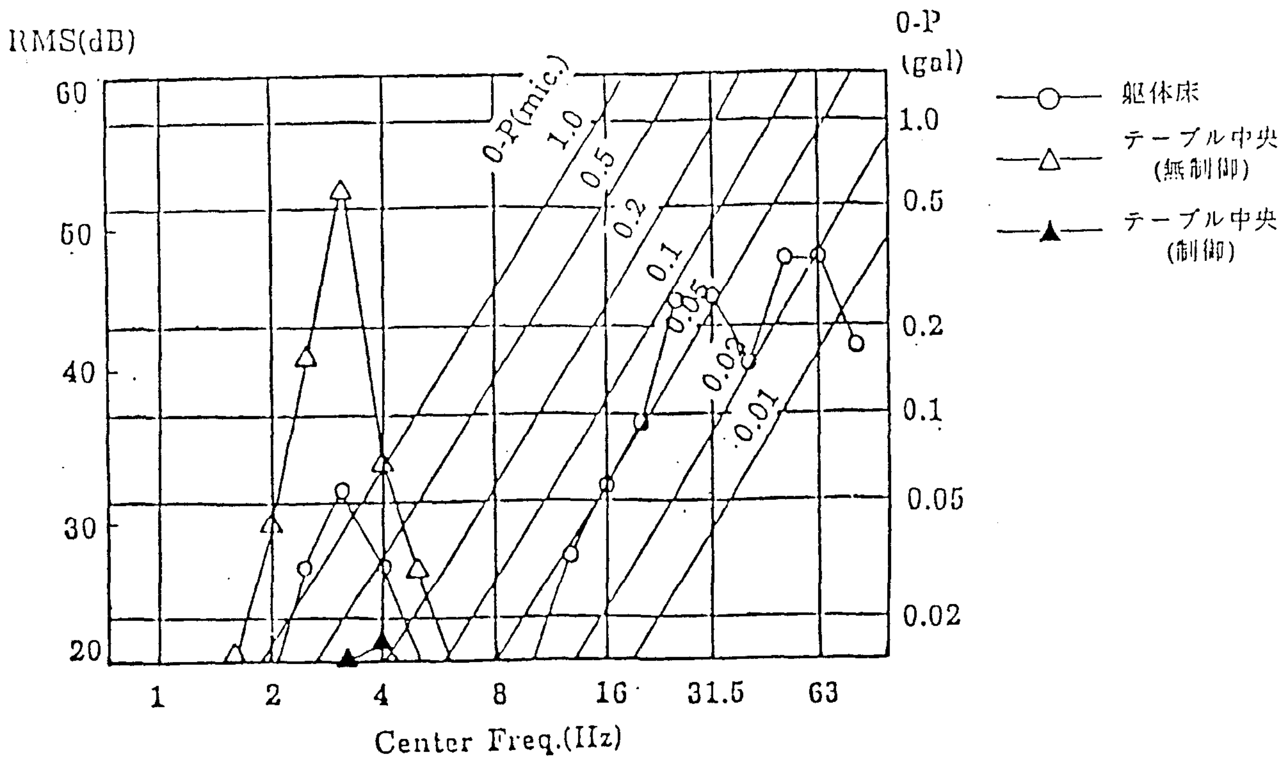

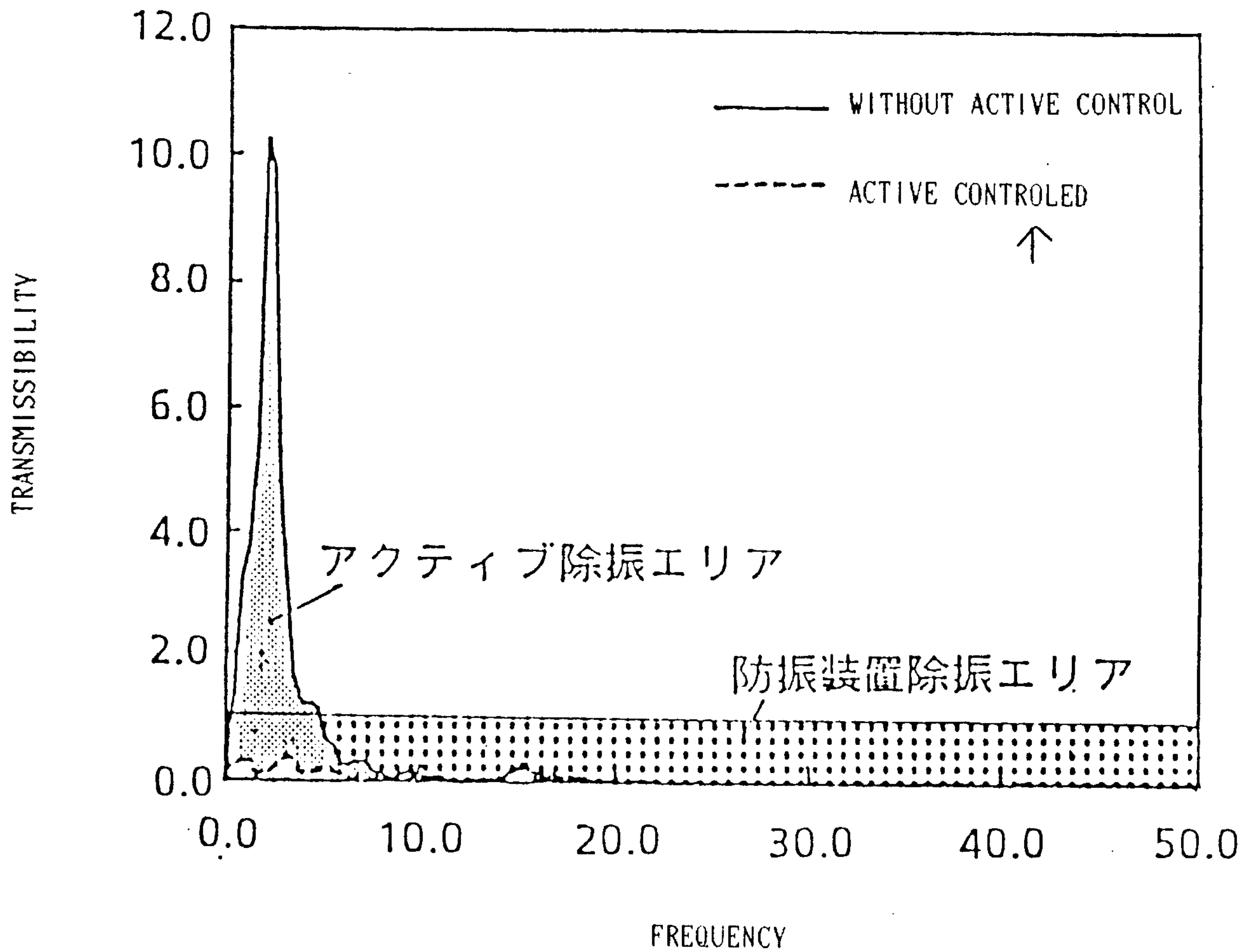

FIGURE-6 VIBRATIONAL TRANSFER CHARACTERISTICS of TACMI SYSTEM

FINAL FOCUS TEST BEAM ALIGNMENT
- - A DRAFT PROPOSAL –

G. E. Fischer, R. E. Ruland

Stanford Linear Accelerator Center

Stanford University, Stanford, CA.

1. Introduction

1.1. General Outline of the Final Focus Test Beam

In its present form, the Final Focus Test Beam (FFTB)[1] is a transport line designed to transmit 50 GeV electron beams of SLC emittance (3×10^{-10} radian-meters) straight through the central arm of the Beam Switchyard (BSY C line) with a final focus point out in the Research Yard but relatively near the end of the switchyard tunnel. The axis of the incident beam coincides with that of the SLAC linear accelerator; the final focus, some 300 meters downstream of the end of the accelerator, is displaced from this axis by about 2 meters horizontally.

1.2. Origin of General Alignment Specifications

Several optical designs for this transport system have been developed and studied by Oide[2]. So that the promise of extraordinarily small final focus spots ($\sigma_x \approx 3$ micrometers, $\sigma_y \approx 60$ nanometers) may be realized, focusing elements, (quadrupoles and sextupoles), should be placed on the design trajectory to absolute accuracies of order fractional to several microns in transverse position. These values, calculated for each element as if it alone were out of place, derive from the fact that off axis trajectories are subject the variations of phase advance and dispersion thereby causing growth of the spot's area at the final focus by a factor of $\sqrt{2}$. For reasons that will become more evident later, we will call these values *single element incoherent "jitter" tolerances.*

As early as the fall of 1988, J. J. Murray had taken one of the Oide proposed cases (FFTF34)[3] and analysed the effects of permitting much larger (perhaps surveyable) imperfections in the position and strength of all magnets and beam position monitors and found that the system was "correctable" without a "significant" (no more than say $\approx 30\%$) loss of performance (effective luminosity). Other cases (for example FFTB59) are currently under consideration and appear to exhibit similar sensitivity to imperfection. Further detailed work on "tuning the beam" was performed by Oide (Ref. 2) which showed that initial alignment errors could be as large as 30 μ in the vertical and 100 μ in the horizontal directions. We will use these values as a guide in the following discussion. Clearly, the better (ie. smaller) such "standard tolerances" achievable, the higher will be the probability of achieving the goals of this project with the minimum of tuning. For the moment we will define the range 5 to 10 micrometers in transverse displacement error as the "specification" for the "ab initio" tolerances for this alignment proposal. The much smaller stability values originally calculated by Oide, which we have called jitter[4] are "operational tolerances" which, if exceeded, call for operational orbit correcting and retuning of the beam.

1.3. Scope of this proposal

The hardware, methods and procedures outlined in this proposal are dedicated to measuring the placement of mechanical objects with respect to certain defined geometric axes. We wish to emphasize that the problems of locating (a) the effective magnetic axes of focusing elements, (b) the effective electrical center of beam position monitors and (c) even the effective axis of the incident beam relative to mechanical reference surfaces are treated elsewhere.[5] In the following we consider only the problem of measurement. The task of mechanical repositioning of elements on-line, although implied, is not yet addressed.

2. Concept

2.1. Outline of Method

The narrow forward geometry of the FFTB lends itself to the method of "survey by offsets". The main task is, therefore, the establishment of an absolutely straight line whose axis can be related to that of the linear accelerator, the agency which provides, presumably with little or no steering, the beam's input direction to the system.

Fortunately, the original planners of the SLAC BSY provided just such a straight line[6] which was used to layout the geometry of the energy defining slits in the A and B lines, as well as providing a C line reference. As will be shown later, with some reconfiguration and additions, the BSY laser alignment system should have adequate resolution and accuracy to serve as the primary reference line, independent of tunnel monuments that may shift with time or the effects of atmospheric refraction. Moreover, this laser based system can be used while the beam is in operation, thereby providing the means for on-line check on the straightness of the reference line and hence indirectly on the coordinates of components.

The steepest angle the beam trajectory makes with respect to the reference line is of order 20 milliradians. This means that offset measurements between the trajectory and the reference line must be made at "s" and "z" distances known to better than 0.1 millimeters if the error introduced in transverse measurements is to be kept less than 2 microns. For the long simple longitudinal distances of this problem, 0.1 mm accuracy can be reached using an "electronic distance meter" (Kern Mekometer ME5000) or with certain restrictions the interferometer calibrated "distinvar wire".[7]

Figure 1 depicts a crossection of the BSY C line tunnel taken at a point sufficiently downstream so that the FFTB trajectory has diverged from the laser reference line. We discuss, in following sections, the details of the components and their expected performance.

2.2. Placement Resolution of a BSY Laser Alignment Fresnel Lens.

The concept of the SLAC laser alignment system is depicted in Figures 2 and 3. The idea is disarmingly simple. If all lens centers lie along a perfectly straight line, all will focus the divergent light from the source onto the same spot in the far focal plane. If some lens is off a defined axis by an amount $\Delta x, y$, the focal spot is displaced by an amount

$$\Delta x', y' = \frac{(r+s)}{r} \times \Delta x, y \qquad (1)$$

in which "r" is the distance from the source to the lens and "s" is the distance from the lens to the focal plane. By making r small with respect to s very large optical levers can be effected.

The resolution in the measured $\Delta x', y'$ is also related to the size of the image. The diffraction limited full width at half maximum w of the central image is given as:[8]

$$w = \sqrt{5}/\pi \left(\frac{\lambda s}{D} \right) \qquad (2)$$

in which λ is the wavelength of the light (normally red light of wavelength 632.8 nanometers), and D is the effective diameter of the lens.

If we were to use the configuration of the *existing* BSY system, we note that the source is near the far eastern end of the BSY tunnel but the focal plane is at far western end of the accelerator located over two miles away. This arrangement has the advantages of sharing a common detector with the accelerator laser alignment system and high sensitivities due to large lever arms.

Inserting values typical of the BSY target coordinates, $r = 299'$, $s = 10,637'$, $D = 5.5"/12" = 0.46'$, we find a calculated width w of 10.5 mm.

Assuming for the moment that the detector is able to locate the center of the image to 1/100th of its size*, and applying the lever arm of Equation (1), the resolution to which the position of the lens can be located is: about 3 micrometers. Depending on axial target coordinate in the BSY, this value varies between 2 and 9 μ. Of course it should be realized that in order to use the presently existing BSY equipment for the new transport line, the existing lens holders and the laser station will need to be relocated. The foregoing was a sample calculation to show that resolutions consistent with requirements are achievable.

2.3. Repeatability of BSY Laser Target Insertion

The efficacy of the method depends on the ability of inserting BSY type lenses, one by one, with repeatabilities of position to better than the suggested resolution. Since it has been known for some time that some of the hinge mechanisms along the accelerator suffer from a lack of repeatabilty, a test was performed on a spare BSY lens actuator. This device (shown in Figure 4) was mounted within the working aperture of a large, three axis, coordinate measuring machine and exercised by hand. The results of many insertions demonstrate a repeatability in the vertical direction (radial with respect to the shaft roller bearing) with a full width of about 1.5 microns. The horizontal spread (in line with the axis of the hinge shaft) is about 7.5 microns but can most probably be improved by a addition of a spring. These tests do not prove that the other 20 or so units installed in the BSY will perform entirely satisfactorily, (tests will have to be performed), but lead one to the notion that they too can be used.

2.4. Coordinate transfer from center of Fresnel lens to new tooling outside the vacuum enclosure

Having established that lenses can be inserted into the laser line of sight in a repeatable way, the coordinates of the lens axes (See Figure 5) must be transferred to new reference tooling located outside the vacuum enclosure. The original tooling, a K & E mirrored target for x and z, and a tooling ball for the y coordinates were meant to be used in connection with the "standard optical alignment" methods employed 25 years ago. Such methods will not suffice for micron accuracies or permit the monitoring of positions while the beam is in operation. New tooling

---

⋆ This value depends in detail on the type of detector employed and will be discussed in Section 3.5

is required and the aforementioned CMM will be used to locate their coordinates. distances with micron accuracies. It should be added that these CMMs, equipped with optical probes (TV microscopes) can be used to examine the fresnel lenses for asymmetric errors of construction that would lead to systematic errors in the positions of their laser light images.

2.5. Coordinate transfer from the laser tooling station to a component tooling station

Figure 1 shows a possible "offset arm" to relate the coordinates of the tooling on a quadrupole, for example, to that on a laser station. We have not decided exactly what form of measurement will prove to be the most appropriate. The suggestions listed below should be followed up experimentally and developed into reliable and cost effective solutions.

Horizontal What ever reading mechanism is proposed, it seems useful to provide a mechanical, albeit floating, bridge to support the instrumentation across the, up to two meter, span.

1. Interferometry

Perhaps the most accurate absolute measurement of distance between the tooling on the component and that on the reference housing is by means of standard metrological interferometry. Over a flight path of two meters, the distance uncertainty should remain below about 1 micron in spite of the combined errors due to temperature, pressure and humidity of the intervening air as well as the uncertainty in the instruments' stabilized wavelength and its ability to resolve fringes.[9] It must be pointed out however that this technique is relatively expensive and not too well suited to being employed in the field. This is particularly true if used in multiple widely separated areas or for remote reading during beam operation. We believe, however, that the tooling and the "arm bridge" should be designed so that initial standardization and recalibration of other instrument types be possible by this method.

2. Invar rod method

It is entirely possible to suppose that the arm bridge carry a fixed calibrated invar rod, one end of which is fastened to the tooling on one side, the position of the other end read by sensing elements having micron resolution. Since these elements have to read stably over relatively short distances (say 1 mm to 1 cm), a wide variety of radiation resistant instrument heads come to mind. Among these are the SONY Magnascale and high precision LVDTs, magnetic or capacitance proximity gauges.

3. Plain rod method

The expense of Invar rods can be traded against the necessity of measuring the average temperature of an ordinary metal transfer rod. What is gained in capital cost is lost in computer read instrumentation channel cost and extra laboratory calibration. This tradeoff has not yet been evaluated.

Vertical We propose to transfer vertical coordinates by means of hydrostatic levels whose liquid containing tubes are carried by the bridge and whose wells are fixed to the tooling at each end. By keeping the riser heights below, say one centimeter, temperature effects will be minimized. We have not yet chosen the fluid or method of height read out. Mercury has been used with excellent results[10]. The difficulties of using water with a high precision capacitance read out appear to have been solved by Roux[11].

Although we do not need to consider the effects of perturbations of the local gravity vector on the average geoid at SLAC over the short offset distances involved, it should be pointed out that very careful attention most be paid to the coordinate systems of the linac and of the BSY laser systems. They are neither parallel to each other nor normal to the local gravity vector at any point along their length. For this reason carefully machined shim blocks are called for to compensate for the resulting height differences of the various components along the beam line.

2.6. Roll, Yaw and Pitch

So far we have described the precision measurement of the transverse and, to a lesser accuracy, the longitudinal coordinates of components. A solid is, however, defined by six parameters. Assuming for the moment we can mount the coordinate tooling to reference the nodal point of a component, (the effective electrical center) studies have shown that we do not need to measure pitch and yaw with extreme accuracy (Milliradians are sufficient). For this reason we presume that they can be set up by more conventional means. The roll angle (θ_z) tolerances are under investigation. Fortunately there exist today remote reading tiltmeters of sufficient accuracy, near zero angle, to solve this problem.

3. Recent Experiences with the BSY Laser Alignment System

The BSY system has been in disuse since the onset of the SLC construction program in summer 1984. At that time high-power slits were removed to make room for the Arc transport system and some target stations are therefore no longer in service. To the best of our knowledge the system was not used till February of this year when a new laser was installed.

We are pleased to be able to report the following observations:

1. The Fresnel targets of all but one of the remaining 17 target stations could be inserted on demand.
2. With the exception of the last target (No.20), the widths of the images observed over 10,000 ft downstream, were consistent with those calculated. The last target is so close to the source, it is suspected that the finite phase space of the laser adds to the image size.
3. Relative to the double target at the end of the accelerator (Station 30-9), a very cursory look indicates that Stations 12, 13, 14, 15, 17, 18, 19 appear to be on a straight line to within about 0.1 mm. Since it is very unlikely that the mountings have been realigned in the last 5 years (perhaps two decades), this observation speaks for the remarkable stability of the downstream part of the Beam Switchyard Tunnel floor and of the original laser target housings. Target 16 is misaligned by about 1mm. We note that it is mounted on an stand made of bolted together dexion angle steel.
4. Figure 6 is a photograph of the image from a BSY Fresnel lens. This picture shows that the far wings of the pattern can be used to determine the relative roll of target stations.
5. The image plane of the observation station has been equipped with a new form of position readout. The oscillating image differentiating scanner has been replaced by a modern CCD camera shown in Figure 7. In its first form, suitable for image widths below 1 cm, the light falls directly on the array. The image is digitized on a gray scale and may be enhanced by a series of filter-programs resident on a local PC. The computer and its digitized output are shown in Figure 8. Various algorithms have been written to find the "center" of the image. Tests are under way to determine the best methods. For images larger than those easily accommodated, a simple demagnifying lens is called for. It goes without saying that the whole panoply of todays computer aided image enhancement techniques may be employed to rapidly find centers of images to better than 1/100th of their width. During recent exercises with the main accelerator laser alignment system using targets in Linac sectors 1

and 2, early results in a semi-automated data acquisition mode resulted in overall position repeatabilities in the 4 micron range.

4. The Proposal

From the aforesaid discussion one is led to the notion that technology existing at SLAC demonstrably permits the establishment of a *straight line reference system* from which the coordinates of beam-line components may be determined, monitored and maintained. The proposal, therefore, is to extend such a reference system into the research yard to whatever length is required and to develop the necessary ancillary measurement equipment and software for rapid realignment. We stress the word rapid because the favorable conditions of ground stability observed in the tunnel will not obtain in the yard; a region which will be subject to changes of loading and major diurnal temperature fluctuations.

We propose to equip every focussing element with an associated laser target station. (Current versions of the FFTB optics contain 29 Quads) Flat field bending magnets, which in principle have loose transverse tolerances, will be placed by conventional means. We assume for the purpose of this proposal that sextupoles will be aligned and permanently fixed to their associated quadrupoles in a precision laboratory environment. The mechanical mounting of beam position monitors will be treated in a similar way.

Although there are more modern[12] methods, we believe this proposal is competitive, both technically and financially, for the following reasons:

1. A great deal of the required hardware already exists. This includes: the laser, its mounting, the input mirror box, some 16 Fresnel target actuators and their vacuum housings, some 600 ft of 10" vacuum pipe and bellows joints, the double targets to reference to the accelerator, a detector room with its CCD Camera and precision slide readout.
2. By virtue of the system's very large lever arm, it achieves the type of resolution required.
3. The existing mechanical parts can achieve the required repeatabilities. Engineering designs exist and additional stations can be manufactured from existing drawings.
4. Because it is unlikely that the old BSY lenses will fit into the extended system perfectly, a new program for the so called artwork has already been written. The manufacture of new lenses by chemical machining is today about an order of magnitude less expensive than it was 25 years ago due to advances in microelectronics technology.

5. It is well to remember that in the micron world, steel behaves like butter. The existing designs of the housings attest to their stability and rugged resistance to abuse.

6. No matter what scheme is adopted for an optical reference line, the difficult problems of coordinate transfer must be solved.

At this moment of writing we are not ready to evaluate, with complete confidence, all the ingredients of the error budget for either the resolution or the accuracy of the system. On the basis of other investigators experiences[13] we believe that entering the micron world may present unexpected effects. We believe this fact is consistent with the exploratory nature of the Final Focus Test Beam's mission.

5. Acknowledgements

It is a pleasure to be able to acknowledge the help of A. Lisin and B. Denton for their work in cost and time estimating. Many thanks to V. Hamilton and Vincent Bressler for his work in setting up and programming the CCD readout.

REFERENCES

1. For preliminary parameters see, for example, T. Fieguth, "Final Focus Test Beam(s)" presentation to the FF working group, International Workshop on Next Generation Linear Colliders, SLAC Report 335, December 1988 p. 312.

2. K. Oide, "Design of Optics for the Final Focus Test Beam at SLAC", Proceedings of the 1989 IEEE Particle Accelerator Conference, Chicago, March 1989, Vol. 2, p. 1319

3. Computer file MISALIGN OIDE C1, on disk JJM193, dated November 3, 1988

4. The term "jitter" derives from the notion that high frequency errors are not correctable by conventional means. Since high frequency countermeasures have already been proposed for highly sensitive beams, the term jitter is probably a misnomer and should be more clearly defined.

5. For example "Finding the Magnetic Center of a Quadrupole to High Resolution" G. E. Fischer, J. K. Cobb, D. R. Jensen SLAC-TN-89-01 March 1989 and these proceedings.

6. For a general description of the SLAC linear accelerator laser alignment system see: R. B. Neal "The Stanford Two Mile Accelerator" Benjamin, New York, 1968 Lib. Congress Cat Card 68-23364, Chapter 22, p. 821 - 885, Support and Alignment. This chapter also contains a discussion of the BSY system. More readily available is W. B. Herrmannsfeldt et al. "Precision Alignment Using a System of Large Rectangular Fresnel Lenses", Applied Optics, Vol. 7, p. 995, (1968)
7. See for example: W.Coosemans et al. "Automation by Microcomputer of Geodetic Distance Measuring Instrument: The Distinvar" CERN 85-16 November 8, 1985.
8. See Reference 6. The BSY system is described in greater detail in "Precision Alignment of a large Beam Transport System" Herrmannsfeldt et al. IEEE Trans. Nucl. Sci. NS-14 No. 3, 903-7 (1967) and additional calculations can be found in SLAC-TN-65-034 April 1965.
9. For a brief discussion of measurements in the micron range the reader may find it useful to refer to the report "Some thoughts on Linear Collider Alignment and Mechanical Stability" G.E.Fischer and M.Mayoud [CERN-LEP-RF-SU-88-07] March 1988 pages 24-30
10. P. F. Pellissier, Trans. IEEE on Nuclear Science Vol. NS 12, No. 3 p. 19 (1965)
11. D. Roux, Note ALGE 88-04, March 1988, ESRF Grenoble France. and Note ALGE 88-06 November 1988.
12. See, for example, the very detailed proposal: "Magnetic Axis Alignment and the Poisson Alignment Reference System" Lee V. Griffith et al. Lawrence Livermore National Laboratory, UCID 21591 January 31, 1989 used to align an FEL.
13. "Microns, Microns, Everywhere and All of Them Out of Line" W. B. Davison et al. Steward Observatory, University of Arizona, Tucson, Ar 85721 and presented in SPIE Vol. 608 Optical Alignment III, (1986)

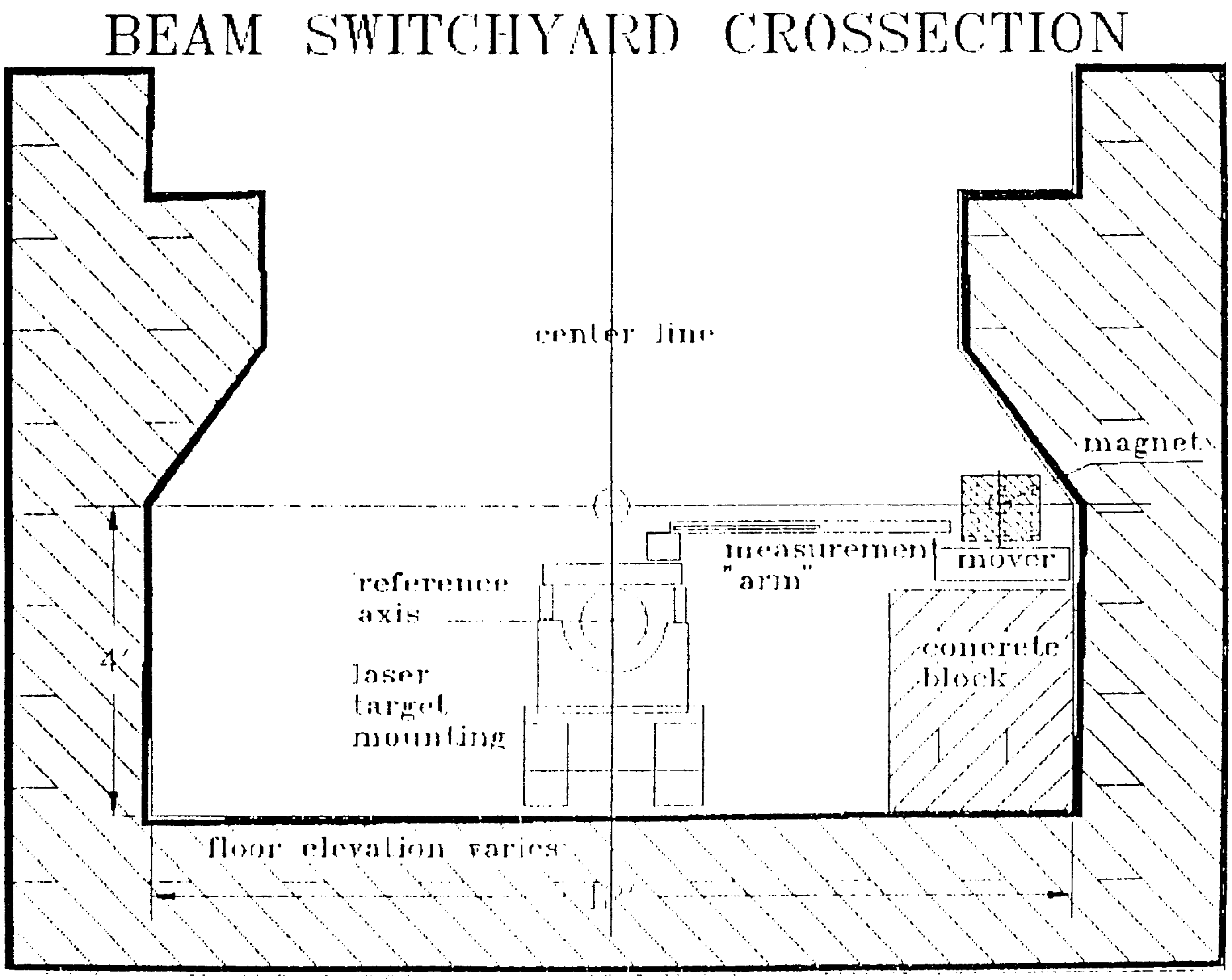

BEAM SWITCHYARD CROSSECTION
center line
magnet
measurement "arm"
mover
reference axis
laser target mounting
concrete block
4'
floor elevation varies

Figure 1.

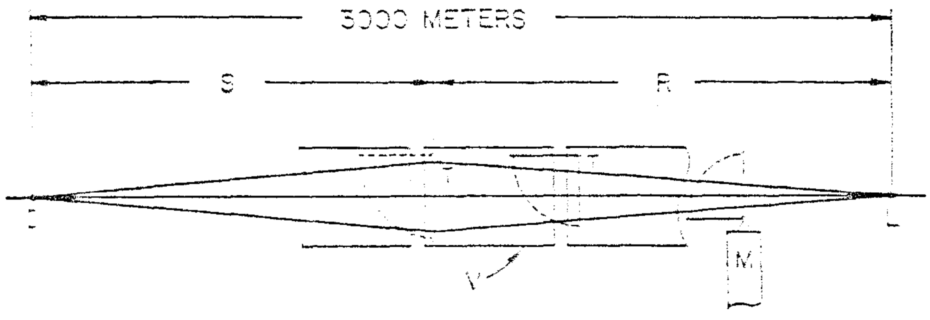

Figure 2. Schematic illustration of the SLAC alignment system. A typical target T, which is actually a rectangular Frensel lens, focuses the laser light source L to an image at the detector D. There are 294 alignment targets and three monument targets such as at M, which are attached to deep pillars. V is the 60-cm diam vacuum pipe, 12 m long.

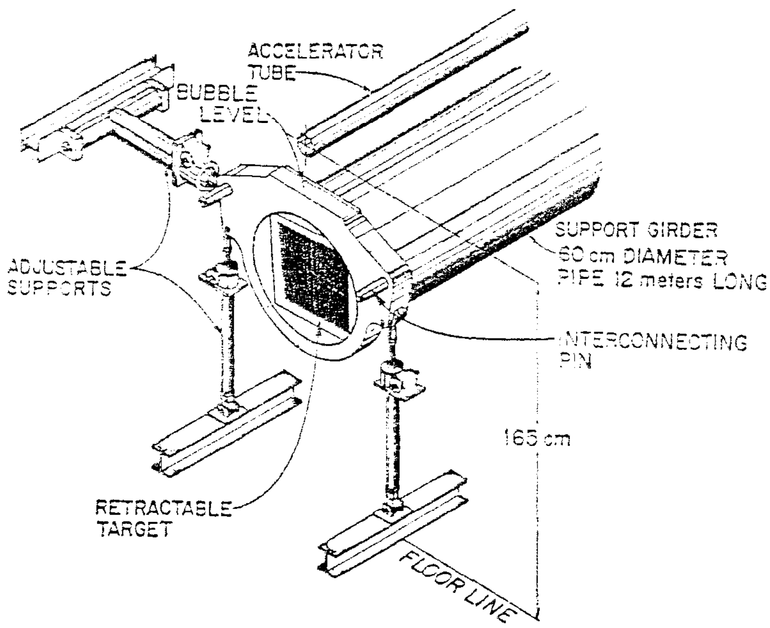

Figure 3. The mounting arrangemnet at the target end of each accelerator support girder. The target is shown in the inserted position. When retracted, the target is positioned horizontally along the top of the pipe.

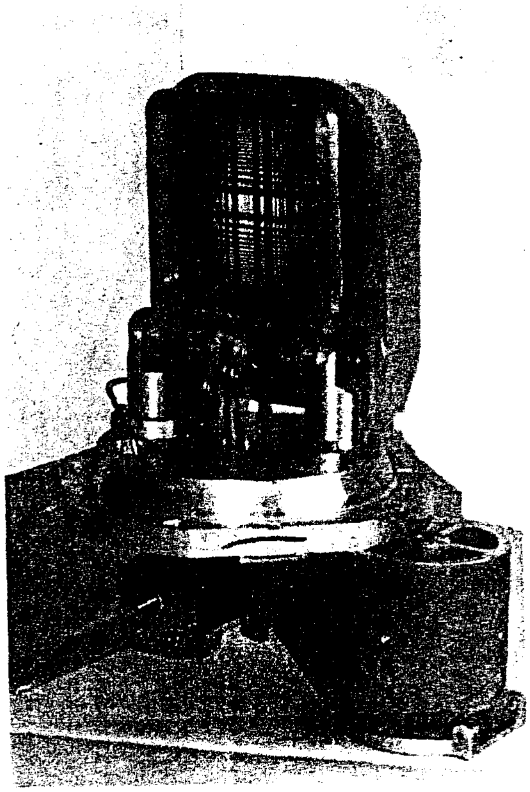

Figure 4.

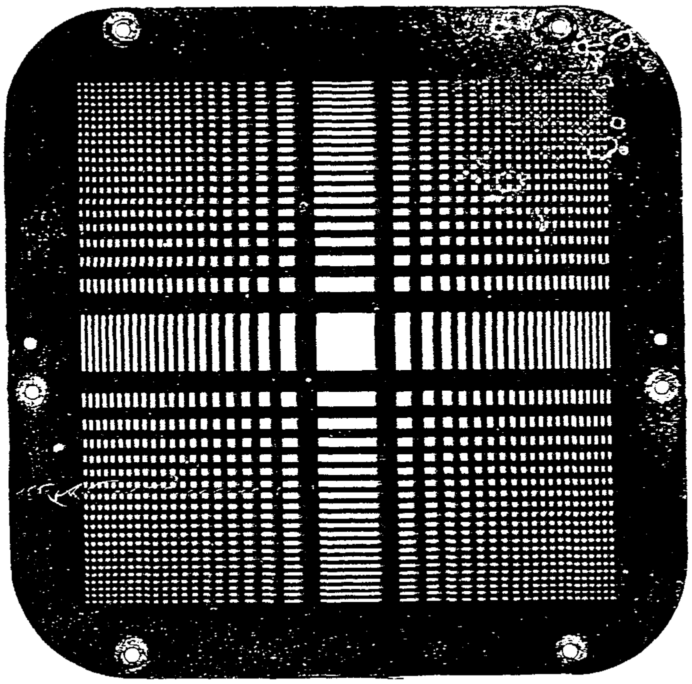

Figure 5.

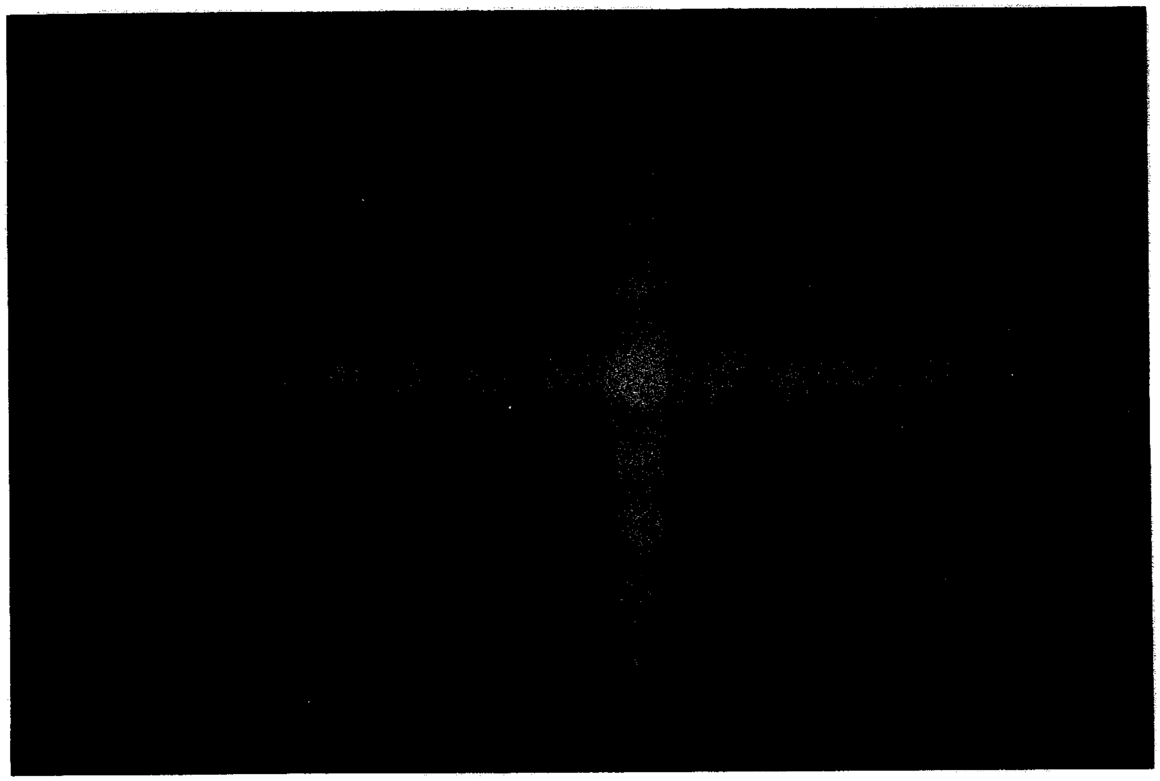

Figure 6.

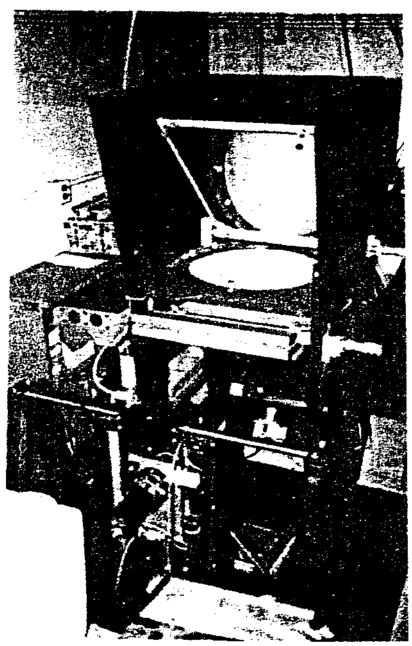

Figure 7.

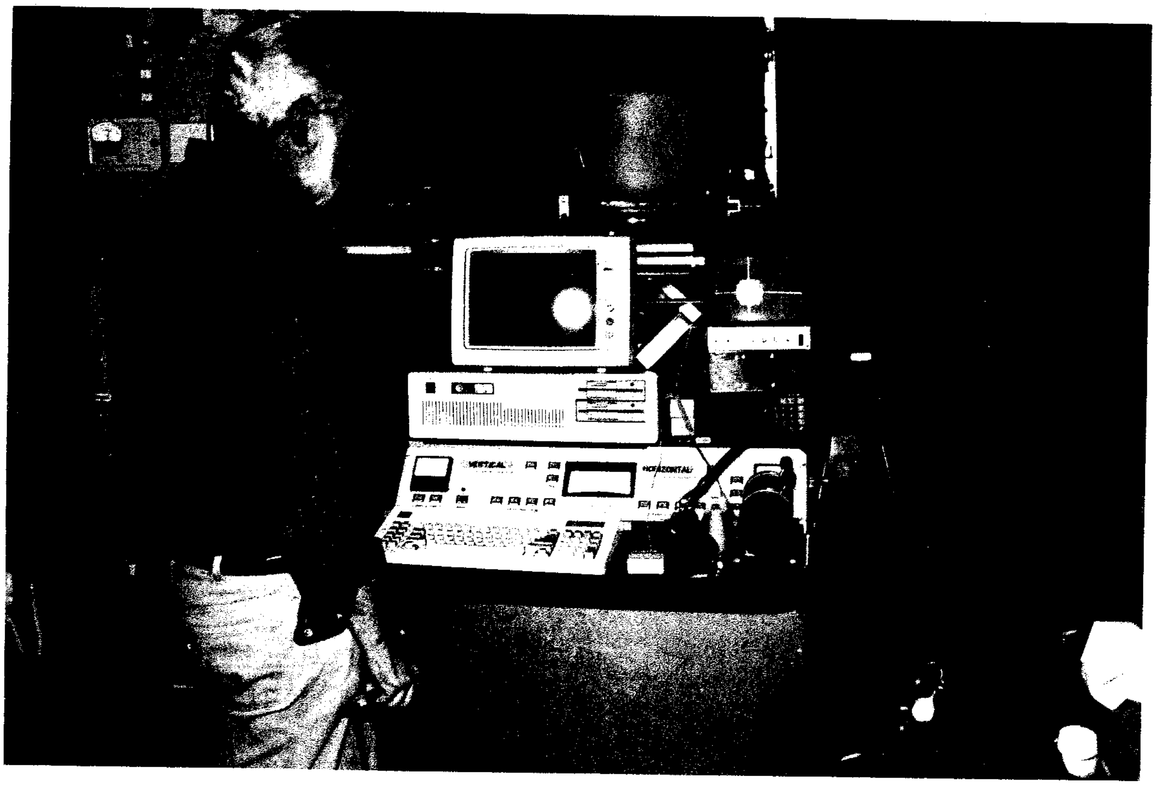

Figure 8.